Amélioration de la modélisation des variables hydrologiques et évaluation de l'impact des changements climatiques au Québec

par

Frédéric TALBOT

MÉMOIRE PAR ARTICLES PRÉSENTÉ À L'ÉCOLE DE TECHNOLOGIE SUPÉRIEURE COMME EXIGENCE PARTIELLE À L'OBTENTION DE LA MAÎTRISE AVEC MÉMOIRE EN GÉNIE DE LA CONSTRUCTION
M. Sc. A.

MONTRÉAL, LE 26 MARS 2025

ÉCOLE DE TECHNOLOGIE SUPÉRIEURE
UNIVERSITÉ DU QUÉBEC

PRÉSENTATION DU JURY

CE MÉMOIRE A ÉTÉ ÉVALUÉ

PAR UN JURY COMPOSÉ DE :

M. Richard Arsenault, directeur de mémoire
Département de génie de la construction à l'École de technologie supérieure

M. Jean-Daniel Sylvain, codirecteur de mémoire
Direction de la recherche forestière du Ministère des Ressources naturelles et des Forêts

M. François Brissette, président du jury
Département de génie de la construction à l'École de technologie supérieure

M. Jean-Luc Martel, membre du jury
Département de génie de la construction à l'École de technologie supérieure

IL A FAIT L'OBJET D'UNE SOUTENANCE DEVANT JURY ET PUBLIC

LE 14 MARS 2025

À L'ÉCOLE DE TECHNOLOGIE SUPÉRIEURE

REMERCIEMENTS

La réalisation de ce mémoire n'aurait pas été possible sans le soutien de plusieurs personnes et organisations, que je tiens à remercier chaleureusement.

Je tiens tout d'abord à exprimer ma plus profonde gratitude à mon directeur de mémoire, Monsieur Richard Arsenault. Richard, lorsque tu m'as contacté à la fin de mon baccalauréat pour m'offrir l'opportunité de faire un stage en recherche, je n'avais alors aucune idée de ce qu'était véritablement la recherche. Mais, plus important encore, je ne pouvais imaginer à quel point cette expérience allait transformer mon parcours et éveiller en moi une véritable passion. Si aujourd'hui, je suis autant passionné par la recherche, c'est en grande partie grâce à toi. Tu as su, dès le premier jour, me transmettre ton enthousiasme et ta curiosité pour le domaine, tout en m'offrant un environnement où j'ai pu repousser mes limites. Tu as toujours cru en moi, m'encourageant à aller plus loin à chaque étape. Ton mentorat a été exceptionnel et ton soutien indéfectible. Tu es une source d'inspiration, et je ne saurais assez te remercier pour la confiance que tu m'as accordée, pour les discussions enrichissantes et pour les conseils précieux qui ont grandement contribué à la réussite de ce travail, ainsi qu'à mon développement professionnel et personnel. Ce projet n'aurait pas été le même sans toi, et pour cela, je te serai toujours reconnaissant.

Un grand merci également à mon codirecteur de mémoire, Monsieur Jean-Daniel Sylvain, du Ministère des Ressources naturelles et des Forêts, pour ton soutien durant ce projet. Tes conseils avisés sur la rédaction scientifique et ta patience m'ont été d'une aide précieuse dans la rédaction de mes premiers articles scientifiques. Merci pour ton accompagnement, ta vision et ton expertise qui ont grandement contribué à la qualité de ce travail.

Je souhaite également remercier, Monsieur Guillaume Drolet, du Ministère des Ressources naturelles et des Forêts, et Monsieur Simon Ricard, de l'Université Laval, pour leur collaboration et leurs idées constructives qui ont permis de pousser cette recherche encore plus loin.

Je n'oublie pas les professeurs du département de génie de la construction qui m'ont soutenu et encouragé tout au long de mon parcours. Un immense merci à Madame Annie Poulin, Monsieur Jean-Luc Martel, Monsieur François Brissette et Monsieur Patrice Dion pour leurs conseils et leur disponibilité. Vos enseignements et votre expertise ont joué un rôle essentiel dans l'accomplissement de ce mémoire.

Je souhaite également remercier les institutions qui m'ont soutenu financièrement, notamment l'École de technologie supérieure, le Ministère des Ressources naturelles et des Forêts et Hydro-Québec. Leur appui m'a permis de me concentrer entièrement sur mes recherches, et sans ce soutien, ce travail n'aurait pu aboutir.

Sur le plan personnel, je veux exprimer ma reconnaissance à mes collègues et amis du groupe de recherche Hydrologie, Climat et Changements Climatiques (HC3). Vous avez été une source de motivation et d'encouragement tout au long de cette aventure. Nos discussions stimulantes et les moments partagés m'ont permis de rester concentré et de traverser les périodes plus difficiles.

Je tiens également à remercier chaleureusement ma famille. Maude et Carol, mes parents, et mes frères, Jérémie et Benjamin, merci pour votre compréhension, vos encouragements constants et votre amour inconditionnel. Votre soutien m'a permis de garder le cap, même dans les moments les plus exigeants de ce parcours.

Enfin, je réserve mes plus profonds remerciements à ma conjointe, Audrey. Tu as été à mes côtés durant toutes ces soirées et fins de semaine consacrées à mon travail de recherche. Merci d'avoir écouté avec patience mes histoires parfois ennuyeuses, d'avoir nourri mes ambitions et d'avoir toujours cru en moi. Ta patience, ton amour et ton soutien m'ont permis de surmonter les moments les plus difficiles. Sans toi, ce cheminement n'aurait tout simplement pas été possible. Tu es une femme extraordinaire et je t'en serai toujours reconnaissant. Je t'aime et je suis infiniment heureux de t'avoir à mes côtés.

Amélioration de la modélisation des variables hydrologiques et évaluation de l'impact des changements climatiques au Québec

Frédéric TALBOT

RÉSUMÉ

Ce mémoire vise à améliorer la modélisation des variables hydrologiques et à évaluer les impacts des changements climatiques sur les bassins versants du Québec, en mettant l'accent sur l'application du modèle hydrologique WaSiM et les projections climatiques issues de CMIP6. La recherche se concentre sur trois aspects clés : l'optimisation de la configuration du modèle hydrologique, la comparaison entre les méthodes de modélisation conventionnelle et asynchrone, et l'évaluation des impacts des changements climatiques sur les variables hydrologiques.

Dans le premier volet de l'étude, trois configurations du modèle WaSiM sont comparées. La configuration intégrant la recharge de la nappe phréatique dans la calibration des paramètres du modèle, bien que moins performante en termes de reproduction des débits observés, offre une précision supérieure dans la modélisation des variables hydrologiques internes, soulignant l'importance d'une calibration multi-variable pour limiter le phénomène d'équifinalité lors de l'optimisation du modèle et améliorer la représentation des variables hydrologiques.

Le deuxième volet de l'étude compare les performances des méthodes de modélisation conventionnelle et asynchrone. L'approche asynchrone, qui élimine la dépendance aux données météorologiques historiques, présente des avantages potentiels dans les régions où les données d'observation sont limitées ou peu fiables. Toutefois, elle montre des lacunes dans la représentation temporelle des événements hydrologiques, en particulier la fonte des neiges. Cette méthode souffre d'une incohérence dans la synchronisation des processus saisonniers. Cela souligne la nécessité d'intégrer une forme de synchronicité dans la méthode asynchrone, afin d'améliorer la fiabilité des projections hydrologiques.

Le troisième volet porte sur l'évaluation des impacts des changements climatiques dans 34 bassins versants du sud du Québec. Les résultats montrent une augmentation des précipitations totales et des températures, avec une transition significative des précipitations neigeuses à la pluie, une réduction de l'accumulation de neige, et un décalage des crues printanières vers des périodes plus précoces. Les projections indiquent également une augmentation de la recharge des nappes phréatiques en hiver et au printemps, tandis que l'évapotranspiration s'intensifie durant les mois plus chauds. Les résultats de cette étude fournissent des informations cruciales pour la gestion des ressources en eau dans un contexte de changements climatiques.

Ce mémoire met en évidence l'importance d'une calibration multi-variable et l'utilisation des dernières projections climatiques pour améliorer la modélisation hydrologique.

Mots-clés : Modélisation hydrologique, changements climatiques, calibration, modèle hydrologique spatialement distribué

Improving hydrological variables representation and assessing the impact of climate change in Quebec

Frédéric TALBOT

ABSTRACT

This thesis aims to improve the modeling of hydrological variables and assess the impacts of climate change on watersheds in Quebec, with a focus on the application of the WaSiM model and climate projections from CMIP6. The research addresses three key aspects: optimizing the configuration of the hydrological model, comparing conventional and asynchronous modeling methods, and evaluating the impacts of climate change on hydrological variables.

In the first part of the study, three calibration configurations of the WaSiM model are compared. The configuration that incorporates recharge into the model's calibration, while slightly less accurate in reproducing observed streamflow, provides superior precision in simulating internal hydrological processes. This highlights the importance of multi-variable calibration to limit equifinality and improve the representation of hydrological variables.

The second part of the study compares the performance of conventional and asynchronous modeling methods. The asynchronous approach, which eliminates the reliance on historical meteorological data, presents potential advantages in regions where observational data are limited or unreliable. However, it shows shortcomings in accurately capturing the timing of hydrological events, particularly snowmelt. This method suffers from inconsistencies in synchronizing seasonal processes, underlining the need for future research to incorporate some form of synchronicity in the asynchronous method to improve the reliability of hydrological projections.

The third part evaluates the impacts of climate change across 34 watersheds in southern Quebec. The results indicate an increase in total precipitation and temperature, with a significant shift from snowfall to rainfall, reduced snow accumulation, and earlier spring peak flows. The projections also show an increase in groundwater recharge during winter and spring, while evapotranspiration intensifies during the warmer months. These findings provide critical insights for water resource management in the context of climate change.

This thesis emphasizes the importance of multi-variable calibration and the use of the latest climate projections to enhance hydrological modeling.

Keywords : Hydrological modeling, climate change, calibration, physically based distributed hydrological model

TABLE DES MATIÈRES

Page

LISTE DES TABLEAUX

Page

LISTE DES FIGURES

LISTE DES ABRÉVIATIONS, SIGLES ET ACRONYMES

BL	Configuration du modèle WaSiM nommée « Baseline »
C_0	Paramètre du modèle hydrologique : degree-day factor
CMIP	Coupled Model Intercomparison Project
CMIP5	Coupled Model Intercomparison Project Phase 5
CMIP6	Coupled Model Intercomparison Project Phase 6
C_{rfr}	Paramètre du modèle hydrologique : coefficient for refreezing
C_{WH}	Paramètre du modèle hydrologique : water storage capacity of snow
DDS	Dynamically Dimensioned Search
DEM	Digital Elevation Model
DSM	Digital Surface Model
d_r	Paramètre du modèle hydrologique : drainage density for interflow
d_z	Paramètre du modèle hydrologique : soil layer thickness
ECMWF	European Center for Medium-Range Weather Forecasts
ERA5	ECMWF Reanalysis v5
ETa	Actual evapotranspiration
ETP	Potential evapotranspiration
FAO	Food and Agriculture Organization of the United Nations
$fi,_{summer}$	Paramètre du modèle hydrologique : summer correction factors for ETP
$fi,_{fall}$	Paramètre du modèle hydrologique : fall correction factors for ETP
$fi,_{winter}$	Paramètre du modèle hydrologique : winter correction factors for ETP
$fi,_{spring}$	Paramètre du modèle hydrologique : spring correction factors for ETP
Fig	Figure

$H_{geo,0}$	Geodetic altitude of the soil surface
H_{gw}	Groundwater table height
IDW	Inverse Distance Weighting
k_B	Paramètre du modèle hydrologique : scaling factor for baseflow
k_D	Paramètre du modèle hydrologique : storage coefficient for surface runoff
k_H	Paramètre du modèle hydrologique : storage coefficient for interflow
Kol	Paramètre du modèle hydrologique : colmation of the river links
k_{rec}	Paramètre du modèle hydrologique : recession constant for hydraulic conductivity
k_s	Saturated hydraulic conductivity
k_{xy}	Paramètre du modèle hydrologique : saturated horizontal conductivity (x-y direction)
GCM	Global Climate Model
GIEC	Groupe d’experts intergouvernemental sur l’évolution du climat
GRACE	Gravity Recovery and Climate Experiment
GRHQ	Géobase du réseau hydrographique du Québec
GW	Configuration du modèle WaSiM nommée « Physically based groundwater »
GW-RC	Configuration du modèle WaSiM nommée « Physically based groundwater and recharge calibration »
IPCC	Intergovernmental Panel on Climate Change
KGE	Kling-Gupta efficiency
LCCS	Land Cover Classification System
MBCn	Multivariate Bias Correction with N-dimensional distribution mapping
MDDELCC	Ministère de l’Environnement, de la Lutte contre les changements climatiques, de la Faune et des Parcs
MGC	Modèle global du climat

MRNF	Ministère des Ressources naturelles et des Forêts
N/A	Not applicable
NALCMS	North American Land Change Monitoring System
NASA	National Aeronautics and Space Administration
PACES	Projets d'acquisition de connaissances sur les eaux souterraines
Q_b	Baseflow
QD_{Snow}	Paramètre du modèle hydrologique : fraction of surface runoff on snowmelt
Qobs	Débits observés à la station hydrométrique
Qsim	Débits simulés par le modèle hydrologique
r	Coefficient de corrélation
RMSE	Root-Mean-Square error
Sect	Section
SIIGSOL	Carte des propriétés du sol
SSP	Shared Socio-economic Pathways
SSP5-8.5	Shared Socio-economic Pathways category fossil-fueled development
SST	Split-sample test
SRTMGL1	NASA Shuttle Radar Topography Mission version 3.0 Global 1 arc second
SWE	Snow water equivalent
T_0	Paramètre du modèle hydrologique : temperature limit for snowmelt
$T_{R/S}$	Paramètre du modèle hydrologique : transition temperature snow/rain
Ts	Land surface temperature
USDA	United States Department of Agriculture
VCF	Paramètre du modèle hydrologique : Vegetation cover fraction

WaSiM	Water balance Simulation Model
Z_0	Paramètre du modèle hydrologique : Roughness length

LISTE DES SYMBOLES ET UNITÉS DE MESURE

Longueur	
m	mètre
mm	millimètre
km	kilomètre
Aire	
km^2	kilomètre carré
Volume	
m^3	mètre cube
Unité de temps	
s	seconde
h	heure
d	jour
yr	année
Unité calorifique	
˚C	degré Celsius (unité calorifique)

INTRODUCTION

0.1 Contexte

Les changements climatiques figurent parmi les plus grands défis auxquels nous sommes confrontés aujourd'hui. En raison de l'augmentation des émissions de gaz à effet de serre, le réchauffement global perturbe le système climatique et le régime hydrologique (Calvin et al., 2023; Yue & Gao, 2018).

Le Québec devrait connaître une hausse des températures plus marquée que la moyenne mondiale, entraînant des modifications significatives du régime hydrologique (Estrada, Kim, & Perron, 2021). Cette transformation rapide du climat modifie la disponibilité, la qualité et la répartition des ressources hydriques, avec des répercussions sur les écosystèmes et les sociétés humaines (Calvin et al., 2023; Yue & Gao, 2018). Cette situation est particulièrement préoccupante pour des secteurs sensibles aux changements climatiques tels que l'agriculture, la foresterie, la production hydroélectrique et pour la gestion des inondations.

Par exemple, les inondations majeures survenues au Québec en 2011, 2017, 2019 et 2022 ont engendré des centaines de millions de dollars de dommages et ont mis en évidence les limites des systèmes de prévision actuels, particulièrement face à la combinaison de fortes précipitations et de fontes des neiges rapides durant la période de dégel (Riboust & Brissette, 2016; Teufel et al., 2019). En agriculture, les changements de régimes hydrologiques pourraient réduire les rendements et augmenter la demande en irrigation (Nand & Qi, 2023), tandis que dans la foresterie, les sécheresses plus fréquentes menacent la santé des forêts et augmentent le risque d’incendies (Gaudreau, Perez, & Drapeau, 2016; Le Goff, Leduc, Bergeron, & Flannigan, 2005; van Bellen, Garneau, & Bergeron, 2010). De plus, dans le secteur hydroélectrique, la gestion des réservoirs devient plus complexe avec des régimes de débits modifiés, posant des défis supplémentaires pour l'approvisionnement énergétique et la gestion des inondations (Haguma, Leconte, Côté, Krau, & Brissette, 2014; Minville, Brissette, Krau, & Leconte, 2009).

Pour atténuer les répercussions négatives du réchauffement global et maximiser les opportunités qui pourraient en découler, l'adaptation aux changements climatiques est un processus essentiel (Fankhauser, 2017). Dans les décennies à venir, il sera important de s'adapter en ajustant nos activités, nos prises de décisions et nos façons de penser. Une adaptation aux changements climatiques réussie permet de réduire la gravité et les coûts associés, tout en renforçant la résilience des infrastructures, des écosystèmes et des sociétés (Antwi, Burkhardt, Boakye-Danquah, Doucet, & Abolina, 2024; Bauer & Steurer, 2014; Lemieux & Scott, 2011; Picketts, Andrey, Matthews, Déry, & Tighe, 2016).

Pour mettre en œuvre une adaptation efficace, il est essentiel de bien quantifier les impacts futurs des changements climatiques. Dans ce contexte, les modèles hydrologiques jouent un rôle clé en permettant de simuler les variables hydrologiques cruciales, telles que les précipitations, les débits des rivières, la recharge des nappes phréatiques et l'évapotranspiration (de Lima Ferreira & da Paz, 2024; Schulla, 2021; Valencia Giraldo, Ricard, & Anctil, 2023). Ces projections sont indispensables pour anticiper les impacts des changements climatiques et soutenir une gestion efficace des ressources hydriques (Milly, Dunne, & Vecchia, 2005; Sivakumar, 2011). Par exemple, des simulations précises de l'humidité du sol sont essentielles en agriculture pour optimiser l'irrigation et préserver les rendements (Nand & Qi, 2023). La modélisation de la recharge des nappes phréatiques est cruciale pour l'approvisionnement en eau potable et la gestion durable des aquifères (Dubois, Larocque, Gagné, & Braun, 2022), tandis que la simulation du ruissellement de surface est vitale pour la conception des infrastructures urbaines et la prévention des inondations (Guo, Guan, & Yu, 2021; Jehanzaib, Ajmal, Achite, & Kim, 2022). Enfin, la prévision des débits des rivières est nécessaire pour la gestion des réservoirs hydroélectriques, permettant d'optimiser la production d'énergie tout en réduisant les risques d'inondations (Haguma et al., 2014; Minville et al., 2009).

Des défis persistent quant à la capacité des modèles actuels à évaluer de manière précise les impacts des changements climatiques sur les variables hydrologiques (de Lima Ferreira &

da Paz, 2024; Mei et al., 2023). L'un des principaux défis réside dans l'amélioration des techniques de calibration des modèles. Actuellement, la majorité des modèles sont calibrés principalement sur les débits des cours d'eau, ce qui peut entraîner une sous-représentation des autres variables hydrologiques, telles que l'humidité du sol ou la recharge des nappes phréatiques (Acero Triana, Chu, Guzman, Moriasi, & Steiner, 2019; Mei et al., 2023; Yassin et al., 2017). Ces lacunes dans la calibration risquent de compromettre la précision des simulations, affectant ainsi la gestion des ressources en eau, la prévention des inondations et la planification de l'adaptation aux changements climatiques (Farjad, Gupta, & Marceau, 2016; Pradhan & Indu, 2019).

De nouvelles approches, comme la méthode asynchrone (Ricard, Lucas-Picher, & Anctil, 2021; Ricard, Lucas-Picher, Thiboult, & Anctil, 2023; Ricard, Sylvain, & Anctil, 2019, 2020), remettent en question l'efficacité des méthodes de modélisation traditionnelles, qui s'appuient souvent sur des corrections de biais des modèles globaux du climat (MGC). Contrairement aux approches conventionnelles, la méthode asynchrone intègre directement les données des MGC sans recourir à des corrections, ce qui simplifie la chaîne de modélisation.

Ce mémoire se penchera sur l'amélioration de la modélisation hydrologique, en mettant l'accent sur l'optimisation de la représentation des variables hydrologiques, tout en évaluant l'impact des changements climatiques dans 34 bassins versants du Québec. Une telle analyse est essentielle pour améliorer notre compréhension des dynamiques hydroclimatiques et ainsi orienter les stratégies d’adaptation et optimiser la gestion des ressources en eau face aux défis climatiques à venir.

0.2 Organisation du mémoire

Ce mémoire est structuré en six chapitres, chacun abordant un aspect spécifique de la recherche. Le premier chapitre établit le cadre théorique en présentant les éléments essentiels pour comprendre les défis liés à la modélisation hydrologique en contexte de changements climatiques. Le deuxième chapitre décrit les éléments généraux de la méthodologie employée dans les trois articles scientifiques qui forment le cœur de cette recherche. Ces articles sont ensuite détaillés dans les chapitres suivants.

Le chapitre 3 introduit le premier article intitulé « Enhancing physically-based and distributed hydrological modeling », soumis à *Hydrology and Earth System Sciences*. Cet article explore l'efficacité de différentes approches de calibration avec le modèle hydrologique WaSiM afin d'améliorer la qualité des simulations des variables hydrologiques. En testant trois configurations distinctes du modèle, l'étude évalue l'impact de chacune sur la précision des simulations. Les résultats démontrent que l'une des configurations se distingue par sa capacité à mieux représenter les processus hydrologiques, offrant ainsi une base solide pour les travaux présentés dans les chapitres suivants.

Le chapitre 4 est consacré au second article intitulé « Towards semi-asynchronous methods for hydrological modelling under climate change », également soumis à *Hydrology and Earth System Sciences*. Cet article évalue l'efficacité de la méthode asynchrone, une approche novatrice de modélisation hydrologique qui diffère de la méthode conventionnelle en calibrant directement les distributions des débits sans recourir aux observations météorologiques historiques. L'étude compare ces deux méthodes en termes de capacité à simuler les processus hydrologiques dans divers bassins versants, offrant ainsi un aperçu des avantages et des limites de chaque approche.

Le chapitre 5 présente le troisième article, intitulé « Assessing hydroclimatic impacts of climate change in snowy catchments using a physically-based hydrological model », soumis à *Journal of Hydrology : Regional Studies*. Cet article se concentre sur les impacts des changements climatiques sur les processus hydrologiques dans 34 bassins versants du sud du Québec. En utilisant le modèle hydrologique WaSiM et les MGC du CMIP6, l'étude explore les effets des changements climatiques sur diverses variables hydrologiques clés, telles que le débit des rivières, l'équivalent en eau de la neige, la recharge des nappes phréatiques, le ruissellement de surface, l'évapotranspiration et l'humidité relative du sol.

Le mémoire se conclut par une discussion générale des résultats obtenus (chapitre 6), suivie d'une conclusion qui synthétise les principaux apports de la recherche. Enfin, des recommandations sont également proposées pour guider les futures études dans le domaine de la modélisation hydrologique, en particulier dans le contexte des changements climatiques.

CHAPITRE 1

REVUE DE LITTÉRATURE

Ce chapitre présente une revue de la littérature sur la modélisation hydrologique, en mettant l'accent sur les différentes approches et applications des modèles, ainsi que sur les avancées récentes dans le domaine. Les techniques de calibration, la modélisation hydroclimatique et l'impact des changements climatiques sur les variables hydrologiques y sont examinés. Ces trois axes constituent les bases méthodologiques de ce mémoire et sont développés en détail dans les articles associés. Cette section offre une vue d'ensemble des concepts fondamentaux de ce mémoire.

1.1 Les modèles hydrologiques

Les modèles hydrologiques sont des outils indispensables pour comprendre, prévoir et gérer les ressources en eau. En s'appuyant sur des équations physiques ou des approximations empiriques, ces modèles permettent de simuler le cycle de l'eau et de fournir des prédictions fiables concernant des variables hydrologiques essentielles telles que les précipitations, l'écoulement de surface, la recharge des nappes phréatiques et l'évapotranspiration (Devia, Ganasri, & Dwarakish, 2015).

Depuis les travaux de Mulvany (1850) et Darcy (1856), les modèles hydrologiques n'ont cessé d'évoluer (Singh, 2018). Avec l'avènement des ordinateurs dans les années 1960, des modèles numériques comme le Stanford Watershed Model (Crawford & Linsley, 1966) ont vu le jour, jetant les bases des modèles modernes. Aujourd'hui, il existe une vaste gamme de modèles hydrologiques, allant des modèles conceptuels simples aux modèles distribués à base physique, jusqu'à l'utilisation de l'intelligence artificielle avec des approches comme les réseaux de neurones (K. J. Beven, 2012). Chaque type de modèle a ses avantages et ses limites, qui varient selon l'échelle de représentation spatiale et temporelle et la complexité des processus à modéliser. Ces aspects seront approfondis dans la section suivante.

Les modèles hydrologiques sont désormais des outils essentiels pour la gestion des ressources en eau et la prévision des phénomènes extrêmes comme les inondations ou les sécheresses. Ils sont également utilisés pour la conception des infrastructures hydrauliques, la modélisation des processus hydrologiques comme le ruissellement, l'humidité du sol ou l'accumulation de neige, ainsi que pour l'évaluation des impacts des changements climatiques sur les systèmes hydriques (K. J. Beven, 2012). Ces modèles sont donc indispensables pour la prise de décisions éclairées en matière de gestion durable de l'eau.

1.1.1 Types de modèles hydrologiques

Les modèles hydrologiques peuvent être différenciés par la manière dont ils représentent les processus hydrologiques (Devia et al., 2015). Les modèles conceptuels, par exemple, offrent une représentation simplifiée de ces processus. Faciles à utiliser et rapides à exécuter, ils conviennent lorsque seul le débit à l'exutoire d'un bassin versant est d'intérêt. Toutefois, ils ne capturent pas les spécificités locales et peinent à modéliser des processus complexes, tels que la recharge des nappes phréatiques ou la dynamique de la couverture neigeuse (K. J. Beven, 2012; Devia et al., 2015; Okiria et al., 2022).

En revanche, les modèles à base physique visent à modéliser ces processus de manière plus détaillée, en s'appuyant sur des lois physiques bien établies. Souvent distribués, ces modèles intègrent les variabilités spatiales au sein des bassins versants, offrant ainsi une représentation plus fidèle des dynamiques internes. Ils sont particulièrement utiles lorsque l'analyse des variables internes est nécessaire. Cependant, leur calibration est plus complexe et ils nécessitent des quantités importantes de données d'entrée, ce qui peut constituer une limite en cas de données manquantes (K. J. Beven, 2012; Poulin, Brissette, Leconte, Arsenault, & Malo, 2011).

Les modèles basés sur des réseaux de neurones, quant à eux, sont performants pour estimer certaines variables comme le débit (Fan et al., 2020; Kim & Kim, 2021; Ley, Bormann, & Casper, 2023; Sabzipour et al., 2023). Toutefois, leur nature de type « boîte noire » rend difficile l’interprétation des résultats et freine encore leur adoption à grande échelle (Kumar et al., 2024; Samek & Müller, 2019).

Les modèles hydrologiques se différencient également par l’échelle de représentation spatiale à laquelle ils opèrent. Les modèles globaux, souvent conceptuels, sont utilisés pour simulé les processus à plus faible résolution sur de larges territoires, ce qui ne permet pas de capturer les détails locaux (Han et al., 2021). Les modèles semi-distribués divisent un bassin versant en sous-bassins homogènes et simulent les processus hydrologiques individuellement pour chaque zone. Ils offrent un compromis entre la simplicité des modèles conceptuels et la précision des modèles distribués (K. Ajami, Gupta, Wagener, & Sorooshian, 2004; Khakbaz, Imam, Hsu, & Sorooshian, 2012). Les modèles distribués offrent une représentation détaillée des hétérogénéités spatiales au sein d’un bassin et sont capables de simuler des variables à différentes résolutions. Cependant, ils demandent d’importantes ressources en termes de données et de calcul (K. J. Beven, 2012).

Le choix du modèle dépend donc des objectifs de l’étude et des besoins de l’utilisateur. Pour des prévisions simples du débit à l'exutoire d’un bassin, un modèle conceptuel global peut être suffisant (Perrin, Michel, & Andréassian, 2003). Cependant, dans le cas où l’objectif est d’optimiser la représentation des variables hydrologiques afin d'évaluer l'impact des changements climatiques, un modèle à base physique et distribué est plus approprié.

1.2 Représentation des variables hydrologiques

Une représentation précise et cohérente des variables hydrologiques est essentielle pour réussir l’adaptation aux changements climatiques. L'ajustement des pratiques agricoles, la planification des infrastructures hydrauliques et la gestion des risques liés aux inondations et aux sécheresses dépendent largement de la capacité à modéliser correctement les réponses hydrologiques des écosystèmes en conditions climatiques futures. Une telle représentation permet d’orienter les décisions stratégiques et d’optimiser la gestion des ressources naturelles face au réchauffement global (Banda, Dzwairo, Singh, & Kanyerere, 2022; Gleick, 1989; Milly et al., 2005; Sivakumar, 2011).

1.2.1 Calibration des modèles hydrologiques

La méthode classique pour calibrer un modèle hydrologique consiste à évaluer sa capacité à reproduire le débit à l'exutoire d'un bassin versant, en comparant les résultats du modèle aux données observées aux stations hydrométriques (Arsenault, Brissette, & Martel, 2018; Arsenault, Poulin, Côté, & Brissette, 2014; Shen, Tolson, & Mai, 2022). Les données de débit observé servent de référence pour ajuster les paramètres du modèle et réduire l’écart entre les résultats simulés et les observations.

Plusieurs métriques d'évaluation sont utilisées pour quantifier la performance des modèles calibrés (Diskin & Simon, 1977; Jie, Chen, Xu, Zeng, & Tao, 2015; Kling, Fuchs, & Paulin, 2012). Parmi les plus courantes, on trouve le coefficient Kling-Gupta Efficiency (KGE), qui mesure l'adéquation entre les débits simulés et observés en combinant trois métriques qui permettent d’exprimer la performance du modèle, tels que la corrélation, le biais et la variabilité (Kling et al., 2012). Lorsque les performances atteignent un seuil jugé satisfaisant, selon la métrique choisie, le modèle est considéré comme calibré. Le niveau de généralisation du modèle est ensuite évalué par une phase de validation sur une période indépendante des données de calibration.

Comme le processus de calibration des modèles hydrologiques vise généralement à optimiser la représentation du débit, il est possible que les processus internes ne soient pas adéquatement représentés (de Lima Ferreira & da Paz, 2024; Mei et al., 2023; Pool, Fowler, & Peel, 2024; Schäfer, Fäth, Kneisel, Baumhauer, & Ullmann, 2023). Ces lacunes peuvent poser problème lorsqu’une étude nécessite une analyse détaillée de ces variables, en particulier dans un contexte de changements climatiques.

En conséquence, l’utilisation et l’analyse des variables hydrologiques internes, comme les volumes de ruissellement, la recharge des nappes phréatiques ou l'humidité du sol, pourraient s’avérer inadéquates si le processus de calibration n’intègre pas explicitement ces variables (Förster, Garvelmann, Meißl, & Strasser, 2018; Rössler, Diekkrüger, & Löffler, 2012; Valencia Giraldo et al., 2023). Ce problème est lié au phénomène d’équifinalité, où différentes combinaisons de paramètres produisent des résultats similaires pour le débit, tout en générant des représentations divergentes des processus internes.

1.2.2 Équifinalité

L’équifinalité est un phénomène bien documenté dans la calibration des modèles hydrologiques (K. Beven, 2006; K. Beven & Freer, 2001; Ebel & Loague, 2006; Hankin & Beven, 1998; Poulin et al., 2011). Elle survient lorsque différents ensembles de paramètres aboutissent à des résultats similaires pour le débit à l'exutoire du bassin versant, tout en produisant des dynamiques internes très différentes dans le modèle. Autrement dit, même si le modèle reproduit correctement les débits observés, la représentation des variables hydrologiques internes telles que l'humidité du sol, l'évaporation ou la recharge des nappes phréatiques peuvent varier considérablement selon les combinaisons de paramètres utilisées, créant ainsi un risque d’incohérence dans la représentation des processus internes.

Par exemple, Bouaziz *et al.* (2021) ont évalué les performances de huit groupes de recherche ayant calibré douze modèles hydrologiques sur le même bassin versant en suivant un protocole identique. Bien que les performances des modèles en termes de débit soient similaires, des différences significatives ont été observées dans la représentation des processus internes, tels que l’interception annuelle, les taux d'évaporation saisonniers, le nombre de jours annuels avec de l'eau stockée sous forme de neige, et le stockage maximal annuel moyen de neige. Ces disparités dans la représentation des processus internes montrent que ces modèles ne peuvent pas être simultanément proches de la réalité en ce qui concerne leurs états hydrologiques internes. Ce constat souligne l'importance d'améliorer les techniques de calibration afin de prendre en compte non seulement les débits à l'exutoire, mais également d'autres variables hydrologiques cruciales pour une meilleure représentation des dynamiques du cycle de l'eau.

1.2.3 Approches de calibration intégrant les variables hydrologiques

Pour atténuer le problème d’équifinalité et améliorer la représentation des processus hydrologiques internes, de nombreuses études ont mis en évidence les avantages d’intégrer des variables hydrologiques supplémentaires dans la calibration des modèles (Dembélé, Ceperley, et al., 2020; Dembélé, Hrachowitz, Savenije, Mariéthoz, & Schaefli, 2020; Immerzeel & Droogers, 2008; Rajib, Evenson, Golden, & Lane, 2018; Yassin et al., 2017). En se basant uniquement sur le débit à l'exutoire, les modèles risquent de mal représenter les variables internes, telles que l'humidité du sol ou l'évapotranspiration. L'intégration de ces variables dans la calibration permet d'obtenir des simulations plus réalistes et cohérentes des processus hydrologiques.

Par exemple, Pool *et al.* (2024) ont démontré que l'intégration de l'évapotranspiration et de l'humidité du sol en complément du débit lors de la calibration d’un modèle hydrologique a considérablement amélioré la performance du modèle pour ces variables. Cette approche a permis de mieux capturer la dynamique globale des variables hydrologiques, bien qu'elle ait entraîné une légère diminution de la performance des simulations du débit.

De manière similaire, de Lima Ferreira et da Paz (2024) ont montré que l’utilisation de données d’évapotranspiration obtenues par télédétection, combinées aux débits observés, a significativement amélioré la capacité du modèle à simuler à la fois l’évapotranspiration et le débit.

Mei *et al.* (2023) ont également souligné l'importance d'inclure des variables telles que l'humidité du sol et l'évapotranspiration dans la calibration des modèles, en particulier dans les bassins où les données hydrologiques sont limitées. Leur étude a révélé que l'ajout de données sur l'humidité du sol a amélioré les prévisions d'évapotranspiration tout en réduisant les biais dans la modélisation des variables hydrologiques.

Ces exemples mettent en lumière les avantages de l’intégration des variables hydrologiques internes dans la calibration des modèles hydrologiques, notamment en réduisant l’équifinalité et en améliorant la précision des simulations pour des variables telles que l’humidité du sol et l’évapotranspiration. Toutefois, cette approche introduit un compromis : bien que la prise en compte de variables supplémentaires permette une meilleure représentation des processus hydrologiques internes, elle peut également entraîner une légère dégradation de la performance du modèle pour la simulation du débit (Mei et al., 2023; Pool et al., 2024).

1.3 La chaîne de modélisation hydroclimatique

La chaîne de modélisation hydroclimatique désigne l'ensemble des étapes méthodologiques nécessaires pour étudier l’impact des changements climatiques sur les variables hydrologiques. Cette chaîne se compose de plusieurs éléments clés, dont chacun joue un rôle essentiel selon la méthode utilisée. Parmi ces éléments figurent les données climatiques et la correction des biais, qui seront abordés en détail dans les sections suivantes. Ces étapes permettent de s’assurer que les projections hydrologiques sont cohérentes avec les scénarios climatiques, la résolution des modèles et les dynamiques hydrologiques locales, favorisant ainsi une représentation plus robuste pour la gestion des ressources en eau dans un contexte de changements climatiques.

1.3.1 Scénarios et données climatiques

Les données issues de MGC jouent un rôle central dans la chaîne de modélisation hydroclimatique, car elles constituent la base des projections sur l’évolution future des variables hydrologiques. Les MGC simulent les interactions complexes entre l’atmosphère, les océans et la surface terrestre pour prévoir les changements des conditions météorologiques sur de longues périodes.

L'histoire de l'utilisation des données climatiques dans la recherche remonte à plusieurs décennies, avec l'émergence des premiers modèles climatiques dans les années 1960 (Manabe et Bryan, 1969). Ces premiers modèles étaient relativement simples, ne tenant compte que de quelques variables atmosphériques. Depuis, les avancées technologiques et scientifiques ont permis de développer des MGC de plus en plus sophistiqués, capables de capturer des interactions climatiques complexes à des échelles de représentation spatiales et temporelles de plus en plus fines (Edwards, 2011).

Les rapports du Groupe d'experts intergouvernemental sur l'évolution du climat (GIEC ou IPCC en anglais), publiés périodiquement depuis 1990, ont joué un rôle clé dans l'évaluation des projections climatiques et des scénarios d'émissions (Calvin et al., 2023; Gupta, 2010). Chaque rapport a contribué à affiner les modèles climatiques, en améliorant la précision des projections tout en introduisant de nouveaux scénarios représentant divers futurs possibles en fonction des trajectoires d'émissions de gaz à effet de serre (Edwards, 2011).

L'un des projets les plus influents dans le développement des modèles climatiques est le Coupled Model Intercomparison Project (CMIP) (Meehl, Boer, Covey, Latif, & Stouffer, 2000), un projet international coordonné qui permet la comparaison des résultats entre différents modèles climatiques. La Phase 6 de ce projet (Eyring et al., 2016), CMIP6, marque une amélioration notable par rapport à la phase précédente, CMIP5 (Taylor, Stouffer, & Meehl, 2012). Parmi les avancées, on note une meilleure représentation des rétroactions entre les composantes du climat, une résolution plus fine des modèles, ainsi qu'une prise en compte plus précise des forçages anthropiques et naturels. Les projections issues de CMIP6 offrent ainsi une vue plus détaillée des futurs climatiques potentiels, notamment en ce qui concerne les extrêmes climatiques, essentiels à l'évaluation des impacts hydrologiques (H. Chen, Sun, Lin, & Xu, 2020; Eyring et al., 2016; Martel et al., 2022).

Parmi les scénarios étudiés dans le cadre de CMIP6, le SSP5-8.5 (Shared Socioeconomic Pathways) (Calvin et al., 2023) représente un scénario à forte émission de gaz à effet de serre, dans lequel la société continue de dépendre lourdement des combustibles fossiles et où les efforts d’atténuation des émissions sont limités. Ce scénario projette une augmentation des températures globales excédant les 4 degrés Celsius d'ici 2100, illustrant un cadre de réchauffement climatique extrême. L’utilisation de ce scénario dans les études hydrologiques permet d’explorer les impacts possibles dans les pires cas d'évolution climatique, fournissant ainsi des perspectives critiques sur les défis auxquels les systèmes hydrologiques pourraient être confrontés. Bien que certains experts, comme Hausfather *et al.* (2022), considèrent ces modèles dits « chauds » comme peu réalistes, ce point de vue reste un sujet de débat au sein de la communauté scientifique.

1.3.2 Correction des biais

Les modèles climatiques, malgré leur sophistication croissante, présentent encore des écarts systématiques par rapport aux observations météorologiques historiques. Ces écarts, appelés biais, peuvent affecter la précision des projections climatiques, en particulier lorsqu'ils sont utilisés pour des analyses hydrologiques ou d'impact.

La correction des biais consiste à comparer les données climatiques simulées par les modèles aux données météorologiques historiques, et à ajuster les projections futures en fonction des écarts observés (Maraun, 2016; Piani, Haerter, & Coppola, 2010). Cette procédure repose sur l’hypothèse que les écarts entre les données simulées et observées restent relativement constants au fil du temps (Teutschbein & Seibert, 2013). Ainsi, une fois que les biais sont corrigés pour une période de référence passée, ces ajustements peuvent être appliqués aux données climatiques projetées, afin de produire des simulations plus réalistes pour les périodes futures.

Cependant, les méthodes de correction des biais peuvent perturber la cohérence physique entre les variables climatiques simulées et affecter les signaux de changement climatique à long terme (J. Chen, Arsenault, Brissette, & Zhang, 2021; Lee, Lu, Im, & Bae, 2019). Cela est particulièrement vrai lorsque les biais sont non stationnaires, c’est-à-dire qu’ils varient au fil du temps (Chen et al., 2021).

De plus, les méthodes conventionnelles de correction des biais dépendent souvent de données météorologiques de haute qualité, qui peuvent être rares dans certaines régions (Ricard et al., 2023). Pour répondre à certaines de ces limitations, des techniques plus avancées comme la méthode MBCn (Multivariate Bias Correction with N-dimensional distribution mapping) (Cannon, 2018) ont été développées. MBCn corrige simultanément les biais sur plusieurs variables climatiques tout en conservant les interactions entre elles, ce qui permet d'obtenir des ajustements plus cohérents et précis. Cette méthode se révèle particulièrement utile dans le cadre de la modélisation hydrologique, où les interactions entre variables telles que la température et les précipitations jouent un rôle crucial dans la précision des simulations. Plusieurs études ont vanté cette approche, qui permet d'améliorer la cohérence des simulations dans divers contextes climatiques (Adeyeri, Laux, Lawin, & Oyekan, 2020; Cannon, 2018; Dieng et al., 2022; Miralha et al., 2021).

1.3.3 Sources d’incertitudes

Le processus conventionnel de modélisation hydroclimatique (Fig. 1.1) repose sur l'utilisation de données météorologiques observées pour calibrer les modèles hydrologiques, puis sur l'application de méthodes de correction de biais aux données des modèles climatiques (Arsenault, Brissette, Chen, Guo, & Dallaire, 2020; J. Chen et al., 2021). Une fois que les données climatiques sont corrigées, elles sont utilisées avec le modèle hydrologique calibré pour produire des simulations des variables hydrologiques sous des conditions climatiques futures. Ce processus, bien que largement adopté, est soumis à de nombreuses incertitudes à chaque étape, ce qui peut affecter la précision des projections.

La chaîne de modélisation hydroclimatique est souvent représentée sous forme d'une cascade d'incertitudes, où chaque étape du processus contribue à l’accumulation d’incertitudes. Parmi les principales sources d'incertitude, on retrouve le choix du modèle hydrologique, les paramètres de calibration, le choix de la fonction-objectif, le choix des modèles climatiques, les scénarios d’émission, ainsi que la correction des biais (Arsenault et al., 2020; Brigode, Oudin, & Perrin, 2013; J. Chen, Brissette, & Leconte, 2011; Clark et al., 2016; Minville, Brissette, & Leconte, 2008; Poulin et al., 2011). Chacune de ces décisions méthodologiques peut introduire des variations significatives dans les projections finales.

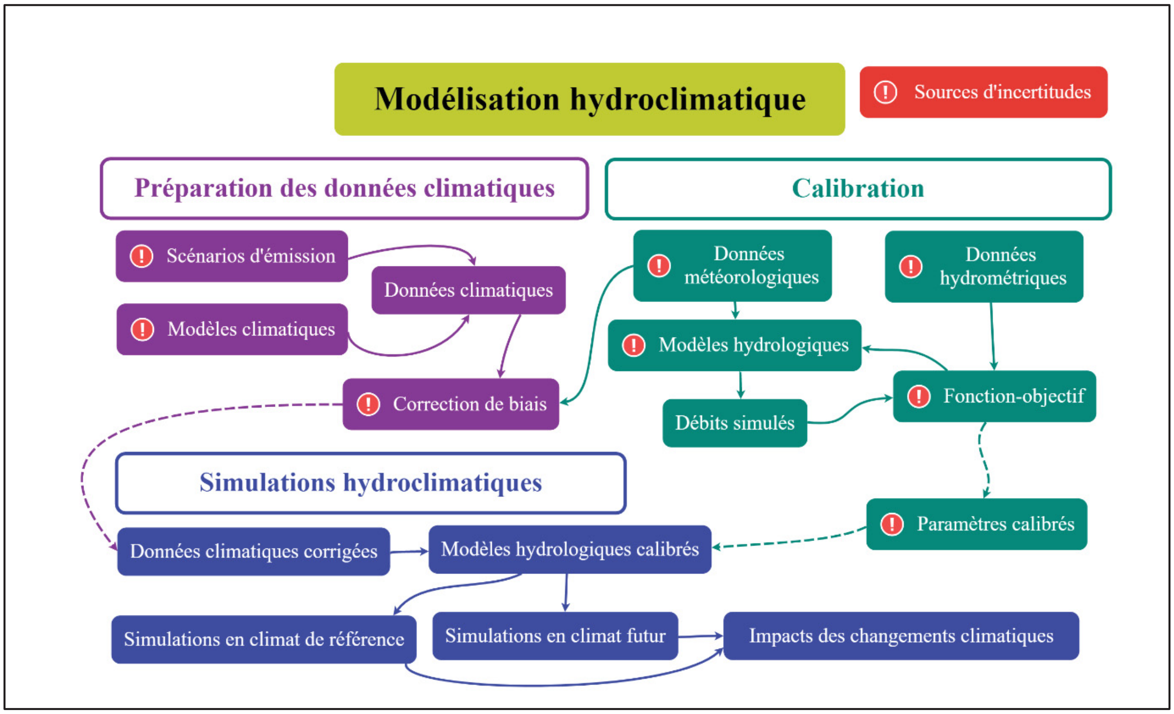

Figure 1.1 Schéma de la chaîne de modélisation hydroclimatique conventionnelle

Le choix des modèles climatiques représente l'une des plus grandes sources d'incertitude dans les projections hydrologiques futures (J. Chen et al., 2011; Minville et al., 2008; Teutschbein & Seibert, 2013). Les modèles globaux du climat diffèrent non seulement dans leur représentation des processus atmosphériques et océaniques, mais également dans la manière dont ils simulent les réponses régionales aux forçages climatiques. Cette variabilité est accentuée par le choix des scénarios socioéconomiques, comme les scénarios d'émission, qui déterminent l'évolution des émissions de gaz à effet de serre dans les futures simulations. Il est essentiel de prendre en compte cette variabilité pour obtenir des projections fiables. L'intégration de plusieurs modèles permet ainsi de mieux cerner les risques potentiels pour les ressources en eau sous des conditions climatiques futures variées.

1.3.4 Modélisation asynchrone

Les méthodes traditionnelles de modélisation hydroclimatique reposent sur la correction des biais des données climatiques avant de les intégrer dans les modèles hydrologiques. Cependant, cette approche fait l'objet de critiques (Alfieri, Feyen, Dottori, & Bianchi, 2015; J. Chen, Brissette, & Chen, 2018; Lee et al., 2019; Ricard et al., 2023). Elle perturbe la cohérence physique entre les variables climatiques, peut altérer les tendances des signaux climatiques, et exige des observations météorologiques de haute qualité, souvent indisponibles, en particulier pour des variables comme la vitesse du vent ou l'humidité relative (Ricard et al., 2020).

Contrairement aux méthodes conventionnelles qui appliquent des ajustements pour corriger les biais dans les simulations climatiques, la méthode asynchrone propose de contourner cette étape (Ricard et al., 2023, 2019, 2020). Elle repose sur l’hypothèse que les modèles hydrologiques peuvent être directement calibrés à partir des données climatiques brutes issues des MGC. En supprimant l’étape de correction des biais, cette méthode minimise les perturbations potentielles des signaux climatiques, qui peuvent affecter les relations physiques entre les variables climatiques (J. Chen et al., 2021; Lee et al., 2019).

Cette approche présente des avantages notables, surtout dans les régions où les données météorologiques sont limitées ou inexistantes puisqu’elle ne requiert aucune observation météorologique. En effet, les méthodes de correction des biais traditionnelles requiert des observations fiables, ce qui peut poser problème dans les zones éloignées ou sous-équipées.

1.4 Les changements climatiques sur les variables hydrologiques au Québec

Les régions boréales, comme le Québec, sont particulièrement vulnérables aux changements climatiques. Situées à des latitudes élevées, elles subissent des hausses de température plus rapides que la moyenne mondiale (Estrada et al., 2021), hausses qui pourraient contribuer à modifier de manière significative les processus hydrologiques et, par conséquent, la gestion des ressources en eau.

De nombreuses études ont exploré les impacts des changements climatiques sur les régimes hydrologiques au Québec. Ces travaux projettent notamment des modifications des régimes d'écoulement des cours d'eau (Aygün, Kinnard, & Campeau, 2020; Castaneda-Gonzalez, 2018; Cochand, Therrien, & Lemieux, 2019; Gombault et al., 2015; Minville et al., 2008; Nolin et al., 2023; Riboust & Brissette, 2015; Valencia Giraldo et al., 2023), des retards et des réductions dans l'accumulation et la fonte de la neige (Aygün et al., 2020; Cochand et al., 2019; Mudryk et al., 2018; Nolin et al., 2023; Novotná, van Bochove, & Thériault, 2013; Valencia Giraldo et al., 2023), ainsi que des changements dans l'humidité du sol et les variations annuels de recharge des nappes phréatiques (Cochand, 2014; Dubois et al., 2022; Houle, Bouffard, Duchesne, Logan, & Harvey, 2012; Sulis, Paniconi, Rivard, Harvey, & Chaumont, 2011). Par ailleurs, ces études suggèrent des changements dans les processus hydrologiques, tels que la répartition saisonnière des écoulements et les interactions entre la neige et l'eau souterraine (Gombault et al., 2015; Novotná et al., 2013; Valencia Giraldo et al., 2023).

Bien que ces recherches fournissent des perspectives précieuses sur les effets potentiels des changements climatiques sur les ressources en eau, elles sont également confrontées à certaines limites. Tout d'abord, beaucoup de ces études se sont basées sur les modèles climatiques de la phase 5 (CMIP5) (Taylor et al., 2012), qui ont depuis été remplacés par les modèles plus avancés de la phase 6 (CMIP6) (O'Neill et al., 2016). Martel *et al.* (2022) ont démontré que les études d'impact réalisées avec CMIP5 devraient être répétées avec CMIP6 en raison des améliorations apportées à la représentation des processus dans ces nouveaux modèles. De plus, la majorité des modèles hydrologiques utilisés dans ces études sont soit conceptuels, soit agrégés, ce qui limite leur capacité à capturer les processus locaux et les hétérogénéités à une échelle plus fine (Han et al., 2021; McDonnell, Spence, Karran, van Meerveld, & Harman, 2021).

1.5 Limitations actuelles

Les méthodologies employées dans les études existantes présentent des limitations importantes, notamment en ce qui concerne la capacité des modèles à représenter les processus hydrologiques complexes à des échelles fines. Les modèles conceptuels utilisés dans plusieurs études simplifient les processus hydrologiques et reposent souvent sur des hypothèses de stationnarité des paramètres, qui peuvent ne pas être valides dans un climat en évolution (Coron, Andréassian, Perrin, Bourqui, & Hendrickx, 2014; Duethmann, Blöschl, & Parajka, 2020). Cela réduit la capacité de ces modèles à représenter fidèlement les impacts des changements climatiques sur les régimes hydrologiques futurs.

Un autre défi majeur réside dans le problème d'équifinalité, particulièrement lorsque l'étude d'une variable hydrologique interne repose sur un modèle hydrologique calibré uniquement sur le débit. Différentes combinaisons de paramètres peuvent générer des simulations de débit similaires, mais avec des dynamiques internes très différentes (K. Beven, 2006; Bouaziz et al., 2021). Ainsi, un modèle qui reproduit fidèlement les débits observés peut néanmoins sous-estimer ou surestimer des variables internes essentielles, telles que l'humidité du sol, la recharge des nappes phréatiques ou l'évapotranspiration, compromettant la validité des résultats pour l'analyse des processus internes et réduisant la confiance envers le modèle en conditions futures (Mei et al., 2023; Yassin et al., 2017).

Pour surmonter ces limitations, l'adoption de modèles à base physique est recommandée pour améliorer la représentation et la robustesse des processus hydrologiques (Devia et al., 2015; Jones, Chiew, Boughton, & Zhang, 2006). Ces modèles permettent de capturer plus précisément les interactions complexes entre les variables hydrologiques, comme la neige, l'évapotranspiration, et les eaux souterraines. En intégrant des principes physiques directement liés aux conditions environnementales, ils offrent une meilleure capacité de généralisation face aux changements climatiques. Par ailleurs, pour réduire les problèmes liés à l'équifinalité, l'intégration de méthodes de calibration multi-variable s'avère essentielle. Le recours à des variables hydrologiques autres que le débit lors de la calibration des modèles, permet de raffiner la représentation des processus internes et d'améliorer la représentation de la dynamique spatiale et temporelle de variables clés, notamment l'humidité du sol et la recharge des nappes phréatiques.

1.6 Objectifs de recherche

L'objectif principal de ce mémoire est d'améliorer la représentation des variables hydrologiques en modélisation hydrologique tout en évaluant l'impact des changements climatiques dans 34 bassins versants du Québec. Pour atteindre cet objectif global, trois objectifs spécifiques ont été définis, chacun répondant à des lacunes identifiées dans la littérature et abordées dans les chapitres suivants :

(1) **Optimiser la calibration d'un modèle hydrologique spatialement distribué et à base physique :** La calibration des modèles hydrologiques repose souvent sur le seul ajustement des débits observés, ce qui peut entraîner un problème d'équifinalité et limiter la représentation réaliste des processus hydrologiques internes, tels que l'humidité du sol ou la recharge des nappes phréatiques (Bouaziz et al., 2021; Yassin et al., 2017). L'objectif est d'évaluer comment l'intégration d'une variable hydrologique supplémentaire et l'utilisation d'approches de calibration multi-variable influencent la représentation des processus hydrologiques. Cette analyse comparative permettra d'identifier la configuration offrant la meilleure représentation des variables hydrologiques, tout en contribuant à l'élaboration de meilleures pratiques de calibration des modèles hydrologiques (chapitre 3).

(2) **Comparer les méthodes de modélisation hydrologique conventionnelle et asynchrone :** La méthode asynchrone a été proposée comme une alternative à la modélisation hydrologique conventionnelle pour éviter la correction des biais climatiques et améliorer la représentativité des projections hydrologiques sous climat futur (Ricard et al., 2021, 2023, 2019, 2020). Cette étude compare donc les performances des deux méthodes afin d'évaluer leur précision et leur applicabilité pour la modélisation hydrologique sous différents scénarios climatiques (chapitre 4).

(3) **Évaluer les impacts des changements climatiques sur les variables hydrologiques à l'aide d'un modèle spatialement distribué:** De nombreuses études sur l'impact des changements climatiques en hydrologie s'appuient sur des modèles simplifiés, limitant la compréhension des dynamiques hydrologiques complexes en climat futur. Dans ce mémoire, les impacts des changements climatiques seront évalués en utilisant un modèle hydrologique spatialement distribué et à base physique, calibré selon une approche multi-variable. Cette configuration optimale, identifiée dans le Chapitre 3, sera couplée à la méthode de modélisation retenue dans le Chapitre 4. L'évaluation portera sur l'évolution des variables hydrologiques, incluant la variabilité des précipitations, l'accumulation et la fonte des neiges, la recharge des nappes phréatiques, ainsi que les variations d'évapotranspiration. (chapitre 5).

En répondant à ces trois objectifs, ce mémoire vise à améliorer la précision et la robustesse de la modélisation hydrologique, tout en fournissant des outils mieux adaptés à l'évaluation des impacts des changements climatiques sur les variables hydrologiques.

CHAPITRE 2

ÉLÉMENTS GÉNÉRAUX DE LA MÉTHODOLOGIE

Cette section présente les bases méthodologiques utilisées dans ce mémoire. Elle décrit la zone d'étude, le modèle hydrologique employé et les approches de modélisation hydroclimatique adoptées dans les chapitres 3, 4 et 5.

2.1 Zone d'étude

La zone d'étude comprend 34 bassins versants situés dans le sud du Québec (Fig. 2.1), sélectionnés pour leur diversité physiographique et hydrométéorologique. Ces bassins, dont la superficie varie entre 525 km² et 6 840 km², sont répertoriés dans l'Atlas hydroclimatique du Québec méridional (« Hydroclimatic Atlas of Southern Québec », 2022). Les bassins sélectionnés sont majoritairement exempts de barrages et de réservoirs, préservant ainsi l'intégrité naturelle des processus hydrologiques.

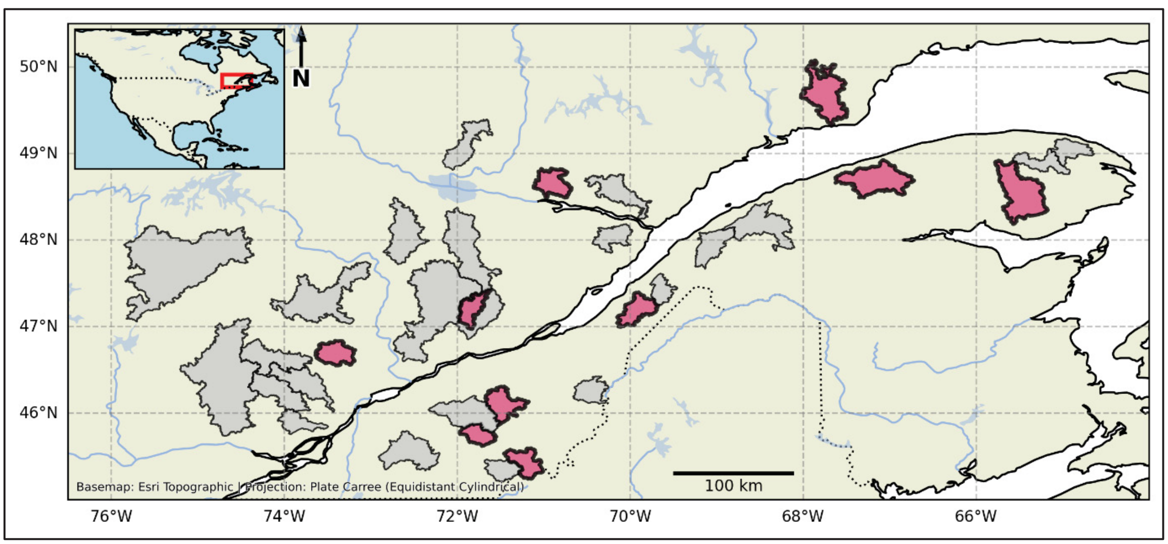

Figure 2.1. Localisation des 34 bassins versants étudiés dans le sud du Québec

Parmi ces 34 bassins versants, un sous-ensemble de 10 bassins (en rose sur la Fig. 2.1) a été sélectionné pour l'analyse de la modélisation asynchrone présentée au chapitre 4. Cette sélection permet de réduire les temps de calcul tout en maintenant une bonne représentativité climatique et hydrologique de l'ensemble de la zone d'étude. En revanche, les analyses présentées aux chapitres 3 et 5 utilisent l'ensemble des 34 bassins.

La région étudiée est principalement classifiée comme Dfb selon la classification de Köppen (climat continental humide), bien que certaines zones plus nordiques présentent un climat Dfc (climat subarctique) (Beck et al., 2018). Ce climat entraîne une forte variabilité saisonnière, influençant les processus hydrologiques des bassins versants. Les hivers sont rigoureux, avec des températures journalières moyennes descendant fréquemment sous -10 °C, et des précipitations majoritairement sous forme de neige. En été, les températures peuvent atteindre 25 °C en juillet, avec des précipitations sous forme de pluie.

Cette variabilité climatique influence directement le régime hydrologique des bassins, qui est dominé par une crue printanière liée à la fonte des neiges. En moyenne, les bassins versants reçoivent entre 933 mm et 1 395 mm de précipitations annuelles.

2.2 Modèle hydrologique utilisé

L'ensemble des analyses présentées dans les chapitres 3, 4 et 5 repose sur le même modèle hydrologique, le Water balance Simulation Model (WaSiM) (Schulla, 2021), reconnu pour sa capacité à simuler avec précision les variables hydrologiques.

WaSiM est un modèle distribué à base physique, reconnu pour sa capacité à simuler avec précision les variables hydrologiques à une fine résolution spatiale. Il peut être utilisé pour modéliser divers processus hydrologiques, tels que l'humidité du sol, la recharge des nappes phréatiques et la dynamique de la couverture neigeuse.

De nombreuses études ont démontré l'efficacité de WaSiM dans différents contextes géographiques. Par exemple, Jasper *et al.* (2006) ont analysé les modifications des schémas d'humidité des sols en été en réponse aux changements climatiques, montrant que WaSiM pouvait capturer les changements des réponses hydrologiques selon différents scénarios climatiques. De même, Natkhin *et al.* (2012) ont utilisé WaSiM pour évaluer les impacts combinés du changement climatique et de la croissance forestière sur la recharge des nappes phréatiques dans le nord-est de l'Allemagne. Rößler et Löffler (2010) et Rössler *et al.* (2012) ont étudié les dynamiques de l'humidité des sols dans des bassins versants de haute montagne, soulignant à la fois les avantages et les limites de WaSiM dans ces environnements extrêmes. De plus, Bormann et Elfert (2010) ont exploré l’influence des changements d’utilisation du territoire sur la génération des écoulements, tandis que Förster *et al.* (2017, 2018) ont comparé les résultats internes du modèle à des mesures réelles en milieu forestier. Ils ont notamment analysé les interactions complexes telles que l'interception par le couvert végétal et la dynamique de la fonte des neiges, démontrant ainsi la robustesse de WaSiM pour modéliser ces processus.

Bien que WaSiM ait principalement été employé en Europe, quelques études ont exploré son application au Québec. Par exemple, Valencia Giraldo *et al.* (2023) ont évalué les impacts des changements climatiques sur le bilan hydrique annuel, observant des réductions significatives de la neige et des variations marquées des débits d'étiage. Ricard *et al.* (2019, 2020) ont, quant à eux, proposé une approche innovante en utilisant des fonctions objectives asynchrones pour étudier la distribution des débits sous l'effet des changements climatiques dans des bassins versants québécois.

L’utilisation de WaSiM dans ce mémoire permet d’évaluer les impacts des changements climatiques sur 34 bassins versants du sud du Québec, en prenant en compte les dynamiques hydroclimatiques complexes de la région.

2.3 Modélisation hydroclimatique

Les chapitres 4 et 5 intègrent une modélisation hydroclimatique afin d’évaluer les effets des changements climatiques sur les variables hydrologiques des bassins étudiés.

Les modèles climatiques sélectionnés reposent sur le scénario d'émissions SSP5-8.5, représentant un futur caractérisé par une forte croissance économique et une utilisation intensive des énergies fossiles. Ce scénario permet de simuler des conditions climatiques extrêmes et plausibles pour la région, afin de mieux cerner les risques potentiels associés à un réchauffement accéléré et d'orienter les stratégies d’adaptation nécessaires pour faire face à ces impacts.

Pour réduire les incertitudes associées aux projections climatiques, 18 modèles du CMIP6 ont été sélectionnés. Ce choix vise à capter l'étendue des incertitudes liées aux modèles climatiques, qui demeurent la source d'incertitude la plus importante dans la chaîne de modélisation hydroclimatique (J. Chen et al., 2011; Minville et al., 2008; Teutschbein & Seibert, 2013). L'intégration de plusieurs modèles permet ainsi de mieux cerner les risques potentiels pour les ressources en eau sous des conditions climatiques futures variées.

Les biais systématiques des modèles climatiques sont corrigés à l’aide de la méthode MBCn (Cannon, 2018), qui ajuste simultanément plusieurs variables climatiques tout en préservant leurs interdépendances physiques. Cette correction améliore la cohérence des projections et renforce la fiabilité des simulations hydrologiques.

En résumé, ce mémoire s’appuie sur une modélisation hydrologique distribuée et à base physique, intégrant une calibration multi-variable, des méthodes avancées de correction des biais et les scénarios climatiques les plus récents. Cette approche permet d’améliorer la précision des simulations hydrologiques et de mieux quantifier les impacts des changements climatiques sur les bassins versants du Québec. Les résultats obtenus fournissent ainsi une base scientifique pour orienter les stratégies d’adaptation et optimiser la gestion des ressources en eau face aux défis climatiques à venir.

CHAPITRE 3

ARTICLE 1: ENHANCING PHYSICALLY BASED AND DISTRIBUTED HYDROLOGICAL MODEL CALIBRATION THROUGH INTERNAL STATE VARIABLE CONSTRAINTS

Frédéric Talbot[1], Jean-Daniel Sylvain[2], Guillaume Drolet[2], Annie Poulin[1] et Richard Arsenault[1]

[1] Département du Génie de la Construction, École de technologie supérieure, Université du Québec, Montréal, H3C 1K3, Canada.
[2] Direction de la recherche forestière, Ministère des Ressources naturelles et des Forêts, Québec, G1P 3W8, Canada.

Article soumis à la revue « Hydrology and Earth System Sciences », octobre 2024

Abstract

This study investigates the effectiveness of various calibration approaches within the Water Balance Simulation Model (WaSiM) to enhance the representation of hydrological variables. We assess the impact of three distinct configurations: Baseline (BL), Physical Groundwater Model (GW), and Physical Groundwater with Recharge Calibration (GW-RC) on the representation of hydrological variables. The analysis demonstrates that while traditional calibration primarily enhances streamflow prediction, integrating recharge and groundwater dynamics significantly refines the model's ability to depict subsurface processes. The GW-RC configuration, with minimal emphasis on recharge in the objective function, shows a marked improvement in representing both the spatial and seasonal variability of groundwater recharge, suggesting that even small and targeted calibration adjustments can significantly enhance the accuracy and realism of model outputs. Although this approach may reduce the model's flexibility in mirroring observed streamflow, it enhances the precision with which other hydrological processes are represented, providing a more accurate reflection of watershed dynamics. Our findings underscore the importance of multi-variable calibration frameworks, which incorporate both streamflow and internal hydrological variables, in developing robust models capable of adapting to anticipated hydrological shifts due to

climate change. This approach provides a more accurate reflection of watershed dynamics and offers valuable insights for calibration strategies in hydrological modelling, water resource management and climate adaptation strategies.

3.1 Introduction

Accurately representing watershed processes under climate change remains a central challenge in the evolving field of hydrology (Persaud et al., 2020). Recent advances in hydrological modeling have offered valuable insights into water resource management and climate adaptation strategies (Chen et al., 2011; Wang, Deng, & Jian, 2023; Xu, Widén, & Halldin, 2005). However, the complexity of watershed dynamics, especially in snow dominated catchments, necessitates models that can accurately simulate both surface and subsurface hydrological processes (Farjad, Gupta, & Marceau, 2016; T. W. Chu & A. Shirmohammadi, 2004).

The need for detailed, physically based hydrological modeling goes beyond immediate concerns of water management and climate impact assessments. Groundwater dynamics play a critical role in forest health (Iacob, Brown, & Rowan, 2017; Maitre, Scott, & Colvin, 1999), as stable water availability, shaped by hydrological processes, underpins forest ecosystem resilience (Cunningham, Thomson, Mac Nally, Read, & Baker, 2011; Orellana, Verma, Loheide, & Daly, 2012). By enhancing the accuracy of groundwater simulation and recharge calibration, we can improve our ability to forecast forest growth and resilience under changing climatic conditions (Ford, Laseter, Swank, & Vose, 2011; Grant, Tague, & Allen, 2013). This linkage underscores the importance of detailed hydrological modeling and aligns with broader environmental, economic, and ecological management goals aimed at sustaining forest productivity in the face of environmental change. Such integrative approaches are vital as they provide the groundwork for informed decision-making in forest management, ensuring that forests continue to thrive (Sun et al., 2023; Vose et al., 2011).

The Water balance Simulation Model (WaSiM) (Schulla, 2021) is a distributed and physically based hydrological model that stands out for its complexity, fine spatial resolution and comprehensive approach to modeling key hydrological processes. This capability is particularly advantageous for yielding reliable results in intermediate variables analysis within hydrological studies. Several studies exemplify the application of WaSiM for examining internal hydrological variables across diverse geographic settings and scenarios. For example, Jasper, Calanca, & Fuhrer (2006) analyzed summer soil water pattern shifts due to climatic changes, demonstrating that WaSiM could effectively model the substantial alterations in hydrological responses to varying climate scenarios. Natkhin et al. (2012) used WaSiM to differentiate the impacts of climate change and forest growth dynamics on groundwater recharge in Northeast Germany. Similarly, two separate studies (Rössler, Diekkrüger, & Löffler, 2012; Rößler & Löffler, 2010) analyzed soil moisture dynamics using WaSiM, discussing the modeling potentials and limitations in high mountain catchments and the broader impact of climate on soil moisture. Bormann & Elfert (2010) investigated how land use changes influence various runoff generation processes such as surface runoff, interflow, and baseflow. Furthermore, Förster et al. (2017, 2018) conducted detailed comparisons of internal state variables with actual forest measurements, including meteorological variables and snow cover dynamics, highlighting the refined capabilities of WaSiM to model complex interactions like snow cover and canopy interception. These studies collectively demonstrate the model's utility in capturing a wide range of hydrological variables.

Recent advances in hydrological modeling have revealed critical challenges in accurately representing watershed dynamics, particularly when calibrating hydrological models based solely on streamflow data (de Lima Ferreira & da Paz, 2024; Mei et al., 2023; Pool, Fowler, & Peel, 2024; Schäfer, Fäth, Kneisel, Baumhauer, & Ullmann, 2023). While streamflow is a key indicator for capturing temporal fluctuations in water systems, it offers limited insights into the internal hydrological processes (Rajib, Evenson, Golden, & Lane, 2018). This reliance on streamflow can result in models that perform well in reproducing observed flows but misrepresent underlying processes—a phenomenon known as equifinality, where different parameter sets produce the same outputs but for the wrong reasons (Acero Triana, Chu, Guzman, Moriasi, & Steiner, 2019; Kirchner, 2006; Mei et al., 2023; Yassin et al., 2017). Therefore, focusing only on streamflow in model calibration can hide important differences in how hydrological processes are represented.

In pursuit of better representing hydrological processes at the catchment scale, several studies have explored hydrologic scaling and parameter transferability (Imhoff, van Verseveld, van Osnabrugge, & Weerts, 2020; Mizukami et al., 2017; Samaniego et al., 2017; Samaniego, Kumar, & Attinger, 2010). Notably, Samaniego et al. (2010) introduced the multiscale parameter regionalization to tackle overparameterization and the non-transferability of parameters across different scales. Ficchì, Perrin, & Andréassian (2019) also proposed a model structure that considers flow accuracy and fluxes match on different modelling timesteps, adjusting the structure and parameters to ensure robust simulation across various time scales. Additionally, Peters-Lidard et al. (2017) advocated for adopting the fourth paradigm of data-intensive science in hydrology, which leverages emerging datasets to refine our understanding of hydrological models and processes. This paradigm posits that advancements in computational science—considered a new methodological branch alongside empiricism, theory, and computational simulation—can revolutionize science through the intensive use of data, facilitating the discovery and testing of theories and models. This approach emphasizes the integration of comprehensive datasets and computational tools into conventional scientific workflows, thereby enhancing the capacity for scientific innovation and synthesis in hydrology.

Recent studies have advocated for a shift towards integrating additional hydrological variables and data sources, such as remote sensing products and in-situ measurements, into the calibration process (Dembélé *et al.*, 2020; Meyer Oliveira *et al.*, 2021; Liu *et al.*, 2022; Mei *et al.*, 2023; Schäfer *et al.*, 2023; de Lima Ferreira and da Paz, 2024; Pool *et al.*, 2024). Mei *et al.* (2023) found that including gridded soil moisture alongside gauged streamflow improved evapotranspiration simulations across 20 catchments in the Lake Michigan watershed. Schäfer *et al.* (2023) used WaSiM to simulate the water balance of a forested catchment in Germany, showing that including plant-available water and evapotranspiration data significantly enhanced model accuracy. De Lima Ferreira and da Paz (2024) similarly improved model performance by incorporating actual evapotranspiration estimates into a hydrological model of a Brazilian semi-arid basin, highlighting the benefits of multi-variable calibration and the need to test distinct data sources.

Although many studies have successfully used variables such as soil moisture, evapotranspiration, and groundwater head in model calibration, there remains a gap in understanding how other variables, like groundwater recharge, can improve the representation of hydrological processes. Addressing this gap is important for both the theoretical advancement of hydrological sciences and the practical applications of water resource management, flood risk assessment, and climate change mitigation (Pradhan & Indu, 2019). By adopting a calibration approach that integrates a more holistic view of watershed processes, models become more reflective of complex hydrological interactions and gain robustness in the face of non-stationary climate conditions (Wang et al., 2023). This enhanced process representation and strengthens confidence in model projections, making them more reliable for future applications.

In this study, we implement three distinct model configurations of the WaSiM hydrological model, configuration BL (baseline model), configuration GW (physical groundwater model), and configuration GW-RC (physical groundwater and recharge calibration model)—to investigate how integrating additional hydrological variables and different calibration approaches influence the representation of hydrological processes over a set of 34 catchments in Nordic conditions. Through comparative analysis of these configurations, we aim to expose the nuances in model performance and hydrological variable representation, contributing to the ongoing debate on the best practices for hydrological model calibration.

3.2 Methods

3.2.1 Study area

This study examines 34 catchments in Southern Quebec, Canada, each with distinct physiographic and hydrometeorological features. The catchments range in size from 525 to

6,840 km² (see Fig. 3.1). These specific catchments were selected for their inclusion in the Hydroclimatic Atlas of Southern Québec (MDDELCC, 2022) due to the availability of comprehensive streamflow data and their representation of the diverse hydrological conditions prevalent throughout Southern Quebec. Selected catchments are unaffected by the presence of dams and reservoirs, preserving the natural integrity of hydrological processes.

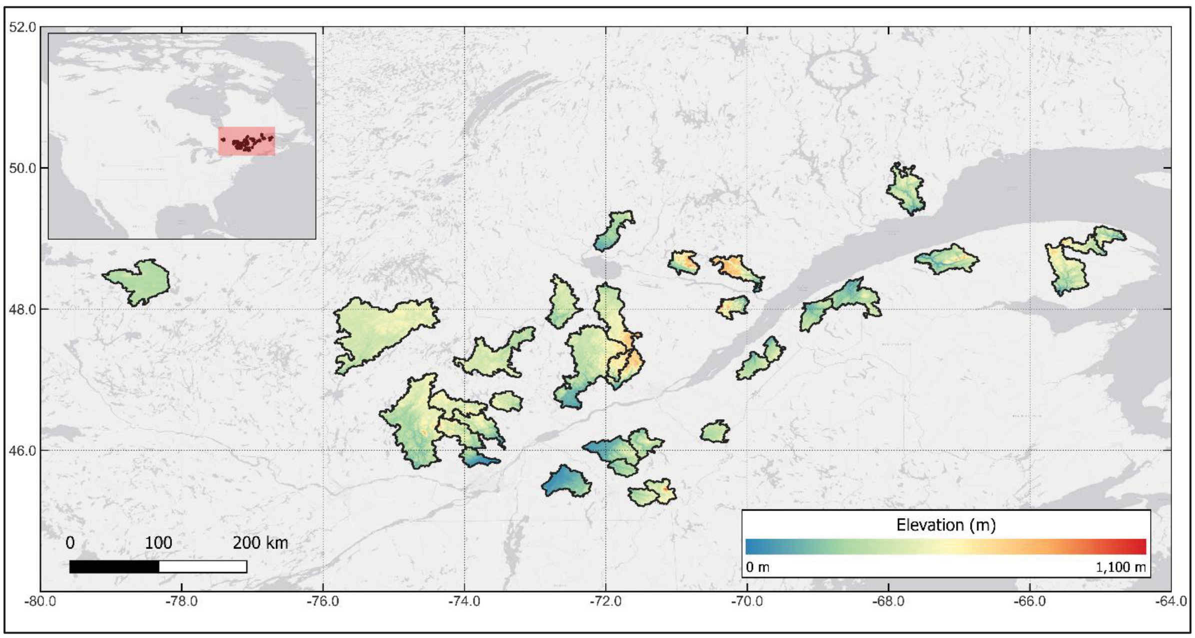

Figure 3.1 Elevation map of study catchments in southern Quebec

The Köppen-Geiger Climate Classification designates most of the study area (28 catchments) as belonging to class Dfb (humid continental mild summer, wet all year), except a small part (six catchments) located in the northern portion that belongs to class Dfc (subarctic with cool summers and year-round precipitation) (Beck et al., 2018). The region experiences four distinct seasons. Winters are characterized by frequent sub-freezing temperature and significant snowfall. As spring arrives, temperatures gradually rise, leading to significant snowmelt which, along with increasing rainfall, influences streamflow and water availability. Summer brings warmer temperatures, peaking in July, with rainfall remaining relatively high. Fall sees a gradual cooling and a transition from rain to increasing snowfall, setting the stage for another winter cycle. This climatic diversity induces complex hydrological processes at catchment scale, as the interplay between snowmelt and precipitation patterns has a significant influence on streamflow and water availability. These dynamics are not unique to Québec but are indicative of broader hydrological upheavals occurring across boreal regions globally under climate change.

To contextualize the environmental and hydrological setting of the selected catchments, Table 3.1 presents a synthesis of key descriptors. The table shows the minimum and maximum values for a set of hydrological and geophysical characteristics for each catchment, providing an at-a-glance perspective of the environmental variation within the study area.

Table 3.1 Hydrological and geophysical characteristics of the study catchments

Catchment characteristics	**Minimum**	**Maximum**
Area (km^2)	525	6840
Mean elevation (m)	137	568
Predominant soil type	Sandy loam	
Predominant land use	Coniferous forest and deciduous forest	
Annual total precipitation (mm)	785	1547
Annual extreme daily temperature (°C)	-37.7	28.6
Annual streamflow ($m^3 s^{-1}$)	10	130

3.2.2 Data

3.2.2.1 Hydrometeorological data

This study utilizes meteorological data, specifically total precipitation and mean temperature on a daily time step, sourced from ECMWF's Reanalysis v5 (ERA5) (Hersbach et al., 2020). These datasets effectively overcome the limitations of observational data and have demonstrated performance on par with observational records in this region (Tarek, Brissette, & Arsenault, 2020). The collected meteorological data spans the period from 1981 to 2020.

Observed streamflow data from 1981 to 2010 was used, recorded at a daily resolution. This data was obtained from the Hydroclimatic Atlas of Southern Québec (MDDELCC, 2022). The dataset contains occasional gaps, primarily during winter months when ice cover and ice jams can significantly distort river flow measurements. To ensure the accuracy of the study, these periods were excluded from the dataset.

3.2.2.2 Elevation data

A hydrologically conditioned digital surface model was derived from the NASA Shuttle Radar Topography Mission version 3.0 Global 1 (SRTMGL1) to account for terrain elevation. The SRTMGL1, originally boasting a spatial resolution of 30 meters at the equator, underwent resampling to 50 meters resolution and filtering using multiple moving average windows to mitigate the impact of local noise, which could lead to erroneous hydrological behaviours (MacMillan, Pettapiece, Nolan, & Goddard, 2000). To ensure hydrological consistency, we applied hydrological corrections based on data from provincial agencies (« Géobase du réseau hydrographique du Québec (GRHQ)—Données Québec », 2016). The elevation values along established hydrological networks were adjusted downward by 5 meters burning the stream network into the digital surface model (DSM) with the SAGA GIS software (Conrad et al., 2015). The resulting DSM accurately captures the hydrological characteristics of the study area and is used for catchment delineation. Additionally, the DSM was resampled to spatial resolutions of 250 and 1000 meters. This resampling process was conducted to optimize computational efficiency while preserving the essential characteristics of the catchments. The minimum value resampling method was used to preserve hydrological connectivity within the study area.

Following this, the Tanalys software (Schulla, 2021) was used to generate key topographic layers, including slope, aspect, and river depth, all formatted for hydrological modeling within WaSiM.

3.2.2.3 Soil type data

To capture the spatial variability of soil hydraulic properties, we utilized the SIIGSOL 100 meters database (Sylvain, Anctil, & Thiffault, 2021), which provides information on soil composition. The SIIGSOL database provides detailed descriptions of the proportions of sand, clay, and silt within the soil profile (Ministère des Ressources Naturelles et des Forêts, 2022). In this study, we converted the reported proportions of sand, silt, and clay layers into soil texture classes based on the classification system of the United States Department of Agriculture (USDA). The USDA soil classification system categorizes soils into various texture classes such as loam, clay, sand, silt, and combinations thereof, which are determined based on the percentage composition of each type. This classification aids in understanding the soil's physical characteristics which are crucial factors in hydrological modeling and in predicting soil-water interactions in the studied catchments (Weil & Brady, 2017).

We derived soil hydraulic properties from generated soil type maps, using established relationships between soil texture classes and hydraulic parameters. For the soil type maps, WaSiM generates soil layers of specified thickness based on the control file settings. By default, if there is only one soil type present in the catchment, the soil depth is uniformly distributed throughout the entire area. To account for soil depth variability, we divided soil types into three distinct sections based on their relative elevation within catchment: narrow, normal, and deep. Pixels with elevations below the 33rd percentile were classified as deep, while those with elevations above the 66th percentile were classified as shallow. The remaining soil type rasters fell into the normal category. This classification was based on the imperfect but useful hypothesis that higher elevations correspond to a closer proximity of bedrock to the surface, while lower elevations indicate a greater depth of soil cover in a post-glacial landscape (Akumu et al., 2016; Jeong, Hong, & Song, 2022).

3.2.2.4 Land use data

For land use attribution, we used the 2015 North American Land Change Monitoring System (NALCMS) 30 meters land cover dataset (Commission for Environmental Cooperation, 2020; Latifovic et al., 2012). The classification scheme used in this map adheres to the widely recognized Land Cover Classification System (LCCS) standard established by the Food and Agriculture Organization (FAO) of the United Nations. This standardized approach ensures the consistency and comparability of land cover information, enabling meaningful regional scale assessments and studies. The nearest neighbor resampling method was employed to align land use maps with the other raster maps used in WaSiM. Land use exerts a substantial influence on various hydrological parameters, and more specifically for the context of this study, it significantly affects parameters such as root distribution, vegetation cover fraction (VCF), roughness length (Z0), and albedo within the hydrological model. The distribution and characteristics of land cover types, ranging from forests to urban areas, directly impact these parameters, thereby influencing processes such as evapotranspiration, runoff, and infiltration.

3.2.2.5 Groundwater recharge data

In 2008, the Government of Quebec initiated the “Projets d’acquisition de connaissances sur les eaux souterraines” (PACES; roughly translated as “groundwater knowledge acquisition projects”) (Buffin-Bélanger et al., 2015; Carrier et al., 2013; Cloutier et al., 2013, 2015; Comeau et al., 2013; M. Larocque et al., 2015; Marie Larocque, Gagné, Tremblay, & Meyzonnat, 2013; Lefebvre et al., 2015; Rouleau et al., 2013), aimed at enhancing understanding of the groundwater resources availability in Southern Quebec area. In addition to PACES, numerous studies conducted across the region have estimated groundwater recharge rates, which vary from 50 mm yr^{-1} to over 500 mm yr^{-1} depending on the location and years studied (Croteau *et* al., 2010; Chemingui *et* al., 2015; Larocque *et* al., 2019; Dubois *et* al., 2021; Boumaiza *et* al., 2022).

Of the 34 catchments in this study, fourteen were entirely or partially covered by the PACES project. Table 3.2 lists these catchments, detailing their areas, associated PACES region reports, the percentage of each catchment's area covered by PACES, and the mean and standard deviation of groundwater recharge for the areas covered.

Table 3.2 PACES data coverage and recharge statistics for covered catchments

Catchment name	**Area (km^2)**	**Region**	**Cover**[1]	**PACES recharge**	
				Mean (mm yr^{-1})	**Std. (mm yr^{-1})**
Matane	1650	Bas-Saint-Laurent	31%	179	78
Rimouski	1610	Bas-Saint-Laurent	29%	213	81
Des Trois-Pistoles	932	Bas-Saint-Laurent	38%	74	34
Ouelle	795	Chaudière-Appalaches	62%	180	35
Famine	691	Chaudière-Appalaches	100%	186	46
Bécancour	919	Chaudière-Appalaches and Bécancour	100%	209	83
Nicolet Sud-Ouest	549	Nicolet-Saint-François	100%	242	64
Nicolet	1540	Nicolet-Saint-François	95%	224	82
Noire	1490	Montérégie-Est	93%	133	98
Rouge	5460	Outaouais	26%	310	40
Kinojévis	2590	Abitibi-Témiscamingue	55%	172	87
Petit Saguenay	712	Saguenay-Lac-Saint-Jean	80%	69	78
Petite rivière Péribonca	1090	Saguenay-Lac-Saint-Jean	29%	142	103
Valin	746	Saguenay-Lac-Saint-Jean	73%	221	85
[1] Fraction of total catchment area covered by PACES data.			Median	183	80

3.2.3 Hydrological modelling

3.2.3.1 WaSiM model

In this study, we employed WaSiM for hydrological modeling (Schulla, 2021). Hydrological processes were analyzed through three specific configurations: BL (baseline), which serves as the standard comparison model; GW (physical groundwater model), which incorporates detailed groundwater dynamics; and GW-RC (physical groundwater model with constrained recharge), which further refines the groundwater variables by incorporating constrained recharge calibrations. Detailed descriptions of these configurations can be found in Sect. 3.2.4 of this study.

WaSiM consists of two versions: WaSiM version I, originally developed using the Topmodel approach for simulating subsurface flows based on variable saturation areas, and WaSiM version II, an extended version with the process-oriented Richards approach. The Richards version, which considers hydraulic head gradients and detailed soil physical properties (pF-curve, k(u) function), was selected for this study due to its more physically based nature.

WaSiM follows a modular structure, composed of multiple sub-models that can be activated based on data availability and the specific research objectives. The model operates using a consistent time step, while internally employing flexible sub-time steps to optimize computational efficiency. It accommodates both regular and irregular raster grids, enabling the analysis of diverse spatial configurations. During each time step, the sub-models are sequentially processed across the entire model grid, enabling parallelization to aid computational optimization and facilitate faster model execution.

One of the key process modules within WaSiM is the unsaturated zone model, which plays a crucial role in calculating various hydrological variables such as surface runoff, groundwater recharge, interflow, and baseflow. Interflow refers to water moving laterally through the upper soil layers, contributing to streamflow, while baseflow is the portion of streamflow sustained by groundwater flow. These variables are essential for understanding the water balance and hydrological dynamics within the study area. Table 3.3 provides an overview of the hydrological model configuration used in this study.

Table 3.3 Overview of WaSiM characteristics and sub-models used

Sub-model	**Method**	**Reference**
Meteorological interpolation	Inverse distance interpolation	(Shepard, 1968)
Potential evapotranspiration	Hamon approach	(Hamon, 1963)
Actual evapotranspiration	Richards equation using the Van Genuchten parameters	(Richards, 1931; van Genuchten, 1980)
Snow melt	Temperature-index approach	(Hock, 2003)
Interception	Classic bucket approach dependent on LAI	-
Lake modelling	Integrated approach to model natural and artificial lakes, considering interactions with unsaturated zone, routing, snow, evaporation, interception, and groundwater models.	-
Unsaturated zone flow	Richards equation using the Van Genuchten parameters	(Richards, 1931; van Genuchten, 1980)
Groundwater flow	Integrated two-dimensional groundwater model	-
Routing	Kinematic wave approach	(Lighthill & Whitham, 1955)

Meteorological data interpolation was an essential step in the hydrological modeling process. The chosen hydrological model, WaSiM, performed the interpolation of daily precipitation and temperature inputs between ERA5 points. For each simulation, the model creates grids that incorporate the interpolated meteorological values at the model's spatial resolution, effectively representing the climatic conditions for each individual pixel. The inverse distance weighting method was used as recommended by WaSiM model description report (Schulla, 2021).

3.2.3.2 Calibration parameters

Calibration of WaSiM involved the optimization of 17 parameters, selected in accordance with WaSiM documentation (Schulla, 2021), while the remaining parameters in the control file were set to their default values. Table 3.4 provides a detailed description of upper and lower limits set for calibrating the 17 parameters in WaSiM, with each parameter adjusted to two decimal places within the specified calibration range.

Table 3.4 Description of the parameters used for the calibration of WaSiM

No.	Code	Description	Unit	Sub-Model	Range
1	k_D	Storage coefficient for surface runoff	h	Unsaturated zone	[1, 25]
2	k_H	Storage coefficient for interflow	h	Unsaturated zone	[1, 25]
3	d_r	Drainage density for interflow	m^{-1}	Unsaturated zone	[1, 50]
4	QD_{Snow}	Fraction of surface runoff of snow melt	-	Unsaturated zone	[0.1, 1]
5	c_0	Degree-Day factor	$mm°C^{-1}d^{-1}$	Snow	[0, 3]
6	T_0	Temperature limit for snow melt	°C	Snow	[-4, 4]
7	$T_{R/S}$	Transition temperature snow/rain	°C	Snow	[-4, 4]
8	C_{WH}	Water storage capacity of snow	-	Snow	[0.1, 0.3]
9	C_{rfr}	Coefficient for refreezing	-	Snow	[0.1, 1]
10	$f_{i,summer}$	ETP summer correction factors	-	ETP	[0.1, 2]
11	$f_{i,fall}$	ETP fall correction factors	-	ETP	[0.1, 2]
12	$f_{i,winter}$	ETP winter correction factors	-	ETP	[0.1, 2]
13	$f_{i,spring}$	ETP spring correction factors	-	ETP	[0.1, 2]
14	K_{rec}	Recession constant for hydraulic conductivity	-	Soil table	[0.1, 0.99]
15	d_z[a]	Soil layer thickness	-	Soil table	[0.8, 1.4]
16_A	K_B	Storage coefficient for base flow	m	Unsaturated zone	[0.1, 8]
17_A	Q_0	Scaling factor for base flow	$mm\ h^{-1}$	Unsaturated zone	[0.1, 5]
16_B	Kol[b]	Colmation of the river links	-	Input grid	[1, 100]
17_B	K_{XY}[c]	Saturated horizontal conductivity	$m\ s^{-1}$	Input grid	[0.2, 4]

[a] Calibration coefficient, ranging from 0.8 to 1.4, is applied to adjust the total soil depth, which is predetermined to be 8 meters for shallow, 14 meters for normal, and 20 meters for deep soil conditions.

[b] Calibration coefficient, ranging from 0.8 to 1.4, is applied to adjust the colmation grid, which is predetermined to be $1x10^{-6}$.

[c] Calibration coefficient, ranging from 0.2 to 4, is applied to adjust the saturated conductivity grid, which is predetermined at $4x10^{-5} m\ s^{-1}$.

Parameters 16_A (K_B) and 17_A (Q_0) are calibrated in the configuration BL when groundwater model is not activated and instead uses a conceptual approach to compute groundwater flow within the unsaturated zone sub-model. Groundwater flow is assessed using Eq. (3.1) (Schulla, 2021), which calculates baseflow as a function of several parameters including the scaling factor for baseflow (Q_0) and the recession constant for baseflow (K_B).

$$Q_B = Q_0 * K_s * e^{(h_{GW} - h_{geo,0})/K_B}, \tag{3.1}$$

where Q_B is baseflow (m s^{-1}), Q_0 is a scaling factor for baseflow, K_s is the saturated hydraulic conductivity (m s^{-1}), h_{GW} is the groundwater table height (m), $h_{geo,0}$ is the geodetic altitude of the soil surface (m) and K_B is the recession constant for baseflow (m).

In the configurations used in GW and GW-RC, which activate groundwater model, parameters 16_A and 17_A are replaced by parameters 16_B and 17_B to obtain a more physically based representation of groundwater processes. Parameters 16_B and 17_B adjust values associated to two input grids that allow to account for the colmation of the river links and saturated horizontal conductivity. This distinction ensures a consistent number of calibrated parameters across all configurations, facilitating an unbiased comparison of model performance.

3.2.3.3 Model optimization

Parameters optimization was performed independently for each catchment through the dynamically dimensioned search algorithm (DDS; (Tolson & Shoemaker, 2007)), following the recommendation of Arsenault et al. (2014). This algorithm is specifically designed for efficiently calibrating complex hydrological models with a large parameter range given a finite computing budget. During optimization, it dynamically adapts its search strategy based on the number of evaluations performed and performance metrics. To manage computational demands effectively while ensuring thorough exploration of the parameter space, a two-phase calibration strategy was employed, albeit the approaches differ for the constrained groundwater configurations.

Initially, 1000 simulations were performed for each catchment at a broader spatial resolution (1000 meters) using a broader range of values for each parameter (Table 3.4). This phase aimed to identify an approximation of the optimal values for each parameter. Subsequently, these values were used to initialize the second calibration step at a finer spatial resolution (250 meters). This sequential calibration strategy allows to refine the model's performance progressively. By first identifying a set of parameters that achieves reasonable model performance at a coarser scale, we then fine-tune the model at a higher resolution to enhance the spatial distribution of hydrological simulations.

The objective functions used vary by configuration: For BL and GW, the objective is to optimize the Kling-Gupta Efficiency (KGE, (Kling, Fuchs, & Paulin, 2012)), as discussed in Sect. 3.2.5.1. Conversely, the GW-RC configuration employs a modified objective function that seeks to optimize KGE and constrain groundwater recharge rates and variability. This approach is described in Sect. 3.2.4.3 and Sect. 3.2.5.2.

The study employed split-sample test (SST) framework for the parameter optimization assessment. This widely used approach involves dividing the available data into two sets: one for calibrating the model and the other for validating its performance on unseen time periods. The calibration period (2000-2009) and the validation period (1990-1999) were chosen based on the availability of comprehensive and reliable hydrological data. A five year spin-up period was performed before each simulation to allow the model to reach a stable state, eliminating the influence of unstable initial conditions on the model's performance metrics. However, data gaps were noted for three catchments: Croche, Petit Saguenay, and Sainte-Marguerite Nord-Est. Specifically, Croche lacked data from 2001 to 2004, Petit Saguenay from 2000 to 2010, and Sainte-Marguerite Nord-Est from 1998 to 2010. To accommodate these gaps, adjustments were made to the calibration and validation periods for the affected catchments. The calibration periods were shortened to later years: 1995 to 1999 for Croche and Petit Saguenay, and 1992 to 1996 for Sainte-Marguerite Nord-Est. Correspondingly, the validation periods were adjusted to precede the missing data: 1991 to 1994 for Croche, 1986 to 1994 for Petit Saguenay, and 1986 to 1991 for Sainte-Marguerite Nord-Est.

3.2.4 Model configurations

The primary objective of this research is to examine how different model configurations influence the representation of hydrological processes. To ensure a consistent comparison of model configuration and calibration, we designed a modelling framework that allow to compare three configurations that incrementally incorporate more complex hydrological variables.

3.2.4.1 Baseline

The first configuration (BL), serving as baseline configuration, employs the standard calibration of the model without activating the groundwater module. This configuration is aligned with the traditional application of WaSiM, where the focus is predominantly on streamflow, and groundwater flow is modeled using Eq. (3.1) within the unsaturated zone sub-model. This configuration is comparable to what has been frequently adopted in numerous studies, providing a common basis for comparative analysis (Förster et al., 2018; Markhali, Poulin, & Boucher, 2022; Rössler et al., 2012; Valencia Giraldo, Ricard, & Anctil, 2023).

3.2.4.2 Physical groundwater module

The second configuration, GW (physical groundwater), marks a departure from the BL configuration by activating WaSiM's groundwater module. This adjustment allows for groundwater flow to be simulated within a designated sub-model, transitioning from a conceptual to a more physically based representation. This configuration, used in numerous studies (Bormann & Elfert, 2010; Gädeke, Hölzel, Koch, Pohle, & Grünewald, 2014; Natkhin et al., 2012; Schäfer et al., 2023), is recommended by the WaSiM documentation for catchments where groundwater dynamics play a pivotal role in the hydrological cycle, particularly in lowland areas with extensive sediment layers.

3.2.4.3 Physical groundwater module and constrained recharge

For configuration GW-RC (physical groundwater and constrained recharge), we incorporate groundwater recharge into the calibration process to achieve a better representation of hydrological variables such as baseflow, interflow, and runoff. By introducing recharge into the calibration, we restrict hyperplane exploration and ensure that the model's representation of the hydrological cycle is more accurately simulating groundwater recharge dynamics. This is particularly useful if model hydrological variables are an important input to another analysis or process, such as for better understanding groundwater movement and evolution under climate change for certain types of vegetation, for example.

The calibration for configuration GW-RC was conducted in two distinct phases. The initial phase involved defining new parameter ranges for parameters that impact baseflow (dr, QDSnow, Krec, Kol, Kxy). We therefore first conducted 200 evaluations at a spatial resolution of 1000 meters, followed by 50 evaluations at 250 meters using the objective function presented in Eq. (3.6). Essentially, the aim here is to constrain the parameter set to a single value that performs well overall and provides realistic internal variables. Similar approaches have been used in studies such as Duethmann et al. (2024), which underscores the benefits of integrating Landsat-derived land surface temperature (Ts) data into model calibration. Landsat, a series of Earth-observing satellites, provides crucial Ts data used in this study. By including satellite-derived Ts, the study demonstrated improvements in the model's ability to capture spatial anomalies and ecosystem stress responses, while maintaining streamflow accuracy, illustrating the advantages of multi-variable constraints in model calibration.

Following pre-calibration at both spatial resolutions, the resulting calibrated parameter sets were analyzed to define new parameter ranges for the calibration phase. This analysis involved adjusting the minimum and maximum values of parameters influencing baseflow (dr, QDSnow, Krec, Kol, Kxy) by ±10% to establish new calibration ranges.

In the second and most important calibration phase, the process continued with the adjusted parameter ranges, employing a less restrictive objective function (Eq. (3.7)) to better accommodate uncertainties in the recharge data. This phase involved a comprehensive series of 1000 evaluations at 1000 meters and 50 at 250 meters resolutions. The modified objective function primarily emphasized the KGE while incorporating the standard deviation of recharge at a reduced influence of 4%. This modification was crucial to allow the model flexibility to adapt the groundwater recharge rate according to the specific hydrological characteristics and precipitation patterns of each catchment. Given that the initial recharge rate of 250 mm yr^{-1} was a preliminary estimate and not necessarily reflective of individual catchment conditions, this approach enabled a more tailored calibration.

Table 3.5 shows an overview of the three methods to ease comparisons between configurations.

Table 3.5 Summary of configurations

Settings	BL	GW	GW-RC
Groundwater Modelling	Conceptual within unsaturated zone sub-model	Physically based within the groundwater sub-model	Physically based within the groundwater sub-model
Calibration Parameters	17 parameters (including KB and Q0)	17 parameters (including Kol and Kxy)	17 parameters (including Kol and Kxy)
Precalibration	N/A	N/A	1. 200 simulations at 1000 meters 2. 50 simulations at 250 meters
Calibration	1. 1000 simulations at 1000 meters 2. 50 simulations at 250 meters	1. 1000 simulations at 1000 meters 2. 50 simulations at 250 meters	1. 1000 simulations at 1000 meters 2. 50 simulations at 250 meters
Objective Function	Kling-Gupta efficiency	Kling-Gupta efficiency	Constrained Kling-Gupta efficiency

3.2.5 Performance assessments

3.2.5.1 Kling-Gupta efficiency

The KGE (Kling et al., 2012) was chosen as the objective function to assess the model's performance during the calibration process.

The KGE is computed using Eq. (3.2):

$$KGE = 1 - \sqrt{(r-1)^2 + (\beta - 1)^2 + (\gamma - 1)^2}, \quad (3.2)$$

where r is the correlation coefficient, calculated as:

$$r = \frac{\sum_{i=1}^{n}(O_i - \bar{O}) * (S_i - \bar{S})}{\sqrt{\sum_{i=1}^{n}(O_i - \bar{O})^2 * \sum_{i=1}^{n}(S_i - \bar{S})^2}}, \quad (3.3)$$

here, O_i and S_i are the daily observed and daily simulated streamflow values, respectively, for each day i in the series. $\bar{O}$ and $\bar{S}$ are the average values of these daily observed and simulated streamflow across the entire series.

β is the bias ratio, defined as:

$$\beta = \frac{\mu_{sim}}{\mu_{obs}}, \tag{3.4}$$

A bias ratio of 1 indicates no bias. Values less than 1 suggest underestimation by the model, while values greater than 1 suggest overestimation.

γ is the variability ratio, calculated as:

$$\gamma = \frac{\sigma_{sim}/\mu_{sim}}{\sigma_{obs}/\mu_{obs}}, \tag{3.5}$$

The variability ratio assesses how effectively the model reproduces the variability in streamflow. It considers differences in the amplitude of variations in simulated and observed streamflow. Again, values less than 1 suggest underestimation by the model, while values greater than 1 suggest overestimation.

The resulting KGE values range from -∞ to 1, where a KGE of 1 indicates a perfect match between observed and simulated streamflow. According to Knoben et al. (2019), a KGE value greater than -0.41 indicates that the model's performance is an improvement over using the mean flow as a benchmark.

3.2.5.2 Constrained Kling-Gupta efficiency

An arbitrary baseline groundwater recharge rate of 250 mm yr^{-1} and a standard deviation of 80 mm yr^{-1} have been established as representative benchmarks for the studied catchments.

These values are based on PACES data and additional studies conducted in Quebec, as described in Sect. 3.2.2.5. The objective function for the pre-calibration of configuration GW-RC, outlined in Eq. (3.6), aims to balance KGE with these established recharge metrics. Specifically, the function assigns a weight of 70% to KGE, 20% to the annual recharge standard deviation, and 10% to the mean annual recharge. This specific weighting was chosen based on preliminary tests, where various weight combinations were evaluated on a test catchment. This objective function was designed to ensure both the quantity and variability of recharge were realistically modeled without sacrificing performance in terms of overall streamflow quality through the KGE.

The objective function employed in the pre-calibration of GW-RC configuration is formulated as follows:

$$Precalibration\ function = 1 - (0.7 * KGE + 0.2 * \lceil \sigma_{r_{sim}} - 0.08 \rceil + 0.1 * \lceil \overline{r_{sim}} - 0.25 \rceil), \tag{3.6}$$

where $\sigma_{r_{sim}}$ is the simulated annual recharge standard deviation (m yr^{-1}), $\overline{r_{sim}}$ is the simulated mean annual recharge (m yr^{-1}) and KGE is the Kling-Gupta efficiency.

Groundwater recharge simulations were performed at the pixel level, ensuring detailed local representation. The simulated mean annual recharge reflects the average amount of recharge occurring annually across the entire catchment during the calibration period. Similarly, the simulated annual standard deviation quantifies the variability in annual recharge across all pixels within the catchment during the same period. Introducing pixel level standard deviation helps in curbing extreme values in groundwater recharge, thus stabilizing the simulation outputs. The mean annual recharge is employed to verify that the model accurately captures the overall recharge volume expected for the study area.

For the main calibration phase of the GW-RC configuration, the objective function is simplified to focus more intensively on streamflow accuracy:

$$Calibration\ function = 1 - (0.96 * KGE + 0.04 * \lceil \sigma_{r_{sim}} - 0.08 \rceil), \quad (3.7)$$

where $\sigma_{r_{sim}}$ is the annual recharge standard deviation (m yr^{-1}) and KGE is the Kling-Gupta efficiency.

3.2.6 Statistical analysis

To assess the performance of the hydrological model configurations, statistical analyses were conducted to compare calibration and validation performance across different configurations. The primary metric used was the KGE, which evaluates the accuracy of simulated streamflow against observed data. The performance metrics were analyzed for each configuration during both the calibration period (2000-2009) and validation period (1990-1999), ensuring robust evaluation across varying hydrological conditions.

All statistical comparisons were made using the Kruskal-Wallis test, a non-parametric method chosen due to its suitability for non-normally distributed data. This test was employed to detect significant differences in the performance and hydrological responses between the model configurations. Where significant differences were identified, multiple comparison post-hoc tests were conducted to ascertain the specific pairs of configurations that differed significantly.

Pearson's correlation coefficients were used to explore the influence of calibration parameters on hydrological variables. This statistical approach provided insights into how variations in parameter settings across different configurations could affect the representation of hydrological processes like surface runoff, interflow, and groundwater recharge.

3.3 Results

3.3.1 Calibration and validation performance

Throughout the calibration (2000-2009) and validation (1990-1999) periods, all configurations yielded KGE values above 0.5. Calibration and validation performances were very similar, with a deviation less than 5%, demonstrating the robustness of the simulations. KGE values for all catchments and configurations, for both the calibration and validation periods, are presented in Table 3.B.

Figure 3.2 reveals a clear trend where catchments with high KGE values during calibration tend to maintain similar performance during validation. This consistency underpins the robustness of the configurations across different validation periods. During the validation period, median KGE values were higher for configurations BL (0.824) and GW (0.830) compared to GW-RC (0.770), demonstrating superior performance in the models without groundwater recharge constraints. However, GW-RC demonstrates more consistent KGE values between calibration and validation, suggesting it may offer more stability in model performance despite its slightly lower KGE scores.

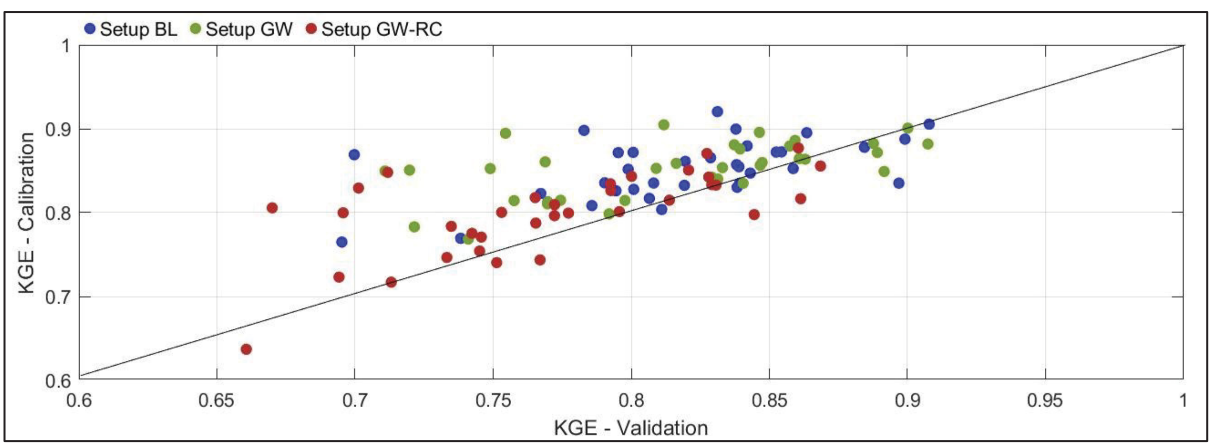

Figure 3.2 Comparison of Kling-Gupta Efficiency values between calibration and validation periods for three configurations

It is important to note that the KGE values for configuration GW-RC are slightly lower than those from configurations BL and GW, which is expected given the supplementary constraints imposed during calibration.

3.3.2 Hydrological variables analysis

This section delves into the simulated hydrological variables, examining their range and distribution across the various model configurations during the calibration and validation periods. The variables in focus include surface runoff, baseflow, interflow, groundwater recharge, and actual evapotranspiration (ETa).

Figure 3.3 illustrates the annual totals (means for groundwater level and soil moisture) for simulated hydrological variables for both calibration and validation periods and for all catchments. Notably, there is a consistency in the distribution of hydrological variables of each model configuration between the calibration and validation periods, which allows us to focus our detailed analysis solely on the validation period for conciseness.

A comparative assessment reveals distinct patterns in the simulated hydrological variables among the configurations. Specifically, configuration GW-RC simulates higher surface runoff and lower interflow, and infiltration compared to configurations BL and GW. Conversely, configuration BL is characterized by higher actual evapotranspiration, lower groundwater recharge, and a higher groundwater level. Configuration GW shares similarities with both configuration BL (in terms of runoff, interflow, and infiltration) and configuration GW-RC (regarding baseflow, groundwater recharge, actual evapotranspiration, and groundwater level).

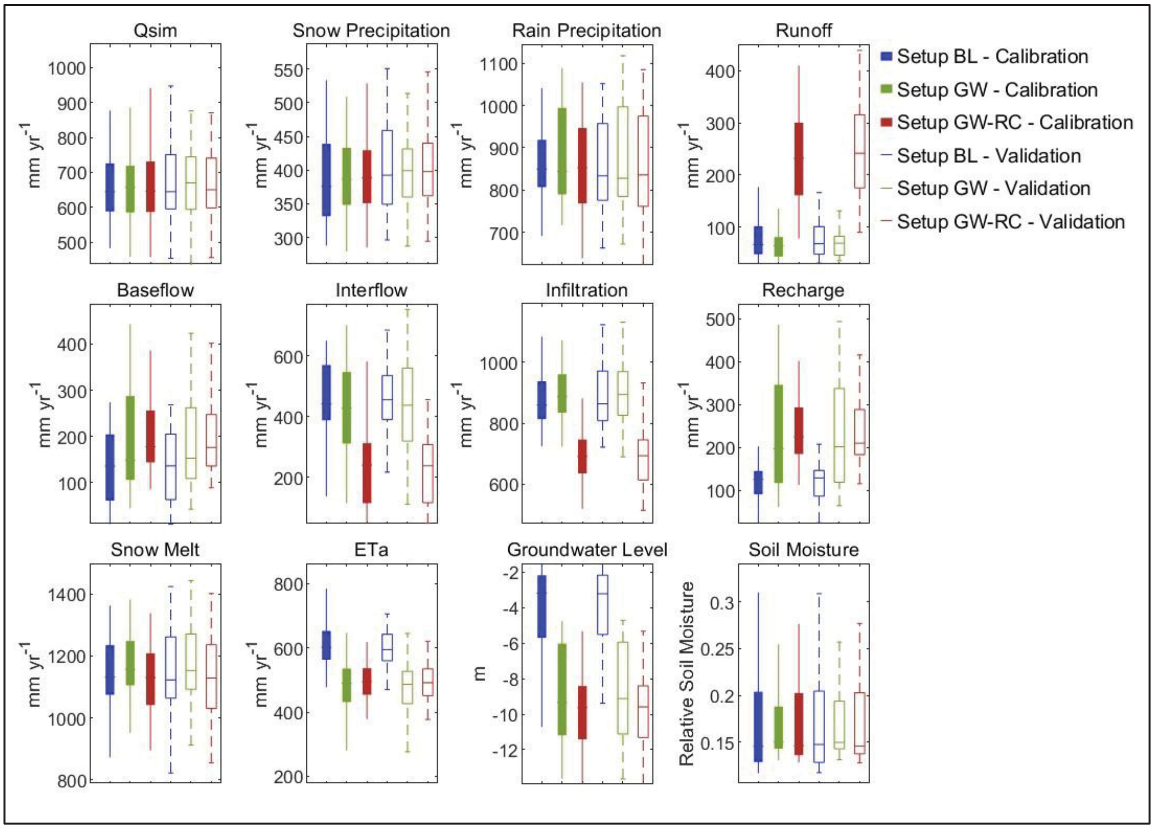

Figure 3.3 Boxplots illustrating annual totals (means for groundwater level and soil moisture) variability of model internal variables

Figure 3.4 presents the proportional distribution of surface runoff, baseflow, interflow, and actual evapotranspiration for the three hydrological model configurations (BL, GW, and GW-RC). The charts effectively compare the relative contribution of each process to the total water cycle within the modeled catchments.

The figure highlights that configuration GW-RC simulates a notably higher proportion of surface runoff (21%) and baseflow (17%) with a lower proportion of interflow (20%). Conversely, configuration BL has a higher proportion of actual evapotranspiration (47%) and less baseflow (11%). Finally, configuration GW has similarities with both BL (surface runoff and interflow) and GW-RC (baseflow and actual evapotranspiration) configurations.

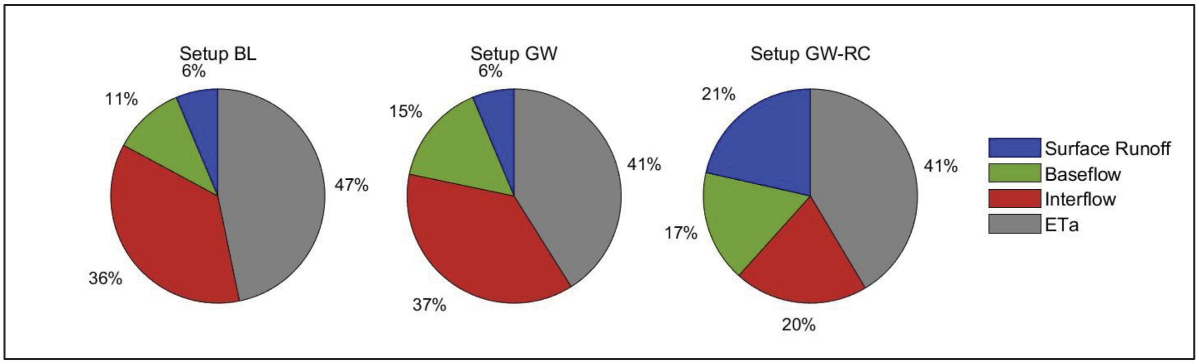

Figure 3.4 Proportional distributions of key hydrological variables for the BL, GW and GW-RC hydrological model configurations

Table 3.6 shows that the observed similarities in surface runoff and interflow between configurations BL and GW are substantiated by statistical significance in their mean groupings. Furthermore, the parallels drawn between configurations GW and GW-RC in terms of actual evapotranspiration and groundwater recharge are also supported by significant statistical evidence. However, the apparent similarity in baseflow between configurations GW and GW-RC does not hold statistical significance.

Table 3.6 Statistical analysis of the differences in estimated hydrological variables from the three configurations BL, GW and GW-RC

Hydrological Variables	**BL vs. GW**	**BL vs. GW-RC**	**GW vs. GW-RC**
Surface runoff	0	1	1
Baseflow	1	1	1
Interflow	0	1	1
Actual evapotranspiration	1	1	0
Groundwater recharge	1	1	0
			(Not Different = 0; Different = 1)

Figure 3.5 illustrates the distribution of key hydrological variables for the 34 catchments and for each configuration. Consistent trends in hydrological responses are observed across the

catchments for each model configuration. For instance, configuration GW-RC typically shows higher runoff and lower interflow values across most catchments. Similarly, configuration BL consistently reports higher actual evapotranspiration and lower groundwater recharge. These patterns, initially observed in Fig. 3.3 and Fig. 3.4, are corroborated across most catchments, aligning with the statistical findings presented in Table 3.6.

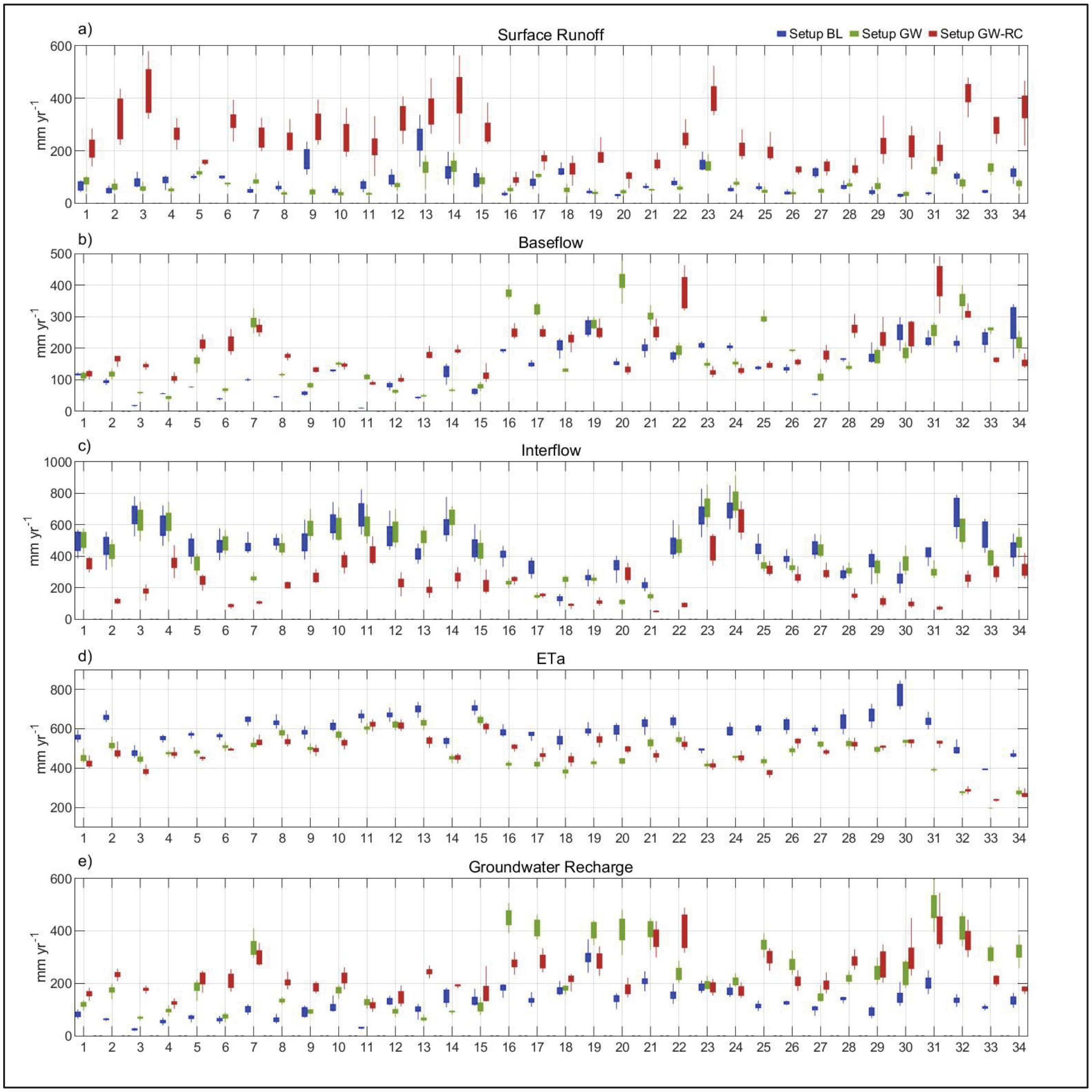

Figure 3.5 Boxplots of annual values for key hydrological variables predicted by WaSiM for the 34 catchments and three configurations

Figure 3.6 presents the relationships between key hydrological variables and selected calibration parameters. All subplots show high levels of correlations, shedding light on how varying the magnitude of calibration parameters influence model behavior. Notably, surface runoff exhibits a strong correlation ($r = 0.899$) with the parameter QDsnow, which determines the proportion of runoff from snowmelt. Actual evapotranspiration shows a notable correlation (r = 0.683) with the correction factors for potential evapotranspiration (ETp), and interflow is similarly strongly linked (r = 0.801) to the drainage density parameter. Baseflow and groundwater recharge display a strong correlation (r = 0.850) across all configurations. For configurations GW and GW-RC, baseflow is inversely but strongly correlated (r = -0.875) with drainage density, whereas in configuration BL, it correlates (r = 0.715) with the scaling factor for baseflow, Q0. It is also observed that configuration GW-RC generally has a higher QDsnow parameter and a lower drainage density. Additionally, configuration BL is characterized by larger correction factors for ETp.

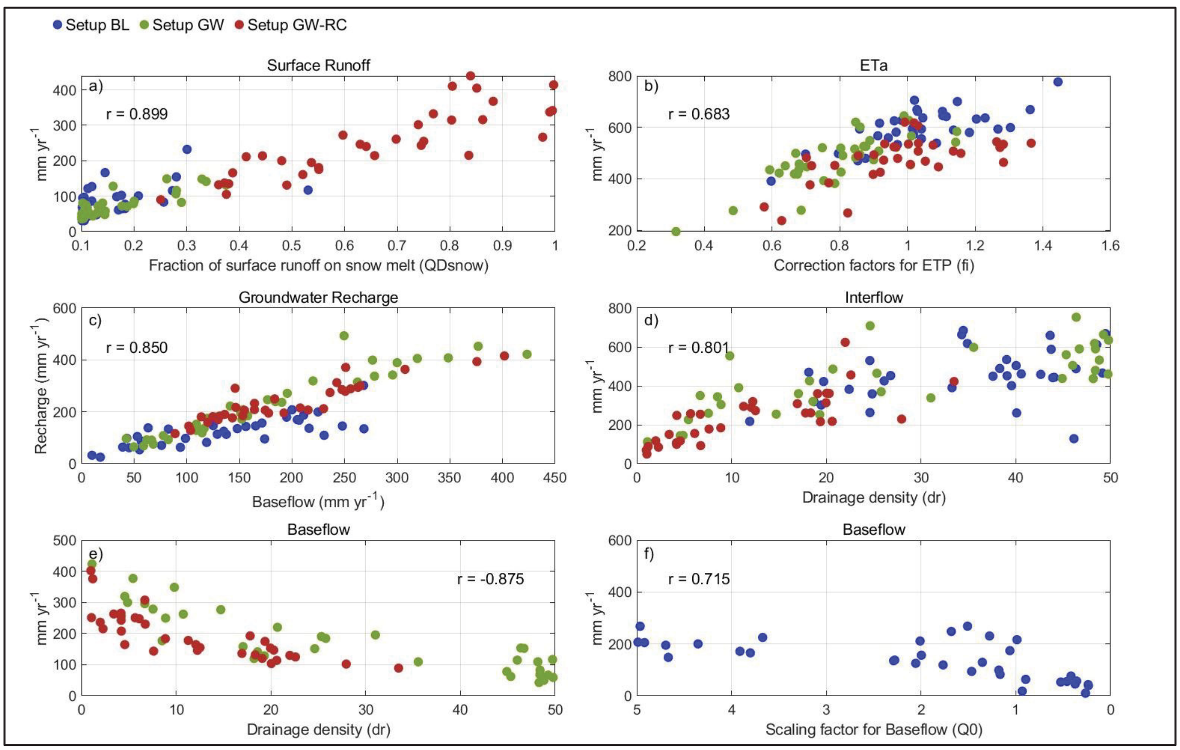

Figure 3.6 Correlations between key hydrological variables and calibration parameters for three model configurations

3.3.3 In-depth analysis of the Matane catchment

This section explores the temporal dynamics of streamflow and hydrological variables in the Matane catchment, which was selected as a representative example from the study's catchments. Figure 3.7 contrasts observed and simulated streamflow for the Matane catchment during both calibration and validation periods, across the three configurations This figure highlights the high similarity in the simulated streamflow between all configurations for both calibration and validation periods with the largest differences happening between April and July. This period aligns with seasonal high flows due to snowmelt. While configurations BL and GW exhibit higher KGE values during these periods, configuration GW-RC demonstrates a slightly reduced performance, in alignment with observations from Sect. 3.3.1. Nonetheless, all configurations show good performance, highlighting their robustness throughout both the calibration and validation periods.

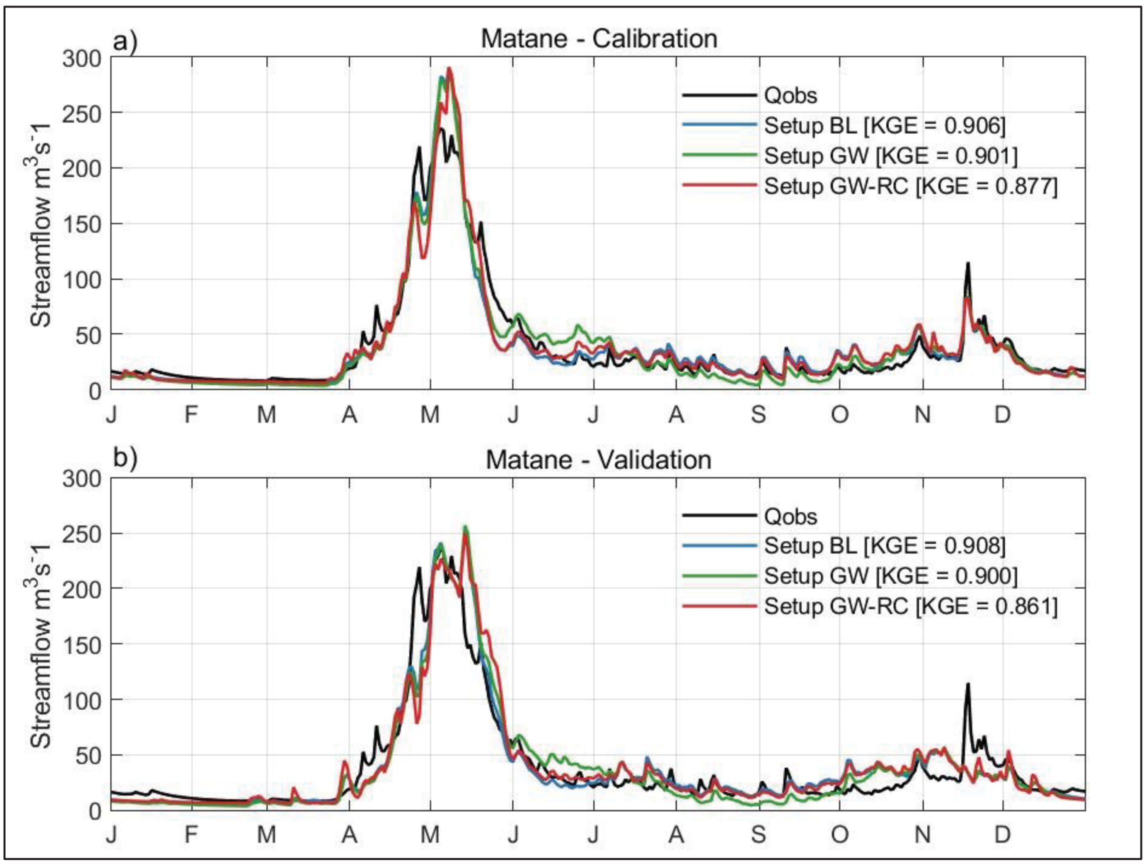

Figure 3.7 Comparative hydrographs for Matane catchment showing modeling results from the three configurations as well as streamflow observations (Qobs)

Figure 3.8 reveals consistent patterns in hydrological variable behavior across all configurations during both the calibration and validation periods. Consequently, the following discussions will focus primarily on the validation period. Generally, interflow is the major contributor to simulated streamflow in configurations BL and GW throughout the year. In contrast, configuration GW-RC is characterized by a significant increase in surface runoff during the seasonal high flow and high precipitation periods in the fall, while predominantly exhibiting interflow contributions during other times of the year.

Configuration GW-RC is also marked by higher levels of surface runoff and baseflow, but lower interflow compared to the other configurations. Configuration BL is distinguished by having the highest levels of annual actual evapotranspiration. Configuration GW aligns closely with configuration BL in terms of interflow, surface runoff, and baseflow, demonstrating similar hydrological dynamics between these two configurations.

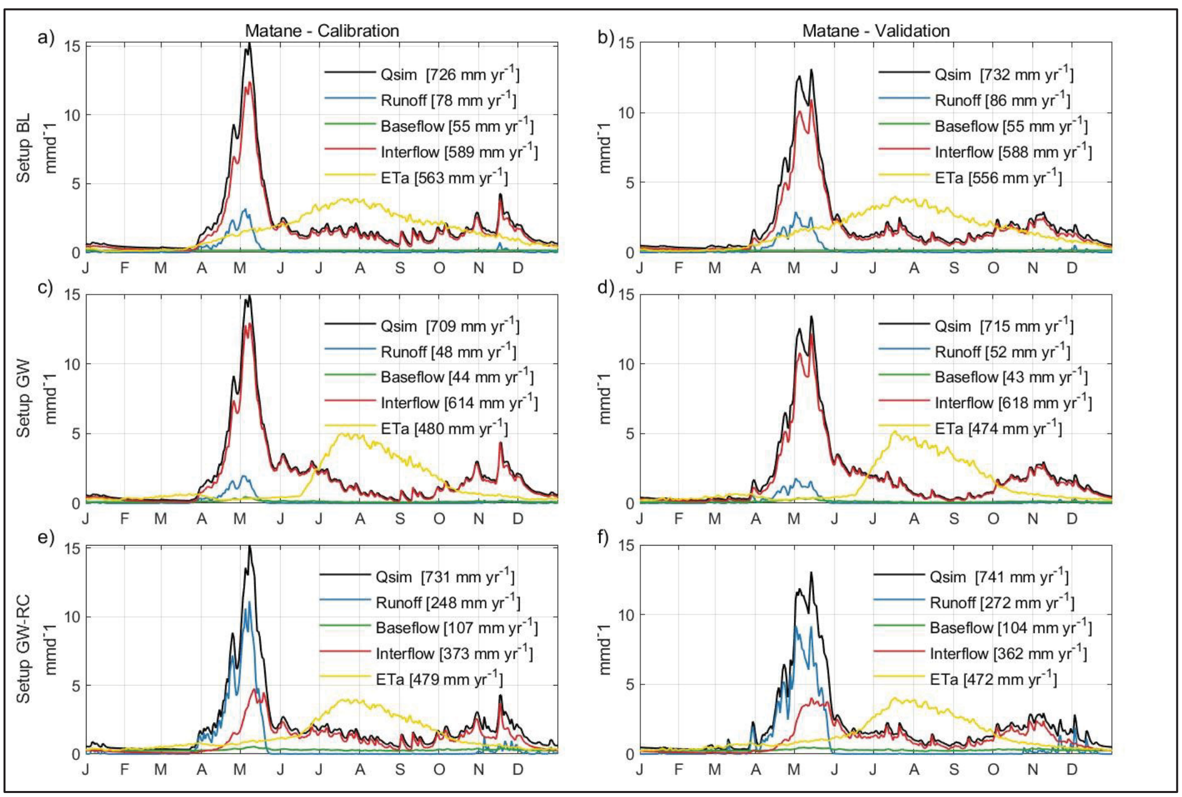

Figure 3.8 Detailed hydrological variable hydrograph for Matane catchment during both the calibration and validation phases and for the three configurations

Figure 3.9 reveals seasonal variations that correlate with hydrological responses to climatic conditions. Surface runoff and interflow differ significantly during periods of high flow, typically driven by snowmelt. Configurations BL and GW primarily attribute high flows to interflow, whereas configuration GW-RC reflects these peaks with increased surface runoff. Groundwater recharge in configuration BL exhibits more pronounced seasonal fluctuations compared to the patterns observed in configurations GW and GW-RC. Similarly, configuration BL maintains a consistent baseflow year-round, unlike configurations GW and GW-RC, which show seasonal baseflow variations. In terms of actual evapotranspiration, configuration BL consistently exhibits higher rates in the spring and fall, GW peaks during the summer, and GW-RC displays a pattern that blends characteristics of both BL and GW across different seasons.

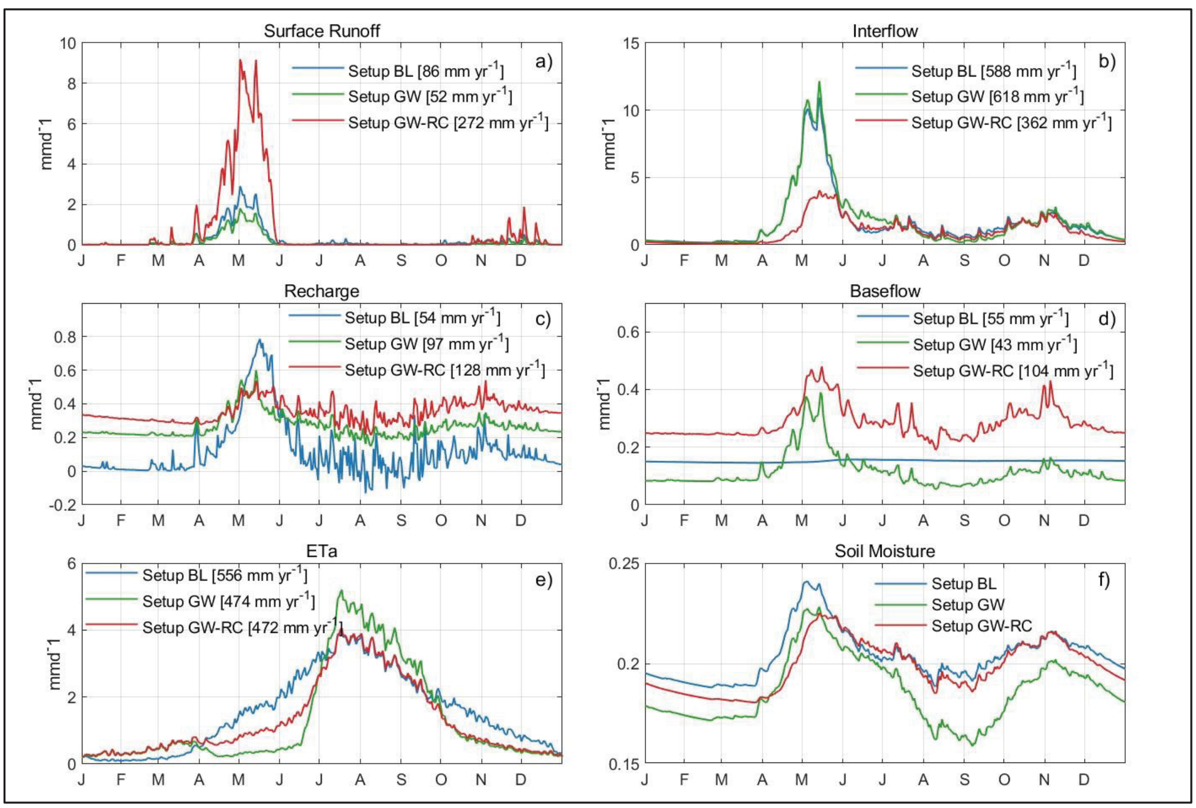

Figure 3.9 Seasonal distribution of hydrological variables in the Matane catchment

3.3.4 Groundwater recharge analysis

This section evaluates groundwater recharge, focusing on the influence of differing model configurations within WaSiM. Figure 3.9 panel C illustrates the daily groundwater recharge in the Matane catchment for each configuration. A common seasonal pattern is evident across all configurations: recharge decreases in winter, rises significantly during snowmelt, and then exhibits marked variability throughout summer and autumn. Notably, configuration GW-RC shows a lower dynamic range during snowmelt compared to configurations BL and GW, which exhibit more pronounced peaks. Throughout the winter, summer, and autumn months, configuration GW-RC consistently shows higher recharge rates than the other configurations. The trends observed in the Matane catchment are also representative of the behaviors seen across all studied catchments

Further analysis involves distributed maps of annual recharge (Fig. 3.C), calculated at the pixel level for seven catchments, comparing PACES data with model outputs. Visually, configurations GW and GW-RC show recharge distributions that are more consistent with the PACES dataset, suggesting a better spatial accuracy in these configurations compared to BL.

Figure 3.10 presents the boxplots of the annual recharge of each pixel for all configurations and the PACES data for the seven catchments. Configuration GW-RC's recharge estimates generally align more closely with the PACES data, indicating its ability in capturing the annual recharge dynamics at a finer spatial resolution. The other configurations follow, with GW also showing a reasonable approximation of PACES data, whereas BL appears less representative.

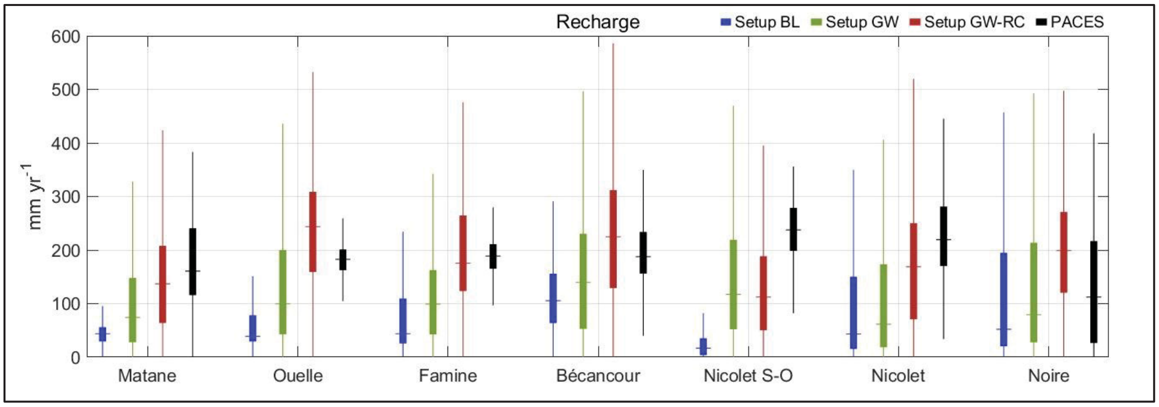

Figure 3.10 Distributions of annual groundwater recharge across seven catchments, for the three configurations and the PACES data

3.4 Discussion

3.4.1 Performance against representation

This study aimed to analyze how varying model configurations affect the representation of hydrological variables estimated by WaSiM. Through the comparative analysis of three distinct calibration configurations, BL (baseline model), GW (activated groundwater simulation), and GW-RC (groundwater simulation and recharge calibration), this study provides insights into how internal hydrological processes are represented in a physically based model.

KGE values were consistently higher for the BL and GW configurations compared to GW-RC during both calibration and validation periods. Configuration GW-RC's modestly lower performance on KGE is reflective of its calibration not solely focusing on optimizing KGE but also in incorporating a broader suite of hydrological dynamics.

This finding aligns with prior research, which suggests that adding constraints to model parameters can often improve the representation of other hydrological processes, such as groundwater dynamics and soil moisture, albeit at the cost of lower validation performance.

For instance, Yassin *et* al. (2017) emphasized that incorporating additional data, such as from the Gravity Recovery and Climate Experiment (GRACE), can lead to more comprehensive and physically realistic model. Similarly, Dembélé *et* al. (2020) showed that incorporating spatial patterns from satellite data significantly improve the model's representation of soil moisture and evapotranspiration. Similarly, Bouaziz *et* al. (2021) found substantial disparities in internal process representation among models calibrated to the same streamflow data, highlighting the limitations of relying solely on discharge data for model validation. Lastly, Pool *et* al. (2024) demonstrated that incorporating variables such as actual evapotranspiration and total water storage alongside discharge in model calibration can significantly enhance the simulation accuracy for these variables.

3.4.2 Hydrological variables analysis

Regarding the distribution of hydrological variables, configuration BL demonstrated the highest actual evapotranspiration rates, alongside the lowest groundwater recharge and baseflow. Conversely, GW-RC was noted for the highest surface runoff and the lowest interflow. Configuration GW demonstrated characteristics that were intermediate between the other two configurations, mirroring BL in terms of interflow and surface runoff while aligning more closely with GW-RC in terms of groundwater recharge, actual evapotranspiration, and baseflow.

Baseflow is closely correlated ($r = -0.875$) with the drainage density parameter (scaling parameter for interflow) for configurations GW and GW-RC. The constrained parameter range in configuration GW-RC explains the minor differences in baseflow rates observed between these configurations. In contrast, the baseflow in configuration BL is significantly correlated ($r = 0.715$) with the scaling factor for baseflow. The differences in groundwater recharge and baseflow across the configurations can be primarily attributed to the activation of the groundwater flow sub-model. In WaSiM, the simulation of groundwater processes can either follow a more conceptual or physically based pathway. Our results indicated that GW and GW-RC, which incorporate more complex mechanisms between groundwater and surface processes, lead to more dynamic and possibly more accurate representations of baseflow and recharge dynamics.

The disparities in interflow of configuration GW-RC are mostly linked to the restricted calibration of the drainage density parameter with a strong correlation ($r = 0.801$) noted between interflow rates and the parameter value, highlighting how constraining the groundwater recharge during calibration can impact other hydrological variables like interflow. Similarly, variations in surface runoff in configuration GW-RC are tied to the calibration restrictions on the QDsnow parameter (fraction of surface runoff on snow melt), which is strongly correlated ($r = 0.899$) with surface runoff rates, indicating a significant control over this hydrological variable. Also, configuration GW-RC showed the highest value for QDsnow parameter and the lowest value for the drainage density parameter consequently leading to the highest surface runoff and lowest interflow rates. This observation indicates that interflow is a flexible variable within the model, with configurations BL and GW appearing to prioritize it over surface runoff and baseflow. This prioritization allows the optimization algorithm greater latitude to enhance performance metrics like KGE and more accurately reproduce observed streamflow patterns. Conversely, configuration GW-RC, constrained by groundwater recharge, tends to prioritize baseflow and surface runoff. While this approach may reduce the model's flexibility in mirroring observed streamflow, it enhances the precision with which other hydrological processes are represented as detailed in Sect. 3.4.3. The same trend was found for the Matane catchment, underlining the broader applicability of these findings across different geographical contexts. Such a representation offers essential information that can be pivotal for water management strategies.

3.4.3 Pinpointing the optimal model configuration

The differences in surface runoff during the snowmelt season across configurations can be largely attributed to the parameter QDsnow. WaSiM employs a singular parameter

(QDsnow) to account for surface runoff from snowmelt. This parameter is calibrated between 0 and 1, and its precise setting critically influences the model's surface runoff predictions.

Analysis of Fig. 8 reveals that configurations BL and GW exhibit lower surface runoff from snowmelt, where melted snow predominantly percolates into the soil, contributing to interflow rather than surface runoff. This behavior is unexpected because, in fully frozen soil conditions, significant surface runoff is typically anticipated due to reduced infiltration.

Conversely, configuration GW-RC, which integrates groundwater recharge into the calibration process, follows a more typical hydrological pattern. Higher surface runoff is observed at the onset of snowmelt, gradually decreasing as infiltration and interflow increase when the soil thaws. This progression aligns with the expected hydrological responses in frozen terrains, illustrating how the inclusion of groundwater recharge can improve the model's simulation of seasonal transitions. This trend of higher surface runoff during snowmelt was observed consistently across all catchments in the study. Configuration GW-RC showed increased surface runoff during the snowmelt period compared to the other configurations. However, for 11 out of the 34 catchments, the surface runoff results were notably elevated. Figure 4.A illustrates an example where nearly all of the spring discharge was attributed to surface runoff, suggesting that the value assigned to the QDsnow parameter, when set too close to 1, may lead to an overestimation of runoff. Careful calibration of this parameter is essential to avoid misrepresentations in the hydrological processes.

The analysis of groundwater recharge, as detailed in Sect. 3.3.4, reveals significant differences in seasonal dynamics and spatial distribution among the configurations. Notably, GW-RC displays less dynamic recharge rates during the snowmelt period compared to configurations BL and GW. This is indicative of a distinct interplay between surface runoff and infiltration processes within configuration GW-RC, where higher surface runoff during the spring results in reduced infiltration. Additionally, GW-RC exhibits higher recharge rates during summer, fall, and winter, with a peak in fall.

Spatial analysis through distributed maps and boxplot representations of annual recharge (Fig. 3.10) demonstrates that configuration GW-RC's recharge estimates align more closely with PACES data than the other configurations. Similarities between both datasets suggests that configuration GW-RC provides a more precise representation of spatial variability in recharge, indicating its enhanced ability to capture the real-world spatial distribution of recharge processes across diverse landscapes effectively.

Supporting these observations, Chemingui *et* al. (2015) found the average recharge rates across different seasons at three locations in the “des Anglais” catchment. The numbers retrieve in their work closely align with those simulated by the GW-RC configuration: winter (58 vs 50 mm), spring (58 vs 54 mm), summer (92 vs 60 mm), and fall (52 vs 72 mm).

Furthermore, Rivard *et* al. (2014) utilized the HELP infiltration model to simulate recharge for a catchment in Eastern Canada, reporting average recharge rates of 67 mm in winter, 62 mm in spring, 27 mm in summer, and 76 mm in fall. These findings align with our results from configuration GW-RC, which also show peak recharge occurring in fall rather than in spring, differentiating it from the other configurations. Configuration GW aligns less precisely with these specific seasonal patterns, with a peak recharge in spring, but still outperforms BL in terms of matching the documented recharge rates from PACES.

Recharge rates from GW-RC align well with the PACES spatial distribution and compare favorably with observed seasonal fluctuations in the literature. Overall, GW-RC's alignment with empirical data and its ability to simulate hydrological processes more accurately make it a preferable model configuration for studying and predicting hydrological dynamics under varied climatic conditions.

In this study, the GW-RC configuration demonstrated that assigning a minor weight to recharge in the objective function can significantly enhance WaSiM’s capability to represent hydrological variables accurately, even with non-exact prior recharge data. This approach underscores, again, the potential of leveraging prior information to refine model outputs, suggesting that even a modest emphasis on recharge within the calibration framework can lead to substantial improvements in model realism. This finding is particularly noteworthy as it implies that effective model calibration does not necessarily require precise initial recharge estimates if the calibration process is appropriately managed. It also points to the broader applicability of using informed yet flexible calibration strategies to improve hydrological models under varied conditions, highlighting a path forward for enhancing model accuracy with limited prior data.

3.4.4 Practical implications, general applicability and limitations

The practical implications of this research extend beyond hydrological process modeling. Integrating groundwater recharge into model calibration, as demonstrated in the GW-RC configuration, offers a more comprehensive approach to representing key hydrological variables. This approach is particularly valuable for improving predictions of water resources under varying climate conditions, as it enhances the accuracy of inputs critical to models of forest growth (Ford et al., 2011; Grant et al., 2013). As climate change continues to alter hydrological dynamics, the reliance on physically based models becomes crucial. These models are favored over conceptual ones or even machine learning based models because they can be adapted more readily to varying conditions, ensuring more robust predictions under climate change scenarios. For example, a strong recent trend is the use of deep learning architectures in hydrological modelling (Arsenault et al., 2023; Kratzert et al., 2019; Kratzert, Klotz, Brenner, Schulz, & Herrnegger, 2018). These models simulate streamflow with generally better accuracy than traditional hydrological models, but they lack any mechanism to investigate internal and intermediate hydrological variables. Such adaptability is also critical for effective water resource management and mitigation of climate impacts (Ludwig et al., 2009; Poulin, Brissette, Leconte, Arsenault, & Malo, 2011; Wilby, 2005).

This research emphasizes the need to calibrate hydrological models using not only streamflow but also other variables such as groundwater recharge. This approach aligns with findings from other studies such as Yassin *et* al. (2017) and Dembélé *et* al. (2020), which advocate for multi-objective calibrations that enhance model reliability across different hydrological variables. By integrating measurements from diverse sources such as satellite data and in-situ measurements, models can avoid the pitfalls of calibration based solely on streamflow, which might not capture the full spectrum of watershed dynamics. Bouaziz *et* al. (2021) further illustrate this point by demonstrating how hydrological models calibrated solely on streamflow can yield differing results when validated against other hydrological variables, underscoring the risk of equifinality where different parameter sets produce similar results for streamflow but diverge for other variables. Without proper constraints—such as incorporating groundwater recharge into the calibration process—models may produce seemingly accurate streamflow simulations while failing to capture the underlying hydrological processes like configurations BL and GW.

The methodology developed in this study has broad applicability beyond the specific context of Southern Québec. This approach can be valuable in a variety of geographic regions and hydrological settings, given similar contexts of equifinality (i.e. more processes and parameters than the data can support). Moreover, this multi-variable calibration method can enhance the accuracy of other distributed hydrological models by improving the representation of groundwater recharge related processes. Similar calibration techniques using remote-sensing data have been applied successfully in different settings, demonstrating that incorporating additional hydrological variables in calibration improves model performance.

Nevertheless, it is crucial to address the limitations of this study. The models' performance in replicating hydrological processes like soil frost impacts and its implications on runoff and recharge remain unknown. Future studies would benefit from incorporating field measurements alongside a broader range of climatic and hydrological conditions. Expanding the research to include different geographic regions with similar soil and climate characteristics could significantly enhance the validation and applicability of the findings.

Moreover, the uncertainty inherent in modeling, especially with configurations that involve complex interactions of multiple variables, poses a continuous challenge. The study's reliance on specific data sets like PACES also introduces potential biases that could influence the generalizability of the findings. It's essential for future research to explore these limitations, perhaps by expanding the range of observational data used for model validation.

In terms of practical implementations and further research, continuing to refine the calibration of hydrological models to include diverse hydrological variables can enhance their utility in real-world applications. Such efforts will help in developing more accurate flood forecasting models, improving water resource management strategies, and crafting more effective climate adaptation measures for forest, agricultural and anthropogenic ecosystems.

Overall, while this study lays a solid foundation for using advanced calibration techniques in hydrological modeling, the journey towards fully reliable and universally applicable hydrological models continues.

3.5 Conclusion

This study examined the nuances of hydrological modeling under different calibration settings using WaSiM model across 34 catchments classified under climate zones Dfb and Dfc in Eastern North America. By implementing three distinct model configurations, BL (baseline model), GW (physical groundwater model), and GW-RC (physical groundwater and recharge calibration model), this research has demonstrated that incorporating groundwater recharge alongside streamflow during calibration process leads to a more accurate representation of hydrological variables.

The results indicate that the GW-RC configuration, enhanced with groundwater recharge calibration, aligns more closely with estimated groundwater recharge rates, thereby providing a more precise representation of groundwater behaviour both spatially and seasonally. The study also underscores the importance of extending calibration beyond traditional streamflow metrics to include other hydrological variables like groundwater recharge. This approach helps to mitigate the risks of equifinality.

Given the successful application of these methodologies within Eastern North American catchments, it presents an intriguing premise for their applicability to other geographical areas with similar hydrological contexts. Further research could explore how these calibration techniques perform under different hydrological conditions, potentially broadening our understanding of these relationships.

3.6 Acknowledgements

This work was funded jointly by the ministère des Ressources naturelles et des Forêts (Quebec, Canada, project number 112332187 conducted at the Direction de la recherche forestière and led by Jean-Daniel Sylvain) and the Forest research service contract number 3322-2022-2187-01 obtained by Richard Arsenault from the Ministère des Ressources naturelles et des Forêts (Quebec, Canada). The authors also acknowledge the use of ChatGPT-4 for assistance in correcting spelling mistakes and improving the flow of text during the manuscript preparation process. The base map in Fig. 3.1 was created using ArcGIS® software by Esri. ArcGIS® and ArcMap™ are the intellectual property of Esri and are used herein under license. Copyright © Esri. All rights reserved. For more information about Esri® software, please visit www.esri.com.

3.7 References

Acero Triana, J. S., Chu, M. L., Guzman, J. A., Moriasi, D. N., & Steiner, J. L. (2019). Beyond model metrics : The perils of calibrating hydrologic models. *Journal of Hydrology*, *578*, 124032. https://doi.org/10.1016/j.jhydrol.2019.124032

Akumu, C. E., Woods, M., Johnson, J. A., Pitt, D. G., Uhlig, P., & McMurray, S. (2016). GIS-fuzzy logic technique in modeling soil depth classes : Using parts of the Clay

Belt and Hornepayne region in Ontario, Canada as a case study. *Geoderma*, *283*, 78-87. https://doi.org/10.1016/j.geoderma.2016.07.028

Arsenault, R., Huard, D., Martel, J.-L., Troin, M., Mai, J., Brissette, F., … Langlois, S. (2023). The PAVICS-Hydro platform : A virtual laboratory for hydroclimatic modelling and forecasting over North America. *Environmental Modelling & Software*, *168*, 105808. https://doi.org/10.1016/j.envsoft.2023.105808

Arsenault, R., Poulin, A., Côté, P., & Brissette, F. (2014). Comparison of Stochastic Optimization Algorithms in Hydrological Model Calibration. *Journal of Hydrologic Engineering*, *19*(7), 1374-1384. https://doi.org/10.1061/(ASCE)HE.1943-5584.0000938

Beck, H. E., Zimmermann, N. E., McVicar, T. R., Vergopolan, N., Berg, A., & Wood, E. F. (2018). Present and future Köppen-Geiger climate classification maps at 1-km resolution. *Scientific Data*, *5*(1), 180214. https://doi.org/10.1038/sdata.2018.214

Bormann, H., & Elfert, S. (2010). Application of WaSiM-ETH model to Northern German lowland catchments : Model performance in relation to catchment characteristics and sensitivity to land use change. Dans *Advances in Geosciences* (Vol. 27, pp. 1-10). Copernicus GmbH. https://doi.org/10.5194/adgeo-27-1-2010

Bouaziz, L. J. E., Fenicia, F., Thirel, G., de Boer-Euser, T., Buitink, J., Brauer, C. C., … Hrachowitz, M. (2021). Behind the scenes of streamflow model performance. *Hydrology and Earth System Sciences*, *25*(2), 1069-1095. https://doi.org/10.5194/hess-25-1069-2021

Boumaiza, L., Walter, J., Chesnaux, R., Lambert, M., Jha, M. K., Wanke, H., … Stumpp, C. (2022). Groundwater recharge over the past 100 years : Regional spatiotemporal assessment and climate change impact over the Saguenay-Lac-Saint-Jean region, Canada. *Hydrological Processes*, *36*(3), e14526. https://doi.org/10.1002/hyp.14526

Buffin-Bélanger, T., Chaillou, G., Cloutier, C.-A., Touchette, M., Hétu, B., & McCormack, R. (2015). *Programme d'acquisition de connaissance sur les eaux souterraines du nord-est du Bas-Saint-Laurent (PACES-NEBSL) : Rapport final*. Rimouski, Québec: Université du Québec à Rimouski, Département de biologie, chimie et géographie.

Carrier, M.-A., Lefebvre, R., Rivard, C., Parent, M., Ballard, J.-M., Benoit, N., … Lavoie, D. (2013). *Portrait des ressources en eau souterraine en Montérégie Est, Québec, Canada* (Rapport No. INRS R-1433). Québec: Institut national de la recherche scientifique (INRS), Commission géologique du Canada (CGC), Organisme de bassin versant de la Yamaska (OBV Yamaska), Institut de recherche et développement en agroenvironnement (IRDA).

Chemingui, A., Sulis, M., & Paniconi, C. (2015a). An assessment of recharge estimates from stream and well data and from a coupled surface-water/groundwater model for the des Anglais catchment, Quebec (Canada). *Hydrogeology Journal*, *23*(8), 1731-1743. https://doi.org/10.1007/s10040-015-1299-1

Chemingui, A., Sulis, M., & Paniconi, C. (2015b). An assessment of recharge estimates from stream and well data and from a coupled surface-water/groundwater model for the des Anglais catchment, Quebec (Canada). *Hydrogeology Journal*, *23*(8), 1731-1743. https://doi.org/10.1007/s10040-015-1299-1

Chen, J., Sudicky, E., Gula, J., Peltier, W., Park, Y., & Ross, M. (2011). Impact of Climate Change on Canadian Surface Water and Groundwater Resources : A Continental-scale Hydrologic Modelling Study using Multiple High-resolution RCM Projections. Repéré à https://www.semanticscholar.org/paper/Impact-of-Climate-Change-on-Canadian-Surface-Water-Chen-Sudicky/656fb52b68b58b782d7cde413126ebaf6844bb1d

Cloutier, V., Blanchette, D., Dallaire, P.-L., Nadeau, S., Rosa, E., & Roy, M. (2013). *Projet d'acquisition de connaissances sur les eaux souterraines de l'Abitibi-Témiscamingue (partie 1)* (Rapport No. P001). Québec: Groupe de recherche sur l'eau souterraine, Institut de recherche en mines et en environnement, Université du Québec en Abitibi-Témiscamingue.

Cloutier, V., Rosa, E., Nadeau, S., Dallaire, P.-L., Blanchette, D., & Roy, M. (2015). *Projet d'acquisition de connaissances sur les eaux souterraines de l'Abitibi-Témiscamingue (partie 2)* (Rapport No. P002.R3). Québec: Groupe de recherche sur l'eau souterraine, Institut de recherche en mines et en environnement, Université du Québec en Abitibi-Témiscamingue.

Comeau, G., Talbot-Poulin, M. C., Tremblay, Y., Ayotte, S., Molson, J., Lemieux, J. M., … Fabien-Ouellet, G. (2013). *Projet d'acquisition de connaissances sur les eaux souterraines en Outaouais*. Québec: Département de géologie et de génie géologique, Université Laval.

Commission for Environmental Cooperation. (2020). 2015 Land Cover of North America ar 30 meters. *Commission for Environmental Cooperation*. Repéré à http://www.cec.org/north-american-environmental-atlas/land-cover-30m-2015-landsat-and-rapideye/

Conrad, O., Bechtel, B., Bock, M., Dietrich, H., Fischer, E., Gerlitz, L., … Böhner, J. (2015). System for Automated Geoscientific Analyses (SAGA) v. 2.1.4. *Geoscientific Model Development*, *8*(7), 1991-2007. https://doi.org/10.5194/gmd-8-1991-2015

Croteau, A., Nastev, M., & Lefebvre, R. (2010). Groundwater Recharge Assessment in the Chateauguay River Watershed. *Canadian Water Resources Journal / Revue canadienne des ressources hydriques*, *35*(4), 451-468. https://doi.org/10.4296/cwrj3504451

Cunningham, S. C., Thomson, J. R., Mac Nally, R., Read, J., & Baker, P. J. (2011). Groundwater change forecasts widespread forest dieback across an extensive floodplain system : Groundwater change forecasts forest dieback. *Freshwater Biology*, *56*(8), 1494-1508. https://doi.org/10.1111/j.1365-2427.2011.02585.x

de Lima Ferreira, P. M., & da Paz, A. R. (2024). Enhanced calibration of a distributed hydrological model in the Brazilian Semi-Arid : Integrating spatiotemporal evapotranspiration and streamflow data. *Environmental Earth Sciences*, *83*(11), 345. https://doi.org/10.1007/s12665-024-11663-6

Dembélé, M., Hrachowitz, M., Savenije, H. H. G., Mariéthoz, G., & Schaefli, B. (2020a). Improving the Predictive Skill of a Distributed Hydrological Model by Calibration on Spatial Patterns With Multiple Satellite Data Sets. *Water Resources Research*, *56*(1), e2019WR026085. https://doi.org/10.1029/2019WR026085

Dubois, E., Larocque, M., Gagné, S., & Meyzonnat, G. (2021, 26 février). Simulation of long-term spatiotemporal variations in regional-scalegroundwater recharge : Contributions of a water budget approach insouthern Quebec. https://doi.org/10.5194/hess-2021-71

Duethmann, D., Anderson, M., Maneta, M. P., & Tetzlaff, D. (2024). Improving process-consistency of an ecohydrological model through inclusion of spatial patterns of satellite-derived land surface temperature. *Journal of Hydrology*, *628*, 130433. https://doi.org/10.1016/j.jhydrol.2023.130433

Farjad, B., Gupta, A., & Marceau, D. J. (2016). Annual and Seasonal Variations of Hydrological Processes Under Climate Change Scenarios in Two Sub-Catchments of a Complex Watershed. *Water Resources Management*, *30*(8), 2851-2865. https://doi.org/10.1007/s11269-016-1329-3

Ficchì, A., Perrin, C., & Andréassian, V. (2019). Hydrological modelling at multiple sub-daily time steps : Model improvement via flux-matching. *Journal of Hydrology*, *575*, 1308-1327. https://doi.org/10.1016/j.jhydrol.2019.05.084

Ford, C. R., Laseter, S. H., Swank, W. T., & Vose, J. M. (2011). Can forest management be used to sustain water-based ecosystem services in the face of climate change? *Ecological Applications*, *21*(6), 2049-2067. https://doi.org/10.1890/10-2246.1

Förster, K., Garvelmann, J., Meißl, G., & Strasser, U. (2018). Modelling forest snow processes with a new version of WaSiM. *Hydrological Sciences Journal*, *63*(10), 1540-1557. https://doi.org/10.1080/02626667.2018.1518626

Förster, K., Meißl, G., Marke, T., Pohl, S., Garvelmann, J., Schulla, J., & Strasser, U. (2017). A new snow-vegetation interaction extension for the Water Balance Simulation Model (WaSiM), 2620. Communication présentée au EGU General Assembly Conference Abstracts. Repéré à https://ui.adsabs.harvard.edu/abs/2017EGUGA..19.2620F

Gädeke, A., Hölzel, H., Koch, H., Pohle, I., & Grünewald, U. (2014). Analysis of uncertainties in the hydrological response of a model-based climate change impact assessment in a subcatchment of the Spree River, Germany. *Hydrological Processes*, *28*(12), 3978-3998. https://doi.org/10.1002/hyp.9933

Géobase du réseau hydrographique du Québec (GRHQ)—Données Québec. (2016). Repéré à https://www.donneesquebec.ca/recherche/dataset/grhq

Grant, G. E., Tague, C. L., & Allen, C. D. (2013). Watering the forest for the trees : An emerging priority for managing water in forest landscapes. *Frontiers in Ecology and the Environment*, *11*(6), 314-321. https://doi.org/10.1890/120209

Hamon, W. R. (1963). Estimating Potential Evapotranspiration. *Transactions of the American Society of Civil Engineers*, *128*(1), 324-338. https://doi.org/10.1061/TACEAT.0008673

Hersbach, H., Bell, B., Berrisford, P., Hirahara, S., Horányi, A., Muñoz-Sabater, J., … Thépaut, J.-N. (2020). The ERA5 global reanalysis. *Quarterly Journal of the Royal Meteorological Society*, *146*(730), 1999-2049. https://doi.org/10.1002/qj.3803

Hock, R. (2003). Temperature index melt modelling in mountain areas. *Journal of Hydrology*, *282*(1), 104-115. https://doi.org/10.1016/S0022-1694(03)00257-9

Hydroclimatic Atlas of Southern Québec. (2022). Repéré à https://www.cehq.gouv.qc.ca/atlas-hydroclimatique/index-en.htm

Iacob, O., Brown, I., & Rowan, J. (2017). Natural flood management, land use and climate change trade-offs : The case of Tarland catchment, Scotland. *Hydrological Sciences Journal*, *62*(12), 1931-1948. https://doi.org/10.1080/02626667.2017.1366657

Imhoff, R. O., van Verseveld, W. J., van Osnabrugge, B., & Weerts, A. H. (2020). Scaling Point-Scale (Pedo)transfer Functions to Seamless Large-Domain Parameter Estimates for High-Resolution Distributed Hydrologic Modeling : An Example for the Rhine River. *Water Resources Research*, *56*(4), e2019WR026807. https://doi.org/10.1029/2019WR026807

Jasper, K., Calanca, P., & Fuhrer, J. (2006). Changes in summertime soil water patterns in complex terrain due to climatic change. *Journal of Hydrology*, *327*(3), 550-563. https://doi.org/10.1016/j.jhydrol.2005.11.061

Jeong, S., Hong, M., & Song, J. (2022). Soil depth estimation in mountainous areas by using GIS and satellite images. *Landslides*, *19*(11), 2711-2726. https://doi.org/10.1007/s10346-022-01919-2

Kirchner, J. W. (2006). Getting the right answers for the right reasons : Linking measurements, analyses, and models to advance the science of hydrology. *Water Resources Research*, *42*(3). https://doi.org/10.1029/2005WR004362

Kling, H., Fuchs, M., & Paulin, M. (2012). Runoff conditions in the upper Danube basin under an ensemble of climate change scenarios. *Journal of Hydrology*, *424-425*, 264-277. https://doi.org/10.1016/j.jhydrol.2012.01.011

Kratzert, F., Klotz, D., Brenner, C., Schulz, K., & Herrnegger, M. (2018). Rainfall–runoff modelling using Long Short-Term Memory (LSTM) networks. *Hydrology and Earth System Sciences*, *22*(11), 6005-6022. https://doi.org/10.5194/hess-22-6005-2018

Kratzert, F., Klotz, D., Herrnegger, M., Sampson, A. K., Hochreiter, S., & Nearing, G. S. (2019). Toward Improved Predictions in Ungauged Basins : Exploiting the Power of Machine Learning. *Water Resources Research*, *55*(12), 11344-11354. https://doi.org/10.1029/2019WR026065

Larocque, M., Gagné, S., Barnetche, D., Meyzonnat, G., Graveline, M.-H., & Ouellet, M. A. (2015). *Projet de connaissance des eaux souterraines du bassin versant de la zone Nicolet et de la partie basse de la zone Saint-François—Rapport final*. Québec:

Ministère du Développement durable, de l'Environnement et de la Lutte contre les changements climatiques.

Larocque, Marie, Gagné, S., Tremblay, L., & Meyzonnat, G. (2013). *Projet de connaissance des eaux souterraines du bassin versant de la rivière Bécancour et de la MRC de Bécancour—Rapport final*. Québec: Ministère du Développement durable, de l'Environnement, de la Faune et des Parcs.

Larocque, Marie, Levison, J., Martin, A., & Chaumont, D. (2019). A review of simulated climate change impacts on groundwater resources in Eastern Canada. *Canadian Water Resources Journal / Revue canadienne des ressources hydriques*, *44*(1), 22-41. https://doi.org/10.1080/07011784.2018.1503066

Latifovic, R., Homer, C., Ressl, R., Pouliot, D. A., Hossian, S., Colditz, R., … Victoria, A. (2012). North American Land Change Monitoring System. *Remote Sensing of Land Use and Land Cover : Principles and Applications*, 303-324. https://doi.org/10.1201/b11964-24

Lefebvre, R., Ballard, J.-M., Vigneault, H., Beaudry, C., Berthot, L., Légaré-Couture, G., … Molson, J. (2015). *Portrait des ressources en eau souterraine en Chaudière-Appalaches, Québec, Canada* (Rapport No. INRS R-1580). Québec: Institut national de la recherche scientifique (INRS), Institut de recherche et développement en agroenvironnement (IRDA), Regroupement des organismes de bassins versants de la Chaudière-Appalaches (OBV-CA).

Lighthill, M. J., & Whitham, G. B. (1955). On kinematic waves I. Flood movement in long rivers. *Proceedings of the Royal Society of London. Series A. Mathematical and Physical Sciences*, *229*(1178), 281-316. https://doi.org/10.1098/rspa.1955.0088

Liu, X., Yang, K., Ferreira, V. G., & Bai, P. (2022). Hydrologic Model Calibration With Remote Sensing Data Products in Global Large Basins. *Water Resources Research*, *58*(12), e2022WR032929. https://doi.org/10.1029/2022WR032929

Ludwig, R., May, I., Turcotte, R., Vescovi, L., Braun, M., Cyr, J.-F., … Mauser, W. (2009). The role of hydrological model complexity and uncertainty in climate change impact assessment. *Advances in Geosciences*, *21*, 63-71. https://doi.org/10.5194/adgeo-21-63-2009

MacMillan, R. A., Pettapiece, W. W., Nolan, S. C., & Goddard, T. W. (2000). A generic procedure for automatically segmenting landforms into landform elements using

DEMs, heuristic rules and fuzzy logic. *Fuzzy Sets and Systems*, *113*(1), 81-109. https://doi.org/10.1016/S0165-0114(99)00014-7

Maitre, D. L., Scott, D., & Colvin, C. (1999). A review of information on interactions between vegetation and groundwater. *Water SA*. Repéré à https://www.semanticscholar.org/paper/A-review-of-information-on-interactions-between-and-Maitre-Scott/b7666786b75c7fda14cbe3e835e70085302c3675

Markhali, S. P., Poulin, A., & Boucher, M.-A. (2022). Spatio-temporal discretization uncertainty of distributed hydrological models. *Hydrological Processes*, *36*(6), e14635. https://doi.org/10.1002/hyp.14635

Mei, Y., Mai, J., Do, H. X., Gronewold, A., Reeves, H., Eberts, S., … Hunt, R. J. (2023). Can Hydrological Models Benefit From Using Global Soil Moisture, Evapotranspiration, and Runoff Products as Calibration Targets? *Water Resources Research*, *59*(2), e2022WR032064. https://doi.org/10.1029/2022WR032064

Meyer Oliveira, A., Fleischmann, A. S., & Paiva, R. C. D. (2021). On the contribution of remote sensing-based calibration to model hydrological and hydraulic processes in tropical regions. *Journal of Hydrology*, *597*, 126184. https://doi.org/10.1016/j.jhydrol.2021.126184

Ministère des Ressources Naturelles et des Forêts. (2022). *SIIGSOL-100m—Carte des propriétés du sol*. Données Québec. Repéré à https://www.donneesquebec.ca/recherche/dataset/siigsol-100m-carte-des-proprietes-du-sol

Mizukami, N., Clark, M. P., Newman, A. J., Wood, A. W., Gutmann, E. D., Nijssen, B., … Samaniego, L. (2017). Towards seamless large-domain parameter estimation for hydrologic models. *Water Resources Research*, *53*(9), 8020-8040. https://doi.org/10.1002/2017WR020401

Natkhin, M., Steidl, J., Dietrich, O., Dannowski, R., & Lischeid, G. (2012). Differentiating between climate effects and forest growth dynamics effects on decreasing groundwater recharge in a lowland region in Northeast Germany. *Journal of Hydrology*, *448-449*, 245-254. https://doi.org/10.1016/j.jhydrol.2012.05.005

Orellana, F., Verma, P., Loheide, S. P., & Daly, E. (2012). Monitoring and modeling water-vegetation interactions in groundwater-dependent ecosystems. *Reviews of Geophysics*, *50*(3), 2011RG000383. https://doi.org/10.1029/2011RG000383

Persaud, E., Levison, J., MacRitchie, S., Berg, S. J., Erler, A. R., Parker, B., & Sudicky, E. (2020). Integrated modelling to assess climate change impacts on groundwater and surface water in the Great Lakes Basin using diverse climate forcing. *Journal of Hydrology*, *584*, 124682. https://doi.org/10.1016/j.jhydrol.2020.124682

Peters-Lidard, C. D., Clark, M., Samaniego, L., Verhoest, N. E. C., van Emmerik, T., Uijlenhoet, R., … Woods, R. (2017). Scaling, similarity, and the fourth paradigm for hydrology. *Hydrology and Earth System Sciences*, *21*(7), 3701-3713. https://doi.org/10.5194/hess-21-3701-2017

Pool, S., Fowler, K., & Peel, M. (2024). Benefit of Multivariate Model Calibration for Different Climatic Regions. *Water Resources Research*, *60*(4), e2023WR036364. https://doi.org/10.1029/2023WR036364

Poulin, A., Brissette, F., Leconte, R., Arsenault, R., & Malo, J.-S. (2011). Uncertainty of hydrological modelling in climate change impact studies in a Canadian, snow-dominated river basin. *Journal of Hydrology*, *409*(3), 626-636. https://doi.org/10.1016/j.jhydrol.2011.08.057

Pradhan, A., & Indu, J. (2019). Uncertainty in Calibration of Variable Infiltration Capacity Model, 89-108. https://doi.org/10.1007/978-3-030-02197-9_4

Rajib, A., Evenson, G. R., Golden, H. E., & Lane, C. R. (2018). Hydrologic model predictability improves with spatially explicit calib ration using remotely sensed evapotranspiration and biophysical parame ters. *Journal of Hydrology*, *567*, 668-683. https://doi.org/10.1016/j.jhydrol.2018.10.024

Richards, L. A. (1931). CAPILLARY CONDUCTION OF LIQUIDS THROUGH POROUS MEDIUMS. *Physics*, *1*(5), 318-333. https://doi.org/10.1063/1.1745010

Rivard, C., Paniconi, C., Vigneault, H., & Chaumont, D. (2014). A watershed-scale study of climate change impacts on groundwater recharge (Annapolis Valley, Nova Scotia, Canada). *Hydrological Sciences Journal*, *59*(8), 1437-1456. https://doi.org/10.1080/02626667.2014.887203

Rössler, O., Diekkrüger, B., & Löffler, J. (2012). Potential drought stress in a Swiss mountain catchment—Ensemble forecasting of high mountain soil moisture reveals a drastic decrease, despite major uncertainties. *Water Resources Research*, *48*(4). https://doi.org/10.1029/2011WR011188

Rößler, O., & Löffler, J. (2010). Potentials and limitations of modelling spatio-temporal patterns of soil moisture in a high mountain catchment using WaSiM-ETH. *Hydrological Processes*, *24*(15), 2182-2196. https://doi.org/10.1002/hyp.7663

Rouleau, A., Daigneault, R., Walter, J., Germaneau, D., Tremblay, M.-L., Lambert, M., … Thouvignon, N. (2013). *Résultats du programme d'acquisition de connaissances sur les eaux souterraines de la région Saguenay-Lac-Saint-Jean*. Chicoutimi, Québec: Centre d'études sur les ressources minérales, Université du Québec à Chicoutimi.

Samaniego, L., Kumar, R., & Attinger, S. (2010). Multiscale parameter regionalization of a grid-based hydrologic model at the mesoscale. *Water Resources Research*, *46*(5). https://doi.org/10.1029/2008WR007327

Samaniego, L., Kumar, R., Thober, S., Rakovec, O., Zink, M., Wanders, N., … Attinger, S. (2017). Toward seamless hydrologic predictions across spatial scales. *Hydrology and Earth System Sciences*, *21*(9), 4323-4346. https://doi.org/10.5194/hess-21-4323-2017

Schäfer, C., Fäth, J., Kneisel, C., Baumhauer, R., & Ullmann, T. (2023). Multidimensional hydrological modeling of a forested catchment in a German low mountain range using a modular runoff and water balance model. *Frontiers in Forests and Global Change*, *6*. https://doi.org/10.3389/ffgc.2023.1186304

Schulla, J. (2021). WaSiM-ETH Documentation. Repéré à http://www.wasim.ch/en/products/wasim_description.htm

Shepard, D. (1968). A two-dimensional interpolation function for irregularly-spaced data. Dans *Proceedings of the 1968 23rd ACM national conference* (pp. 517-524). New York, NY, USA: Association for Computing Machinery. https://doi.org/10.1145/800186.810616

Sun, G., Wei, X., Hao, L., Sanchis, M. G., Hou, Y., Yousefpour, R., … Zhang, Z. (2023). Forest hydrology modeling tools for watershed management : A review. *Forest Ecology and Management*, *530*, 120755. https://doi.org/10.1016/j.foreco.2022.120755

Sylvain, J.-D., Anctil, F., & Thiffault, E. (2021). Using bias correction and ensemble modelling for predictive mapping and related uncertainty : A case study in digital soil mapping. *Geoderma*, *403*, 1-29. https://doi.org/10.1016/j.geoderma.2021.115153

T. W. Chu & A. Shirmohammadi. (2004). EVALUATION OF THE SWAT MODELS HYDROLOGY COMPONENT IN THE PIEDMONT PHYSIOGRAPHIC REGION

OF MARYLAND. *Transactions of the ASAE*, *47*(4), 1057-1073. https://doi.org/10.13031/2013.16579

Tarek, M., Brissette, F. P., & Arsenault, R. (2020). Evaluation of the ERA5 reanalysis as a potential reference dataset for hydrological modelling over North America. *Hydrology and Earth System Sciences*, *24*(5), 2527-2544. https://doi.org/10.5194/hess-24-2527-2020

Tolson, B. A., & Shoemaker, C. A. (2007). Dynamically dimensioned search algorithm for computationally efficient watershed model calibration. *Water Resources Research*, *43*(1). https://doi.org/10.1029/2005WR004723

Valencia Giraldo, M. del C., Ricard, S., & Anctil, F. (2023). Assessment of the Potential Hydrological Impacts of Climate Change in Quebec—Canada, a Refined Neutral Approach. *Water*, *15*(3), 584. https://doi.org/10.3390/w15030584

van Genuchten, M. Th. (1980). A Closed-form Equation for Predicting the Hydraulic Conductivity of Unsaturated Soils. *Soil Science Society of America Journal*, *44*(5), 892-898. https://doi.org/10.2136/sssaj1980.03615995004400050002x

Vose, J. M., Sun, G., Ford, C. R., Bredemeier, M., Otsuki, K., Wei, X., … Zhang, L. (2011). Forest ecohydrological research in the 21st century : What are the critical needs? *Ecohydrology*, *4*(2), 146-158. https://doi.org/10.1002/eco.193

Wang, Q., Deng, H., & Jian, J. (2023). Hydrological Processes under Climate Change and Human Activities : Status and Challenges. *Water*, *15*(23), 4164. https://doi.org/10.3390/w15234164

Weil, R., & Brady, N. (2017). *The Nature and Properties of Soils. 15th edition*. (S.l.): (s.n.).

Wilby, R. L. (2005). Uncertainty in water resource model parameters used for climate change impact assessment. *Hydrological Processes*, *19*(16), 3201-3219. https://doi.org/10.1002/hyp.5819

Xu, C., Widén, E., & Halldin, S. (2005). Modelling hydrological consequences of climate change—Progress and challenges. *Advances in Atmospheric Sciences*, *22*(6), 789-797. https://doi.org/10.1007/BF02918679

Yassin, F., Razavi, S., Wheater, H., Sapriza-Azuri, G., Davison, B., & Pietroniro, A. (2017). Enhanced identification of a hydrologic model using streamflow and sat ellite water storage data : A multicriteria sensitivity analysis and op timization approach. *Hydrological Processes*, *31*(19), 3320-3333. https://doi.org/10.1002/hyp.11267

CHAPITRE 4

ARTICLE 2: TOWARDS A SEMI-ASYNCHRONOUS METHOD FOR HYDROLOGICAL MODELING IN CLIMATE CHANGE STUDIES

Frédéric Talbot[1], Simon Ricard[3], Jean-Daniel Sylvain[2], Guillaume Drolet[2], Annie Poulin[1], Jean-Luc Martel[1] et Richard Arsenault[1]

[1] Département du Génie de la Construction, École de technologie supérieure, Université du Québec, Montréal, H3C 1K3, Canada.
[2] Direction de la recherche forestière, Ministère des Ressources naturelles et des Forêts, Québec, G1P 3W8, Canada.
[3] Sciences et ingénierie, Université Laval, Québec, G1V 0A6, Canada.

Article soumis à la revue « Hydrology and Earth System Sciences », septembre 2024

Abstract

This study assesses the performance of the asynchronous approach used in hydrological modeling, which stands apart from the conventional approach by calibrating streamflow distributions without relying on meteorological observations. The focus is on comparing the two methods within the context of climate change impact studies, particularly in their ability to simulate key hydroclimatic processes across catchments. The analysis, conducted across multiple catchments, including a detailed case study of the Matane catchment in Southern Quebec, explores the potential of the asynchronous method as a viable alternative for future hydrological modeling. By eliminating the dependency on meteorological observations, the asynchronous approach offers potential advantages in regions with limited or unreliable observational data, providing a more flexible tool for climate change impact assessments.

The results reveal that while the asynchronous method effectively captures the overall distribution of streamflow and preserves extreme values, it faces significant challenges in accurately representing the timing of hydrological events, particularly those related to snowmelt. This issue stems, in part, from the method's decision to work directly with the biases present in raw climate model outputs, without adjusting for the timing discrepancies in

meteorological inputs. Consequently, the asynchronous approach inherits these biases, leading to timing inconsistencies and increased variability across different climate models, which raises concerns about the method's ability to reliably simulate critical hydroclimatic variables under future climate scenarios. In contrast, the conventional method, which incorporates bias correction, demonstrates greater reliability in capturing the timing and magnitude of streamflow events, making it a more robust tool for most hydrological applications.

The study also highlights the concept of equifinality, where different methods achieve similar outcomes through potentially flawed mechanisms, particularly in the case of the asynchronous method. Despite projecting changes in hydroclimatic variables similar to those of the conventional method, the asynchronous approach may do so for reasons that are not hydrologically sound, particularly in snow-dominated catchments.

While the asynchronous method shows promise in preserving streamflow extremes, its current implementation requires further refinement to improve its accuracy and reliability, particularly in how it simulates the timing of seasonal dynamics. However, as climate model simulations continue to improve and their biases are progressively reduced, the asynchronous approach is poised to benefit significantly, enhancing its potential for more accurate and reliable future hydrological projections. The conventional method remains the preferred choice for applications requiring hydrological simulations, but future research should focus on developing semi-asynchronous approaches that combine the asynchronous method's strength in preserving extremes with the conventional method's ability to handle event-specific timing.

4.1 Introduction

Climate change is one of the most significant challenges of our time, with profound implications for the Earth's hydrological systems. Alterations in temperature and precipitation regimes affect water availability and the timing of hydrological events.

Understanding these impacts is crucial for effective water resource management and decision-making (Arsenault, Brissette, Malo, Minville, & Leconte, 2013; Calvin et al., 2023). Accurate climate change studies are essential for developing strategies to mitigate and adapt to these changes, ensuring the sustainability of natural resources and the resilience of human and ecological systems (Milly, Dunne, & Vecchia, 2005; Sivakumar, 2011).

The complex dynamics of watersheds require hydrological models capable of precisely simulating both surface and subsurface processes (Farjad, Gupta, & Marceau, 2016; T. W. Chu & A. Shirmohammadi, 2004). Accurate depiction of these processes within hydrological models is essential for assessing the impacts of climate change (Kour, Patel, & Krishna, 2016; Talbot, Sylvain, Drolet, Poulin, & Arsenault, 2024). Physically based and spatially distributed hydrological models, such as the Water Balance Simulation Model (WaSiM) (Schulla, 2021), are particularly valuable due to their detailed representation of key processes including surface runoff, groundwater recharge, interflow, and baseflow. These models enable accurately simulating hydroclimatic variables, which are essential for understanding the physical processes driving water flow and distribution in a catchment (Bormann & Elfert, 2010; Förster et al., 2017; Förster, Garvelmann, Meißl, & Strasser, 2018; Jasper, Calanca, & Fuhrer, 2006; Natkhin, Steidl, Dietrich, Dannowski, & Lischeid, 2012). The use of physically based models like WaSiM, which capture local heterogeneity and finer-scale processes, provides a robust framework for evaluating climate change impacts on hydrology (Devia, Ganasri, & Dwarakish, 2015; Ludwig et al., 2009; Poulin, Brissette, Leconte, Arsenault, & Malo, 2011) and supports stakeholders in making decisions that are both data-driven and aligned with strategic goals.

The conventional method for evaluating climate change impacts on hydrology involves a multi-step modeling chain. This method typically starts with the calibration of a hydrological model using observed meteorological data. Subsequently, raw climate model outputs are corrected using techniques such as quantile mapping (Jakob Themeßl, Gobiet, & Leuprecht, 2011; Mpelasoka & Chiew, 2009) to reduce potential biases in the observed data. The calibrated hydrological model is then driven by these bias-corrected climate data to simulate hydrological processes over both a reference and a future period. By comparing the differences between these two periods, the method estimates the potential effects of climate change on hydroclimatic variables, enabling a clearer understanding of how projected climate changes will influence key hydrological processes.

While widely used, conventional methods have several limitations. Bias correction can disrupt the physical consistency between simulated climate variables and affect long-term climate change signals (Chen, Arsenault, Brissette, & Zhang, 2021; Lee, Lu, Im, & Bae, 2019). Advanced techniques, such as multivariate quantile mapping bias correction (MBCn) (Cannon, 2018), have been developed to address some of these issues, offering a more nuanced approach preserving the inter-variable relationships essential for reliable hydrological modeling.

Chen et al. (2021) further highlights the challenges of maintaining the integrity of climate signals due to the nonstationarity of biases in climate model outputs over time. Their study, which compares pre-processing bias correction of climate model outputs with post-processing corrections applied directly to hydrological model outputs, reveals that while both approaches can significantly reduce biases, they also introduce uncertainties, particularly when dealing with sharp seasonal gradients in correction factors. Despite these challenges, they recommend pre-processing as the preferred method for climate impact studies. Additionally, conventional methods rely on high-quality meteorological observations, which are often unavailable in many regions (Ricard, Lucas-Picher, Thiboult, & Anctil, 2023).

New approaches like asynchronous method have been proposed to address some of these challenges (Ricard et al., 2023; Ricard, Sylvain, & Anctil, 2019, 2020; Valencia Giraldo, Ricard, & Anctil, 2023). This framework avoids the need for bias correction by adapting the hydrological model calibration process to directly use raw climate model projections data. This allows to conduct climate change studies without relying on observed meteorological data. Because the sequence of climatic events within climate model simulations is different from the historical observations, one cannot use the correlation between observed and simulated streamflow during the calibration process. Instead, the asynchronous method focuses on calibrating proxies for the distribution of streamflow rather than reproducing historical time series. Given that most of climate change impact studies assess the projected change in statistical properties between a reference and a future period (Piani, Haerter, & Coppola, 2010), the need for accurate temporal correlation may become less critical (Ricard et al., 2019).

Given its potential advantages, a key question is whether the asynchronous method sacrifices the integrity of hydroclimatic variables in its pursuit of accurately reproducing streamflow distributions. To address this, this study compares hydroclimatic variables simulated by a physically based hydrological model (WaSiM) across 10 catchments, using both the conventional and asynchronous methods for climate change impact assessments. By examining the outcomes of both methods, this research aims to evaluate the asynchronous method's capacity to reliably simulate hydrological processes within catchments. The results highlight the strengths and limitations of the asynchronous framework, offering valuable insights for advancing hydrological modeling in climate change studies.

4.2 Methods and data

4.2.1 Study area

The study focuses on a selection of forested catchments in Southern Quebec, Canada, chosen for their varied sizes and hydrological characteristics. These catchments range in area from 549 km² to 1910 km² (Table 4.1), providing a diverse representation of the region's physiographic and climatic conditions (Fig. 4.1). This subset was selected from catchments previously studied (Talbot et al., 2024), where we have extensive knowledge of their behavior and a well-established baseline for comparison. These catchments are well-suited for hydrological modeling with WaSiM, as their natural hydrological processes remain largely intact and are minimally influenced by human-made structures such as dams. The availability of comprehensive streamflow data further supports their suitability for this study.

The region experiences a humid continental climate, with significant seasonal variation characterized by cold, snowy winters and warm, rainy summers. The Köppen-Geiger Climate Classification designates most of this region as Dfb (Humid Continental Mild Summer Wet All Year), with a smaller northern part classified as Dfc (Subarctic with Cool Summers and Year-round Precipitation) (Beck et al., 2018).

Climatic conditions show marked seasonal variations. Winters, extending from December to February, are cold with significant snowfall, contributing to the snowpack that influences spring runoff. Average temperatures during these months frequently drop below freezing, and snow depths can accumulate substantially, impacting streamflow upon melting.

Summers, from June to August, are characterized by warm temperatures and increased rainfall (Fig. 4.6). The transitional seasons of spring (March to May) and autumn (September to November) exhibit moderate temperatures and variable precipitation, playing a significant role in the hydrological cycle by contributing to groundwater recharge and streamflow variability.

Table 4.1 Physical and meteorological characteristics of the selected catchments in Southern Quebec

Catchments	Area (km^2)	Mean Elevation (m)	Most Common Soil Type	Most Common Land Use	Annual Rainfall [a] (mm)	Annual Snowfall [a] (mm)	Annual Runoff (mm)
Bonaventure	1910	356	Sandy Loam	Coniferous forest	753	446	675
Matane	1650	284	Sandy Loam	Mixed forest	789	480	722
Ouelle	795	315	Sandy Loam	Mixed forest	826	424	604
Bécancour	919	305	Sandy Loam	Deciduous forest	1011	389	743
Nicolet S-O	549	259	Sandy Loam	Cropland	1057	341	719
Au Saumon	738	465	Loam	Deciduous forest	935	446	810
Bras du Nord	642	511	Sandy Loam	Mixed forest	1034	444	952
Du Loup	774	381	Sandy Loam	Mixed forest	795	355	504
Valin	746	441	Sandy Loam	Mixed forest	922	436	988
Godbout	1570	302	Sandy Loam	Coniferous forest	732	434	822

[a] Derived from WaSiM simulations for the period 1981 to 2020, using ERA5 data as input.

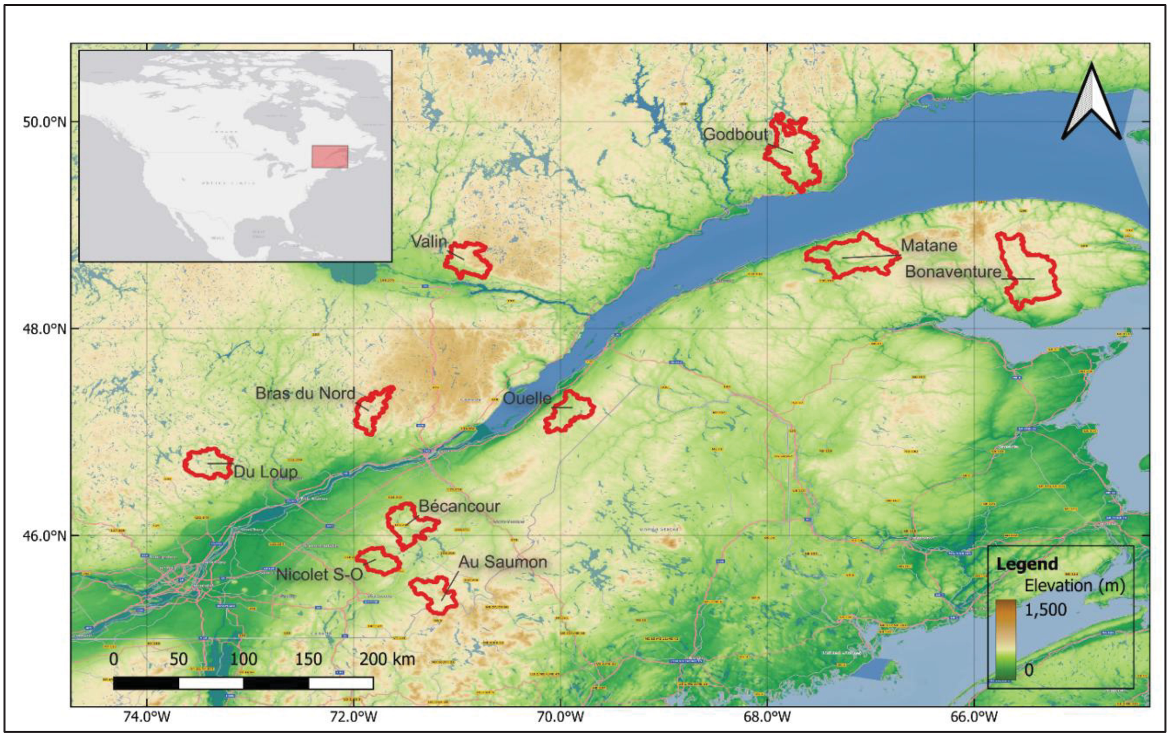

Figure 4.1 Locations of the selected catchments within Southern Quebec

4.2.2 Data

4.2.2.1 Hydrometeorological

This study utilizes daily total precipitation and mean temperature data from the ECMWF Reanalysis v5 (ERA5) (Hersbach et al., 2020) for the period 1981 to 2020. ERA5 was chosen due to its advanced features over previous reanalysis datasets, such as finer spatial resolution, hourly time step, and a more sophisticated data assimilation system that incorporates a wider range of observational inputs (Tarek, Brissette, & Arsenault, 2020). These features make ERA5 a suitable reference dataset for hydrological modeling, as demonstrated in Tarek *et al.* (2020), where ERA5-based hydrological simulations performed equivalently to observational data in most regions, including our study area. Additionally, ERA5 showed reduced biases in temperature and precipitation compared to the ERA-Interim dataset, further justifying its use as a reliable and accurate source of climate data.

Streamflow data was sourced from the *Hydroclimatic Atlas of Southern Québec* (MDDELCC, 2022), covering the period from 1981 to 2010. This dataset provides daily measurements, though some catchments have minor gaps, primarily during winter months due to ice cover and ice jams. These periods were excluded from model calibration and analyses to maintain data accuracy.

4.2.2.2 Elevation

A hydrologically conditioned digital surface model (DEM) was derived from the NASA Shuttle Radar Topography Mission version 3.0 Global 1 arc second (SRTMGL1). Hydrological corrections ensured accurate representation of hydrological networks, with adjustments made using SAGA GIS software (Conrad et al., 2015). Basin delineation and analysis were conducted using QGIS and Tanalys software (Schulla, 2021) to extract essential topographic information for hydrological modeling.

4.2.2.3 Soil type

Soil data was sourced from the SIIGSOL 100 meters database, which provides detailed descriptions of sand, clay, and silt proportions within the soil profile (Ministère des Ressources Naturelles et des Forêts, 2022; Sylvain, Anctil, & Thiffault, 2021). These proportions were converted to soil texture classes based on the USDA classification system (Soil Survey Division Staff, 2017). Soil hydraulic properties were imputed from established relationships between soil texture classes and hydraulic parameters. Elevation data was used to account for soil depth variability, classifying raster cells into deep, normal, and shallow categories based on their relative elevation as described in (Talbot et al., 2024).

4.2.2.4 Land use

Land use data was obtained from the 2015 North American Land Change Monitoring System (NALCMS) 30 meters dataset. This data was resampled using the nearest neighbor method to create land use maps, significantly impacting hydrological parameters such as root distribution, vegetation cover fraction (VCF), roughness length (Z0), and albedo. These parameters influence processes like evapotranspiration, runoff, and infiltration (2015 Land Cover of North America at 30 meters, 2023; Latifovic et al., 2012).

4.2.2.5 Climate models

Projected daily temperature and precipitation data were sourced from the Coupled Model Intercomparison Project Phase 6 (CMIP6) (O'Neill et al., 2016) for both the reference period (1981-2010) and future period (2070-2099). These datasets were accessed and processed through the PAVICS-Hydro platform (Arsenault et al., 2023). The Shared Socioeconomic Pathway 5-8.5 (SSP5-8.5) scenario, which projects very high greenhouse gas emissions, was used to simulate future conditions (Calvin et al., 2023). To address uncertainties related to climate model selection, an ensemble of 18 climate models was employed as it was previously shown that, to ensure robustness, using multiple climate models is required (Arsenault, Brissette, Chen, Guo, & Dallaire, 2020; Lucas-Picher et al., 2021; Minville, Brissette, & Leconte, 2008; Tarek, Brissette, & Arsenault, 2021). This ensemble approach ensures a more robust representation of potential climate outcomes by capturing a range of possible future scenarios.

4.2.3 Hydrological modelling

4.2.3.1 Hydrological model

WaSiM is a physically based, spatially distributed hydrological model designed to simulate water flow processes in catchments. It integrates a comprehensive suite of sub-models to capture key hydrological processes, including surface runoff, groundwater recharge, interflow, and baseflow, within a deterministic framework (Schulla, 2021).

In this study, WaSiM was configured with a spatial resolution of 1000 meters and a temporal resolution of 24 hours. This setup allows for detailed spatial analysis while maintaining computational efficiency. The chosen spatial resolution ensures that the heterogeneity of the landscape is adequately captured, and the daily time step allows for accurate simulation of hydrological processes over time.

WaSiM employs the Richards equation and the Van Genuchten parameters for simulating water flow in the unsaturated zone (Richards, 1931; van Genuchten, 1980). This equation provides a physically based representation of hydraulic head gradients and soil moisture dynamics, incorporating detailed soil physical properties. Groundwater flow is calculated conceptually within the unsaturated zone model.

4.2.3.2 Conventional method

The framework used to calibrate and validate the effectiveness of the conventional method rely on the split sample test (SST) approach, which is widely recognized for its effectiveness in evaluating model performance. This approach involves dividing the data into separate calibration and validation periods, allowing for an assessment of the model's ability to generalize beyond the calibration conditions.

For this method, historical data from ERA5 were used for both calibration and validation. The calibration period spanned from 2000 to 2009, during which simulations were performed over a 15-year period (1995 to 2009), discarding the first 5 years to stabilize the initial conditions of the model. The validation period was set from 1990 to 1999, following the same approach of conducting simulations over a 15-year period (1985 to 1999) and discarding the initial 5 years.

A set of 17 parameters (Table 4.2) was selected for calibration based on model documentation and the configuration used in Talbot, Sylvain, Drolet, et al. (2024). Table 4.2 was taken from Talbot, Sylvain, Drolet, et al. (2024).

Table 4.2 Calibration parameters for the hydrological model WaSiM.

No.	Code	Description	Sub-Model	Range
1	k_D	Storage coefficient for surface runoff (h)	Unsaturated zone	[1, 25]
2	k_H	Storage coefficient for interflow (h)	Unsaturated zone	[1, 25]
3	d_r	Drainage density for interflow (m^{-1})	Unsaturated zone	[1, 50]
4	QD_{Snow}	Fraction of surface runoff on snow melt	Unsaturated zone	[0.1, 1]
5	c_0	Degree-Day factor (mm °C^{-1} d^{-1})	Snow	[0, 3]
6	T_0	Temperature limit for snow melt (°C)	Snow	[-4, 4]
7	$T_{R/S}$	Transition temperature snow/rain (°C)	Snow	[-4, 4]
8	C_{WH}	Water storage capacity of snow	Snow	[0.1, 0.3]
9	C_{rfr}	Coefficient for refreezing	Snow	[0.1, 1]
10	$f_{i,summer}$	Summer correction factors for ETP	Evapotranspiration	[0.1, 2]
11	$f_{i,fall}$	Fall correction factors for ETP	Evapotranspiration	[0.1, 2]
12	$f_{i,winter}$	Winter correction factors for ETP	Evapotranspiration	[0.1, 2]
13	$f_{i,spring}$	Spring correction factors for ETP	Evapotranspiration	[0.1, 2]
14	K_{rec}	Recession constant for hydraulic conductivity	Soil table	[0.1, 0.99]
15	d_z[a]	Soil layer thickness	Soil table	[0.8, 1.4]
16	KB	Storage coefficient for base flow (m)	Unsaturated zone	[0.1, 8]
17	Q0	Scaling factor for base flow (mm h^{-1})	Unsaturated zone	[0.1, 5]

[a] Calibration coefficient, ranging from 0.8 to 1.4, is applied to adjust the total soil depth, which is predetermined to be 8 meters for shallow, 14 meters for normal, and 20 meters for deep soil conditions.

These parameters were optimized based on a single objective function through the Dynamically Dimensioned Search (DDS) algorithm, developed by Tolson and Shoemaker (2007). This algorithm was chosen for its efficiency in handling complex optimization problems for compute-intensive hydrological models, as recommended by Arsenault *et al.* (2014).

The objective function used for calibration was the Kling Gupta-Efficiency (KGE) (Kling, Fuchs, & Paulin, 2012). The KGE metric provides a balanced evaluation of model performance by considering simultaneously correlation, variability, and bias in the simulated streamflow relative to observed streamflow.

The KGE is computed using Eq. (4.1):

$$KGE = 1 - \sqrt{(r-1)^2 + \left(\frac{\sigma_{sim}/\mu_{sim}}{\sigma_{obs}/\mu_{obs}} - 1\right)^2 + \left(\frac{\mu_{sim}}{\mu_{obs}} - 1\right)^2}, \qquad (4.1)$$

where r is the correlation coefficient between simulated and observed streamflow, σ_{sim} is the standard deviation of simulated streamflow, σ_{obs} is the standard deviation of observed streamflow, μ_{sim} is the mean of the simulated streamflow, and μ_{obs} is the mean of the observed streamflow.

A KGE value of 1 indicates a perfect match between the simulated and observed streamflow, reflecting ideal performance across all three components: correlation, variability, and bias.

To address biases in the climate model simulations, the Multivariate Bias Correction algorithm (MBCn) of Cannon (2018) was utilized. This method corrects biases in meteorological data while accounting for spatiotemporal interdependencies between variables and preserving changes in quantiles between the reference (1981-2010) and future (2070-2099) periods. The bias correction was applied to daily total precipitation and daily mean temperature using ERA5 data as the reference over the period 1981-2010 and was used to correct the climate models data for both the reference (1981-2010) and future periods (2070-2099).

For the conventional method, climate change hydrological simulations were performed using the bias-corrected climate models data. Simulations were conducted for each climate model over the reference and future periods using the calibrated hydrological model for each catchment.

4.2.3.3 Asynchronous method

The primary objective of the asynchronous method is to conduct climate change studies without relying on observed meteorological data (Ricard et al., 2023, 2019, 2020) and eliminate the need for bias-correction of climate variables. Instead, the calibration is performed using raw climate model data and observed streamflow, integrating the bias-correction in the calibration step. A significant challenge in this approach is the lack of synchronization between the timings of observed streamflows and those of raw climate model outputs (Ricard et al., 2019), as climate models are not temporally aligned with actual past events. This requires a departure from the conventional calibration framework, which aims to optimize the synchronicity and amplitude of streamflow.

To overcome this obstacle, the objective function optimizes the distribution of observed streamflow over an extended period rather than individual streamflow observations. This approach ensures the hydrological model effectively captures the streamflow distribution, rather than day-to-day natural variability.

Given the calibration objectives of the asynchronous method, the observed streamflow data from 1984 to 2009 was sorted and used to establish a reference distribution of streamflow. This sorted distribution provided a consistent target for both the calibration and validation of the hydrological model. In the context of the asynchronous method, where direct temporal alignment between climate model outputs and observed streamflow is not maintained, relying on the same observed distribution for both calibration and validation ensures that the model is evaluated against a stable and representative reference. Therefore, a 25-year period (1984-2009) was used for both calibration and validation, as it captures a broad range of hydrological conditions, minimizes the influence of short-term climate variability, and mitigates biases that could arise from using shorter time frames. A key hypothesis underlying this approach is the assumption of stationarity—that the hydrological model, with fixed parameters optimized during calibration, will continue to produce reasonable streamflow simulations under future climate conditions. This assumes that despite changing climatic conditions, the model will adequately respond to future scenarios as it did to past conditions. However, if future climate changes introduce conditions outside the model's calibrated range, such as new snow patterns or shifts in seasonal dynamics, the model's performance could be compromised.

The calibration and validation periods are separated based on the total yearly precipitation from October to September. This separation ensures an equal distribution of wet and dry years between both periods. Simulations were performed for the years 1984 to 2011, with the first two years discarded to allow for initial model stabilization. Out of the 26 years of simulations, 13 years were used for calibration, selected based on total yearly precipitation, while all 26 years were utilized for model validation.

To address biases in simulated streamflow resulting from biases in precipitation and temperature in the raw climate data, the simulated streamflow was adjusted by multiplying it by a factor equal to the ratio of the mean observed streamflow Q_{obs} to the mean simulated streamflow Q_{sim}. This adjustment was applied only during the calibration process and not during the reference or future periods simulations. It ensures that the mean simulated streamflow matches the mean observed streamflow, effectively removing bias. This means the simulated absolute streamflow values cannot be directly compared with observations, but changes between the reference and future period can be analyzed.

The Root Mean Square Error (RMSE) was employed as the objective function:

$$RMSE = \sqrt{\frac{1}{n}\sum_{i=1}^{n}\left(Q_{sim_i} - Q_{obs_i}\right)^2} \quad , \qquad (4.2)$$

where Q_{sim} represents the sorted simulated streamflow (mm), Q_{obs} represents the sorted observed streamflow (mm), and n is the number of simulated streamflow values.

Each climate model was calibrated for each catchment, resulting in a total of 180 calibration parameter sets (18 climate models x 10 catchments). In contrast, the conventional method involves 10 calibration parameter sets (one per catchment) which is then applied to all climate models and their bias-corrected outputs. Consequently, the asynchronous method is considerably more computationally intensive than the conventional method in terms of parameter calibration.

The calibration framework for the asynchronous method is similar to that of the conventional method. It involves 1000 trials, uses the same 17 calibration parameters (Table 4.2), and employs DDS optimization algorithm.

For the asynchronous method, climate change simulations were conducted using the calibrated model for each catchment and each projected climate model, but without relying on historical event timing. Raw projected climate data were utilized to perform simulations over both the reference and future periods.

4.2.4 Comparative analysis

The comparative analysis in this study is designed to evaluate the performance of the conventional and asynchronous methods in simulating hydrological processes under both current and future climate conditions. To ensure a fair and unbiased comparison, both methods employed the same WaSiM configuration, including identical calibration parameters, the number of evaluations, and the optimization algorithm. This was performed to ensure minimal calibration bias and to isolate the differences attributable solely to the methodological framework of each approach.

The first step in the comparative analysis involves assessing the calibration and validation performance of each method. Streamflow simulations were evaluated using the KGE for the conventional method and the RMSE of the sorted simulated and observed streamflow for the asynchronous method. These metrics were selected to highlight each method's strengths in different aspects of streamflow simulation—KGE for overall model performance and RMSE for the accuracy of flow distribution.

Beyond streamflow, we also examine the relationships between various hydroclimatic variables, such as groundwater recharge, surface runoff, soil moisture, and snow water equivalent (SWE). By comparing the simulated values from both methods, the analysis seeks to understand how well each method captures the interactions between these variables. This serves to evaluate the internal consistency of the models and assess their ability to realistically simulate the physical processes within the catchments.

The analysis extends to a comparison of the projected changes in hydroclimatic variables between the reference period (1981–2010) and the future period (2070–2099). The magnitude and direction of these changes are assessed to determine how each method projects the impact of climate change on the catchments. This includes examining variables such as changes in snowmelt dynamics, and the consequent effects on streamflow, surface runoff and groundwater recharge.

A detailed spatial analysis is conducted to evaluate the distribution of key variables, such as soil moisture and groundwater recharge, across the catchments. The comparative analysis employs several criteria to determine which method is more effective. These include the accuracy of streamflow simulation (both in terms of overall distribution and event timing), the internal consistency of hydroclimatic variable relationships and the realism of spatial distributions and projected changes under future climate scenarios. The method that consistently demonstrates superior performance across these criteria is considered more reliable for future hydrological modeling and climate impact assessments.

4.3 Results

4.3.1 Streamflow representation performance

For the conventional method, streamflow representation performance was assessed using the KGE metric for each catchment during both the calibration and validation periods.

During calibration, the conventional method achieves KGE values ranging from 0.817 to 0.906, with a mean of 0.863. Similarly, for the validation period, the KGE values ranged from 0.778 to 0.906, with a mean of 0.842. These results indicate that the conventional method maintains a consistent performance in simulating streamflow across different catchments. Detailed KGE results for each catchment are provided in the Appendix C (Table AC.1).

For the asynchronous method, the RMSE was used to evaluate streamflow representation performance during both the calibration and validation periods. During calibration, the RMSE values exhibited a mean of 0.121 mm d^{-1} with a mean standard deviation between climate models of 0.031 mm d^{-1}. In the validation period, the RMSE values demonstrated similar patterns, with a mean of 0.179 mm d^{-1} and a standard deviation of 0.057 mm d^{-1}. Detailed RMSE values are available in the Appendix C (Table AC.2).

Figure 4.2 presents hydrographs of streamflow for both methods during the reference period across the ten catchments, along with observed streamflow for the same period. The asynchronous method shows greater variability between climate models, especially in the timing of peak flows, which often fails to align with the observed data, as expected. This variability suggests that the timing of streamflow events in the asynchronous method is highly sensitive to the specific climate model employed. For instance, in the Matane catchment, the observed and conventional method peak flow occurs at the beginning of May, while the asynchronous method shows a broader range of peak flow timings, extending from early May to late June. This discrepancy might be attributed to challenges in accurately simulating snowmelt processes with the asynchronous method, which are crucial for generating high flows in the study region. Furthermore, in the same catchment, the asynchronous method overestimates summer flows compared to the observed data, indicating potential difficulties in capturing the seasonal dynamics of low-flow periods. Conversely, the conventional method accurately reproduces the annual observed streamflow variability, demonstrating its strength in capturing the timing and magnitude of hydrological events.

Despite these differences, the asynchronous method outperforms the conventional method in terms of annual volume accuracy in 8 out of 10 catchments (Fig. 4.2). This enhanced accuracy can be attributed to the scaling adjustments applied during the calibration period. In the asynchronous method, streamflow is adjusted by multiplying them by a scaling factor to correct biases between simulated and observed means, effectively minimizing the difference between overall volume in simulated and observed streamflow. However, the inability of the asynchronous simulations to replicate the precise timing of streamflow events raises concerns about its representation of underlying hydroclimatic variables, which may impact the model's broader predictive accuracy.

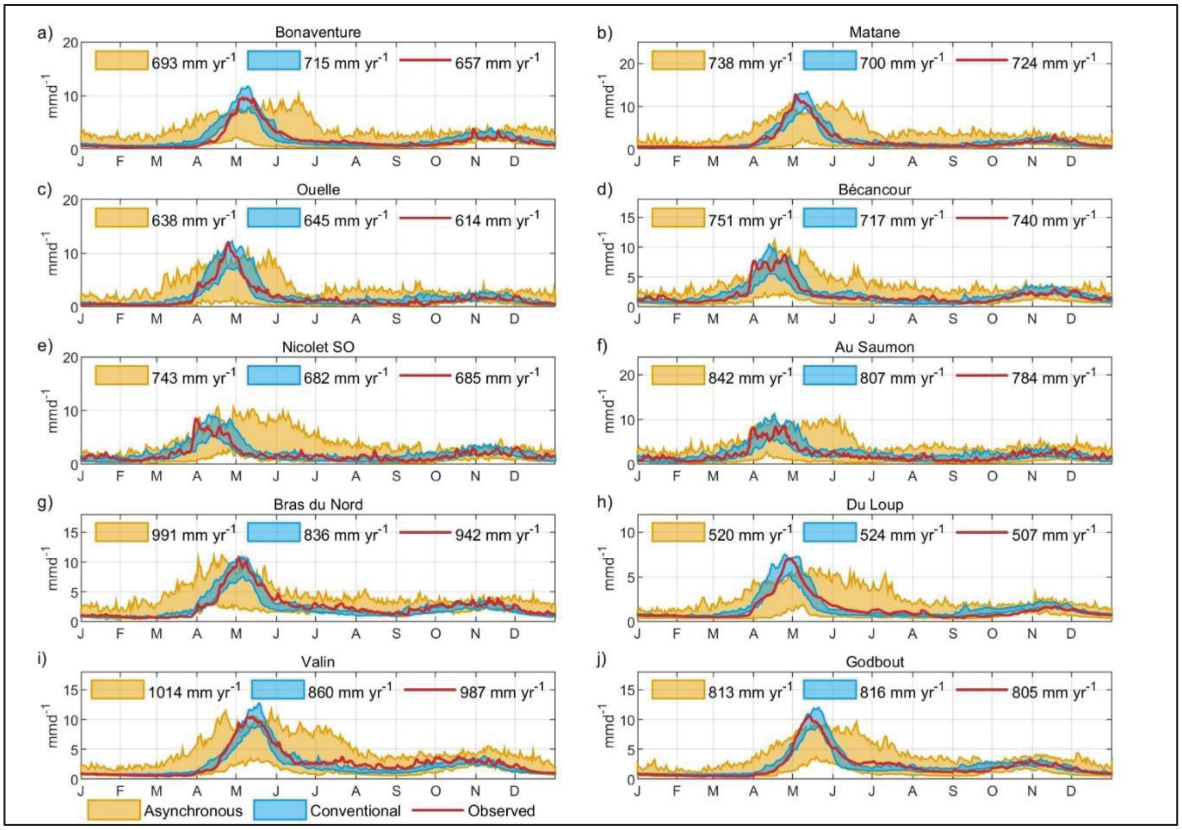

Figure 4.2 Seasonal streamflow comparison between the asynchronous and conventional methods and observed data across ten catchments during the reference period

Figure 4.3 shows the relationship between the sorted streamflow distribution and percentage bias for simulated and observed values using conventional and asynchronous methods during the reference period (1981–2010) for the Matane catchment. Climate models using the conventional method exhibit broader dispersion compared to the asynchronous method. Moreover, the asynchronous method demonstrates a better ability to capture extreme streamflow events, as indicated by its lower percentage bias across a range of streamflow conditions. This suggests that the asynchronous method is more effective in predicting extreme flows and capturing the overall distribution of streamflow, likely due to its calibration focus on streamflow distribution rather than the precise timing of hydrological events.

While these results are specific to the Matane catchment, similar patterns are observed across all catchments studied (Fig. 4.C to Fig. 4.K). This consistency highlights the asynchronous method's strength in capturing the full range of potential streamflow conditions across diverse hydrological settings, particularly in representing extremes.

In contrast, the conventional method excels at capturing the annual fluctuations and timing of the observed streamflow but is more limited in its ability to represent extreme flows. The asynchronous method, optimized for distributions, offers a distinct advantage in this area by more accurately reflecting the range of possible streamflow values, particularly during high and low flow events.

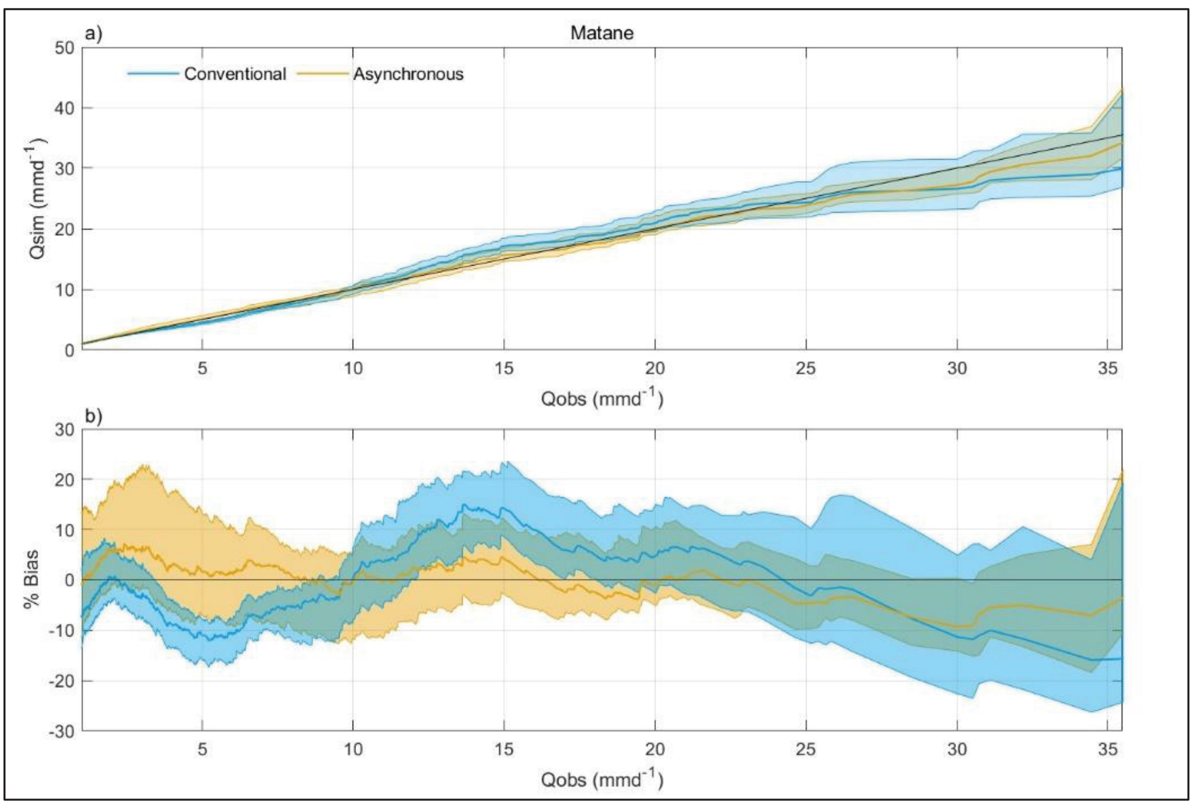

Figure 4.3 Performance comparison between the conventional and asynchronous methods for the Matane catchment during the reference period

Figure 4.4 presents a comparative analysis of streamflow quantiles for both methods across the reference (1981–2010) and future (2070–2099) periods for all ten catchments. When comparing the observed streamflow to the reference period simulations, the asynchronous method shows a closer alignment with the observed distribution, particularly for high flows (Q95% and Q90%), confirming its strength in capturing extreme events. However, it is important to note that the asynchronous method also exhibits a higher dispersion among climate models during the reference period, indicating greater variability in its predictions.

In terms of future projections, both methods demonstrate similar trends, with both projecting decreases in high flows (Q95%) across most catchments. However, the projections for other flow quantiles, such as median (Q50%) and low flows (Q5% and Q10%), show mixed changes that vary depending on the catchment's geographical location. While there is a broad agreement between the methods on the direction of changes from the reference to the future period, the asynchronous method again shows a higher dispersion between climate models, especially for low flows (Q5% and Q10%). This increased variability suggests that while the asynchronous method is effective at representing the distribution of streamflow, it may introduce greater uncertainty in future projections, particularly for low-flow conditions.

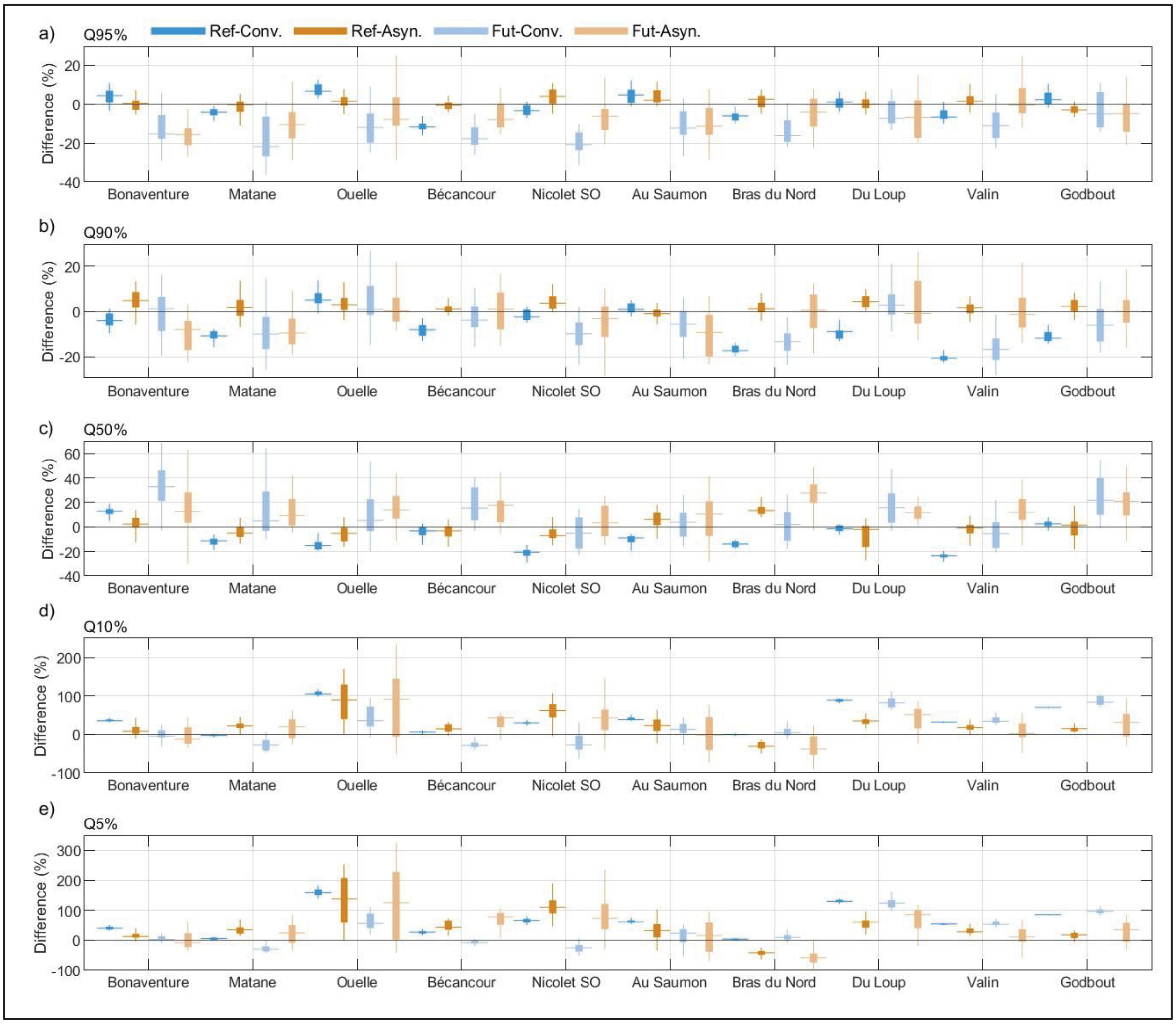

Figure 4.4 Streamflow distribution analysis

4.3.2 Hydroclimatic variables

The primary objective of this study is to compare the conventional and asynchronous methods and evaluate the ability of the asynchronous approach to accurately reproduce the physical processes within catchments. This section expands the analysis beyond streamflow to include a broader range of hydroclimatic variables, providing a more comprehensive assessment of the methods' performance.

Table 4.3 presents the annual averages for several key hydroclimatic variables—such as precipitation, snowfall, streamflow, surface runoff, interflow, actual evapotranspiration (ETa), baseflow, groundwater recharge, SWE, and soil moisture—across both the reference (1981–2010) and future (2070–2099) periods. The table also highlights the relative changes in these variables between the reference and future periods for both the conventional and asynchronous methods.

When comparing the results for the reference and future periods, both methods exhibit similar trends across most hydroclimatic variables. For instance, both methods predict an increase in precipitation and ETa, alongside a significant reduction in snowfall and SWE as a response to the anticipated warming climate.

However, notable differences arise in the representation of certain variables. One of the most significant discrepancies is observed in surface runoff. The asynchronous method predicts more than twice the amount of surface runoff compared to the conventional method, both in the reference and future periods. This substantial difference suggests that the asynchronous method may be simulating surface processes differently than the conventional method.

In terms of relative changes between the reference and future periods, both methods demonstrate similar trends across most variables, indicating agreement on the direction of change due to climate impacts. For example, both methods predict a similar reduction in snowfall (around 33% and 41%) and SWE (around 53% and 58%), reflecting the expected decrease in snow accumulation as temperatures rise. The increase in ETa (31%) is also consistent across both methods, suggesting that higher temperatures will lead to greater evapotranspiration.

Table 4.3 Comparison of hydroclimatic variables

Hydroclimatic Variables	Unit	Conventional			Asynchronous		
		Reference (1981-2010)	Future (2070-2099)	Relative Change	Reference (1981-2010)	Future (2070-2099)	Relative Change
Precipitation	mm yr^{-1}	1276	1463	15%	1328	1507	13%
Snowfall	mm yr^{-1}	409	273	-33%	362	214	-41%
Streamflow	mm yr^{-1}	730	744	2%	771	778	1%
Surface Runoff	mm yr^{-1}	109	77	-29%	256	199	-22%
Interflow	mm yr^{-1}	482	530	10%	400	460	15%
ETa	mm yr^{-1}	554	727	31%	561	733	31%
Baseflow	mm yr^{-1}	140	137	-2%	113	117	3%
Groundwater Recharge	mm yr^{-1}	133	139	4%	118	141	19%
SWE	mm	281	131	-53%	252	106	-58%
Soil Moisture	-	0.188	0.180	-5%	0.203	0.200	-2%

Figure 4.5 illustrates the annual variations of key hydroclimatic variables across different catchments and 18 climate models for both the reference and future periods, comparing the conventional and asynchronous methods. Several noteworthy differences emerge between the two methods, particularly in streamflow, interflow, and groundwater recharge.

The conventional method tends to produce higher peaks for streamflow, interflow and recharge during periods of high streamflow, suggesting a more pronounced response to snowmelt and precipitation events. This method also exhibits greater variability during these high-flow periods. In contrast, the asynchronous method displays higher summer flows.

Both methods predict similar absolute changes in streamflow between the reference and future periods, reflecting a consistent trend across climate projections. However, the conventional method indicates a more substantial decrease in high flows in the future, which could have significant implications for water resource management, particularly in regions where peak flows are crucial for reservoir replenishment and flood control. It is thus important to assess if one of the two methods (conventional vs. asynchronous) can be considered as more reliable than the other as this could affect conclusions of many climate change impact studies.

For surface runoff, the asynchronous method consistently generates higher values compared to the conventional method across both periods. This suggests that the asynchronous method may be simulating more rapid or intense surface processes. Despite these differences in magnitude, both methods exhibit similar trends in absolute change, indicating a projected decrease in surface runoff in the future.

ETa results are closely aligned between the two methods. This consistency suggests that ETa projections are robust across different modeling frameworks, reinforcing confidence in these projections for water balance assessments.

Maximum SWE also shows differences between the two methods. The conventional method predicts higher SWE values, suggesting that it may simulate a more substantial accumulation of snowpack during the winter months. On the other hand, the asynchronous method demonstrates greater variability during the snowmelt period, with snowmelt extending from April to August, compared to a more concentrated snowmelt period from April to June in the conventional method. This extended snowmelt period in the asynchronous method could lead to prolonged high flows in late spring and early summer. However, it is quite unrealistic to observe snow persisting through the summer months, highlighting a significant limitation of the asynchronous method in accurately representing seasonal snow dynamics.

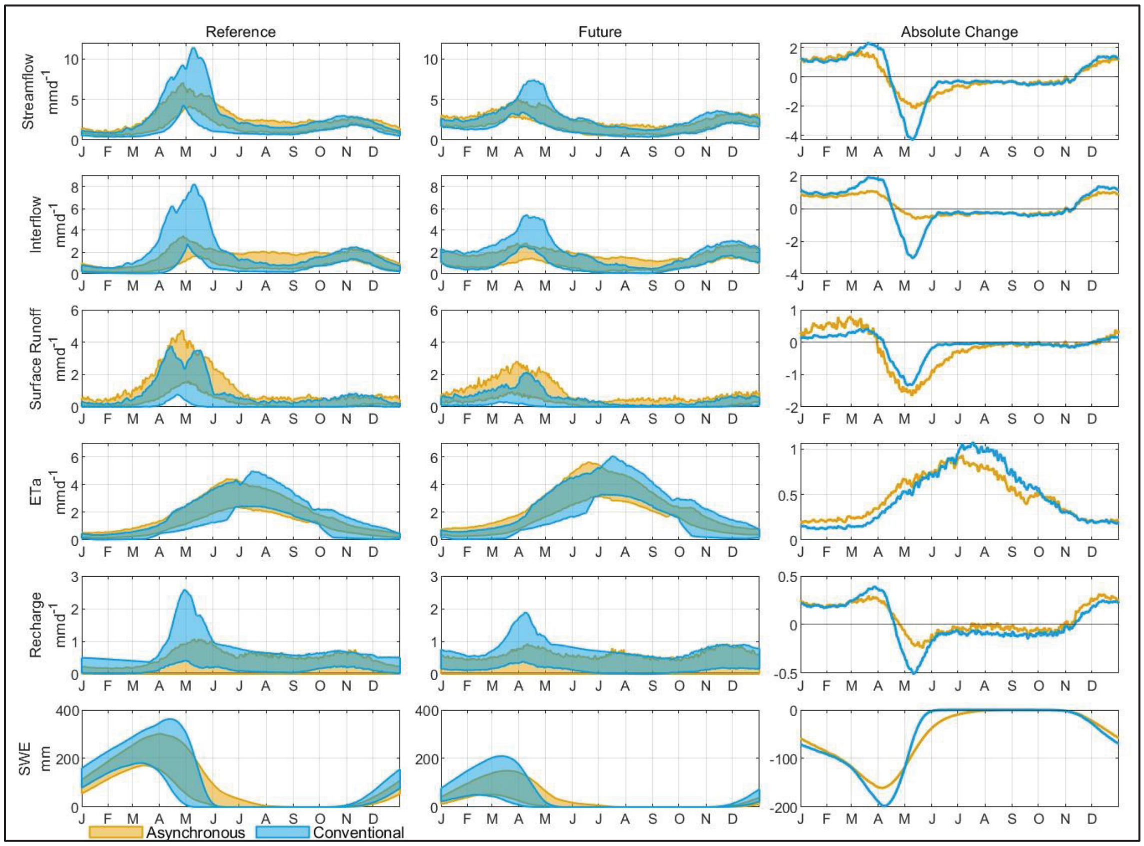

Figure 4.5 Seasonal distribution of key hydroclimatic variables

4.3.3 Case study

To thoroughly assess the asynchronous method's ability to accurately reproduce physical processes within a catchment, the Matane catchment, covering an area of 1650 km², was selected as a case study. This catchment was chosen due to its strong calibration and validation performance under both methods, as well as its representative characteristics of the broader set of studied catchments.

Average monthly temperature and precipitation for the reference period (1981-2010) and the future period (2070-2099) before and after bias-correction using MBCn for the Matane catchment and the climate model ACCESS-ESM1-5 is provided as an example (Fig. 4.6).

In the reference period, a noticeable gap exists between the ERA5 data and the raw climate model data, with the raw climate data showing higher temperatures and increased precipitation for all months except October. The effectiveness of the bias correction is evident, as the bias-corrected climate data closely aligns with the ERA5 data, significantly reducing discrepancies in temperature and precipitation. The same bias trend is observed in the future period, where raw climate model data predicts higher temperatures and increased precipitation compared to the bias-corrected data.

Furthermore, Fig. 4.6 highlights the anticipated changes in precipitation and temperature between the reference and future periods. Temperatures are expected to increase significantly, with projected increases around 6 degrees Celsius across the study area. These projections are in line with the IPCC's forecasts based on SSP5-8.5, and suggest that northern latitudes will experience faster warming compared to the global average (Estrada, Kim, & Perron, 2021). Projections consistently show an annual increase in precipitation ranging from 15 to 20%, with the most significant increases occurring between December and April, as well as in July. The anticipated increases in temperature and changes in precipitation patterns have profound implications for hydrological processes and water resource management.

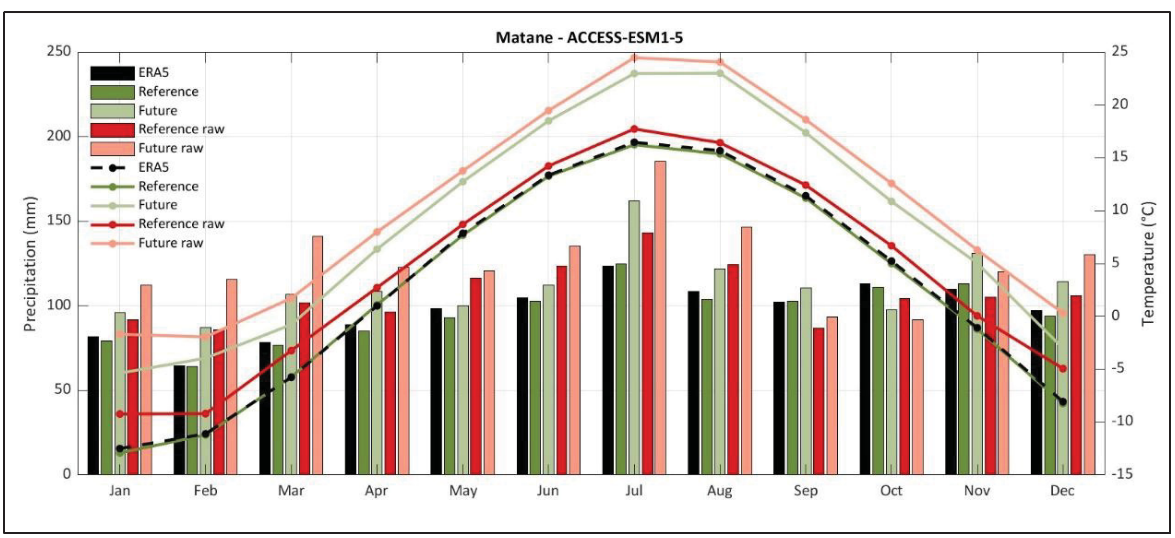

Figure 4.6 Comparison of average monthly precipitation and temperature for the Matane catchment

Figure 4.7 offers a detailed comparison of the annual variations in key hydroclimatic variables for both the reference (1981–2010) and future (2070–2099) periods, using the conventional and asynchronous methods for the Matane catchment. The figure mirrors the approach taken in Fig. 4.5 but focuses specifically on Matane, with the shaded areas indicating the variability across different climate models.

The trends observed in the Matane catchment largely reflect the broader findings across all catchments. For variables such as interflow, streamflow, ETa, surface runoff, and SWE, the asynchronous and conventional methods exhibit patterns that align with the general trends noted in the overall analysis. However, the asynchronous method predicts significantly more groundwater recharge in the Matane catchment compared to the conventional method.

A key observation from Fig. 4.7 is the pronounced variability between climate models when using the asynchronous method. This variability suggests that some climate models may produce an unrealistic representation of physical processes, particularly in relation to snow dynamics. For example, when examining the maximum snow water equivalent, the asynchronous method shows that the snowmelt period can start as early as April and extend as late as July, depending on the climate model. This is problematic, as it is highly unusual to have snow persist into July in the Matane region, making it unrealistic for a 30-year average to show such late snowmelt. This discrepancy raises concerns about the asynchronous method's ability to accurately simulate snow processes, a critical component of the hydrological cycle in regions with significant winter snowfall.

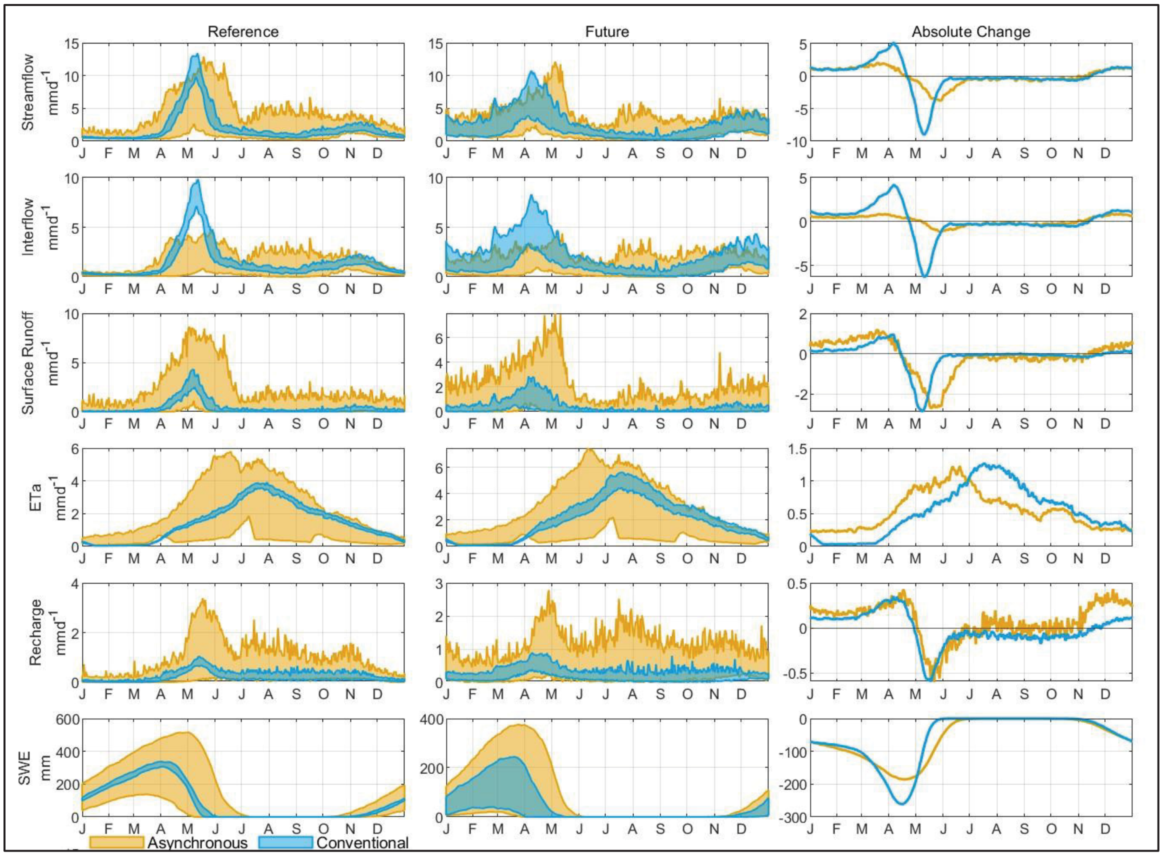

Figure 4.7 Seasonal distribution of key hydroclimatic variables across the Matane catchment for the reference and future period

Figure 8 presents a comparison of SWE for the reference period (1981–2010) across various climate models in the Matane Catchment. Each panel corresponds to a different climate model, with the shaded areas illustrating the range of annual variability. Similar figures for other catchments are provided in Appendix C (Fig. AC.10 to Fig. AC.18).

The figure clearly demonstrates the significant variability in SWE results produced by the asynchronous method compared to the conventional method. This disparity underscores the asynchronous method's challenges in accurately simulating snow patterns. For instance, the asynchronous method exhibits a broad range of SWE values, with the NorESM2-MM model showing only 200 mm of snow cover, while the IPSL-CM6A-LR model projects up to 700 mm for the same period. Additionally, the duration of snow accumulation varies widely within the asynchronous method. NorESM2-MM, for example, depicts snow presence from

November to May, whereas EC-Earth3 suggests snow from October extending into July. These inconsistencies indicate a potential weakness in the asynchronous method's ability to capture snow dynamics.

In contrast, the conventional method consistently produces more stable and realistic results across different climate models, accurately reflecting the expected behaviour of snow accumulation and melt processes.

The poor representation of snow processes for asynchronous method is not limited to the Matane catchment. Other catchments, such as Valin and Godbout, exhibit similar anomalies, with snow present from November to September in some cases. Particularly striking is one climate model simulation in the Godbout catchment, where the asynchronous method predicts snow cover persisting throughout 11 months of the year. In the Bras du Nord catchment, the asynchronous method predicts roughly half the amount of snow compared to the conventional method, further highlighting again inadequate representation of snow accumulation and melt dynamics.

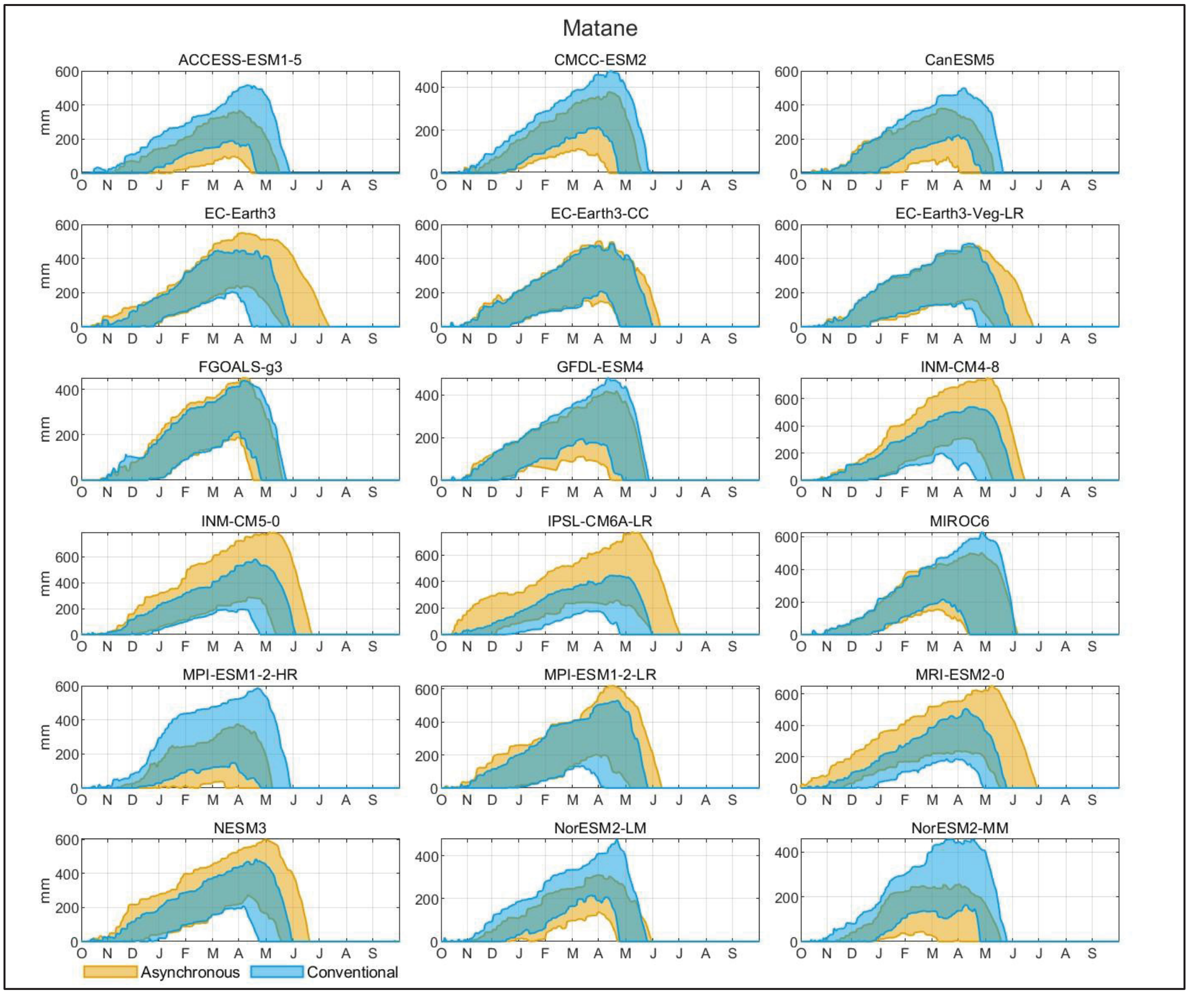

Figure 4.8 Snow water equivalent (SWE) comparison for the Matane catchment

Figure 4.9 illustrates the spatial distribution of annual groundwater recharge rates in the Matane catchment for both the reference (1981–2010) and future (2070–2099) periods, comparing the results from the conventional and asynchronous methods. Both methods exhibit similar spatial patterns, with higher elevations showing reduced recharge rates and lower elevations demonstrating higher recharge rates. An elevation map of the Matane catchment is provided in the Appendix C (Fig. AC.19). The asynchronous method, however, predicts a generally higher magnitude of recharge across the catchment.

When examining the absolute difference between the future and reference periods, both methods project a similar spatial pattern of changes in groundwater recharge, with a noticeable decrease in recharge at lower elevations. However, the asynchronous method projects smaller increases in recharge in certain higher elevation areas, while the conventional method predicts a much more pronounced reduction—3 to 4 times greater—at lower elevations.

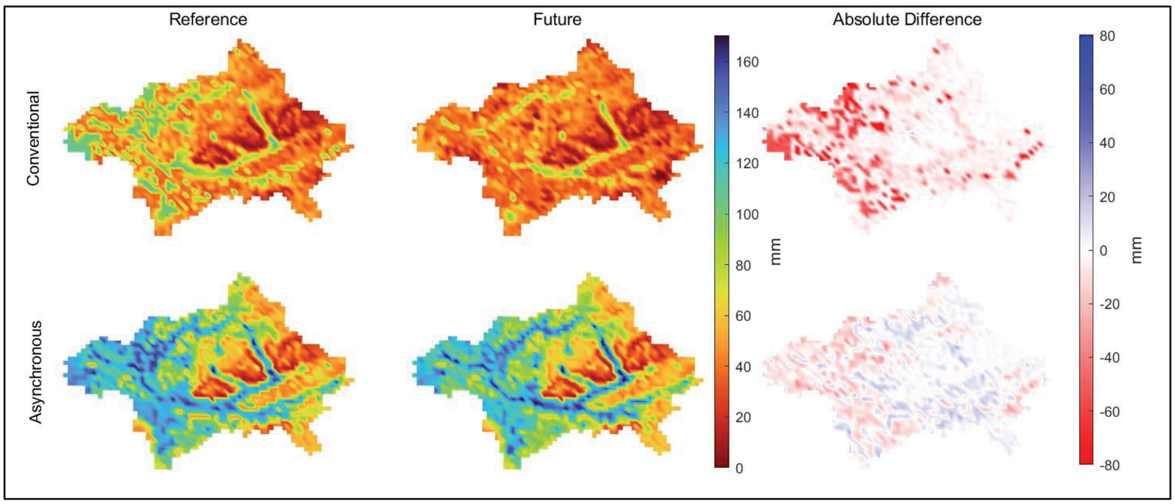

Figure 4.9 Spatial distribution of annual groundwater recharge in the Matane catchment

Figure 4.10 illustrates the spatial distribution of soil moisture across the Matane catchment for both the reference period (1981–2010) and the future period (2070–2099), comparing results from the conventional and asynchronous methods. Both methods demonstrate that soil moisture distribution is heavily influenced by soil type, as indicated by the consistent spatial patterns observed (detailed soil type information is provided in the Appendix 4, Fig. AC.19). The soil moisture maps show that areas with finer soils, such as loam, tend to have higher moisture retention, while coarser soils, such as sandy loams, exhibit lower moisture levels.

The asynchronous method tends to generate slightly higher soil moisture values compared to the conventional method, particularly in areas with inherently higher moisture retention capacity. The asynchronous method also displays greater variability in soil moisture patterns. In terms of absolute changes between the reference and future periods, the conventional method projects a general decrease in soil moisture, predominantly in regions with initially higher moisture values. The asynchronous method, while also projecting a decrease in soil moisture around high moisture areas, shows a more complex pattern with small regions exhibiting increases in soil moisture. Finally, it is noteworthy that the patterns of groundwater and soil moisture during the reference and future periods are spatially consistent and exhibit similar trends.

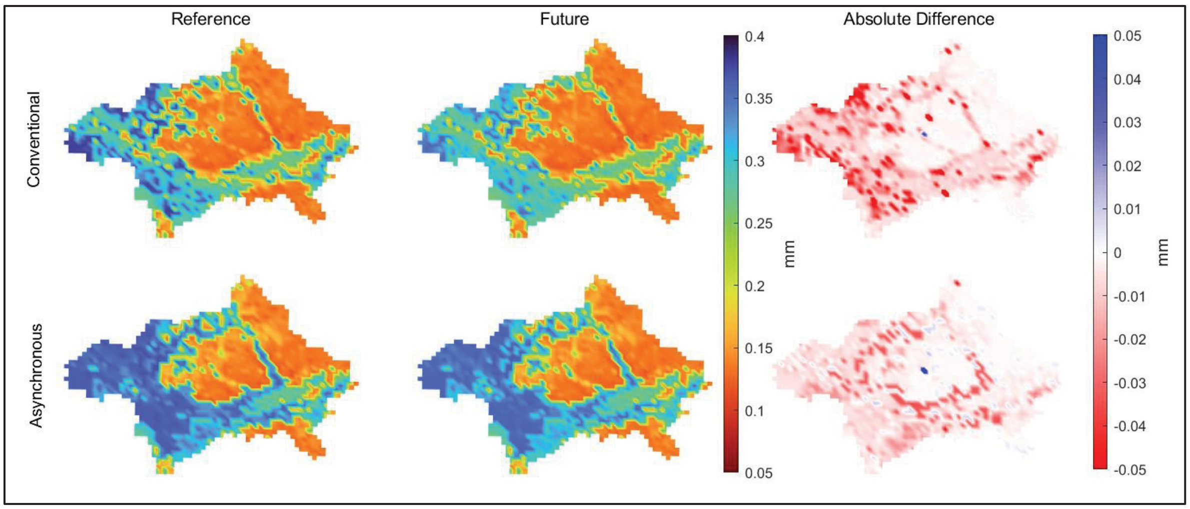

Figure 4.10
Spatial distribution of soil moisture in the Matane catchment

4.4 Discussion

The primary goal of this study was to evaluate the ability of the asynchronous method in reproducing key hydroclimatic processes within a catchment and to compare its performance according to the conventional method. Through detailed analyses across multiple catchments, including a focused case study on the Matane catchment, this study aimed to determine whether the asynchronous method could offer a robust alternative to the conventional method, particularly in the context of climate change impact studies.

4.4.1 Hydroclimatic variables representation

One benefit of the asynchronous method is its ability to better represent extreme higher values (Q95% and Q90%) compared to conventional approach. By aligning the flow distribution with observed data, the asynchronous method effectively reproduces the magnitude of these high flow events, which is critical for managing flood risks under future climate conditions.

However, despite its strengths in representing streamflow distributions, this study's findings align with other research indicating that the asynchronous method struggles to accurately capture the timing of observed streamflow, particularly during spring high-flow events (Ricard et al., 2023). This issue contrasts with earlier findings by Ricard *et al.* (2020), who reported that the asynchronous modeling approach provided a superior representation of the hydrologic regime compared to the conventional method.

The asynchronous method performs comparably to the conventional method when it comes to representing the spatial distribution of hydroclimatic variables such as soil moisture and groundwater recharge. This similarity is likely due to the strong correlation between these hydroclimatic variables and the physical properties of the catchment, such as elevation and soil type (Talbot et al., 2024). The consistent representation of these variables across both methods suggests that the fundamental physical processes driving these patterns are well-captured, irrespective of the methodological differences in how streamflow is simulated.

The asynchronous method shows consistency with the conventional method in predicting the overall trends for several variables, such as increases in precipitation and ETa, as well as decreases in SWE and snowfall. These findings align with broader climate change projections for the region, which anticipate warmer temperatures leading to reduced snow accumulation and altered precipitation patterns (Aygün, Kinnard, Campeau, & Pomeroy, 2022; Nolin et al., 2023; Valencia Giraldo et al., 2023). However, while the overall trends may appear consistent, the underlying processes and the accuracy of the projections differ significantly between the two methods.

Despite these consistencies, a significant issue with the asynchronous method is its high sensitivity to variability in climate models. This problem comes from the biases inherent in climate models, which often lead to the simulation of hydrological processes occurring either too early or too late (Chen et al., 2021; Ricard et al., 2023). The asynchronous method, as currently implemented, adjust the calibration parameters to correct for biases, assuming that these biases remain constant over time. Consequently, if a climate model has a significant or nonstationary biases, the asynchronous method will perpetuate these biases, leading to inaccuracies in the timing of peak flows and the representation of hydroclimatic variables. Ricard *et al.* (2023) also emphasizes this vulnerability, noting that the asynchronous method is particularly prone to producing outlying projections due to the uncorrected biases in raw climate model outputs.

One of the most critical issues highlighted in this study is the concept of equifinality, where different models or methods achieve similar outcomes for different reasons (Mei et al., 2023; Yassin et al., 2017). In the case of the asynchronous method, it appears to replicate certain aspects of the conventional method's projections, but it does so through potentially flawed mechanisms.

The asynchronous method struggles to synchronize streamflow with the actual timing of hydrological events, particularly snowmelt. This lack of synchronization leads to a cascade of flawed mechanisms throughout the model. For instance, when snowmelt occurs too early or too late, the timing and magnitude of surface runoff are inaccurately represented, which can lead to unrealistic increases in surface runoff during inappropriate seasons. This misalignment also affects evapotranspiration and groundwater recharge, causing large, unrealistic variations, further skewing the model's output. Because the streamflow is not properly synchronized with the seasonal dynamics, the asynchronous method ultimately produces streamflow simulations that may match the overall distribution of the observations but do so for the wrong reasons.

Equifinality becomes particularly problematic in this context because the asynchronous method may achieve similar projected changes in hydroclimatic variables as the conventional method, but for reasons that are not hydrologically sound. This brings into question the reliability of its projections, especially when the method demonstrates high variability among different climate models. Such variability, coupled with the method's inability to accurately replicate key hydrological processes, suggests that the asynchronous method, as implemented in this study, may not provide a robust framework for analyzing climate change impacts on hydroclimatic variables.

In contrast, the conventional method excels at addressing the timing of hydrological events due to its optimization process, which incorporates the synchronization between observed and simulated flows. This synchronization allows the model to more accurately capture the timing of hydrological processes, such as snowmelt and peak flows. Given the importance of this synchronicity, it would be beneficial for the asynchronous method to integrate a similar measure of event timing. This adjustment could pave the way for a semi-asynchronous approach that balances the strengths of both methods, offering better overall performance in hydrological simulations.

4.4.2 Advantages and limitations

Both the conventional and asynchronous methods present distinct advantages and limitations. One of the most notable distinctions between the two methods lies in how they handle extremes. The Multivariate Bias Correction (MBCn) approach, typically used in the conventional method, tends to dampen the extremes, smoothing out the peaks. In contrast, the asynchronous method, which calibrates directly on the distribution of streamflow without bias correction, preserves (or attempts to preserve) these extremes (Ricard et al., 2023). Maintaining extreme values may provide a more realistic representation of potential high-impact events.

Another critical consideration is the computational demand of the asynchronous method. Due to its reliance calibration on every climate model, the asynchronous method requires significantly more computational time in the calibration process. This increased computational cost must be weighed against the benefits of using the asynchronous method, particularly when the conventional method might achieve similar results with less computational effort and more established reliability.

The performance of the asynchronous method in snow-dominated catchments has proven to be problematic in this study. The method's inability to accurately capture snowmelt processes, as evidenced by the unrealistic snow retention and melt timing, casts doubt on its utility in regions where snow dynamics play a critical role in the hydrological cycle. Additionally, the high variability observed between climate models when using the asynchronous method suggests that the approach may be overly sensitive to the inherent uncertainties present in raw climate data. This variability complicates the interpretation of results and diminishes confidence in the method’s projections, particularly in scenarios where precise predictions are required for decision-making.

The key takeaway from this study is that while the asynchronous method allowed preserving the distribution of streamflow and maintaining extremes, it does so at the cost of increased variability and potential inaccuracies in simulating critical hydrological processes, particularly those related to snow. Therefore, the asynchronous method, as implemented in this study, should be used with caution, especially in snow-dominated catchments where accurate representation of snowmelt is crucial. However, the asynchronous method could be useful in scenarios where the distribution of extremes is of particular interest, such as in regions where the temporal distribution of streamflow is less critical than the overall volume
The conventional method, which is optimize to account for event-specific dynamics, remains the more reliable option for most applications, particularly when the goal is to simulate the timing and magnitude of streamflow events with a higher degree of accuracy.

Ultimately, these findings aim to inform decision-making in critical sectors such as agriculture, water resource management, urban planning, and environmental conservation. For example, soil moisture data is essential in agriculture for optimizing irrigation and improving crop yields, as well as in environmental management for maintaining wetlands and forest ecosystems. Groundwater recharge data supports sustainable management of aquifers, which is crucial for drinking water supplies, agriculture, and industrial use, while also guiding urban planning to avoid flooding or subsidence. Surface runoff modeling is vital for flood prevention and urban infrastructure design, ensuring stormwater systems can handle heavy rainfall. Lastly, streamflow data is key to water resource management, enabling efficient allocation for agriculture and industry, flood forecasting, and optimizing hydroelectric power generation. By providing detailed projections of these key hydroclimatic variables, this study supports adaptive management strategies across a wide range of sectors impacted by climate change.

4.4.3 Future directions

Looking forward, one of the most promising avenues for improving the asynchronous method is the integration of synchronicity, leading to the development of a semi-asynchronous approach. This hybrid method would combine the strengths of both the conventional and asynchronous methods, offering a more balanced solution that mitigates the weaknesses observed in each. By incorporating synchronicity into the calibration process, the semi-asynchronous method would better align the timing of hydrological events, such as snowmelt, with observed data, improving its ability to capture critical seasonal dynamics.
For instance, modifying the objective function to calibrate based on seasonal or monthly data could enhance the model's ability to simulate hydrological processes. This integration of event timing into the calibration process is crucial for addressing the timing discrepancies that currently limit the asynchronous method's performance.

In parallel, ongoing advancements in climate modeling provide an opportunity to further refine the semi-asynchronous approach. As climate models become more accurate, with fewer biases and enhanced temporal precision, the challenges of synchronization in the current asynchronous method could be significantly alleviated. These improvements would enable the semi-asynchronous method to offer more robust and reliable simulations of hydrological processes under future climate scenarios, positioning it as a more versatile tool for climate impact assessments.

4.5 Conclusion

This study aimed to evaluate the performance of the asynchronous method in comparison to the conventional method for simulating key hydroclimatic variables within catchments, with a focus on the implications for climate change impact studies. Through a detailed analysis of multiple catchments, including a focused case study on the Matane catchment, the study has revealed several important insights into the strengths and limitations of both methods.

The findings indicate that while the asynchronous method shows promise in accurately preserving extreme values, it struggles significantly with the timing of hydrological events, particularly those related to snowmelt. This timing issue is critical in snow-dominated catchments, where accurate snowmelt representation is crucial for reliable hydrological modeling. The asynchronous method's vulnerability to equifinality, nonstationarity and biases in climate models further complicates its application, often leading to increased variability and potential inaccuracies in key hydrological processes which may not be hydrologically sound.

In contrast, the conventional method, with its bias correction step, provides more reliable simulations of event-specific dynamics, particularly in capturing the timing and magnitude of streamflow events, but at cost of underestimating extreme hydrological events. This reliability makes it a more suitable choice for most hydrological applications, especially in regions where precise timing of hydrological events is essential.

From a practical standpoint, while the asynchronous method offers the advantage of preserving extremes, it comes at the cost of increased computational demand and variability in projections, which may limit its utility in certain contexts. The conventional method, on the other hand, remains a robust and reliable tool for simulating hydrological processes under future climate scenarios, particularly when accuracy in timing is a critical factor.

Looking ahead, there are significant opportunities to refine the asynchronous method, particularly by integrating synchronicity into the calibration process to better capture seasonal dynamics. This enhancement could lead to the development of a semi-asynchronous approach that combines the strengths of both the asynchronous and conventional methods, addressing the current challenges related to event timing while preserving the ability to model extremes. Such a hybrid method would offer a more balanced solution, improving accuracy in snowmelt representation and other critical hydrological processes.

Until these refinements are realized, the asynchronous method should be applied with caution, especially in regions where precise seasonal dynamics, such as snowmelt, are critical. Future research should focus on advancing the semi-asynchronous method, ultimately aiming to create a more versatile and robust tool for hydrological modeling in the context of climate change.

4.6 Acknowledgements

This work was funded jointly by the ministère des Ressources naturelles et des Forêts (Quebec, Canada, project number 112332187 conducted at the Direction de la recherche forestière and led by Jean-Daniel Sylvain) and the Forest research service contract number 3322-2022-2187-01 obtained by Richard Arsenault from the Ministère des Ressources naturelles et des Forêts (Quebec, Canada). The authors also acknowledge the use of ChatGPT-4 for assistance in correcting spelling mistakes and improving the flow of text during the manuscript preparation process. The base map in Fig. 4.1 was created using ArcGIS® software by Esri. ArcGIS® and ArcMap™ are the intellectual property of Esri and are used herein under license. Copyright © Esri. All rights reserved. For more information about Esri® software, please visit www.esri.com.

4.7 References

Arsenault, R., Brissette, F., Chen, J., Guo, Q., & Dallaire, G. (2020). NAC2H : The North American Climate Change and Hydroclimatology Data Set. *Water Resources Research*, *56*(8), e2020WR027097. https://doi.org/10.1029/2020WR027097

Arsenault, R., Brissette, F., Malo, J.-S., Minville, M., & Leconte, R. (2013). Structural and Non-Structural Climate Change Adaptation Strategies for the Péribonka Water Resource System. *Water Resources Management*, *27*(7), 2075-2087. https://doi.org/10.1007/s11269-013-0275-6

Arsenault, R., Huard, D., Martel, J.-L., Troin, M., Mai, J., Brissette, F., … Langlois, S. (2023). The PAVICS-Hydro platform : A virtual laboratory for hydroclimatic modelling and forecasting over North America. *Environmental Modelling & Software*, *168*, 105808. https://doi.org/10.1016/j.envsoft.2023.105808

Arsenault, R., Poulin, A., Côté, P., & Brissette, F. (2014). Comparison of Stochastic Optimization Algorithms in Hydrological Model Calibration. *Journal of Hydrologic Engineering*, *19*(7), 1374-1384. https://doi.org/10.1061/(ASCE)HE.1943-5584.0000938

Aygün, O., Kinnard, C., Campeau, S., & Pomeroy, J. W. (2022). Landscape and climate conditions influence the hydrological sensitivity to climate change in eastern Canada. *Journal of Hydrology*, *615*, 128595. https://doi.org/10.1016/j.jhydrol.2022.128595

Beck, H. E., Zimmermann, N. E., McVicar, T. R., Vergopolan, N., Berg, A., & Wood, E. F. (2018). Present and future Köppen-Geiger climate classification maps at 1-km resolution. *Scientific Data*, *5*(1), 180214. https://doi.org/10.1038/sdata.2018.214

Bormann, H., & Elfert, S. (2010). Application of WaSiM-ETH model to Northern German lowland catchments : Model performance in relation to catchment characteristics and sensitivity to land use change. Dans *Advances in Geosciences* (Vol. 27, pp. 1-10). Copernicus GmbH. https://doi.org/10.5194/adgeo-27-1-2010

Calvin, K., Dasgupta, D., Krinner, G., Mukherji, A., Thorne, P. W., Trisos, C., … Péan, C. (2023). *IPCC, 2023 : Climate Change 2023: Synthesis Report. Contribution of Working Groups I, II and III to the Sixth Assessment Report of the Intergovernmental Panel on Climate Change [Core Writing Team, H. Lee and J. Romero (eds.)]. IPCC, Geneva, Switzerland.* Intergovernmental Panel on Climate Change (IPCC). https://doi.org/10.59327/IPCC/AR6-9789291691647

Cannon, A. J. (2018). Multivariate quantile mapping bias correction : An N-dimensional probability density function transform for climate model simulations of multiple variables. *Climate Dynamics*, *50*(1), 31-49. https://doi.org/10.1007/s00382-017-3580-6

Chen, J., Arsenault, R., Brissette, F. P., & Zhang, S. (2021). Climate Change Impact Studies : Should We Bias Correct Climate Model Outputs or Post-Process Impact Model Outputs? *Water Resources Research*, *57*(5), e2020WR028638. https://doi.org/10.1029/2020WR028638

Commission for Environmental Cooperation. (2020). 2015 Land Cover of North America ar 30 meters. *Commission for Environmental Cooperation*. Repéré à http://www.cec.org/north-american-environmental-atlas/land-cover-30m-2015-landsat-and-rapideye/

Conrad, O., Bechtel, B., Bock, M., Dietrich, H., Fischer, E., Gerlitz, L., … Böhner, J. (2015). System for Automated Geoscientific Analyses (SAGA) v. 2.1.4. *Geoscientific Model Development*, *8*(7), 1991-2007. https://doi.org/10.5194/gmd-8-1991-2015

Devia, G. K., Ganasri, B. P., & Dwarakish, G. S. (2015). A Review on Hydrological Models. *Aquatic Procedia*, *4*, 1001-1007. https://doi.org/10.1016/j.aqpro.2015.02.126

Estrada, F., Kim, D., & Perron, P. (2021). Spatial variations in the warming trend and the transition to more severe weather in midlatitudes. *Scientific Reports*, *11*(1), 145. https://doi.org/10.1038/s41598-020-80701-7

Farjad, B., Gupta, A., & Marceau, D. J. (2016). Annual and Seasonal Variations of Hydrological Processes Under Climate Change Scenarios in Two Sub-Catchments of a Complex Watershed. *Water Resources Management*, *30*(8), 2851-2865. https://doi.org/10.1007/s11269-016-1329-3

Förster, K., Garvelmann, J., Meißl, G., & Strasser, U. (2018). Modelling forest snow processes with a new version of WaSiM. *Hydrological Sciences Journal*, *63*(10), 1540-1557. https://doi.org/10.1080/02626667.2018.1518626

Förster, K., Meißl, G., Marke, T., Pohl, S., Garvelmann, J., Schulla, J., & Strasser, U. (2017). A new snow-vegetation interaction extension for the Water Balance Simulation Model (WaSiM), 2620. Communication présentée au EGU General Assembly Conference Abstracts. Repéré à https://ui.adsabs.harvard.edu/abs/2017EGUGA..19.2620F

Hersbach, H., Bell, B., Berrisford, P., Hirahara, S., Horányi, A., Muñoz-Sabater, J., … Thépaut, J.-N. (2020). The ERA5 global reanalysis. *Quarterly Journal of the Royal Meteorological Society*, *146*(730), 1999-2049. https://doi.org/10.1002/qj.3803

Hydroclimatic Atlas of Southern Québec. (2022). Repéré à https://www.cehq.gouv.qc.ca/atlas-hydroclimatique/index-en.htm

Jakob Themeßl, M., Gobiet, A., & Leuprecht, A. (2011). Empirical-statistical downscaling and error correction of daily precipitation from regional climate models. *International Journal of Climatology*, *31*(10), 1530-1544. https://doi.org/10.1002/joc.2168

Jasper, K., Calanca, P., & Fuhrer, J. (2006). Changes in summertime soil water patterns in complex terrain due to climatic change. *Journal of Hydrology*, *327*(3), 550-563. https://doi.org/10.1016/j.jhydrol.2005.11.061

Kling, H., Fuchs, M., & Paulin, M. (2012). Runoff conditions in the upper Danube basin under an ensemble of climate change scenarios. *Journal of Hydrology*, *424-425*, 264-277. https://doi.org/10.1016/j.jhydrol.2012.01.011

Kour, R., Patel, N., & Krishna, A. P. (2016). Climate and hydrological models to assess the impact of climate change on hydrological regime : A review. *Arabian Journal of Geosciences*, *9*(9), 544. https://doi.org/10.1007/s12517-016-2561-0

Latifovic, R., Homer, C., Ressl, R., Pouliot, D. A., Hossian, S., Colditz, R., … Victoria, A. (2012). North American Land Change Monitoring System. *Remote Sensing of Land Use and Land Cover : Principles and Applications*, 303-324. https://doi.org/10.1201/b11964-24

Lee, M.-H., Lu, M., Im, E.-S., & Bae, D.-H. (2019). Added value of dynamical downscaling for hydrological projections in the Chungju Basin, Korea. *International Journal of Climatology*, *39*(1), 516-531. https://doi.org/10.1002/joc.5825

Lucas-Picher, P., Lachance-Cloutier, S., Arsenault, R., Poulin, A., Ricard, S., Turcotte, R., & Brissette, F. (2021). Will Evolving Climate Conditions Increase the Risk of Floods of the Large U.S.-Canada Transboundary Richelieu River Basin? *JAWRA Journal of the American Water Resources Association*, *57*(1), 32-56. https://doi.org/10.1111/1752-1688.12891

Ludwig, R., May, I., Turcotte, R., Vescovi, L., Braun, M., Cyr, J.-F., … Mauser, W. (2009). The role of hydrological model complexity and uncertainty in climate change impact assessment. *Advances in Geosciences*, *21*, 63-71. https://doi.org/10.5194/adgeo-21-63-2009

Mei, Y., Mai, J., Do, H. X., Gronewold, A., Reeves, H., Eberts, S., … Hunt, R. J. (2023). Can Hydrological Models Benefit From Using Global Soil Moisture, Evapotranspiration, and Runoff Products as Calibration Targets? *Water Resources Research*, *59*(2), e2022WR032064. https://doi.org/10.1029/2022WR032064

Milly, P. C. D., Dunne, K. A., & Vecchia, A. V. (2005). Global pattern of trends in streamflow and water availability in a changing climate. *Nature*, *438*(7066), 347-350. https://doi.org/10.1038/nature04312

Ministère des Ressources Naturelles et des Forêts. (2022). *SIIGSOL-100m—Carte des propriétés du sol*. Données Québec. Repéré à https://www.donneesquebec.ca/recherche/dataset/siigsol-100m-carte-des-proprietes-du-sol

Minville, M., Brissette, F., & Leconte, R. (2008). Uncertainty of the impact of climate change on the hydrology of a nordic watershed. *Journal of Hydrology*, *358*(1), 70-83. https://doi.org/10.1016/j.jhydrol.2008.05.033

Mpelasoka, F. S., & Chiew, F. H. S. (2009). Influence of Rainfall Scenario Construction Methods on Runoff Projections. https://doi.org/10.1175/2009JHM1045.1

Natkhin, M., Steidl, J., Dietrich, O., Dannowski, R., & Lischeid, G. (2012). Differentiating between climate effects and forest growth dynamics effects on decreasing groundwater recharge in a lowland region in Northeast Germany. *Journal of Hydrology*, *448-449*, 245-254. https://doi.org/10.1016/j.jhydrol.2012.05.005

Nolin, A. F., Girardin, M. P., Adamowski, J. F., Barzegar, R., Boucher, M.-A., Tardif, J. C., & Bergeron, Y. (2023). Observed and projected trends in spring flood discharges for the Upper Harricana River, eastern boreal Canada. *Journal of Hydrology : Regional Studies*, *48*, 101462. https://doi.org/10.1016/j.ejrh.2023.101462

O'Neill, B. C., Tebaldi, C., van Vuuren, D. P., Eyring, V., Friedlingstein, P., Hurtt, G., … Sanderson, B. M. (2016). The Scenario Model Intercomparison Project (ScenarioMIP) for CMIP6. *Geoscientific Model Development*, *9*(9), 3461-3482. https://doi.org/10.5194/gmd-9-3461-2016

Piani, C., Haerter, J. O., & Coppola, E. (2010). Statistical bias correction for daily precipitation in regional climate models over Europe. *Theoretical and Applied Climatology*, *99*(1), 187-192. https://doi.org/10.1007/s00704-009-0134-9

Poulin, A., Brissette, F., Leconte, R., Arsenault, R., & Malo, J.-S. (2011). Uncertainty of hydrological modelling in climate change impact studies in a Canadian, snow-dominated river basin. *Journal of Hydrology*, *409*(3), 626-636. https://doi.org/10.1016/j.jhydrol.2011.08.057

Ricard, S., Lucas-Picher, P., Thiboult, A., & Anctil, F. (2023). Producing reliable hydrologic scenarios from raw climate model outputs without resorting to meteorological observations. *Hydrology and Earth System Sciences*, *27*(12), 2375-2395. https://doi.org/10.5194/hess-27-2375-2023

Ricard, S., Sylvain, J.-D., & Anctil, F. (2019). Exploring an Alternative Configuration of the Hydroclimatic Modeling Chain, Based on the Notion of Asynchronous Objective Functions. *Water*, *11*(10), 2012. https://doi.org/10.3390/w11102012

Ricard, S., Sylvain, J.-D., & Anctil, F. (2020). Asynchronous Hydroclimatic Modeling for the Construction of Physically Based Streamflow Projections in a Context of Observation Scarcity. *Frontiers in Earth Science*, *8*. Repéré à https://www.frontiersin.org/articles/10.3389/feart.2020.556781

Richards, L. A. (1931). CAPILLARY CONDUCTION OF LIQUIDS THROUGH POROUS MEDIUMS. *Physics*, *1*(5), 318-333. https://doi.org/10.1063/1.1745010

Schulla, J. (2021). WaSiM-ETH Documentation. Repéré à http://www.wasim.ch/en/products/wasim_description.htm

Sivakumar, B. (2011). Global climate change and its impacts on water resources planning and management : Assessment and challenges. *Stochastic Environmental Research and Risk Assessment*, *25*(4), 583-600. https://doi.org/10.1007/s00477-010-0423-y

Sylvain, J.-D., Anctil, F., & Thiffault, E. (2021). Using bias correction and ensemble modelling for predictive mapping and related uncertainty : A case study in digital soil mapping. *Geoderma*, *403*, 1-29. https://doi.org/10.1016/j.geoderma.2021.115153

T. W. Chu & A. Shirmohammadi. (2004). EVALUATION OF THE SWAT MODELS HYDROLOGY COMPONENT IN THE PIEDMONT PHYSIOGRAPHIC REGION OF MARYLAND. *Transactions of the ASAE*, *47*(4), 1057-1073. https://doi.org/10.13031/2013.16579

Talbot, F., Sylvain, J.-D., Drolet, G., Poulin, A., & Arsenault, R. (2024). Enhancing physically based and distributed hydrological model calibration through internal state variable constraints. *EGUsphere*, 1-42. https://doi.org/10.5194/egusphere-2024-3353

Tarek, M., Brissette, F., & Arsenault, R. (2021). Uncertainty of gridded precipitation and temperature reference datasets in climate change impact studies. *Hydrology and Earth System Sciences*, *25*(6), 3331-3350. https://doi.org/10.5194/hess-25-3331-2021

Tarek, M., Brissette, F. P., & Arsenault, R. (2020). Evaluation of the ERA5 reanalysis as a potential reference dataset for hydrological modelling over North America. *Hydrology and Earth System Sciences*, *24*(5), 2527-2544. https://doi.org/10.5194/hess-24-2527-2020

Tolson, B. A., & Shoemaker, C. A. (2007). Dynamically dimensioned search algorithm for computationally efficient watershed model calibration. *Water Resources Research*, *43*(1). https://doi.org/10.1029/2005WR004723

Valencia Giraldo, M. del C., Ricard, S., & Anctil, F. (2023). Assessment of the Potential Hydrological Impacts of Climate Change in Quebec—Canada, a Refined Neutral Approach. *Water*, *15*(3), 584. https://doi.org/10.3390/w15030584

van Genuchten, M. Th. (1980). A Closed-form Equation for Predicting the Hydraulic Conductivity of Unsaturated Soils. *Soil Science Society of America Journal*, *44*(5), 892-898. https://doi.org/10.2136/sssaj1980.03615995004400050002x

Yassin, F., Razavi, S., Wheater, H., Sapriza-Azuri, G., Davison, B., & Pietroniro, A. (2017). Enhanced identification of a hydrologic model using streamflow and sat ellite water storage data : A multicriteria sensitivity analysis and op timization approach. *Hydrological Processes*, *31*(19), 3320-3333. https://doi.org/10.1002/hyp.11267

CHAPITRE 5

ARTICLE 3: ASSESSING HYDROCLIMATIC IMPACTS OF CLIMATE CHANGE IN SNOWY CATCHMENTS USING A PHYSICALLY BASED HYDROLOGICAL MODEL

Frédéric Talbot[1], Jean-Daniel Sylvain[2], Guillaume Drolet[2], Annie Poulin[1], Jean-Luc Martel[1] et Richard Arsenault[1]

[1] Département du Génie de la Construction, École de technologie supérieure, Université du Québec, Montréal, H3C 1K3, Canada.
[2] Direction de la recherche forestière, Ministère des Ressources naturelles et des Forêts, Québec, G1P 3W8, Canada.

Article soumis à la revue « Journal of Hydrology : Regional Studies », décembre 2024

Abstract

Understanding the impacts of climate change on hydrology is crucial for effective water resources management, especially in snowy regions like Quebec, Canada, which are vulnerable to significant climatic shifts. This study employs the Water flow and balance Simulation Model (WaSiM), a physically based distributed hydrological model, combined with the latest Coupled Model Intercomparison Project Phase 6 (CMIP6) climate projections to evaluate future hydroclimatic changes across 34 catchments in Southern Quebec. Key hydroclimatic variables, including precipitation, snow water equivalent (SWE), streamflow, evapotranspiration, soil moisture, and groundwater recharge, were analyzed for both reference (1981-2010) and future (2070-2099) periods under the shared socioeconomics pathways 5-8.5 scenario.

The substantial increases in total precipitation and temperature lead to a notable shift from snowfall to rainfall, reduced snow accumulation, and earlier snowmelt. These changes are expected to alter the seasonal distribution of streamflow, with significant increases in winter low flows and shifts in peak flows from spring to earlier in the year. Furthermore, the study

highlights an increase in groundwater recharge rates during winter and spring, driven by higher precipitation and reduced soil freezing.

A detailed case study of the Matane catchment provides insights into the spatial and temporal variability of hydrological processes, demonstrating the benefits of using a spatially distributed model. The findings indicate a decrease in surface runoff and SWE, and an increase in interflow, baseflow, and actual evapotranspiration. Soil moisture shows mixed responses, with increases during the colder months and decreases during warmer months. This research underscores the importance of employing advanced modeling techniques and the latest climate projections to enhance our understanding of climate change impacts on hydrology. The methodologies and findings presented in this study extend beyond Quebec, offering valuable insights for regions with similar climatic, hydrological and topographical conditions globally. By providing a comprehensive assessment of future hydrological changes, this study supports more informed decision-making and adaptive management practices to mitigate the impacts of climate change on water resources and ecosystems.

5.1 Introduction

The Earth's climate system is undergoing rapid changes, primarily driven by human-induced greenhouse gas emissions (Calvin et al., 2023; Yue & Gao, 2018). These changes have far-reaching implications for hydrological processes, altering water availability and quality (Gleick, 1989). Understanding the impacts of climate change on hydrology is crucial for effective water resources management and planning in the face of evolving climatic conditions (Milly, Dunne, & Vecchia, 2005; Sivakumar, 2011).

Boreal regions are particularly susceptible to climate change, experiencing rapid shifts in temperature and precipitation patterns, changing the duration of snow cover. Because they are located at higher latitudes, boreal regions are poised to see higher levels of warming compared to the world average (Estrada, Kim, & Perron, 2021). Several studies have explored the potential impacts of climate change on hydrology, providing valuable insights into future water resources management. These investigations have projected changes such as altered streamflow regimes (Minville et al., 2008; Gombault et al., 2015; Riboust and Brissette, 2015; Cochand et al., 2019; Aygün et al, 2020; Valencia Giraldo et al., 2023), delayed and shortened snow accumulation and melt periods (Novotná et al., 2013; Mudryk et al., 2018; Cochand et al., 2019; Aygün et al., 2020; Nolin et al., 2023; Valencia Giraldo et al., 2023), changes in soil moisture and groundwater recharge annual patterns (Cochand, 2014; Dubois, Larocque, Gagné, & Braun, 2022; Houle, Bouffard, Duchesne, Logan, & Harvey, 2012; Sulis, Paniconi, Rivard, Harvey, & Chaumont, 2011), and shifts in the dominant hydrological processes (Gombault et al., 2015; Middelkoop et al., 2001; Novotná et al., 2013; Valencia Giraldo et al., 2023).

While these studies offer valuable insights into the potential impact of climate change on regional hydrology, they also face limitations in accurately projecting these changes under future conditions. Firstly, many investigations relied on the Coupled Model Intercomparison Project Phase 5 (CMIP5) models (Taylor, Stouffer, & Meehl, 2012), which have since been succeeded by the more advanced Model Intercomparison Project Phase 6 (CMIP6) models (O'Neill et al., 2016). Martel *et al.* (2022) demonstrated that climate change impact studies using CMIP5 should be repeated with CMIP6 models due to the improvements in processes representation in the new models. Secondly, the spatial scale of hydrological models used in most of these studies has often been lumped or distributed but conceptual in nature, limiting their ability to capture local heterogeneity and finer-scale processes (Han et al., 2021; McDonnell, Spence, Karran, van Meerveld, & Harman, 2021).

Accurate representation of processes within hydrological models is vital when evaluating climate change impacts (Kour, Patel, & Krishna, 2016; Talbot, Sylvain, Drolet, Poulin, & Arsenault, 2024). Conceptual models, which simplify complex hydrological processes, often assume parameter stationarity, which may not hold true under changing climatic conditions (Coron, Andréassian, Perrin, Bourqui, & Hendrickx, 2014; Duethmann, Blöschl, & Parajka, 2020; Milly et al., 2008). Consequently, adopting physically based models can enhance the representation and robustness of hydrological processes, thereby improving our ability to assess future hydrological responses to climate change (Devia, Ganasri, & Dwarakish, 2015; Jones, Chiew, Boughton, & Zhang, 2006; Ludwig et al., 2009; Poulin, Brissette, Leconte, Arsenault, & Malo, 2011; Wilby, 2005).

Recent research has employed advanced models and novel approaches to assess climate change impacts on hydrology, particularly in regions characterized by snowy conditions. One such model is the grid-based Water flow and balance Simulation Model (WaSiM) (Schulla, 2021), which has been effectively used to study hydrological responses to climate change across various regions. For instance, Gädeke *et al.* (2014) explored uncertainties in hydrological responses in Germany's Spree River catchment, finding significant variability due to different downscaling approaches. Bormann and Elfert (2010) evaluated the impacts of land use changes in Northern Germany, noting that WaSiM performed better in sloped and heterogeneous catchments. Additionally, Jasper *et al.* (2006) investigated changes in soil moisture in Switzerland's Thur river basin, demonstrating WaSiM's capability in capturing soil moisture dynamics under changing climatic conditions. In Scotland's Tarland catchment, Iacob *et al.* (2017) analyzed flood management strategies, showing how land use changes could mitigate flood risks, further highlighting WaSiM's versatility.

In Quebec, Canada, WaSiM has been applied to study the hydrological impacts of climate change. Novotná *et al.* (2013) examined water quality in an agricultural watershed, observing increased discharge and related water quality issues. Valencia Giraldo *et al.* (2023) used a refined neutral approach to assess the potential hydrological impacts of climate change in Quebec, revealing significant changes in annual water balances, snow reduction, and differential impacts on low flows. Ricard et al. (2019) explored an alternative framework of the hydroclimatic modeling chain using asynchronous objective functions to evaluate the effects of climate change on streamflow distribution. While these studies have made significant contributions to hydrological modeling, they also have certain limitations. For instance, they did not incorporate the latest advancements in climate modeling, such as the use of CMIP6 models, which could provide more accurate representations of future climate conditions. Additionally, these studies did not utilize the WaSiM groundwater module, which is essential for a comprehensive understanding of hydrological processes.

The use of physically based models like WaSiM, which capture local heterogeneity and finer-scale processes, provides a robust framework for evaluating climate change impacts on hydrology. This approach is particularly crucial in regions with complex hydrological dynamics, such as Quebec, where shifts in temperature, precipitation patterns, and snow cover duration are expected to have a significant impact on water resources availability.

This study aims to fill a gap left by previous research, by integrating projections from the latest CMIP6 climate models with the distributed hydrological model WaSiM to provide a more accurate and comprehensive assessment of climate change impacts on streamflow and hydrological processes in regions characterized by snowy conditions. Focusing on 34 catchments across the province of Quebec, Canada, this research seeks to enhance our understanding of potential future changes in hydroclimatic variables. By comparing our findings with those of previous studies, the study aims to achieve a holistic understanding of hydrological changes, thereby supporting more informed decision-making and adaptive management practices. Additionally, the methodologies and insights gained from this study have broader applicability to other regions with similar climatic and hydrological conditions, such as parts of Europe, North America, and Asia, thereby expanding the scope and relevance of the findings.

5.2 Materials and methods

5.2.1 Study area

The data and methods employed in this study, including study area selection, physiographic data, streamflow measurements, digital elevation model processing, land use classification, soil type determination, and meteorological data interpolation, are consistent with those detailed in (Talbot et al., 2024). Readers are encouraged to refer to that publication for comprehensive information on data sources, processing techniques, and methodological approaches.

The study focuses on 34 catchments located in Southern Quebec, Canada, selected for their diverse physiographic and hydrometeorological characteristics. These catchments, which range in area from 525 km² to 6,840 km² (Fig. 5.1), are key components of the *Hydroclimatic Atlas of Southern Québec* (MDDELCC, 2022).

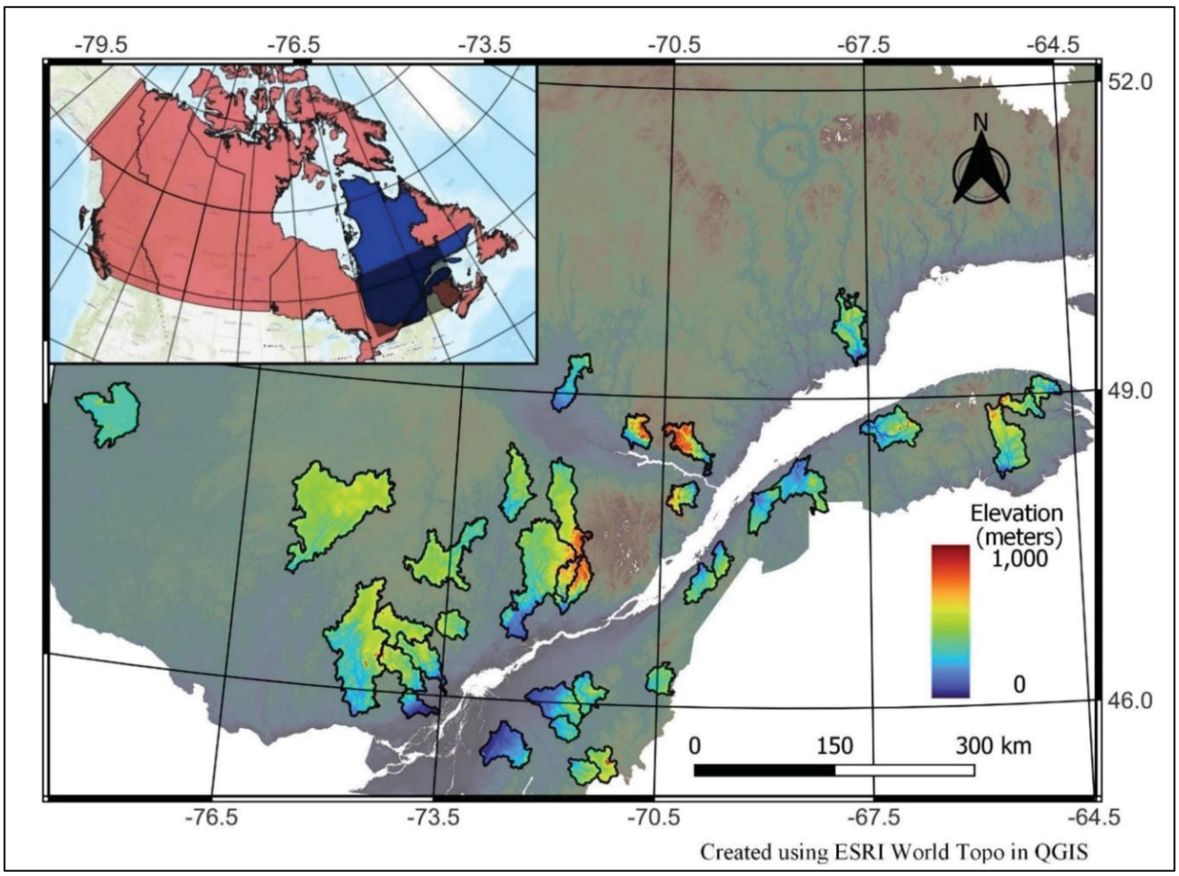

Figure 5.1 Map showing the location of the 34 study catchments within Southern Quebec, Canada

The Köppen climate classification for this region is primarily Dfb (Humid continental mild summer, wet all year), with some areas classified as Dfc (Subarctic with cool summers and year-round precipitation) (Beck et al., 2018). The region experiences significant seasonal climate variability (Fig. 5.2), with cold, snowy winters and warm, rainy summers, influencing the hydrological processes within the catchments.

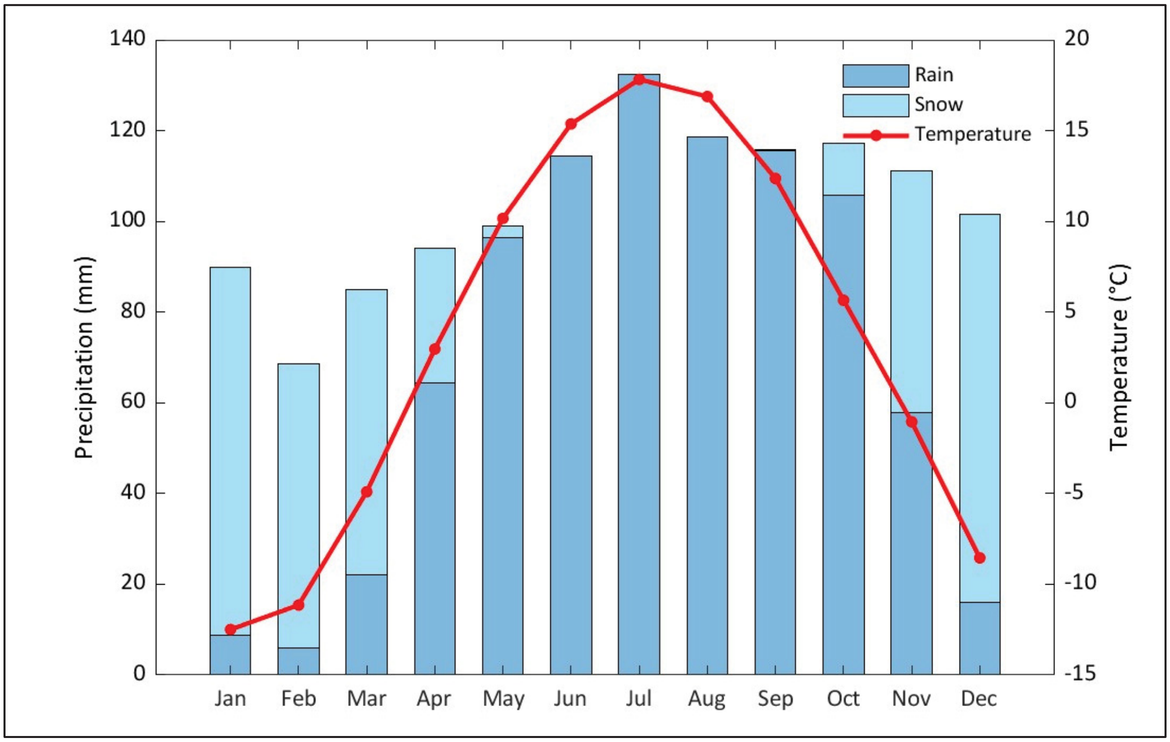

Figure 5.2 Monthly average temperature (°C) and total precipitation (mm) for the study area, averaged over the 34 selected catchments

Key characteristics of the catchments, including area, mean elevation, annual total precipitation, annual extreme daily temperature, and annual streamflow, are summarized in Table 5.1.

Table 5.1 Summary characteristics of key attributes for the 34 selected catchments during the period 1995-2009

Characteristics	**Minimum**	**Median**	**Maximum**
Area (km^2)	525	1185	6840
Mean Elevation (m)	137	365	568
Annual Total Precipitation (mm)	933	1140	1395
Annual Extreme Daily Temperature (°C)	-34.6	3.3	28.3
Annual Daily Streamflow ($m^3 s^{-1}$)	10	24	130

Selected catchments remain mostly unaffected by the presence of dams and reservoirs, preserving the natural integrity of hydrological processes.

The study area encompasses various soil types and land uses. According to Sylvain et al. (2021), sandy loam is the predominant soil texture, constituting 72% of the study area, while loam and loamy sand also feature prominently at 12% and 11%, respectively. Land use patterns reveal that mixed forests cover 38% of the study area, with coniferous and deciduous forests also each accounting for 23% and 22%, respectively. Crops and water are the only other significant land use classes, at 6% and 5% respectively (2015 Land Cover of North America at 30 meters, 2023; Latifovic et al., 2012).

5.2.2 Data

5.2.2.1 Streamflow

This study utilized streamflow data from 1981 to 2010 from the *Hydroclimatic Atlas of Southern Québec* (MDDELCC, 2022). It is provided at the daily timestep and contains some minor periods of missing data. These include winter periods where flows can be affected by ice cover and ice jams and are therefore heavily biased, explaining their removal from the dataset. Most rivers are natural and unregulated. However, some have small weirs that control upstream sections of the watersheds. The resulting flows are considered unregulated despite these small deviations.

5.2.2.2 Digital elevation model

The digital elevation model (DEM) was derived from the NASA Shuttle Radar Topography Mission Global 1 arc second (SRTMGL1) version 3.0. Hydrological corrections based on provincial data ensured the accurate representation of hydrological networks, with adjustments made using SAGA GIS software (Conrad et al., 2015). Tanalys software (Schulla, 2021) was used to extract essential information, including slope, aspect, flow times, and river characteristics, for integration into the WaSiM hydrological model.

5.2.2.3 Land use

Land use data were sourced from the 2015 North American Land Change Monitoring System (NALCMS) 30 meters dataset (2015 Land Cover of North America at 30 meters, 2023; Latifovic et al., 2012) and resampled using the nearest neighbor method at a 250 meters resolution. Land use can have a significant impact on hydrological parameters like root distribution, vegetation cover fraction (VCF), roughness length (Z0), and albedo which, in WaSiM, control processes such as evapotranspiration, runoff, and infiltration.

5.2.2.4 Soil type

To account for the spatial variability of soil hydraulic properties across the study area, we utilized the SIIGSOL 100 meters database (Sylvain et al., 2021). The SIIGSOL database provides detailed descriptions of the proportions of sand, clay, and silt within the soil profile (Ministère des Ressources Naturelles et des Forêts, 2022). Soil type information was converted to soil texture classes based on the United States Department of Agriculture (USDA) classification system (Soil Survey Division Staff, 2017). Soil hydraulic properties were imputed from established relationships between soil texture classes and hydraulic parameters (Soil Survey Division Staff, 2017). SRTM elevation data was used to account for soil depth spatial variability. Higher elevations were assumed to have thinner soil thickness, while lower elevations were considered to have thicker soil. Raster cells with elevations below the 33rd percentile were classified as deep, those above the 66th percentile as shallow, and the remaining as normal.

5.2.2.5 Meteorological data

This study employed meteorological data from the ECMWF Reanalysis v5 (ERA5) dataset (Hersbach et al., 2020), which is known for its ability to mitigate the shortcomings of observational datasets and has demonstrated its effectiveness in this region (Tarek, Brissette, & Arsenault, 2020). We chose ERA5 due to its comprehensive coverage and reliability, particularly in regions where observational data may be sparse or inconsistent. Specifically, we focused on total precipitation and mean temperature, using daily temporal resolution, for a period spanning from 1981 to 2020. Meteorological data were further interpolated for each watershed at the 250 meters spatial resolution used by the model. The interpolation was run directly in WaSiM using the inverse distance weighting (IDW) method as recommended by Schulla (2021).

5.2.2.6 Climate projections

Projected daily temperature and precipitation data were obtained from CMIP6 models (O'Neill et al., 2016) for both the reference (1981-2010) and future period (2070-2099). To address and assess the uncertainty related to the selection of climate models (Arsenault, Brissette, Chen, Guo, & Dallaire, 2020; Lucas-Picher et al., 2021; Minville et al., 2008; Tarek, Brissette, & Arsenault, 2021), an ensemble of 18 climate models was employed, as shown in Table 5.2.

Table 5.2 Global climate models used in the study and their associated institutions

ID	GCM	Source	Institution
CM1	ACCESS-ESM1-5	(Ziehn et al., 2020)	Australian Community Climate and Earth System Simulator, Australia
CM2	CMCC-ESM2	(Lovato et al., 2022)	Centro Euro-Mediterraneo sui Cambiamenti Climatici, Italy
CM3	CanESM5	(Swart et al., 2019)	Canadian Centre for Climate Modelling and Analysis, Canada
CM4	EC-Earth3	(Döscher et al., 2022)	European consortium of national meteorological services and research institutes; Spain, Denmark, Italy, Finland, Germany, Ireland, Portugal, Netherlands, Sweden, Norway, and Belgium.
CM5	EC-Earth3-CC		
CM6	EC-Earth3-Veg-LR		
CM7	FGOALS-g3	(Pu et al., 2020)	Chinese Academy of Sciences, China
CM8	GFDL-ESM4	(Krasting et al., 2018)	Geophysical Fluid Dynamics Laboratory, USA
CM9	INM-CM4-8	(Volodin et al., 2019)	Institute for Numerical Mathematics, Russia
CM10	INM-CM5-0		
CM11	IPSL-CM6A-LR	(Boucher et al., 2020)	Institut Pierre Simon Laplace, France
CM12	MIROC6	(Tatebe et al., 2019)	Japan Agency for Marine-Earth Science and Technology, Japan
CM13	MPI-ESM1-2-HR	(Mauritsen et al., 2019)	Max Planck Institute for Meteorology, Germany
CM14	MPI-ESM1-2-LR		
CM15	MRI-ESM2-0	(Yukimoto et al., 2019)	Meteorological Research Institute, Japan
CM16	NESM3	(Cao et al., 2021)	Nanjing University of Information Science and Technology, China
CM17	NorESM2-LM	(Seland et al., 2020)	Norwegian Climate Centre, Norway
CM18	NorESM2-MM		

The multivariate bias correction algorithm (MBCn) (Cannon, 2018) was utilized to correct biases in the climate model simulations. This method allows to correct biases in meteorological data, while accounting for spatiotemporal interdependencies between variables and preserving changes in quantiles between the reference and future periods. This was performed on daily total precipitation and mean temperature using the ERA5 data as the reference data over the period 1981-2010, then applying the transformation to the climate models data over the reference (1981-2010) and future (2070-2099) periods.

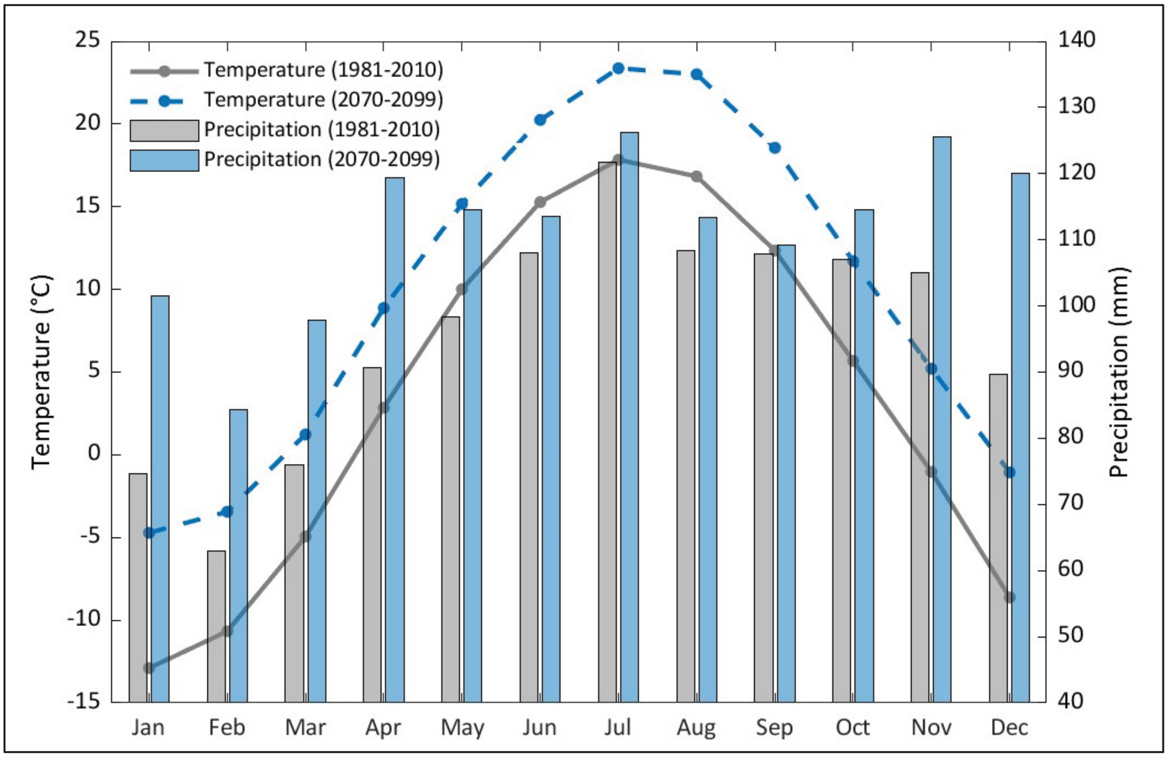

Figure 5.3 Monthly total precipitation and mean temperature for the reference (1981-2010) and future (2070-2099) periods

This study utilized climate simulations from the Shared Socioeconomic Pathway 5-8.5 (SSP5-8.5), a scenario projecting very high greenhouse gas emissions with global warming exceeding 4 degrees Celsius by 2100 (Calvin et al., 2023). While some authors argue that these "hot" models are unrealistic, this remains a subject of much debate in the scientific community (Calvin et al., 2023; Hausfather, Marvel, Schmidt, Nielsen-Gammon, & Zelinka, 2022). In this study, the SSP5-8.5 models were used to provide a picture of the future climate of the region under the worst plausible conditions. Figure 5.3 shows a consistent increase in future monthly precipitation throughout the year across the catchments and models, especially from November to April. Additionally, temperatures are projected to rise significantly, with an increase of 5 to 8 degrees Celsius, consistent with IPCC projections.

This trend aligns with expectations for northern latitudes, which are anticipated to warm faster than the global average (Estrada et al., 2021). Figure 5.4 presents the spatial distribution of annual mean temperatures and annual total precipitation for the reference period as well as projected changes for the future period.

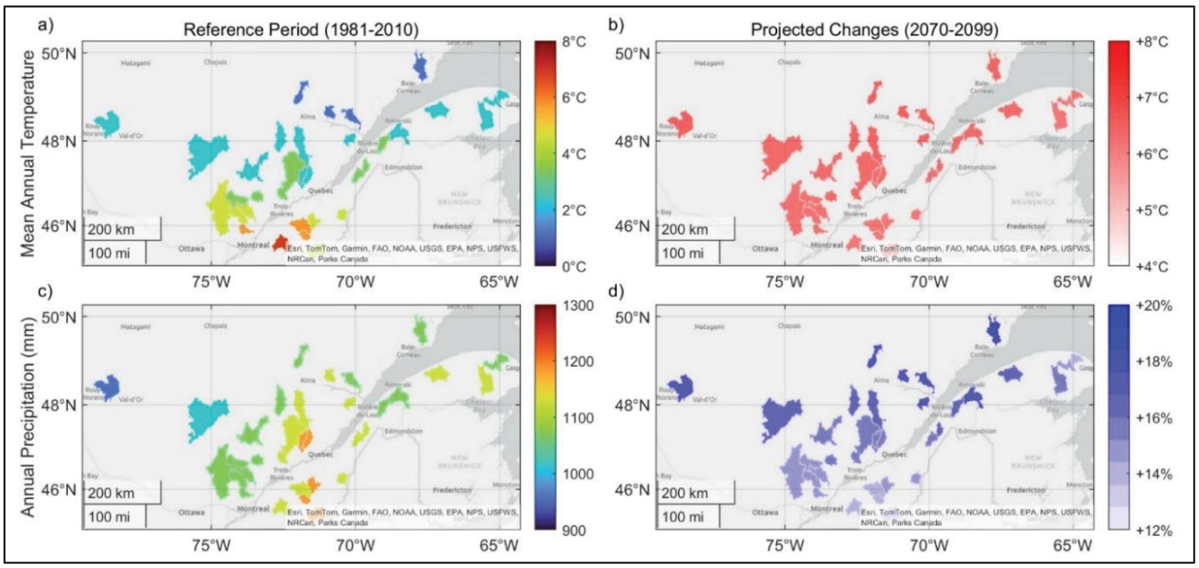

Figure 5.4 Spatial distribution of mean annual temperature (°C) and annual precipitation (mm) across selected catchments

5.2.3 WaSiM model

In this study, the WaSiM version 10.06.00 was utilized for hydrological modeling (Schulla, 2021). WaSiM allow to accurately model key hydrological processes in three dimension through a deterministic and spatially distributed approach (Ricard, Sylvain, & Anctil, 2020). However, WaSiM's complexity involves the necessity for high-quality input data, which can be seen as a limitation of this model due to potential data uncertainties and increased computational demands (Beven, 2001; Blöschl & Sivapalan, 1995).

WaSiM is available in two versions: one using the Topmodel approach and another using the Richards equation (Richards, 1931). We selected the Richards equation version for its physically based simulation of hydraulic head gradients and the integration of soil properties.

Based on research needs, WaSiM allows the activation of specific sub-models, which can be parallelized to optimize efficiency and reduce computational demands.

The configuration used for this study included activating the groundwater flow sub-model using the Gauss-Seidel iteration method and employing the Hamon method for the evapotranspiration sub-model. The remainder of the model configuration mirrors that described in Talbot, Sylvain, *et al.* (2024).

5.2.4 Model calibration

5.2.4.1 Calibration parameters

The calibration process involved fine-tuning 17 parameters (Table 5.3), selected based on the recommendations provided in the WaSiM documentation (Schulla, 2021). The rest of the parameters in the control file were kept at their default values as specified in the documentation. This calibration approach mirrors configuration GW-RC described in Talbot, Sylvain, *et al.* (2024). Table 5.3 was taken from Talbot, Sylvain, *et al.* (2024).

Table 5.3 Parameter description and values used for calibrating WaSiM

No.	Code	Description	Unit	Sub-Model	Range
1	k_D	Storage coefficient for surface runoff	h	Unsaturated zone	[1, 25]
2	k_H	Storage coefficient for interflow	h	Unsaturated zone	[1, 25]
3	d_r	Drainage density for interflow	m^{-1}	Unsaturated zone	[1, 50]
4	QD_{Snow}	Fraction of surface runoff on snow melt	-	Unsaturated zone	[0.1, 1]
5	c_0	Degree-Day factor	mm °$C^{-1}d^{-1}$	Snow	[0, 3]
6	T_0	Temperature limit for snow melt	°C	Snow	[-4, 4]
7	$T_{R/S}$	Transition temperature snow/rain	°C	Snow	[-4, 4]
8	C_{WH}	Water storage capacity of snow	-	Snow	[0.1, 0.3]
9	C_{rfr}	Coefficient for refreezing	-	Snow	[0.1, 1]
10	$f_{i,summer}$	Summer correction factors for ETP	-	Evapotranspiration	[0.1, 2]
11	$f_{i,fall}$	Fall correction factors for ETP	-	Evapotranspiration	[0.1, 2]
12	$f_{i,winter}$	Winter correction factors for ETP	-	Evapotranspiration	[0.1, 2]
13	$f_{i,spring}$	Spring correction factors for ETP	-	Evapotranspiration	[0.1, 2]
14	K_{rec}	Recession constant for hydraulic conductivity	-	Soil table	[0.1, 0.99]
15	d_z[a]	Soil layer thickness	-	Soil table	[0.8, 1.4]
16	Kol[b]	Colmation of the river links	-	Input grid	[1, 100]
17	K_{XY}[c]	Saturated horizontal conductivity	m s^{-1}	Input grid	[0.2, 4]

[a] Calibration coefficient, ranging from 0.8 to 1.4, is applied to adjust the total soil depth, which is predetermined to be 8 meters for shallow, 14 meters for normal, and 20 meters for deep soil conditions.

[b] Calibration coefficient, ranging from 1-100, is applied to adjust the colmation grid, which is predetermined to be $1x10^{-6}$.

[c] A calibration coefficient, ranging from 0.2 to 4, is applied to adjust the saturated horizontal conductivity grid, which is predetermined to be $4x10^{-5}$ m s^{-1}.

5.2.4.2 Calibration framework

For model calibration, the study employed split-sample test (SST) framework. This widely used approach involves dividing the available streamflow data into two sets: one for calibrating the model and the other for validating its performance. This method is particularly useful in hydrology for testing a model's ability to generalize beyond the conditions under which it was calibrated, providing a measure of model’s performance and reliability. The calibration period (2000-2009) was chosen based on the availability of reliable hydrological data, with specific adjustments for certain catchments (Croche: 1995-1999, Petit Saguenay: 1995-1999, and Sainte-Marguerite Nord-Est: 1992-1996). Similarly, the validation period was set for 1990-1999, except for the Croche (1986-1994), Petit Saguenay (1986-1994), and Sainte-Marguerite Nord-Est (1986-1991) catchments. A five year spin-up period was performed before each simulation to allow the model to reach a stable state, limiting the effect of unstable initial conditions on the model's performance metrics (Ekmekcioğlu, Demirel, & Booij, 2022).

The optimization algorithm employed for the calibration process was the dynamically dimensioned search (DDS; (Tolson & Shoemaker, 2007)) algorithm, following the recommendation of Arsenault et al. (2014). This algorithm is specifically designed for efficiently calibrating complex hydrological models with a large parameter range given a finite computing budget. It dynamically adapts its search strategy based on the number of evaluations performed and converges accordingly.

The calibration process was divided into two main phases: pre-calibration and calibration. This sequential calibration is designed to refine the model's performance progressively. The strategy of starting with a wider parameter space and progressively narrowing it ensured a comprehensive and targeted calibration, ultimately enhancing the model's ability to simulate the hydrological dynamics of the catchments, which is critical for an application in climate change conditions.

5.2.4.3 Pre-calibration

The pre-calibration involved defining parameter ranges for parameters that mostly impact baseflow (d_r, QD_{Snow}, K_{rec}, Kol, Kxy). The pre-calibration involved 200 evaluations using grids with a spatial resolution of 1000 meters, followed by 50 evaluations using grids with a resolution of 250 meters. This approach reduces computing time while optimizing the exploration of hyperspace parameters, while still allowing the optimizer to fine-tune parameter values on the more detailed grids, as is often done in surrogate modeling (Meert, Pereira, & Willems, 2018). Balanced Kling-Gupta Efficiency (KGE) with the annual recharge mean (250 mm yr^{-1}) and standard deviation (80 mm yr^{-1}) (Eq. (3)) was used as the objective function, as in Talbot, Sylvain, *et al.* (2024).

Following the pre-calibration at both spatial resolutions, the resulting pre-calibrated parameter sets were used to define new parameter ranges for the calibration phase. This analysis involved adjusting the minimum and maximum values of parameters influencing baseflow by ±10% to establish new calibration ranges. This ensures that the model calibration will respect groundwater recharge and associated hydrogeological processes during the main calibration phase.

5.2.4.4 Calibration

The main calibration phase involved a comprehensive series of 1000 evaluations at 1000 meters resolution and 50 evaluations at 250 meters resolution for final fine-tuning. The objective function is composed of the KGE at a weight of 96% and the standard deviation of recharge at a weight of 4%. This specific weighting was chosen based on preliminary tests, where various weight combinations were evaluated on a test catchment. The 96% for KGE and 4% for recharge standard deviation provided a good balance between maintaining high overall performance in terms of KGE and ensuring reasonable variability in groundwater recharge. The revised objective function is shown in Eq. (5.4).

5.2.4.5 Performance metric

Model performance was assessed with the KGE (Kling, Fuchs, & Paulin, 2012) (Eq. (5.1)), which combines metrics of correlation, variability, and bias and ranges from $-\infty$ to 1, with 1 indicating a perfect match between observed and simulated streamflow:

$$KGE = 1 - \sqrt{(r-1)^2 + \left(\frac{\mu_{sim}}{\mu_{obs}} - 1\right)^2 + \left(\frac{\sigma_{sim}/\mu_{sim}}{\sigma_{obs}/\mu_{obs}} - 1\right)^2}, \tag{5.1}$$

where r is the correlation coefficient, calculated as:

$$r = \frac{\sum_{i=1}^{n}(O_i-\bar{O})*(S_i-\bar{S})}{\sqrt{\sum_{i=1}^{n}(O_i-\bar{O})^2*\sum_{i=1}^{n}(S_i-\bar{S})^2}}, \tag{5.2}$$

here, O_i and S_i are the observed and simulated streamflow values for each day, respectively, and $\bar{O}$ and $\bar{S}$ are their respective means.

The weights used in the objective function for pre-calibration and calibration were determined through preliminary tests. These tests involved evaluating different weight combinations on a test catchment to find an optimal balance between achieving high KGE and maintaining reasonable variability in groundwater recharge. The chosen weightings provided the best compromise, ensuring that the model performs well overall while accurately representing groundwater recharge dynamics.

The objective function used for the pre-calibration and calibration are defined in Eq. (5.3) and Eq. (5.4) respectively.

$$Objective\ function = 1 - (0.7 * KGE + 0.2 * \lceil \sigma_{r_{sim}} - 0.08 \rceil + 0.1 * \lceil \overline{r_{sim}} - 0.25 \rceil), \tag{5.3}$$

$$Objective\ function = 1 - (0.96 * KGE + 0.04 * \lceil \sigma_{r_{sim}} - 0.08 \rceil), \tag{5.4}$$

where $\sigma_{r_{sim}}$ represents the simulated annual recharge standard deviation (m yr^{-1}), $\overline{r_{sim}}$ is the simulated mean annual recharge (m yr^{-1}) and KGE is the Kling-Gupta efficiency.

5.2.5 Climate change assessment

5.2.5.1 Reference and future period simulations

For all catchments, simulations were performed using meteorological data from ERA5 for the reference period (1981-2010). Additionally, simulations were conducted using the 18 climate models from CMIP6 for both the reference period (1981-2010) and the future period (2070-2099). These simulations provided a comprehensive dataset to analyze historical conditions and project future changes.

5.2.5.2 Comparison of hydroclimatic variables

A regional comparative analysis was conducted on key hydroclimatic variables under reference and projected conditions and for ERA5 and CMIP6 data, including precipitation, snowfall, streamflow, surface runoff, interflow, actual evapotranspiration (ETa), baseflow, groundwater recharge, snow water equivalent (SWE), and soil moisture.

First, annual totals (annual means for soil moisture and annual maximums for SWE) of each variable were compared between ERA5 and CMIP6 simulations for the reference period. This comparison aimed to verify the adequacy of bias correction and the effectiveness of CMIP6 simulations in representing hydroclimatic variables for the reference period. Next, the relative changes between future and reference period simulations were calculated using the climate models outputs for both periods. The mean and standard deviation of these relative changes were computed across all catchments to quantify the overall impact of climate change on hydroclimatic variables across the study area and for the future period. Additionally, a comparative analysis of hydroclimatic variables was performed to validate the similarities between ERA5 and CMIP6 simulations for the reference period and to assess the differences between future and reference periods in terms of the timing and magnitude. Furthermore, the contributions of surface runoff, baseflow, interflow, and ETa to the water cycle were calculated for each climate model for both the reference and future periods. This analysis helped in understanding the potential redistribution of water within the hydrological cycle under future climate scenarios.

In addition to the regional analysis, particular emphasis was placed on the Matane catchment due to its representative hydrological characteristics. Specific comparisons of hydroclimatic variables were conducted at a finer scale for this catchment to provide a more granular understanding of climate change impacts. The Matane catchment analysis complements the broader regional assessment by offering insights into localized hydrological responses and variability.

5.2.5.3 Spatial representation of direction and magnitude of change

A spatial representation of the direction and magnitude of change for multiple hydroclimatic variables was performed using criteria from the *Hydroclimatic Atlas of Southern Québec* (MDDELCC, 2022), outlined in Table 4.

Table 5.4 Criteria for determining the direction of change in hydrological variables based on consensus among climate models indicating an increase or decrease

Direction of Change	**Criteria**
Highly Probable Increase	More than 16 climate models indicate an increase.
Probable Increase	12 to 16 climate models indicate an increase.
No Consensus	7 to 11 climate models indicate an increase or decrease. The lack of consensus may indicate a weak change or widely dispersed climate models.
Probable Decrease	12 to 16 climate models indicate a decrease.
Highly Probable Decrease	More than 16 climate models indicate a decrease.

This classification allowed for a detailed spatial analysis, comparing the changes predicted by different climate models and identifying areas with consistent trends. The spatial analysis focused on hydrological indicators such as streamflow, groundwater recharge, and SWE, providing a clear visualization of regional impacts.

5.3 Results

5.3.1 Model calibration and validation

The model consistently achieved KGE scores above 0.5 across all catchments during both the calibration and validation phases.

During the calibration period, the minimum KGE achieved was 0.637 (Eaton), while the maximum was 0.877 (Matane), with a median value of 0.803. For the validation period, the minimum KGE was 0.661 (Eaton), the maximum was 0.869 (Bras du Nord), and the median value was 0.770. These results, including the similarity in KGE values between the calibration and validation periods, indicate an agreement between the observed and simulated streamflow data, supporting the model reliability for climate change assessment.

5.3.2 Regional hydrological changes

5.3.2.1 Comparative analysis of hydrological changes

This section presents a global overview of hydrological changes across the selected catchments. Table 5.5 provides a detailed comparison of various hydroclimatic variables simulated by WaSiM for the reference period (1981-2010), using ERA5 and CMIP6 data, and for the future period (2070-2099) using CMIP6 data only. It presents the mean relative changes, biases and standard deviations across the 34 catchments for each simulated variable, quantifying the impact of climate change on the water cycle.

Table 5.5 Comparison of hydroclimatic variables for reference and future periods across all catchments

Hydroclimatic Variables	Unit	Reference (1981-2010)			Future (2070-2099)		
		ERA5	CMIP6	Relative Bias	CMIP6	Relative change	
						μ	σ
Precipitation	mm yr^{-1}	859	850	-1.04%	1156	36%	5%
Snowfall	mm yr^{-1}	389	386	-0.83%	260	-33%	7%
Streamflow	mm yr^{-1}	661	652	-1.39%	656	0.51%	4%
Surface Runoff	mm yr^{-1}	232	237	1.79%	156	-34%	12%
Interflow	mm yr^{-1}	232	223	-3.77%	278	24%	12%
ETa	mm yr^{-1}	480	482	0.44%	645	34%	5%
Baseflow	mm yr^{-1}	194	190	-2.30%	218	15%	12%
Groundwater Recharge	mm yr^{-1}	236	231	-1.96%	259	12%	11%
SWE	mm	282	283	0.34%	149	-47%	9%
Soil Moisture	-	0.172	0.171	-0.30%	0.172	0.21%	1.48%

The similarity in averaged hydroclimatic variables between the ERA5 and CMIP6 simulations during the reference period indicates the consistency of the hydrological model and the effectiveness of the bias correction implementation.

Comparing the CMIP6 simulations between the reference and future periods reveals several significant differences. There is a notable shift in the ratio of snow to rain, with a 36% increase in rain and a 33% decrease in snow in the future period. Consequently, total precipitation rises from 1236 mm in the reference period to 1416 mm in the future, marking a 15% increase.

Although the annual total streamflow remains similar between the reference and future periods, notable changes occur in the hydroclimatic variables. Surface runoff decreases by

34%, while interflow, baseflow, and ETa increase by 24%, 15%, and 34%, respectively. Groundwater recharge sees a 12% increase, while snow SWE decreases by 47% and soil moisture stays constant (0.21%).

Figure 5.5 presents the annual fluctuation of eight hydroclimatic variables over the reference and future periods for ERA5 and CMIP6 meteorological inputs. Again, the similarity between hydroclimatic variables resulting from simulations driven with ERA5 and CMIP6 datasets, along with the minimal differences between climate models over the reference period, suggests the effectiveness of the bias-correction method. In contrast, the larger variance observed in the CMIP6 simulations for the future period suggests a higher uncertainty associated with the climate simulations in the future.

Comparisons between simulations driven by CMIP6 under reference and future periods reveals a noticeable shift in the timing of seasonal peak flow, moving from May to April, along with an increase in winter flows and a decrease in amplitude of the seasonal peak flow. Similar shifts also occur in interflow, baseflow, surface runoff, and groundwater recharge. Interflow, groundwater recharge, and soil moisture all show an increase during the colder months (November to May) and a slight decrease during the warmer months (June to October). Baseflow follows a similar pattern, with less pronounced decreases during the warmer months. Surface runoff largely increases between December and April. This change in runoff also coincides with a slight reduction in the amplitude of the peak related to snowmelt in the spring. Snow water equivalent consistently decreases throughout the year, which is also consistent with the decrease in snowfall precipitation (-33%, Table 5.5). Actual evapotranspiration increases throughout the year, with a more substantial rise from June to September. The wider range of values in future period simulations depicted variance related to the climate models.

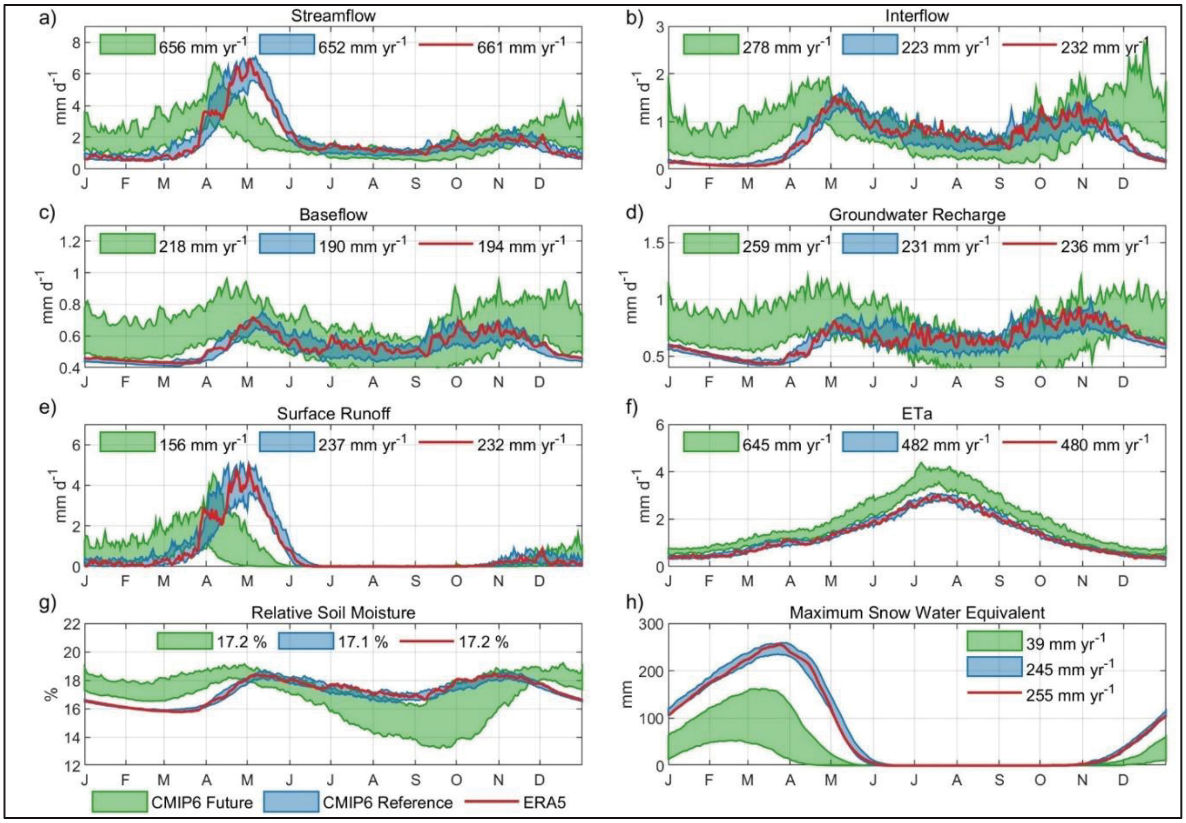

Figure 5.5 Comparative analysis of annual dynamics of daily hydroclimatic variables across all catchments

Figure 5.6 presents the contributions of hydroclimatic variables across all climate models for the reference and future periods. The similarity between climate models for all hydrological processes during the reference period is evident. However, there is increased variability between climate models in the future period, with surface runoff exhibiting the greatest variability. Figures 5.6b and 5.6c reveal significant changes in the contributions of various processes between the two periods, such as an increase in ETa and interflow, and a decrease in surface runoff. Baseflow maintains a consistent proportion during both periods. The most notable changes occur in surface runoff and ETa.

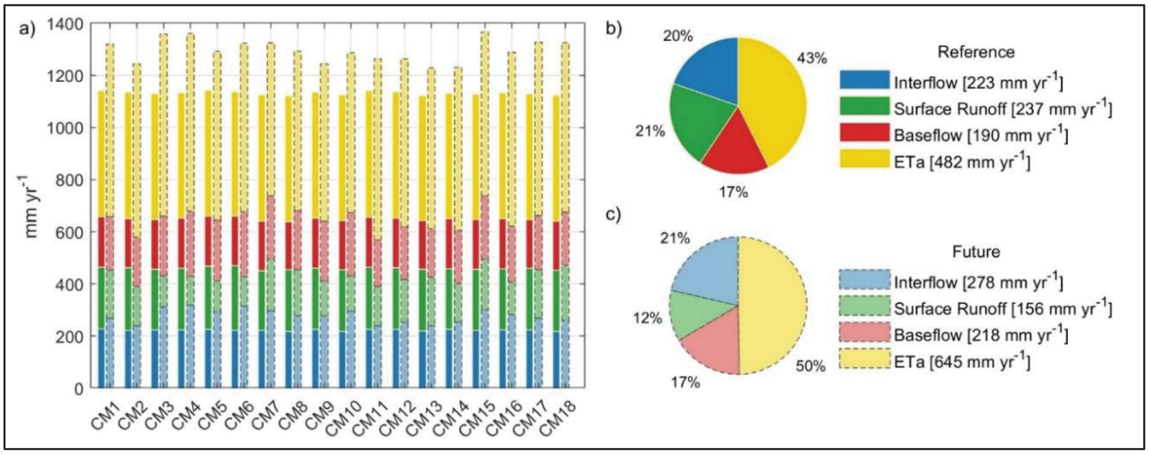

Figure 5.6 Distribution of hydroclimatic variables for reference and future periods across eighteen climate models (CM1 to CM18)

5.3.2.2 Streamflow

Figure 5.7 illustrates the spatial pattern of changes in the direction and magnitude of the annual maximum daily flow with a two-year return period (panels 5.7a and 5.7b). Northeastern catchments predominantly exhibit an increase in maximum flow, while southwestern catchments indicate a decrease. This trend is reflected in the magnitude of changes, with the most southern and northern catchments displaying the highest magnitudes corresponding to their respective directions. Notably, catchments with the highest increases are small catchments with steep slopes.

The direction and magnitude of changes in the annual minimum 7-day mean flow with a two-year return period (panels 5.7c and 5.7d) indicate that almost all catchments show a decrease in flow, except for four catchments that exhibit a significant increase in flow magnitude, with three of them located on the North shore of the St-Lawrence River. Southeastern catchments generally present a higher magnitude of decrease, underscoring a clear spatial trend in the direction and extent of changes across the study area. Furthermore, many catchments show no consensus between climate models, suggesting variability between models and/or that the magnitude of change is close to zero leaving higher uncertainty on the potential impact of climate change in these catchments.

The temporal shifts in annual peak flow (panels 5.7e and 5.7f) highlight a noticeable trend toward earlier peak flows across many catchments, with a general shift of approximately one month. Catchments with peak flows traditionally occurring in May have shifted to April, while those with peak flows in April have moved to March. Notably, one southern catchment exhibits a peak flow in February. On average, the shift in peak flow timing across all catchments is 32 days, with a standard deviation of 8 days, indicating a significant and consistent temporal adjustment in peak flow timing.

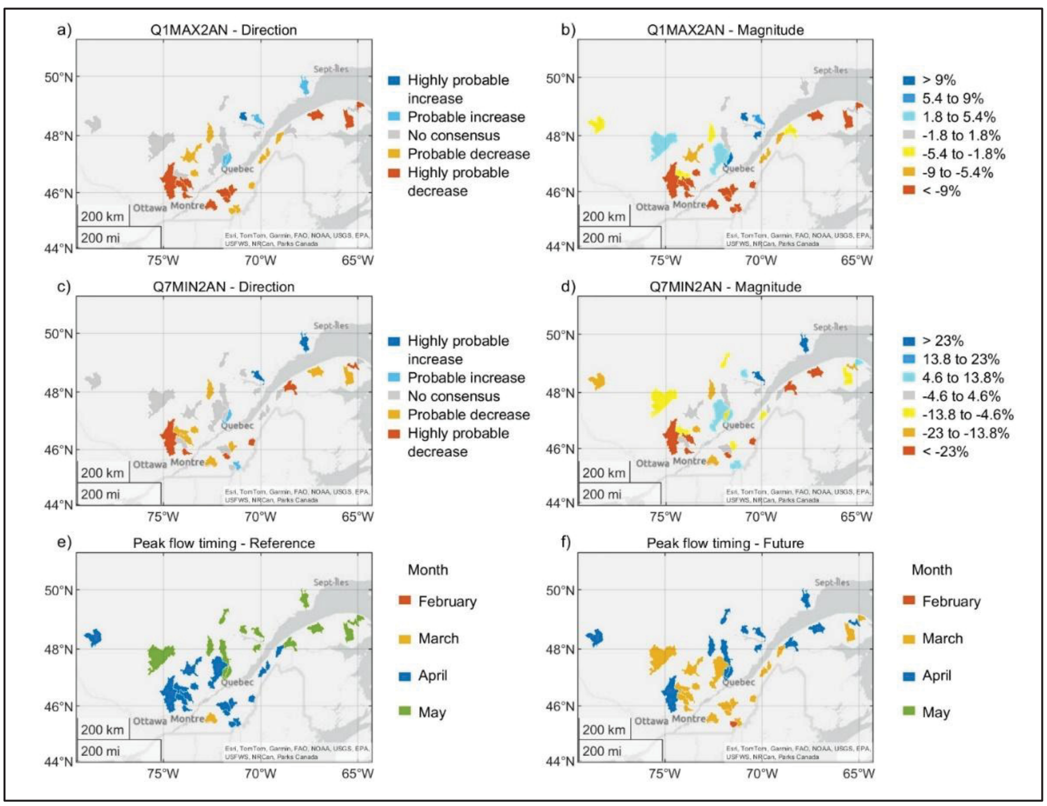

Figure 5.7 Spatial distribution of changes in hydrological indicators and annual peak flow timing

5.3.2.3 Groundwater recharge, SWE and ETa

Figure 5.8 indicate a general increase in groundwater recharge rates (panels 5.8a and 5.8b), with most catchments exhibiting an increase between 12% and 24%. There are no discernible spatial patterns in the distribution of these changes. One catchment shows an unexpected result with a highly probable decrease exceeding 6%.

The results for the annual maximum SWE (panels 5.8c and 5.8d) indicate a clear decrease across all catchments, with magnitudes of change ranging between -25% and -62%. Catchments located in the southern part of the study area tend to exhibit higher magnitudes of decrease, while those further north show relatively lower magnitudes of change. The reduction in SWE is strongly correlated ($r = 0.94$) with a 44% decrease in the average number of consecutive snow days, which drops from 167 days (standard deviation of 20 days) in the reference period to 94 days (standard deviation of 29 days) in the future period. Furthermore, the analysis of correlation coefficient reveals that higher temperature between December and March will decrease the number of consecutive snow days ($r = -0.89$), as expected.

As expected, an increase in temperature and precipitation leads to an increase in mean annual ETa across all catchments (panels 5.8e and 5.8f), with magnitudes of change ranging between 95 and 203 millimeters. There is no distinct pattern in the spatial distribution of these changes, indicating that the increase in ETa is widespread and not confined to specific geographic areas within the study region.

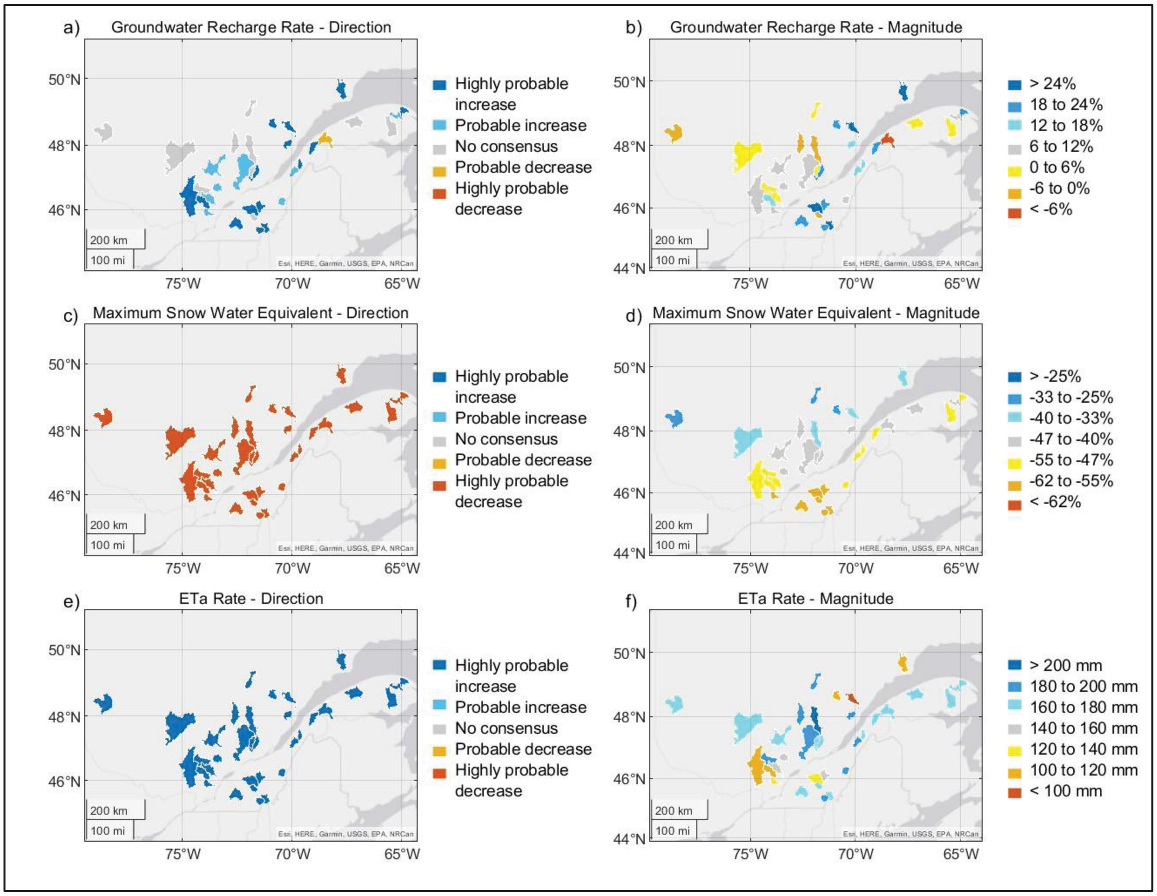

Figure 5.8 Spatial distribution of changes in annual groundwater recharge rate, maximum snow water equivalent (SWE), and actual evapotranspiration rate (ETa)

5.3.3 Case study: Matane catchment

5.3.3.1 Hydroclimatic variables

The Matane catchment was selected for an in-depth case study analysis due to its representative characteristics of the study area. It serves as a valuable example for evaluating the impacts of climate change within the context of a snow-dominated catchment. The findings from the Matane catchment generally align with the broader regional patterns observed in the study, confirming its suitability as a representative case.

For instance, future projections indicate a significant increase in precipitation (42%) and evapotranspiration (36%) alongside a notable decrease in snowfall (-32%) and snow water equivalent (-47%). Similar trends were observed for streamflow, baseflow, interflow, and groundwater recharge, with increases during the colder months.

The Matane catchment also follows the regional trend of earlier seasonal peak flows, increased winter flows, and decreases in surface runoff during the spring peak period. These shifts in the timing and magnitude of hydrological processes reflect the broader impacts of climate change on the region's water cycle. The detailed results for the Matane catchment can be found in Appendix D, where Table AD.1 and Fig. AD.3 provide specific numerical comparisons and graphical representations of the annual dynamics of hydroclimatic variables.

5.3.3.2 Spatial variability of hydrological processes at the catchment scale

Figure 5.9 shows the spatial distribution of groundwater recharge rates across the four seasons. It highlights the annual fluctuation in relative changes between the future and reference periods. There is notable spatial variation in groundwater recharge rates, consistent across both reference and future periods. The most significant spatial variation occurs during spring and summer, with some areas receiving up to 100 mm of recharge while others receive only 5 mm. Groundwater recharge rates closely follow the spatial variation in elevation throughout the catchment (Fig. 5.A panel a), with higher elevations receiving less groundwater recharge while lower elevations receive more. Conversely, higher elevations received more interflow than lower elevations (Fig. 5.B).

The relative and absolute comparison allows for a better distinction of spatial and temporal variability and helps identify areas that are more prone to reductions. When examining the absolute and relative differences between the future and reference periods, winter and spring exhibit an increase in groundwater recharge rates across most of the catchment. Conversely, summer and autumn show a mix of increases and decreases, with both seasons predominantly experiencing decreases across the catchment. Spring receives the most significant absolute increase in groundwater recharge rates, with some areas experiencing increases close to 20 millimeters. In contrast, autumn sees the most substantial decrease in groundwater recharge rates, with certain parts of the catchment experiencing decreases of up to 20 millimeters.

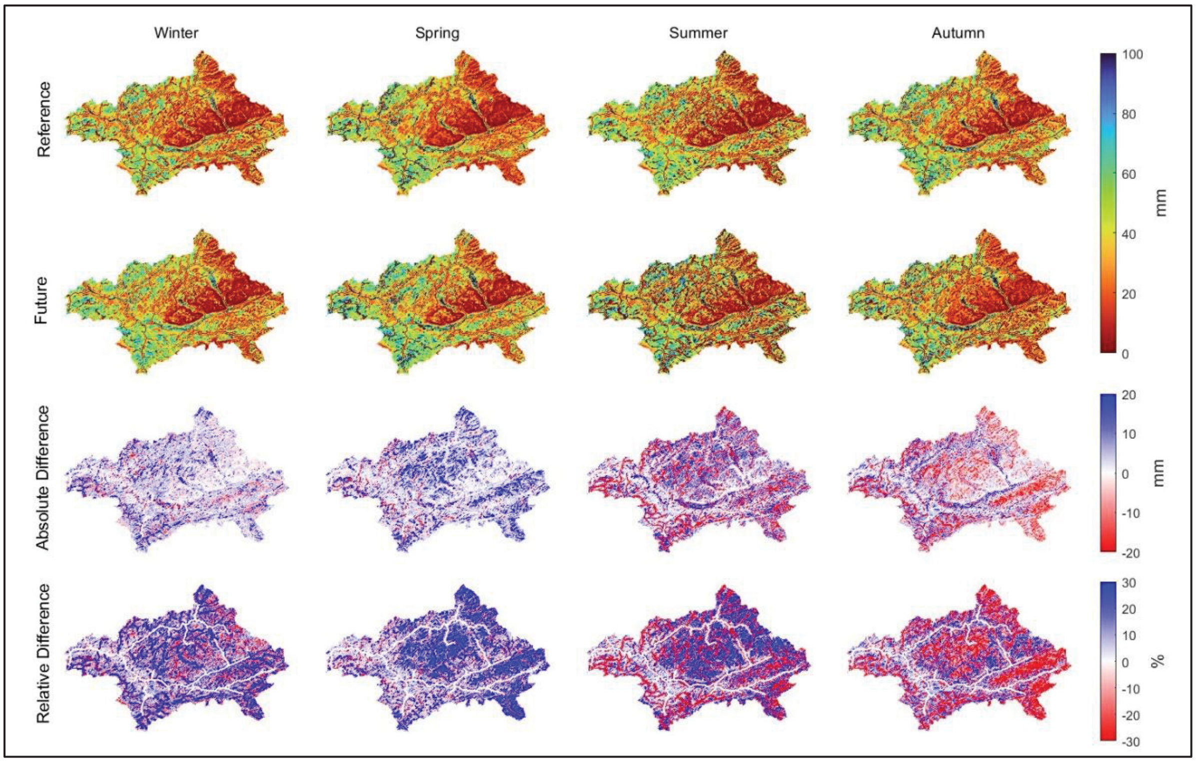

Figure 5.9 Seasonal groundwater recharge rates in the Matane catchment, for reference and future periods, and their differences

Figure 5.10 presents the spatial distribution of soil moisture across the four seasons. When comparing soil moisture with the soil type map of the catchment (Fig. 5.A panel b), there is a clear relationship between soil type and soil moisture. Sandy loam soil, which is more permeable, has the lowest soil moisture levels, around 0.15. Loam soils exhibit soil moisture levels ranging from 0.25 to 0.3, while sandy clay soils have soil moisture levels between 0.3 and 0.35. Although the variability in soil moisture between seasons is small, it appears to be greater for the future period compared to the reference period.

In terms of absolute and relative changes between the future and reference periods, winter and spring show an increase in soil moisture, while summer and autumn exhibit a decrease. These changes are relatively consistent across the entire catchment, with an absolute change of around 0.03 for all four seasons, depending on the direction of change.

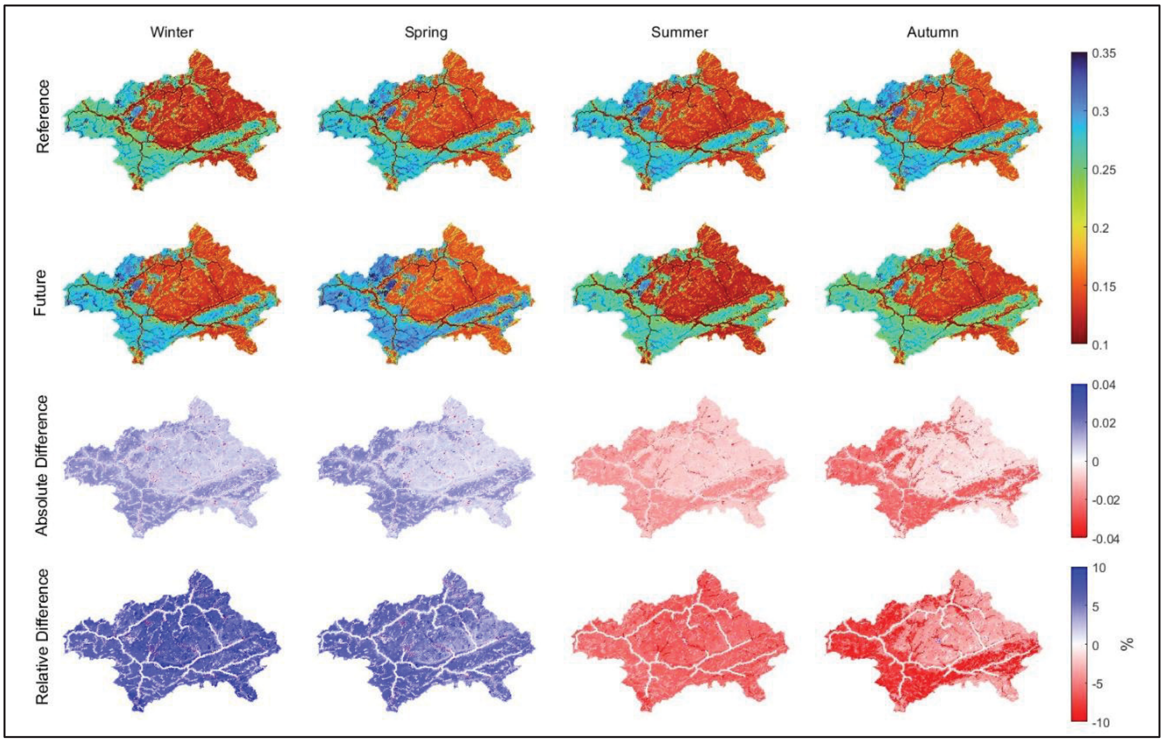

Figure 5.10 Seasonal soil moisture in the Matane catchment, for reference and future periods, and their differences

5.4 Discussion

This study investigates the impacts of climate change on hydrological processes using a spatially distributed and physically based hydrological model, WaSiM, coupled with climate simulations from the SSP5-8.5, which represents a high greenhouse gas emissions scenario. The use of bias corrected CMIP6 climate model data for the future period indicates an increase in total precipitation, particularly pronounced from November to April, along with a significant temperature rise of five to eight degrees Celsius, depending on the climate model.

In the following sections, results will be analyzed in terms of the various hydroclimatic variables.

5.4.1 Regional hydrological changes

5.4.1.1 Snow water equivalent

Projected changes in total precipitation indicate a 15% increase relative to the reference period. However, rising temperatures will result in a 33% decrease in snowfall, with more precipitation falling as rain instead of snow. This is in line with the 20% reduction found by Nolin et al., (2023) for the Upper Harricana River, but less than the 50% reduction in snowfall highlighted in Valencia Giraldo et al. (2023) for the five degrees Celsius warming scenario. This shift leads to a shorter snow accumulation period, with the average number of consecutive snow days projected to decrease significantly, averaging 94 days (standard deviation of 29 days) in the future compared to 167 days (standard deviation of 20 days) in the reference period. This 44% reduction in mean number of snow days is consistent with the 45% reduction for the +6°C scenarios reported by (Valencia Giraldo et al., 2023).

Additionally, the results showed a corresponding decrease in SWE between 25% and 62%, representing a 4% to 11% reduction in SWE per °C, depending on the latitude of the catchment. This is less than the 25%-35% reduction per °C for the 0-2 °C warming zone found by (Aygün et al., 2020) and the 69% decrease found by Cochand et al. (2019), but aligns with the 2.5% to 7.5% reduction per decade for Southern Quebec highlighted by Mudryk et al. (2018), and the 43% reduction found by Novotná et al. (2013).

Catchments in the southern part of the study area show larger decreases in SWE magnitudes (Fig. 8 panel c), whereas those further north exhibit relatively smaller changes—a trend also present in Mudryk et al. (2018). This reduction in SWE is strongly correlated with the absolute change in consecutive snow days ($r = 0.94$). Furthermore, the analysis reveals a strong negative correlation ($r = -0.89$) between the absolute change in consecutive snow days and the mean temperature during the months of December to March in the future period. This suggests that the reduction in consecutive snow days is due to higher temperatures in the southern catchments, bringing them closer to the melting point. Consequently, increases in winter temperatures are a significant factor driving the reduction in snow days and the decrease in SWE.

5.4.1.2 Actual evapotranspiration

The study reveals a change in ETa, increasing from 95 to 203 millimeters, with no distinct pattern in the spatial variability of these changes across the catchments. This aligns with results in Valencia Giraldo et al. (2023) under the 6 degrees Celsius warming scenario, and the 96 millimeters increase found by Novotná et al. (2013). This widespread increase suggests that the factors driving this increase are not localized but affect the entire study area uniformly. One significant factor contributing to this increase is the rise in temperature, which enhances the rate of evapotranspiration. Furthermore, the contribution of ETa to the water cycle is projected to grow substantially. Currently, ETa accounts for 43% of the total water cycle. However, according to our simulation, this rate is expected to rise to 50% in the future. This trend is also highlighted in Valencia Giraldo et al. (2023) under the 6 degrees Celsius warming scenario. This shift raises questions on how such increases in evapotranspiration will impact hydrological processes under future conditions. Higher temperatures increase the potential for water loss through evapotranspiration, leading to a greater proportion of the total precipitation being returned to the atmosphere rather than contributing to runoff and interflow, ultimately impacting streamflow. Additionally, the increase in total precipitation combined to shorter winter period could make more water available for evaporation, further contributing to the rise in ETa.

While this study focuses on ETa, it is important to differentiate it from potential evapotranspiration (ETP), as discussed in other studies (Dallaire, Poulin, Arsenault, & Brissette, 2021). ETP represents the maximum possible evapotranspiration under ideal conditions, whereas ETa provides a better approximation of the actual water loss from land surfaces and vegetation.

The focus on ETa in this study is more useful for informing decision-makers about water availability. ETa reflects the actual conditions in the catchment, considering the availability of water and the specific characteristics of the landscape and vegetation. This makes ETa a more practical measure for assessing the impacts of climate change on water resources and for developing effective water management strategies.

5.4.1.3 Streamflow

Higher temperatures in the future leads to more precipitation falling as rain rather than snow, enhancing streamflow from December to April. This change could be associated with earlier and lower peak flow during the year, shifting by an average of 32 days across all catchments. This shift is less than the three-month shift found by Aygün et al., (2020) but aligns with the worst emission scenario peak discharge shift reported by Cochand et al. (2019) and the results presented by Gombault et al. (2015) and Minville et al. (2008). The shift in timing of peak flows from spring to earlier in the year is due to the reduced snowpack and earlier snowmelt, a consequence of rising temperatures.

The maximum daily flow with a 2-year return period shows changes between -26% and 15%, with most catchments showing changes between -9% and 9%. These results align with the median decrease of 10% to 15% in spring high flows with a 5-year return period found by Riboust and Brissette (2015). Northern catchments predominantly exhibit an increase in maximum flow, while southern catchments indicate a decrease, consistent with the findings in the *Hydroclimatic Atlas of Southern Québec* (MDDELCC, 2022). The relative change in maximum flow is correlated with the relative change in SWE ($r = 0.76$). Southern catchments show a stronger decrease in high flows due to their significant decrease in SWE. Conversely, northern catchments present a smaller magnitude of decrease and even an increase in high flows due to a modest reduction in SWE and an increase in total precipitation. Notably, catchments with the highest increases in streamflow are small northern catchments with steep slopes, where the reduction of SWE was modest and heavy rain could rapidly reach the outlet.

The minimum 7-day flow with a 2-year return period shows changes between -44% to 42%, with most catchments showing changes between -23% and 23%. These results align with the findings in Valencia Giraldo et al. (2023) and the *Hydroclimatic Atlas of Southern Québec* (MDDELCC, 2022). Most southern catchments present a decrease in low flows, while two northern catchments exhibit a strong increase. For the latter, minimum flows typically occur during the winter low-flow period. With the reduction of SWE and the increase in rainfall, winter low flows are expected to be less intense, resulting in increased minimum flows during winter. This contrasts with southern catchments, where low flows occur during the summer months. With the increase in evapotranspiration, it is expected that summer low flows will decrease.

Significant changes are observed across streamflow components for the future period. Annual surface runoff shows a 34% decrease, contrasting with the 11% to 21% increase found by Gombault *et al.* (2015). This reduction in surface runoff is linked to decreased snowfall and snowmelt, consistent with findings in Talbot, Sylvain, *et al.* (2024). The timing of peak surface runoff shifts earlier in the year, corresponding with the change in peak flow timing, and an increase in surface runoff is observed from December to April due to snow melt during these months. Surface runoff's contribution to hydrological processes decreases from 21% during the reference period to 12% in the future, indicating a reduced role of surface runoff in the overall water cycle.

5.4.1.4 Soil moisture

Projected changes in soil moisture reflect a nuanced interplay between increased precipitation, temperature rise, and changes in evapotranspiration rates. For the future, our results show a small increase in soil moisture from December to April and a small decrease from May to November relative to reference conditions.

In the winter months, increases in soil moisture are primarily driven by higher temperatures and increased precipitation. Higher temperatures reduce snow cover and soil freezing depth, allowing water to infiltrate the soil more effectively (Lundberg et al., 2016). This is corroborated by a strong correlation ($r = 0.79$) between soil moisture absolute change and winter temperature increase, as well as by the correlation ($r = 0.67$) with the absolute increase in rainfall during winter. The reduction in soil freezing along with higher winter precipitation enable more water to be retained in the soil, increasing soil moisture levels during these months.

From May to November, soil moisture decreases due to higher evapotranspiration rates driven by increased temperatures. The relative decrease in soil moisture is closely related to the relative increase in ETa, with correlation coefficients of 0.81 in summer and 0.79 in autumn. As temperatures rise, more water is lost through evapotranspiration, reducing the amount of water available to infiltrate the soil. Sulis et al. (2011) and Houle et al. (2012) found similar patterns in soil moisture variability, with increases during winter and spring and decreases in summer and autumn, influenced by topographic and pedologic characteristics.

In the distributed results for the Matane Catchment, soil moisture values range from 0.1 to 0.35, depending on the area. Soil moisture levels are closely related to the saturated hydraulic conductivity of the major soil types of each catchment, with a correlation coefficient r of 0.70. Furthermore, absolute changes in soil moisture and groundwater recharge are positively correlated, with an r value of 0.71. This relationship underscores the interconnectedness of soil moisture and groundwater recharge processes, particularly in response to changes in precipitation and evapotranspiration.

5.4.1.5 Groundwater recharge rate

The annual groundwater recharge rate is projected to increase across most catchments, ranging from 6% to over 24%. Temporally, groundwater recharge rates rise from December to May and decrease from July to November compared to the reference period. This temporal pattern is influenced by seasonal variations in precipitation, temperature, and evapotranspiration.

In winter and spring, the increase in groundwater recharge is driven by higher precipitation and lower evapotranspiration compared to the summer months. The higher winter precipitation and reduced soil freezing allow more water to infiltrate and recharge the groundwater. These findings align with Sulis et al. (2011), who observed similar seasonal variations in the Anglais River basin, where winter recharge increased by 49% due to more rain and snowmelt.

Conversely, in summer and autumn, groundwater recharge rates vary, showing both increases and decreases across the catchments. Decreases in groundwater recharge during these seasons are closely correlated with increased evapotranspiration rates. As temperatures rise, more water is lost to evapotranspiration, reducing the amount available for groundwater recharge. This is supported by a strong correlation ($r = -0.71$) between the absolute change in summer ETa and the absolute change in summer recharge. Higher evapotranspiration rates during summer outweigh the increase in precipitation, leading to a net decrease in groundwater recharge. Similar trends were noted by Cochand (2014) in the Saint-Charles River watershed, where summer recharge decreased due to increased evapotranspiration.

For the Matane Catchment, the spatial distribution of groundwater recharge rates varies significantly across the four seasons. Spring exhibits the largest increase, with some areas experiencing rises of up to 20 millimeters. In contrast, autumn shows the greatest decrease, with reductions of up to 20 millimeters. These variations are influenced by the catchment's topography, highlighting the importance of using high-resolution spatial data in hydrological modeling. Dubois et al. (2022) emphasized the need for detailed spatial analysis to accurately capture such variations in groundwater recharge. Other studies in cold and humid climates or regions with snow-dependent hydrology have reported similar patterns of increased winter recharge and decreased summer recharge (Grinevskiy, Pozdniakov, & Dedulina, 2021; Wright & Novakowski, 2020). These studies consistently highlight the significant impact of warmer winters and increased winter liquid precipitation on enhancing groundwater recharge during colder months, while higher summer temperatures and evapotranspiration rates reduce recharge during warmer months.

The spatial variability in groundwater recharge rates is closely linked to elevation. Higher elevations tend to receive less groundwater recharge, while lower elevations receive more. This is reflected in a mean correlation coefficient r of -0.74 (std = 0.19) between the future period recharge of each sub-catchments and their corresponding mean elevation.

Interestingly, these findings contrast with those of Lindquist et al. (2019), who observed a positive relationship between groundwater recharge and elevation, as well as Sulis et al. (2011), who noted that the strongest responses in relative recharge changes were observed at higher elevations. The discrepancy may be attributable to our specific methodological approach, particularly the soil thickness separation we incorporated. In our study, higher elevations had thinner soil layers, while lower elevations had thicker soil layers, potentially influencing recharge rates.

These results emphasize the importance of considering soil thickness in hydrological studies, as it can significantly impact groundwater recharge dynamics. The differences observed in our study suggest that other research might have overlooked this critical factor, leading to differing results. These findings highlight the need for a comprehensive representation of physical soil attributes in hydrological models to better understand and predict groundwater recharge under future climate scenarios.

It is important to critically examine these results and consider that the observed differences might stem from the structural characteristics of the WaSiM model. The model's configuration, including the way soil thickness was assigned based on elevation, might introduce biases that differ from other studies. Therefore, while our findings contribute to the understanding of groundwater recharge dynamics under future climate scenarios, they also highlight the need for cautious interpretation and further investigation into the model's assumptions and configurations.

5.4.2 Benefits and limitations

This study aims to evaluate the hydrological impacts of climate change using a physically based, spatially distributed hydrological model (WaSiM) and the latest CMIP6 climate projections. The key objectives include understanding future hydroclimatic conditions, improving water resources management, and enhancing adaptive strategies.

The primary benefit of using a physically based, spatially distributed model like WaSiM is its ability to capture local heterogeneity and finer-scale processes. This is particularly important for boreal regions like Quebec, which experience diverse and complex hydrological dynamics. The use of multiple Global Climate Models (GCMs) within the CMIP6 framework provides a more comprehensive representation of potential future climatic conditions, thereby reducing the uncertainty associated with a single model approach.

Additionally, the use of an advanced bias-correction method, MBCn, enhances the robustness of climate projections by maintaining inter-variable correlations and spatiotemporal patterns. This approach ensures that the modeled hydrological responses are more reflective of the actual climatic conditions, thus providing valuable insights for water resources management. By focusing on a high-resolution spatial and temporal analysis, the study provides detailed insights into the seasonal and spatial variability of hydrological processes. This level of detail is crucial for understanding how different parts of the catchments will respond to climate change, aiding in more targeted and effective management practices.

Despite its strengths, this study has limitations that need to be addressed in future research. One limitation is the reliance on a single Shared Socioeconomic Pathway (SSP) scenario. While this study focused on the worst-case SSP5-8.5 scenario to highlight potential extreme impacts, incorporating multiple SSP scenarios would provide a more comprehensive view of potential future climatic conditions and their impacts on hydrological processes. Another limitation is the use of only one hydrological model. Although WaSiM is well-suited for capturing spatiotemporal dynamics, employing multiple hydrological models would provide a more nuanced understanding of hydrological responses and reduce model-related uncertainty. However, this approach would significantly increase computational time and resources.

The calibration of only one set of parameters per catchment introduces additional uncertainty. Despite the model demonstrating strong validation performance along with the use of an integrated calibration approach that enhances the representation of catchment hydrological processes (Talbot et al., 2024), using multiple parameter sets could offer a more comprehensive assessment of the sensitivity and variability of the hydroclimatic variables. However, this would also cause an increase in computational time and complexity. Furthermore, the spatial and temporal resolution of the model, although effective, may overlook some finer-scale processes. Increasing these resolutions could provide more detailed insights, particularly in heterogeneous landscapes and during extreme short-time meteorological events. Nevertheless, this would also result in increased computational time.

This research underscores the importance of employing advanced modeling techniques and the latest climate projections to enhance our understanding of climate change impacts on hydrology. The methodologies and findings from this study, although focused on Quebec, provide valuable insights that can be extrapolated to other regions with similar hydroclimatic and topographic characteristics. For instance, regions in Northern Europe, North America, and parts of Asia that experience cold winters and significant snow cover can benefit from understanding the potential impacts of climate change on their hydrological processes.

Having spatially distributed results is crucial for identifying regions at risk, understanding hydrological dynamics, and developing targeted water management strategies. The spatially explicit modeling approach allows for the identification of specific areas that may be more vulnerable to changes in precipitation, snow cover and depth, soil moisture, and groundwater recharge. This detailed information can guide the implementation of adaptive measures, such as improving infrastructure resilience, protecting critical habitats, and ensuring sustainable water supply.

Overall, the implications of these findings highlight the need for spatially explicit models in water resources management. By providing a comprehensive assessment of future hydrological changes, this study supports more informed decision-making and adaptive management practices to mitigate the impacts of climate change on water resources and ecosystems.

5.5 Conclusion

This study comprehensively assessed the impacts of climate change on hydroclimatic variables in Quebec using a physically based, spatially distributed hydrological model (WaSiM) and CMIP6 climate projections. The findings reveal significant changes in snow water equivalent, evapotranspiration, groundwater recharge, soil moisture, and streamflow dynamics under future climate scenarios.

Key results indicate a considerable increase in total precipitation and temperature, leading to a shift from snowfall to rainfall, reduced snowpack, and earlier snowmelt. This change is expected to cause a seasonal shift in the timing of peak flows and an increase in winter minimum flows. Additionally, the study highlights a significant increase in groundwater recharge rates during the winter and spring months, attributed to higher precipitation and reduced soil freezing.

This research underscores the importance of employing advanced modeling techniques and the latest climate projections to enhance our understanding of climate change impacts on hydrology. The methodologies and findings are not only pertinent to Quebec but also applicable to other regions with similar climatic and hydrological conditions, such as parts of Europe, North America, and Asia. By providing a more accurate and comprehensive assessment of future hydrological changes, this study supports more informed decision-making and adaptive management practices to mitigate the impacts of climate change on water resources and ecosystems globally.

5.6 Acknowledgements

This work was funded jointly by the ministère des Ressources naturelles et des Forêts (Quebec, Canada, project number 112332187 conducted at the Direction de la recherche forestière and led by Jean-Daniel Sylvain) and the Forest research service contract number 3322-2022-2187-01 obtained by Richard Arsenault from the Ministère des Ressources naturelles et des Forêts (Quebec, Canada). The authors also acknowledge the use of ChatGPT-4 for assistance in correcting spelling mistakes and improving the flow of text during the manuscript preparation process. The base map in Fig. 5.1 was created using ArcGIS® software by Esri. ArcGIS® and ArcMap™ are the intellectual property of Esri and are used herein under license. For more information about Esri® software, please visit www.esri.com.

5.7 References

Arsenault, R., Brissette, F., Chen, J., Guo, Q., & Dallaire, G. (2020). NAC2H : The North American Climate Change and Hydroclimatology Data Set. *Water Resources Research*, *56*(8), e2020WR027097. https://doi.org/10.1029/2020WR027097

Arsenault, R., Poulin, A., Côté, P., & Brissette, F. (2014). Comparison of Stochastic Optimization Algorithms in Hydrological Model Calibration. *Journal of Hydrologic Engineering*, *19*(7), 1374-1384. https://doi.org/10.1061/(ASCE)HE.1943-5584.0000938

Aygün, O., Kinnard, C., & Campeau, S. (2020). Impacts of climate change on the hydrology of northern midlatitude cold regions. *Progress in Physical Geography : Earth and Environment*, *44*(3), 338-375. https://doi.org/10.1177/0309133319878123

Aygün, O., Kinnard, C., Campeau, S., & Krogh, S. A. (2020). Shifting Hydrological Processes in a Canadian Agroforested Catchment due to a Warmer and Wetter Climate. *Water*, *12*(3), 739. https://doi.org/10.3390/w12030739

Beck, H. E., Zimmermann, N. E., McVicar, T. R., Vergopolan, N., Berg, A., & Wood, E. F. (2018). Present and future Köppen-Geiger climate classification maps at 1-km resolution. *Scientific Data*, *5*(1), 180214. https://doi.org/10.1038/sdata.2018.214

Beven, K. (2001). How far can we go in distributed hydrological modelling? *Hydrology and Earth System Sciences*, *5*(1), 1-12. https://doi.org/10.5194/hess-5-1-2001

Blöschl, G., & Sivapalan, M. (1995). Scale issues in hydrological modelling : A review. *Hydrological Processes*, *9*(3-4), 251-290. https://doi.org/10.1002/hyp.3360090305

Bormann, H., & Elfert, S. (2010). Application of WaSiM-ETH model to Northern German lowland catchments : Model performance in relation to catchment characteristics and sensitivity to land use change. Dans *Advances in Geosciences* (Vol. 27, pp. 1-10). Copernicus GmbH. https://doi.org/10.5194/adgeo-27-1-2010

Boucher, O., Servonnat, J., Albright, A. L., Aumont, O., Balkanski, Y., Bastrikov, V., … Vuichard, N. (2020). Presentation and Evaluation of the IPSL-CM6A-LR Climate Model. *Journal of Advances in Modeling Earth Systems*, *12*(7), e2019MS002010. https://doi.org/10.1029/2019MS002010

Calvin, K., Dasgupta, D., Krinner, G., Mukherji, A., Thorne, P. W., Trisos, C., … Péan, C. (2023). *IPCC, 2023 : Climate Change 2023: Synthesis Report. Contribution of Working Groups I, II and III to the Sixth Assessment Report of the Intergovernmental Panel on Climate Change [Core Writing Team, H. Lee and J. Romero (eds.)]. IPCC, Geneva, Switzerland.* Intergovernmental Panel on Climate Change (IPCC). https://doi.org/10.59327/IPCC/AR6-9789291691647

Cannon, A. J. (2018). Multivariate quantile mapping bias correction : An N-dimensional probability density function transform for climate model simulations of multiple variables. *Climate Dynamics*, *50*(1), 31-49. https://doi.org/10.1007/s00382-017-3580-6

Cao, J., Ma, L., Liu, F., Chai, J., Zhao, H., He, Q., … Wang, B. (2021). NUIST ESM v3 Data Submission to CMIP6. *Advances in Atmospheric Sciences*, *38*(2), 268-284. https://doi.org/10.1007/s00376-020-0173-9

Cochand, F. (2014). Impact des changements climatiques et du développement urbain sur les ressources en eaux du bassin versant de la rivière Saint-Charles. Repéré à http://hdl.handle.net/20.500.11794/25465

Cochand, F., Therrien, R., & Lemieux, J.-M. (2019). Integrated Hydrological Modeling of Climate Change Impacts in a Snow-Influenced Catchment. *Groundwater*, *57*(1), 3-20. https://doi.org/10.1111/gwat.12848

Commission for Environmental Cooperation. (2020). 2015 Land Cover of North America ar 30 meters. *Commission for Environmental Cooperation*. Repéré à http://www.cec.org/north-american-environmental-atlas/land-cover-30m-2015-landsat-and-rapideye/

Conrad, O., Bechtel, B., Bock, M., Dietrich, H., Fischer, E., Gerlitz, L., … Böhner, J. (2015). System for Automated Geoscientific Analyses (SAGA) v. 2.1.4. *Geoscientific Model Development*, *8*(7), 1991-2007. https://doi.org/10.5194/gmd-8-1991-2015

Coron, L., Andréassian, V., Perrin, C., Bourqui, M., & Hendrickx, F. (2014). On the lack of robustness of hydrologic models regarding water balance simulation : A diagnostic approach applied to three models of increasing complexity on 20 mountainous catchments. *Hydrology and Earth System Sciences*, *18*(2), 727-746. https://doi.org/10.5194/hess-18-727-2014

Dallaire, G., Poulin, A., Arsenault, R., & Brissette, F. (2021). Uncertainty of potential evapotranspiration modelling in climate change impact studies on low flows in North

America. *Hydrological Sciences Journal*, *66*(4), 689-702. https://doi.org/10.1080/02626667.2021.1888955

Devia, G. K., Ganasri, B. P., & Dwarakish, G. S. (2015). A Review on Hydrological Models. *Aquatic Procedia*, *4*, 1001-1007. https://doi.org/10.1016/j.aqpro.2015.02.126

Döscher, R., Acosta, M., Alessandri, A., Anthoni, P., Arsouze, T., Bergman, T., … Zhang, Q. (2022). The EC-Earth3 Earth system model for the Coupled Model Intercomparison Project 6. *Geoscientific Model Development*, *15*(7), 2973-3020. https://doi.org/10.5194/gmd-15-2973-2022

Dubois, E., Larocque, M., Gagné, S., & Braun, M. (2022). Climate Change Impacts on Groundwater Recharge in Cold and Humid Climates : Controlling Processes and Thresholds. *Climate*, *10*(1), 6. https://doi.org/10.3390/cli10010006

Duethmann, D., Blöschl, G., & Parajka, J. (2020). Why does a conceptual hydrological model fail to correctly predict discharge changes in response to climate change? *Hydrology and Earth System Sciences*, *24*(7), 3493-3511. https://doi.org/10.5194/hess-24-3493-2020

Ekmekcioğlu, Ö., Demirel, M. C., & Booij, M. J. (2022). Effect of data length, spin-up period and spatial model resolution on fully distributed hydrological model calibration in the Moselle basin. *Hydrological Sciences Journal*, *67*(5), 759-772. https://doi.org/10.1080/02626667.2022.2046754

Estrada, F., Kim, D., & Perron, P. (2021). Spatial variations in the warming trend and the transition to more severe weather in midlatitudes. *Scientific Reports*, *11*(1), 145. https://doi.org/10.1038/s41598-020-80701-7

Gädeke, A., Hölzel, H., Koch, H., Pohle, I., & Grünewald, U. (2014). Analysis of uncertainties in the hydrological response of a model-based climate change impact assessment in a subcatchment of the Spree River, Germany. *Hydrological Processes*, *28*(12), 3978-3998. https://doi.org/10.1002/hyp.9933

Gleick, P. H. (1989). Climate change, hydrology, and water resources. *Reviews of Geophysics*, *27*(3), 329-344. https://doi.org/10.1029/rg027i003p00329

Gombault, C., Sottile, M.-F., Ngwa, F. F., Madramootoo, C. A., Michaud, A. R., Beaudin, I., & Chikhaoui, M. (2015). Modelling climate change impacts on the hydrology of an agricultural watershed in southern Québec. *Canadian Water Resources Journal /*

Revue canadienne des ressources hydriques, *40*(1), 71-86. https://doi.org/10.1080/07011784.2014.985509

Grinevskiy, S. O., Pozdniakov, S. P., & Dedulina, E. A. (2021). Regional-Scale Model Analysis of Climate Changes Impact on the Water Budget of the Critical Zone and Groundwater Recharge in the European Part of Russia. *Water*, *13*(4), 428. https://doi.org/10.3390/w13040428

Han, F., Zheng, Y., Tian, Y., Li, X., Zheng, C., & Li, X. (2021). Accounting for field-scale heterogeneity in the ecohydrological modeling of large arid river basins : Strategies and relevance. *Journal of Hydrology*, *595*, 126045. https://doi.org/10.1016/j.jhydrol.2021.126045

Hausfather, Z., Marvel, K., Schmidt, G. A., Nielsen-Gammon, J. W., & Zelinka, M. (2022). Climate simulations : Recognize the « hot model » problem. *Nature*, *605*(7908), 26-29. https://doi.org/10.1038/d41586-022-01192-2

Hersbach, H., Bell, B., Berrisford, P., Hirahara, S., Horányi, A., Muñoz-Sabater, J., … Thépaut, J.-N. (2020). The ERA5 global reanalysis. *Quarterly Journal of the Royal Meteorological Society*, *146*(730), 1999-2049. https://doi.org/10.1002/qj.3803

Houle, D., Bouffard, A., Duchesne, L., Logan, T., & Harvey, R. (2012). Projections of Future Soil Temperature and Water Content for Three Southern Quebec Forested Sites. https://doi.org/10.1175/JCLI-D-11-00440.1

Hydroclimatic Atlas of Southern Québec. (2022). Repéré à https://www.cehq.gouv.qc.ca/atlas-hydroclimatique/index-en.htm

Iacob, O., Brown, I., & Rowan, J. (2017). Natural flood management, land use and climate change trade-offs : The case of Tarland catchment, Scotland. *Hydrological Sciences Journal*, *62*(12), 1931-1948. https://doi.org/10.1080/02626667.2017.1366657

Jasper, K., Calanca, P., & Fuhrer, J. (2006). Changes in summertime soil water patterns in complex terrain due to climatic change. *Journal of Hydrology*, *327*(3), 550-563. https://doi.org/10.1016/j.jhydrol.2005.11.061

Jones, R. N., Chiew, F. H. S., Boughton, W. C., & Zhang, L. (2006). Estimating the sensitivity of mean annual runoff to climate change using selected hydrological models. *Advances in Water Resources*, *29*(10), 1419-1429. https://doi.org/10.1016/j.advwatres.2005.11.001

Kling, H., Fuchs, M., & Paulin, M. (2012). Runoff conditions in the upper Danube basin under an ensemble of climate change scenarios. *Journal of Hydrology*, *424-425*, 264-277. https://doi.org/10.1016/j.jhydrol.2012.01.011

Kour, R., Patel, N., & Krishna, A. P. (2016). Climate and hydrological models to assess the impact of climate change on hydrological regime : A review. *Arabian Journal of Geosciences*, *9*(9), 544. https://doi.org/10.1007/s12517-016-2561-0

Krasting, J. P., Blanton, C., McHugh, C., Radhakrishnan, A., John, J. G., Rand, K., … Zeng, Y. (2018, 7 janvier). NOAA-GFDL GFDL-ESM4 model output prepared for CMIP6 C4MIP esm-ssp585. World Data Center for Climate (WDCC) at DKRZ. Repéré à https://hdl.handle.net/21.14106/c74f845181dd8d041cd5823a97f44a6cf444401c

Latifovic, R., Homer, C., Ressl, R., Pouliot, D. A., Hossian, S., Colditz, R., … Victoria, A. (2012). North American Land Change Monitoring System. *Remote Sensing of Land Use and Land Cover : Principles and Applications*, 303-324. https://doi.org/10.1201/b11964-24

Lindquist, L. W., Palmquist, K. A., Jordan, S. E., & Lauenroth, W. K. (2019). Impacts of Climate Change on Groundwater Recharge in Wyoming Big Sagebrush Ecosystems are Contingent on Elevation. *Western North American Naturalist*, *79*(1), 37-48. https://doi.org/10.3398/064.079.0104

Lovato, T., Peano, D., Butenschön, M., Materia, S., Iovino, D., Scoccimarro, E., … Navarra, A. (2022). CMIP6 Simulations With the CMCC Earth System Model (CMCC-ESM2). *Journal of Advances in Modeling Earth Systems*, *14*(3), e2021MS002814. https://doi.org/10.1029/2021MS002814

Lucas-Picher, P., Lachance-Cloutier, S., Arsenault, R., Poulin, A., Ricard, S., Turcotte, R., & Brissette, F. (2021). Will Evolving Climate Conditions Increase the Risk of Floods of the Large U.S.-Canada Transboundary Richelieu River Basin? *JAWRA Journal of the American Water Resources Association*, *57*(1), 32-56. https://doi.org/10.1111/1752-1688.12891

Ludwig, R., May, I., Turcotte, R., Vescovi, L., Braun, M., Cyr, J.-F., … Mauser, W. (2009). The role of hydrological model complexity and uncertainty in climate change impact assessment. *Advances in Geosciences*, *21*, 63-71. https://doi.org/10.5194/adgeo-21-63-2009

Lundberg, A., Ala-Aho, P., Eklo, O., Klöve, B., Kværner, J., & Stumpp, C. (2016). Snow and frost : Implications for spatiotemporal infiltration patterns – a review. *Hydrological Processes*, *30*(8), 1230-1250. https://doi.org/10.1002/hyp.10703

Martel, J.-L., Brissette, F., Troin, M., Arsenault, R., Chen, J., Su, T., & Lucas-Picher, P. (2022). CMIP5 and CMIP6 Model Projection Comparison for Hydrological Impacts Over North America. *Geophysical Research Letters*, *49*(15), e2022GL098364. https://doi.org/10.1029/2022GL098364

Mauritsen, T., Bader, J., Becker, T., Behrens, J., Bittner, M., Brokopf, R., … Roeckner, E. (2019). Developments in the MPI-M Earth System Model version 1.2 (MPI-ESM1.2) and Its Response to Increasing CO2. *Journal of Advances in Modeling Earth Systems*, *11*(4), 998-1038. https://doi.org/10.1029/2018MS001400

McDonnell, J. J., Spence, C., Karran, D. J., van Meerveld, H. J. (Ilja), & Harman, C. J. (2021). Fill-and-Spill : A Process Description of Runoff Generation at the Scale of the Beholder. *Water Resources Research*, *57*(5), e2020WR027514. https://doi.org/10.1029/2020WR027514

Meert, P., Pereira, F., & Willems, P. (2018). Surrogate modeling-based calibration of hydrodynamic river model parameters. *Journal of Hydro-environment Research*, *19*, 56-67. https://doi.org/10.1016/j.jher.2018.02.003

Middelkoop, H., Daamen, K., Gellens, D., Grabs, W., Kwadijk, J. C. J., Lang, H., … Wilke, K. (2001). Impact of Climate Change on Hydrological Regimes and Water Resources Management in the Rhine Basin. *Climatic Change*, *49*(1), 105-128. https://doi.org/10.1023/A:1010784727448

Milly, P. C. D., Betancourt, J., Falkenmark, M., Hirsch, R. M., Kundzewicz, Z. W., Lettenmaier, D. P., & Stouffer, R. J. (2008). Stationarity Is Dead : Whither Water Management? *Science*, *319*(5863), 573-574. https://doi.org/10.1126/science.1151915

Milly, P. C. D., Dunne, K. A., & Vecchia, A. V. (2005). Global pattern of trends in streamflow and water availability in a changing climate. *Nature*, *438*(7066), 347-350. https://doi.org/10.1038/nature04312

Ministère des Ressources Naturelles et des Forêts. (2022). *SIIGSOL-100m—Carte des propriétés du sol*. Données Québec. Repéré à https://www.donneesquebec.ca/recherche/dataset/siigsol-100m-carte-des-proprietes-du-sol

Minville, M., Brissette, F., & Leconte, R. (2008). Uncertainty of the impact of climate change on the hydrology of a nordic watershed. *Journal of Hydrology*, *358*(1), 70-83. https://doi.org/10.1016/j.jhydrol.2008.05.033

Mudryk, L. R., Derksen, C., Howell, S., Laliberté, F., Thackeray, C., Sospedra-Alfonso, R., … Brown, R. (2018). Canadian snow and sea ice : Historical trends and projections. *The Cryosphere*, *12*(4), 1157-1176. https://doi.org/10.5194/tc-12-1157-2018

Nolin, A. F., Girardin, M. P., Adamowski, J. F., Barzegar, R., Boucher, M.-A., Tardif, J. C., & Bergeron, Y. (2023). Observed and projected trends in spring flood discharges for the Upper Harricana River, eastern boreal Canada. *Journal of Hydrology : Regional Studies*, *48*, 101462. https://doi.org/10.1016/j.ejrh.2023.101462

Novotná, B., van Bochove, E., & Thériault, G. (2013). Potential ecological impact of climate change on the water quality of an intensively managed agricultural watershed in Quebec, Canada. *Journal of Water and Climate Change*, *5*(1), 81-99. https://doi.org/10.2166/wcc.2013.121

O'Neill, B. C., Tebaldi, C., van Vuuren, D. P., Eyring, V., Friedlingstein, P., Hurtt, G., … Sanderson, B. M. (2016). The Scenario Model Intercomparison Project (ScenarioMIP) for CMIP6. *Geoscientific Model Development*, *9*(9), 3461-3482. https://doi.org/10.5194/gmd-9-3461-2016

Poulin, A., Brissette, F., Leconte, R., Arsenault, R., & Malo, J.-S. (2011). Uncertainty of hydrological modelling in climate change impact studies in a Canadian, snow-dominated river basin. *Journal of Hydrology*, *409*(3), 626-636. https://doi.org/10.1016/j.jhydrol.2011.08.057

Pu, Y., Liu, H., Yan, R., Yang, H., Xia, K., Li, Y., … Zuo, L. (2020). CAS FGOALS-g3 Model Datasets for the CMIP6 Scenario Model Intercomparison Project (ScenarioMIP). *Advances in Atmospheric Sciences*, *37*(10), 1081-1092. https://doi.org/10.1007/s00376-020-2032-0

Riboust, P., & Brissette, F. (2015). Climate Change Impacts and Uncertainties on Spring Flooding of Lake Champlain and the Richelieu River. *JAWRA Journal of the American Water Resources Association*, *51*(3), 776-793. https://doi.org/10.1111/jawr.12271

Ricard, S., Sylvain, J.-D., & Anctil, F. (2019). Exploring an Alternative Configuration of the Hydroclimatic Modeling Chain, Based on the Notion of Asynchronous Objective Functions. *Water*, *11*(10), 2012. https://doi.org/10.3390/w11102012

Ricard, S., Sylvain, J.-D., & Anctil, F. (2020). Asynchronous Hydroclimatic Modeling for the Construction of Physically Based Streamflow Projections in a Context of Observation Scarcity. *Frontiers in Earth Science*, *8*. Repéré à https://www.frontiersin.org/articles/10.3389/feart.2020.556781

Schulla, J. (2021). WaSiM-ETH Documentation. Repéré à http://www.wasim.ch/en/products/wasim_description.htm

Seland, Ø., Bentsen, M., Olivié, D., Toniazzo, T., Gjermundsen, A., Graff, L. S., … Schulz, M. (2020). Overview of the Norwegian Earth System Model (NorESM2) and key climate response of CMIP6 DECK, historical, and scenario simulations. *Geoscientific Model Development*, *13*(12), 6165-6200. https://doi.org/10.5194/gmd-13-6165-2020

Sivakumar, B. (2011). Global climate change and its impacts on water resources planning and management : Assessment and challenges. *Stochastic Environmental Research and Risk Assessment*, *25*(4), 583-600. https://doi.org/10.1007/s00477-010-0423-y

Sulis, M., Paniconi, C., Rivard, C., Harvey, R., & Chaumont, D. (2011). Assessment of climate change impacts at the catchment scale with a detailed hydrological model of surface-subsurface interactions and comparison with a land surface model. *Water Resources Research*, *47*(1). https://doi.org/10.1029/2010WR009167

Swart, N. C., Cole, J. N. S., Kharin, V. V., Lazare, M., Scinocca, J. F., Gillett, N. P., … Winter, B. (2019). The Canadian Earth System Model version 5 (CanESM5.0.3). *Geoscientific Model Development*, *12*(11), 4823-4873. https://doi.org/10.5194/gmd-12-4823-2019

Sylvain, J.-D., Anctil, F., & Thiffault, E. (2021). Using bias correction and ensemble modelling for predictive mapping and related uncertainty : A case study in digital soil mapping. *Geoderma*, *403*, 1-29. https://doi.org/10.1016/j.geoderma.2021.115153

Talbot, F., Sylvain, J.-D., Drolet, G., Poulin, A., & Arsenault, R. (2024). Enhancing physically based and distributed hydrological model calibration through internal state variable constraints. *EGUsphere*, 1-42. https://doi.org/10.5194/egusphere-2024-3353

Tarek, M., Brissette, F., & Arsenault, R. (2021). Uncertainty of gridded precipitation and temperature reference datasets in climate change impact studies. *Hydrology and Earth System Sciences*, *25*(6), 3331-3350. https://doi.org/10.5194/hess-25-3331-2021

Tarek, M., Brissette, F. P., & Arsenault, R. (2020). Evaluation of the ERA5 reanalysis as a potential reference dataset for hydrological modelling over North America. *Hydrology and Earth System Sciences*, *24*(5), 2527-2544. https://doi.org/10.5194/hess-24-2527-2020

Tatebe, H., Ogura, T., Nitta, T., Komuro, Y., Ogochi, K., Takemura, T., … Kimoto, M. (2019). Description and basic evaluation of simulated mean state, internal variability, and climate sensitivity in MIROC6. *Geoscientific Model Development*, *12*(7), 2727-2765. https://doi.org/10.5194/gmd-12-2727-2019

Taylor, K. E., Stouffer, R. J., & Meehl, G. A. (2012). An Overview of CMIP5 and the Experiment Design. *Bulletin of the American Meteorological Society*, *93*(4), 485-498. https://doi.org/10.1175/BAMS-D-11-00094.1

Valencia Giraldo, M. del C., Ricard, S., & Anctil, F. (2023). Assessment of the Potential Hydrological Impacts of Climate Change in Quebec—Canada, a Refined Neutral Approach. *Water*, *15*(3), 584. https://doi.org/10.3390/w15030584

Volodin, E., Mortikov, E., Gritsun, A., Lykossov, V., Galin, V., Diansky, N., … Emelina, S. (2019, 30 mai). INM INM-CM4-8 model output prepared for CMIP6 CMIP. World Data Center for Climate (WDCC) at DKRZ. Repéré à https://hdl.handle.net/21.14106/7c23e83ce8071b5c0079a65af16b51d81b27a2a9

Wilby, R. L. (2005). Uncertainty in water resource model parameters used for climate change impact assessment. *Hydrological Processes*, *19*(16), 3201-3219. https://doi.org/10.1002/hyp.5819

Wright, S. N., & Novakowski, K. S. (2020). Impacts of warming winters on recharge in a seasonally frozen bedrock aquifer. *Journal of Hydrology*, *590*, 125352. https://doi.org/10.1016/j.jhydrol.2020.125352

Yue, X.-L., & Gao, Q.-X. (2018). Contributions of natural systems and human activity to greenhouse gas emissions. *Advances in Climate Change Research*, *9*(4), 243-252. https://doi.org/10.1016/j.accre.2018.12.003

Yukimoto, S., Kawai, H., Koshiro, T., Oshima, N., Yoshida, K., Urakawa, S., … Ishii, M. (2019). The Meteorological Research Institute Earth System Model Version 2.0, MRI-ESM2.0 : Description and Basic Evaluation of the Physical Component. *気象集誌. 第2輯*, *97*(5), 931-965. https://doi.org/10.2151/jmsj.2019-051

Ziehn, T., Chamberlain, M. A., Law, R. M., Lenton, A., Bodman, R. W., Dix, M., … Srbinovsky, J. (2020). The Australian Earth System Model : ACCESS-ESM1.5.

Journal of Southern Hemisphere Earth Systems Science, *70*(1), 193-214. https://doi.org/10.1071/ES19035

CHAPITRE 6

DISCUSSION

6.1 Représentation des variables hydrologiques

6.1.1 Calibration

La calibration des modèles hydrologiques est une étape cruciale pour assurer la précision et la fiabilité des variables hydrologiques. Traditionnellement, la calibration vise à reproduire des débits observés à l'exutoire d'un bassin versant. Cependant, comme le souligne la revue de littérature (Bouaziz et al., 2021; Yassin et al., 2017), calibrer un modèle uniquement sur le débit ne garantit pas une représentation adéquate des variables hydrologiques internes telles que l'humidité du sol, la recharge des nappes phréatiques ou l'évapotranspiration. Cela peut entraîner des modèles équifinaux, où différentes combinaisons de paramètres produisent des débits similaires mais des variables hydrologiques divergentes.

Les résultats du chapitre 3 de ce mémoire illustrent parfaitement ce problème. Trois configurations de calibration distinctes ont été analysées : BL (modèle de base), GW (simulation à base physique des eaux souterraines) et GW-RC (simulation à base physique des eaux souterraines et calibration de la recharge). Bien que les configurations BL et GW aient obtenu des valeurs de KGE plus élevées durant les périodes de calibration et de validation, la configuration GW-RC, a démontré une meilleure représentation des variables hydrologiques. L'intégration de la recharge des nappes phréatiques dans la métrique de performance a permis de réduire l'espace paramétrique et permettant une calibration plus ciblée sur plusieurs variables hydrologiques simultanément.

La calibration multi-variable a démontré son efficacité dans l'amélioration de la représentation des variables hydrologiques (de Lima Ferreira & da Paz, 2024; Dembélé, Hrachowitz, et al., 2020; Mei et al., 2023; Pool et al., 2024; Yassin et al., 2017). L'intégration de la recharge des nappes phréatiques dans la configuration GW-RC a amélioré la représentation des variables hydrologiques. En particulier, elle a permis une meilleure simulation des dynamiques hydrologiques, notamment en prenant en compte le dégel du sol lors de la fonte des neiges. Plus de détails sont disponibles au chapitre 3.

De plus, il est important d'analyser ou de valider explicitement la représentation des variables hydrologiques internes. Bingeman *et al.* (2006) ont démontré que la validation explicite de variables comme l'humidité du sol, l'évapotranspiration, l'accumulation et la fonte de la neige, ainsi que le flux des eaux souterraines, est essentielle pour garantir que le modèle offre une bonne représentation des processus hydrologiques. L'analyse de la représentation des variables hydrologiques du modèle permet de détecter des incohérences internes, de réduire les risques liés au problème d'équifinalité et d'améliorer la robustesse du modèle pour l'analyse de l'impact des changements climatiques.

Dans l'optique où les variables hydrologiques sont d'intérêt, la calibration des modèles hydrologiques doit aller au-delà de la simple optimisation du débit et inclure plusieurs variables hydrologiques d'intérêt. Cette approche, conjointement avec une validation des variables hydrologiques, permet de réduire le problème d'équifinalité et d'améliorer la représentation des processus internes, comme démontré par les résultats du chapitre 3. L'intégration de variables supplémentaires dans la calibration, soutenue par des études antérieures, conduit à des simulations hydrologiques plus réalistes et robustes, essentielles pour une gestion efficace des ressources en eau face aux changements climatiques.

6.1.2 Chaîne de modélisation hydroclimatique

La chaîne de modélisation hydroclimatique est un processus essentiel pour évaluer les impacts des changements climatiques sur les systèmes hydrologiques. Elle repose sur plusieurs étapes clés, allant des scénarios climatiques à l'intégration dans des modèles hydrologiques, en passant par des techniques de correction de biais et de calibration des modèles. Chaque étape contribue à introduire des incertitudes, qui peuvent influencer les résultats des simulations. Le chapitre 4 de ce mémoire s'est concentré sur l'évaluation d'une nouvelle approche dans la chaîne de modélisation : la méthode asynchrone, qui se distingue des méthodes conventionnelles en évitant la correction des biais et en intégrant directement les données brutes des modèles climatiques.

Les résultats du chapitre 4 mettent en lumière les limites de cette approche pour représenter les variables hydrologiques de manière cohérente. En particulier, la synchronisation temporelle des processus hydrologiques, comme l'accumulation et la fonte de la neige, est souvent inadéquate. Par exemple, certaines simulations climatiques produisaient de fontes de neige en plein été, un résultat inattendu qui perturbe le partitionnement de l'eau et compromet la représentativité des autres variables hydrologiques.

Cette incohérence dans la synchronisation des événements hydrologiques est un défi majeur pour la méthode asynchrone, qui repose sur des données climatiques brutes souvent biaisées. Ces biais peuvent entraîner des projections où les processus hydrologiques, tels que la fonte des neiges, se produisent trop tôt ou trop tard, compromettant ainsi la précision des prévisions (J. Chen et al., 2021; Ricard et al., 2023). Cette sensibilité aux biais non corrigés est un point faible de la méthode asynchrone, particulièrement dans les régions où les dynamiques hydrologiques sont fortement influencées par les conditions climatiques saisonnières.

Un autre point soulevé dans le chapitre 4 est l'incertitude accrue dans les projections hydrologiques lorsque la méthode asynchrone est utilisée. Les résultats montrent que cette approche est plus sensible aux variations entre les différents modèles climatiques, ce qui entraîne une plus grande variabilité dans les projections des débits et d'autres variables hydrologiques. Cette sensibilité accrue est due à l'absence de correction des biais qui, en utilisant les mêmes observations, pourrait autrement atténuer les écarts entre les différents modèles climatiques (Ricard et al., 2023).

Enfin, les résultats du chapitre 4 mettent en évidence la nécessité de futures améliorations à la méthode asynchrone. Une voie prometteuse serait de développer une approche semiasynchrone qui intègre des éléments de synchronisation, permettant ainsi une meilleure représentation temporelle des processus hydrologiques tout en conservant les avantages de la méthode asynchrone.

6.2 Impact des changements climatiques sur les variables hydrologiques

Les changements climatiques ont un impact considérable sur les variables hydrologiques, en particulier dans les régions plus nordiques telles que le Québec. Les résultats de cette étude, présentés au chapitre 5, confirment certaines tendances identifiées dans la littérature tout en apportant des perspectives nouvelles sur l'évolution des processus hydrologiques sous l'influence des changements climatiques.

Les résultats du chapitre 5 révèlent une augmentation globale des précipitations dans la région étudiée, particulièrement marquée entre novembre et avril. Cette hausse s'accompagne d'une augmentation significative des températures. Cette élévation des températures a pour conséquence un changement notable de la nature des précipitations, une part importante des précipitations hivernales passant de la neige à la pluie. Cette transition a des répercussions directes sur la dynamique de l'enneigement et sur les régimes d'écoulement. Les mois d’hiver verront probablement une augmentation des écoulements en raison (1) des redoux hivernaux causant une fonte de neige précoce et (2) de la pluie supplémentaire. De plus, la réduction de l’accumulation de neige, tant en quantité qu’en durée, entraînera une diminution du nombre de jours consécutifs de couverture neigeuse. Le déplacement de la crue printanière montre que les débits de pointe se produisent en moyenne 32 jours plus tôt, avec des débits de pointe généralement plus faibles, particulièrement dans les bassins versants situés au sud de la région d’étude.

De plus, les projections indiquent une augmentation de l’évapotranspiration, conséquence directe de l’élévation des températures et d'une plus grande disponibilité de l'eau en raison des précipitations hivernales. L'augmentation de l’évapotranspiration a des répercussions importantes sur l’humidité des sols et la recharge des nappes phréatiques. Avec des températures plus élevées et des taux d'évaporation accrus, l’humidité des sols pourrait diminuer pendant les mois d’été et d’automne, entraînant des sols plus secs. Cette augmentation de l’évapotranspiration contribue également à la baisse des débits d’étiage, un facteur préoccupant pour la gestion de l’eau en période de sécheresse, particulièrement dans les bassins versants où les ressources en eau sont déjà limitées.

Enfin, les résultats du chapitre 5 montrent une augmentation de la recharge en hiver et au début du printemps, due à une infiltration accrue résultant de la réduction des périodes de gel et de l'augmentation des précipitations hivernales sous forme liquide. Cependant, cette augmentation saisonnière est partiellement compensée par une diminution de la recharge pendant les mois d’été et d’automne, où l’évapotranspiration plus intense réduit la quantité d’eau disponible pour la recharge. De plus, les résultats mettent en évidence une variabilité spatiale importante des taux de recharge, influencée par l’altitude et les caractéristiques géomorphologiques des bassins versants. Toutefois, ces projections sont issues du scénario SSP5-8.5 uniquement, qui représente une trajectoire à fortes émissions de gaz à effet de serre, et les résultats pourraient différer sous des scénarios plus modérés.

6.3 Implications

En revenant à l’introduction de ce mémoire, il est clair que l’un des défis majeurs de notre époque est l’adaptation aux changements climatiques. Ce mémoire a contribué à cet effort en offrant une évaluation détaillée de l'impact des changements climatiques sur les variables hydrologiques au Québec, avec un accent particulier sur l'amélioration de la représentation de ces variables dans les modèles hydrologiques. À travers trois articles, ce travail a permis de mieux comprendre les dynamiques hydrologiques sous des conditions climatiques futures, en identifiant plusieurs configurations du modèle hydrologique WaSiM et en comparant diverses approches de modélisation.

Les implications de cette recherche sont multiples. D'une part, l'amélioration des modèles hydrologiques permettra aux gestionnaires de l'eau de prendre des décisions mieux informées face aux défis croissants liés aux précipitations, à l'évapotranspiration et à la disponibilité de l'eau. En particulier, la réduction des périodes de gel et l'augmentation des écoulements hivernaux suggèrent que des ajustements seront nécessaires dans la gestion des infrastructures de retenue et dans les prévisions hydrologiques saisonnières.

D'autre part, cette recherche souligne l'importance de l’adaptation aux changements climatiques en tant que processus dynamique et multidimensionnel. Les résultats présentés démontrent que, bien que le changement climatique entraîne des défis importants pour la gestion de l’eau, une modélisation précise et améliorée des variables hydrologiques peut offrir des informations cruciales permettant de renforcer la résilience des infrastructures, des écosystèmes et des activités humaines. Ces conclusions sont directement liées aux enjeux soulevés dans l’introduction, notamment la nécessité d’une adaptation proactive pour atténuer les effets des changements climatiques et optimiser les opportunités potentielles dans des secteurs clés comme l’agriculture, la foresterie et la production d’énergie hydroélectrique.

En résumé, cette recherche contribue à un meilleur pilotage des stratégies d’adaptation aux changements climatiques, en apportant des outils de modélisation robustes et en anticipant les modifications des régimes hydrologiques dans des régions sensibles comme le Québec. La prochaine étape sera d’explorer comment ces résultats peuvent être traduits en politiques publiques et en stratégies de gestion de l'eau qui tiennent compte des incertitudes futures, tout en maximisant les bénéfices des approches de modélisation avancées mises en œuvre dans cette étude.

CONCLUSION

Ce mémoire a exploré en profondeur la modélisation des variables hydrologiques ainsi que l'impact des changements climatiques sur les régimes hydrologiques de plusieurs bassins versants au Québec. Les objectifs définis au début de ce travail étaient

(1) déterminer la configuration optimale du modèle hydrologique WaSiM afin d'améliorer la représentation des variables hydrologiques et la robustesse des simulations,
(2) comparer les méthodes de modélisation conventionnelle et asynchrone, et
(3) évaluer les impacts des changements climatiques sur les variables hydrologiques dans 34 bassins versants.

Ces objectifs ont guidé l'organisation et le contenu des trois articles constitutifs de ce mémoire.

Tout d’abord, nous avons démontré que la calibration intégrant la recharge de la nappe phréatique du modèle hydrologique WaSiM offre une meilleure représentation des processus internes par rapport à une calibration axée uniquement sur le débit à l'exutoire. Cela permet de mieux appréhender les dynamiques complexes du cycle de l’eau, élément essentiel pour une gestion durable des ressources hydriques. Ensuite, la comparaison des méthodes de modélisation conventionnelle et asynchrone a permis de mettre en lumière les avantages et les limites de chacune. La méthode asynchrone, bien que simplifiant la chaîne de modélisation, présente des défis importants en termes de synchronisation des processus hydrologiques. Finalement, les résultats ont révélé des changements notables dans les régimes hydrologiques futurs en raison des augmentations de température et des précipitations, mettant en évidence les enjeux climatiques auxquels le Québec devra faire face.

Le problème initial à résoudre dans ce mémoire concernait la nécessité de mieux comprendre et modéliser les impacts des changements climatiques sur les variables hydrologiques afin de soutenir des stratégies d'adaptation efficaces. Ce travail a montré que des approches de modélisation avancées, combinées à des scénarios climatiques récents comme ceux issus de CMIP6, permettent de fournir des projections plus fiables, essentielles pour anticiper et mitiger les effets du réchauffement climatique sur les ressources en eau. Ces résultats renforcent la pertinence de la modélisation hydrologique distribuée et à base physique pour une gestion éclairée des ressources hydriques.

Cependant, cette étude n’est pas sans limites. D'une part, la complexité des modèles à base physique, comme WaSiM, exige des données de haute qualité, qui ne sont pas toujours disponibles pour toutes les régions ou toutes les variables. D'autre part, bien que la méthode asynchrone présente un potentiel intéressant, elle nécessite encore des améliorations, notamment pour mieux gérer la synchronisation des événements hydrologiques critiques.

Ce mémoire a permis de mieux comprendre les dynamiques hydrologiques sous l'effet des changements climatiques dans les bassins versants du Québec, tout en ouvrant la voie à de nouvelles approches méthodologiques pour améliorer la précision des simulations hydrologiques. Il est impératif de continuer à développer et à affiner ces modèles pour répondre aux défis croissants posés par les changements climatiques sur les ressources en eau, garantissant ainsi une gestion durable et résiliente des écosystèmes et des infrastructures humaines.

RECOMMANDATIONS

Les résultats présentés dans ce mémoire ont mis en lumière plusieurs aspects essentiels de la modélisation hydrologique. En se basant sur ces résultats, voici quelques recommandations pratiques et pour de futurs travaux qui pourraient guider les prochaines études et les applications pratiques dans ce domaine.

- Une validation des variables hydrologiques internes, telles que l'humidité du sol, l’accumulation de neige ou la recharge des nappes, doit être réalisée pour s'assurer que les simulations sont réalistes et fiables. Cette validation peut se faire à partir de données observées ou de mesures sur le terrain, afin de garantir que les modèles représentent fidèlement les processus internes. Lorsque des données observées ou des mesures sur le terrain ne sont pas disponibles, le recours à un jugement expert peut permettre d'évaluer la représentativité des processus.

- Lorsque les variables hydrologiques internes, telles que l'humidité du sol, l'évapotranspiration ou la recharge des nappes phréatiques, sont d’intérêt, il est essentiel de privilégier une calibration intégrant à la fois le débit et au moins une variable hydrologique interne. Cette approche permet de réduire le problème d’équifinalité, où plusieurs configurations de paramètres peuvent produire des résultats similaires pour le débit, mais avec des dynamiques internes divergentes. Cela améliore ainsi la représentation des processus hydrologiques clés.

- La calibration avec des variables internes mérite d’être explorée davantage, notamment par l'intégration de données obtenues par télédétection ou des mesures in situ. Des études futures devraient se pencher sur les avantages de combiner ces données avec des modèles hydrologiques pour améliorer la précision et la robustesse des simulations.

- Bien que la méthode asynchrone présente des avantages, ses limitations en termes de synchronisation des processus hydrologiques, comme la fonte des neiges, nécessitent des améliorations. De futurs travaux pourraient se concentrer sur l'intégration de certaines formes de synchronicité dans cette méthode afin de mieux représenter les processus hydrologiques critiques tout en conservant les avantages de l'approche asynchrone.

- Répéter l'étude en utilisant différents modèles hydrologiques distribués et divers scénarios SSP afin d'évaluer plus précisément l'impact de ces choix sur les incertitudes des résultats obtenus.

APPENDICE A

CHAPITRE 1 - LISTE DES CONTRIBUTIONS SCIENTIFIQUES

1. Articles scientifiques – journaux avec jury (soumis)

Talbot, F., Sylvain, J.-D., Drolet, G., Poulin, A., et Arsenault, R. (2025) Enhancing physically based and distributed hydrological model calibration through internal state variable constraints. 42p. (Soumis à Hydrology and Earth System Sciences en octobre 2024)

Talbot, F., Ricard, S., Sylvain, J.-D., Drolet, G., Poulin, A., Martel, J.-L. et Arsenault, R. (2025). Towards a semi-asynchronous method for hydrological modeling in climate change studies. 51p. (Soumis à Hydrology and Earth System Sciences en septembre 2024)

Talbot, F., Sylvain, J.-D., Drolet, G., Poulin, A., Martel, J.-L. et Arsenault, R. (2025). Assessing hydroclimatic impacts of climate change in snowy catchments using a physically based hydrological model. 45p. (Soumis à Journal of Hydrology: Regional Studies en décembre 2024)

Pouryousefi Markhali, S., Boucher, M.-A., Poulin, A., Rahemipour, M., **Talbot, F.** et Arsenault, R. (2025). Regionalization of a Distributed Hydrology Model Using Random Forest. 34p. (Soumis à Hydrological Processes en décembre 2024)

2. Conférences internationales/nationales/provinciales – avec jury

Talbot, F., Sylvain, J.-D., Drolet, G., Poulin, A., Martel, J.-L. & Arsenault, R. (2025, janvier). *L'impacts des changements climatiques sur le cycle de l'eau au Québec*. Affiche présentée à la 10^{e} édition du Symposium Ouranos, Montréal, Canada.

APPENDICE B

CHAPITRE 3 - MATÉRIELS SUPPLÉMENTAIRES DE L'ARTICLE 1

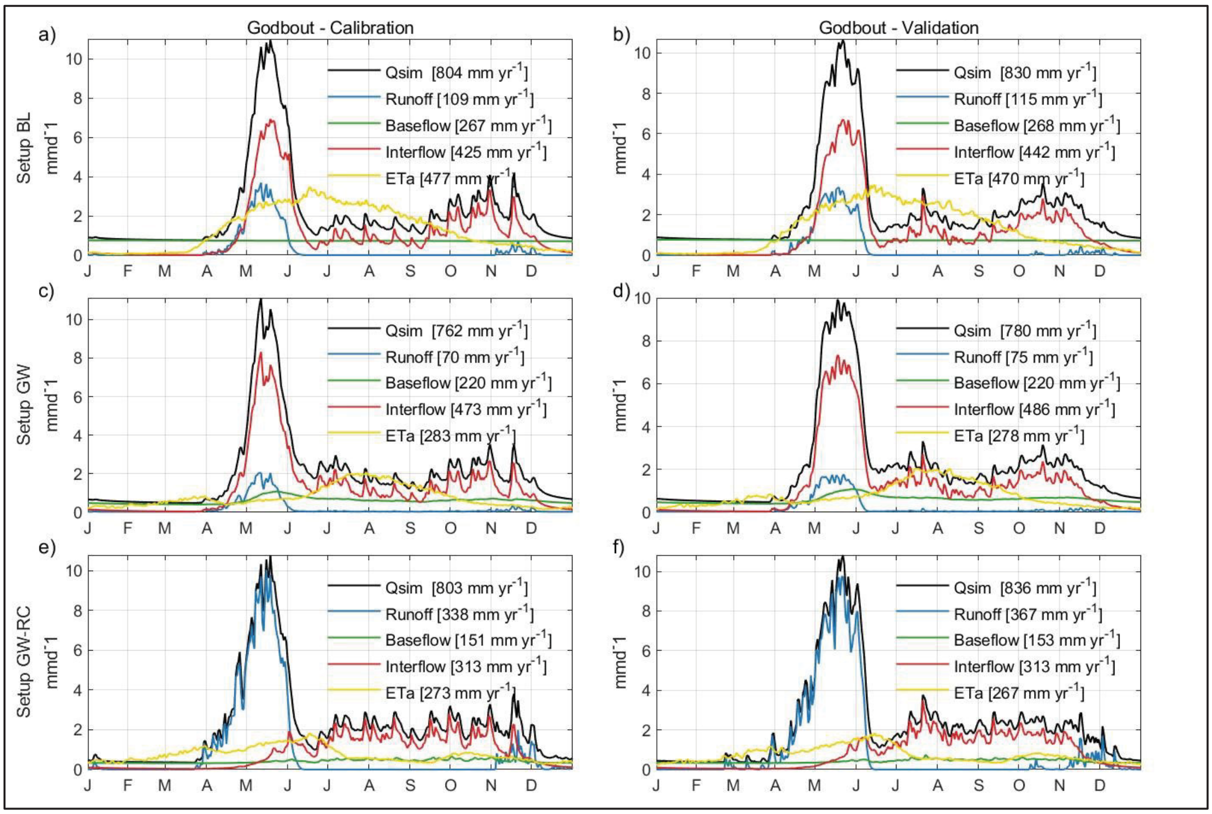

Figure AB.1 Detailed hydrological variable hydrograph for Godbout catchment during both the calibration and validation phases and for the three configurations

Table AB.1 Kling-Gupta efficiency values across studied catchments during calibration and validation periods, for the three calibrations configurations

Catchment		Calibration			Validation		
Code	**Name**	**BL**	**GW**	**GW-RC**	**BL**	**GW**	**GW-RC**
10802	Bonaventure	0.835	0.849	0.817	0.897	0.892	0.861
20404	York	0.847	0.872	0.815	0.843	0.889	0.814
20602	Dartmouth	0.888	0.882	0.842	0.899	0.907	0.828
21601	Matane	0.906	0.901	0.877	0.908	0.900	0.861
22003	Rimouski	0.920	0.905	0.870	0.831	0.812	0.827
22301	Des Trois-Pistoles	0.898	0.895	0.848	0.783	0.754	0.712
22507	Du Loup	0.872	0.852	0.800	0.795	0.749	0.696
22704	Ouelle	0.900	0.896	0.834	0.838	0.846	0.792
23422	Famine	0.826	0.814	0.754	0.794	0.798	0.745
24003	Bécancour	0.861	0.859	0.788	0.820	0.816	0.765
30101	Nicolet Sud-Ouest	0.828	0.810	0.771	0.801	0.770	0.746
30103	Nicolet	0.804	0.799	0.744	0.811	0.792	0.767
30234	Eaton	0.769	0.768	0.637	0.738	0.741	0.661
30282	Au Saumon	0.836	0.815	0.717	0.790	0.774	0.713
30304	Noire	0.823	0.813	0.723	0.767	0.770	0.694
40204	Rouge	0.830	0.842	0.798	0.838	0.829	0.844
40830	Gatineau	0.817	0.840	0.796	0.807	0.831	0.772
43012	Kinojévis	0.765	0.850	0.784	0.695	0.711	0.735
50119	Mattawin	0.852	0.814	0.740	0.799	0.758	0.751
50135	Croche	0.835	0.835	0.833	0.839	0.840	0.831
50144	Vermillon	0.835	0.853	0.747	0.808	0.809	0.733
50304	Batiscan	0.878	0.856	0.801	0.884	0.847	0.796
50408	Sainte-Anne	0.872	0.860	0.833	0.852	0.847	0.829
50409	Bras du Nord	0.853	0.864	0.856	0.859	0.863	0.869
52212	Ouareau	0.855	0.881	0.818	0.839	0.837	0.765
52219	L'Assomption	0.865	0.886	0.851	0.829	0.859	0.821
52233	De l'Achigan	0.869	0.851	0.829	0.700	0.720	0.701
52805	Du Loup	0.808	0.783	0.800	0.786	0.721	0.753
60101	Petit Saguenay	0.895	0.879	0.843	0.864	0.857	0.800
61801	Petite rivière Péribonca	0.833	0.876	0.775	0.819	0.839	0.742
61502	Métabetchouane	0.872	0.861	0.806	0.801	0.769	0.670
62701	Valin	0.880	0.882	0.826	0.842	0.888	0.793
62802	Sainte-Marguerite Nord-Est	0.872	0.854	0.810	0.854	0.833	0.772
71401	Godbout	0.857	0.864	0.799	0.838	0.861	0.777

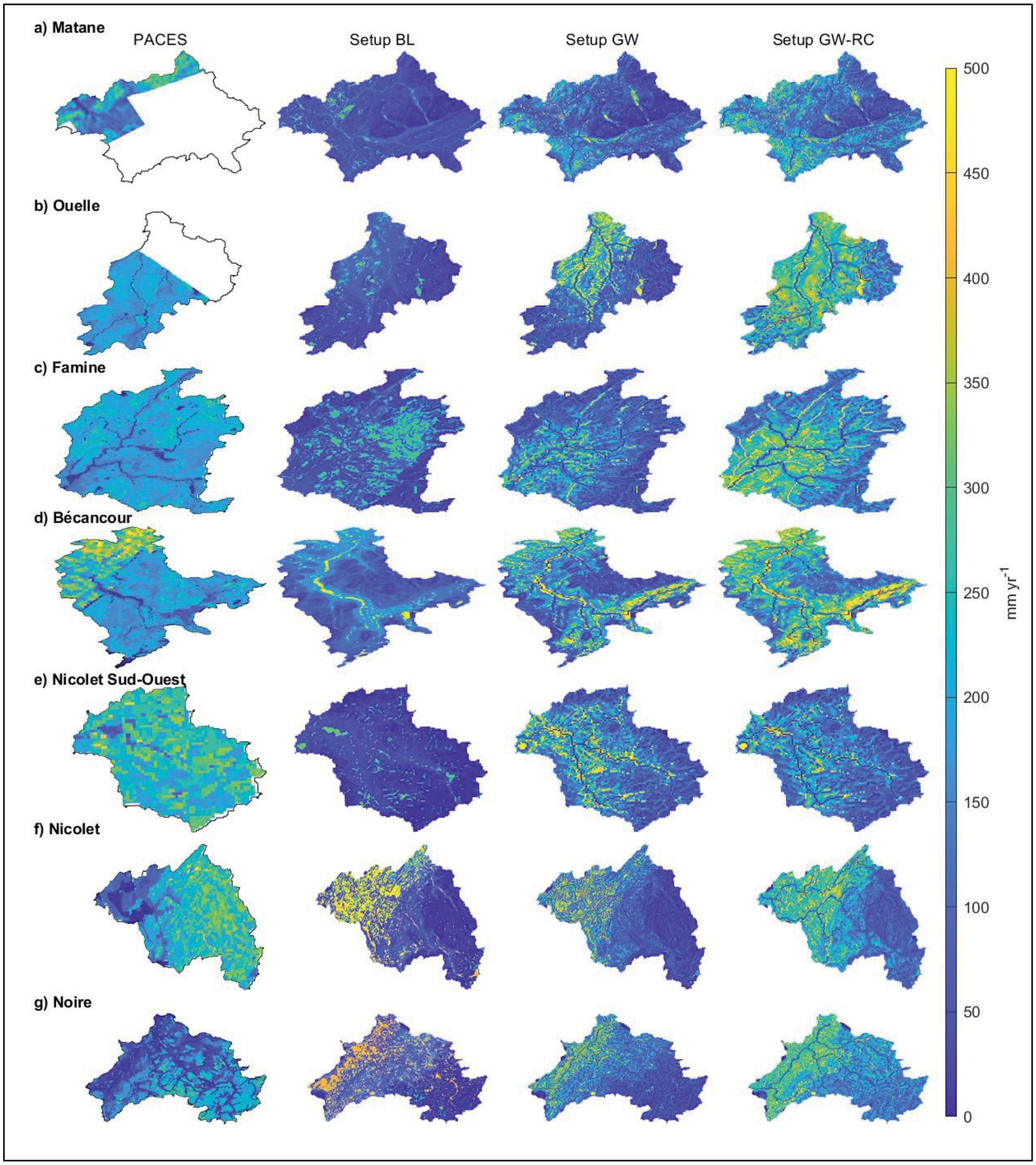

Figure AB.2 Spatial distribution of annual total recharge for PACES data and hydrological model calibration configurations

APPENDICE C

CHAPITRE 4 - MATÉRIELS SUPPLÉMENTAIRES DE L'ARTICLE 2

Table AC.1 Kling-Gupta Efficiency (KGE) values for the conventional method during the calibration and validation periods across ten catchments

Conventional Method		**KGE**	
Name	Area (km^2)	Calibration	Validation
Bonaventure	1910	0.847	0.889
Matane	1650	0.906	0.906
Ouelle	795	0.894	0.834
Bécancour	919	0.850	0.807
Nicolet Sud-Ouest	549	0.817	0.786
Au Saumon	738	0.831	0.778
Bras du Nord	642	0.873	0.872
Du Loup	774	0.838	0.804
Valin	746	0.902	0.885
Godbout	1570	0.869	0.863
	Mean	0.863	0.842

Table AC.2 Root Mean Square Error (RMSE) values for the asynchronous method during the calibration and validation periods across ten catchments

Asynchronous Method		**RMSE**			
Name	Area (km^2)	Calibration		Validation	
		Mean	Std	Mean	Std
Bonaventure	1910	0.108	0.031	0.154	0.047
Matane	1650	0.124	0.021	0.180	0.034
Ouelle	795	0.125	0.027	0.167	0.043
Bécancour	919	0.095	0.019	0.158	0.048
Nicolet Sud-Ouest	549	0.125	0.034	0.200	0.097
Au Saumon	738	0.156	0.054	0.209	0.053
Bras du Nord	642	0.175	0.044	0.243	0.063
Du Loup	774	0.085	0.019	0.165	0.091
Valin	746	0.109	0.036	0.162	0.055
Godbout	1570	0.110	0.032	0.157	0.037
	Mean	0.121	0.031	0.179	0.057

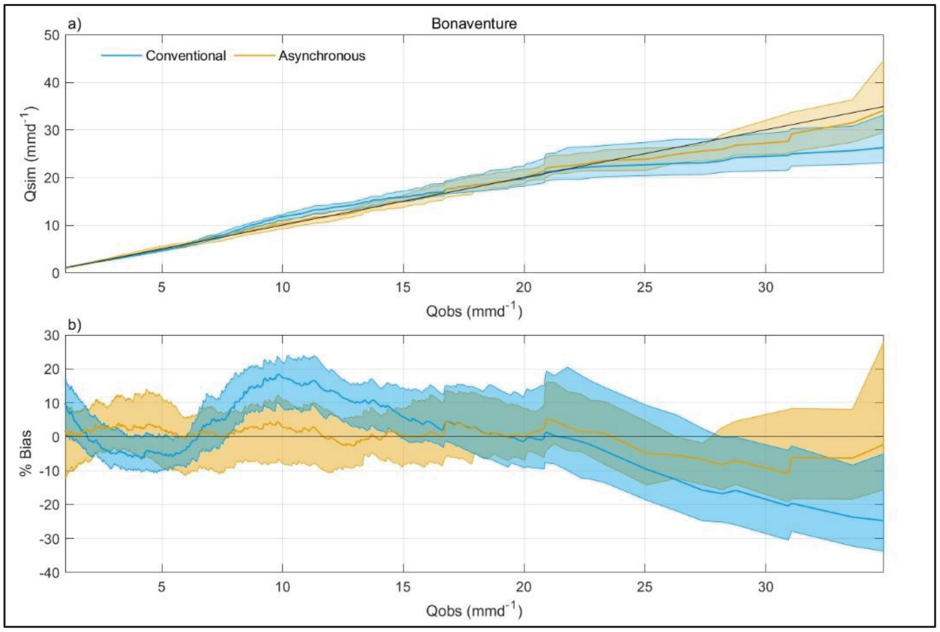

Figure AC.1 Performance comparison between the conventional and asynchronous methods for the Bonaventure catchment during the reference period (1981–2010)

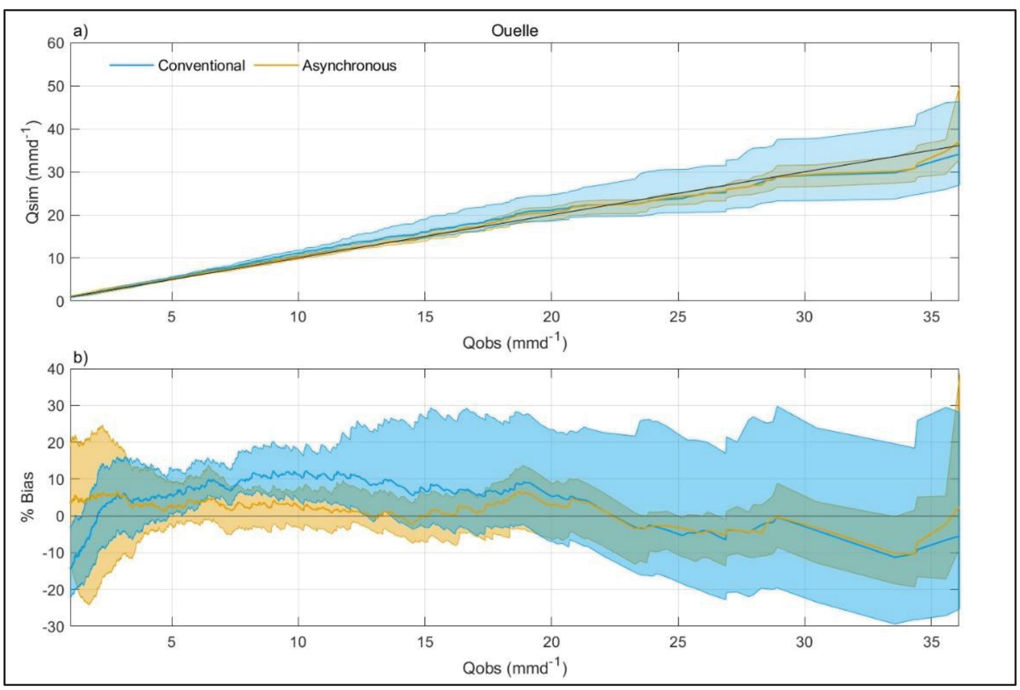

Figure AC.2 Same as Fig. AC.1, but for Ouelle catchment

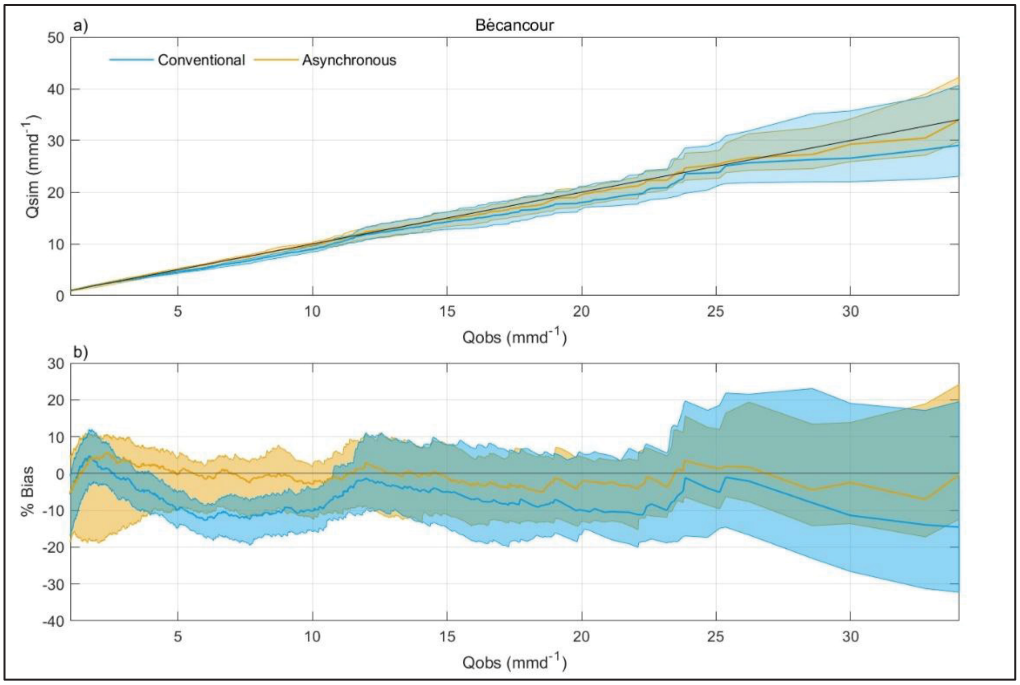

Figure AC.3 Same as Fig. AC.1, but for Bécancour catchment

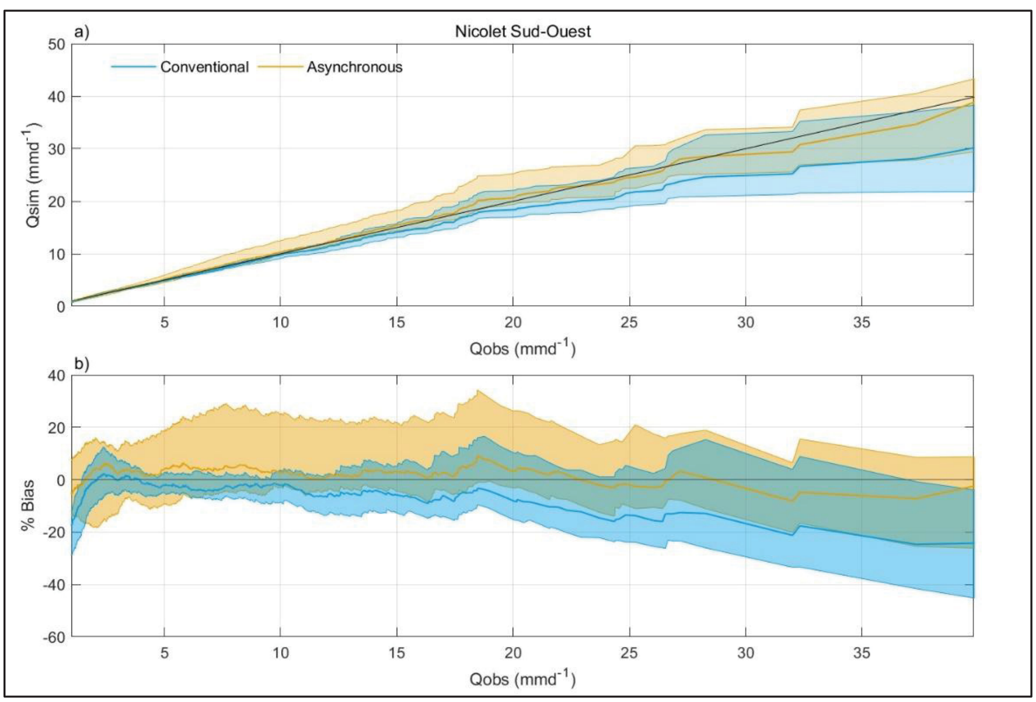

Figure AC.4 Same as Fig. AC.1, but for Nicolet Sud-Ouest catchment

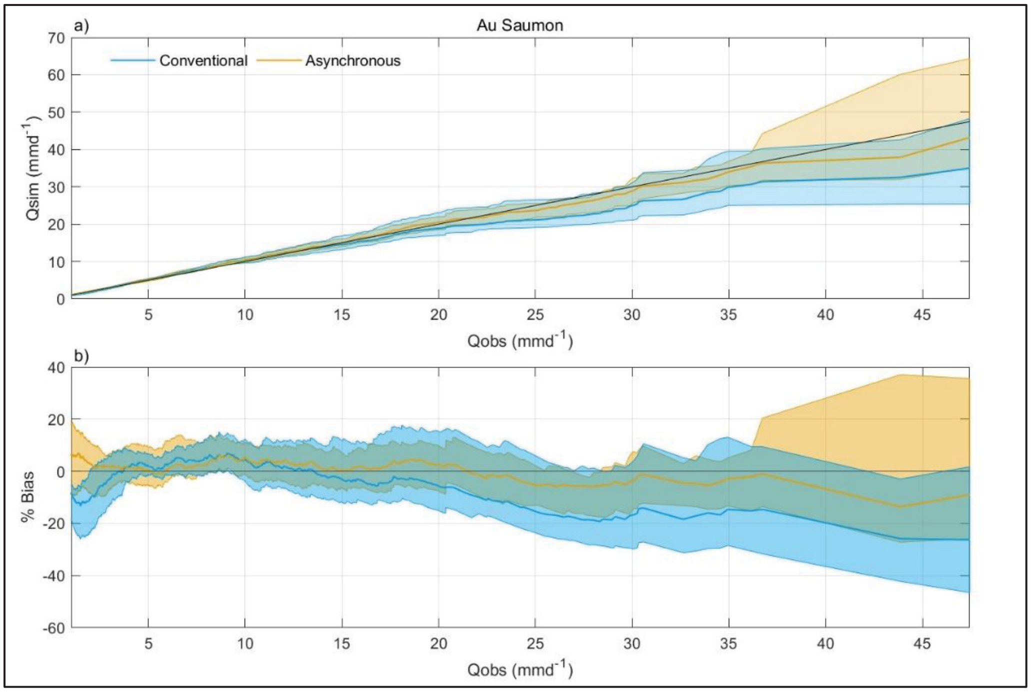

Figure AC.5 Same as Fig. AC.1, but for Au Saumon catchment

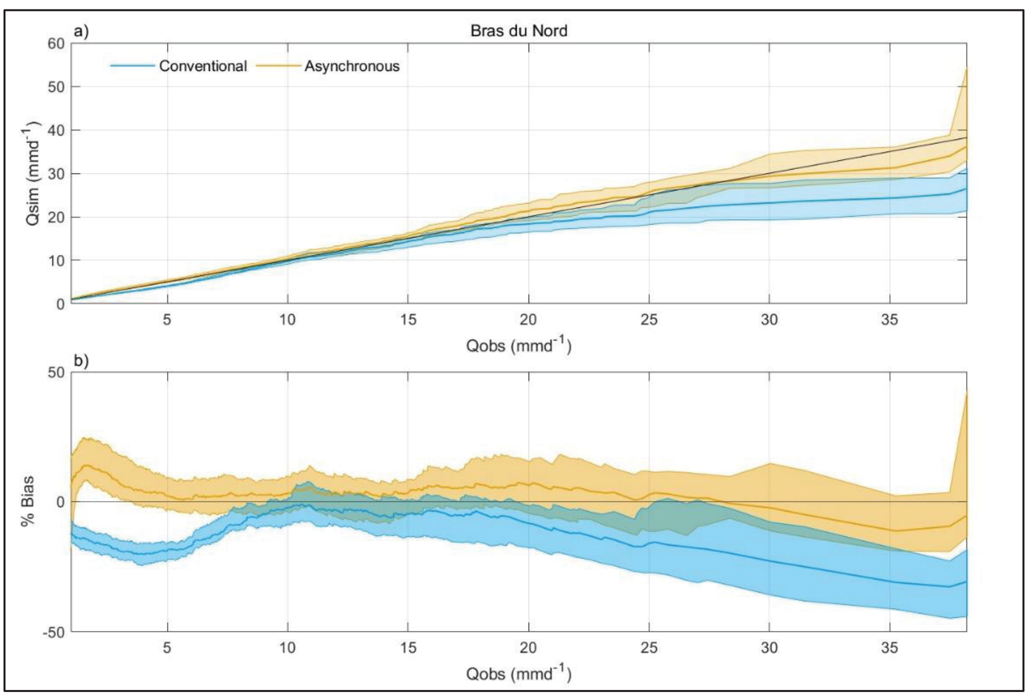

Figure AC.6 Same as Fig. AC.1, but for Bras du Nord catchment

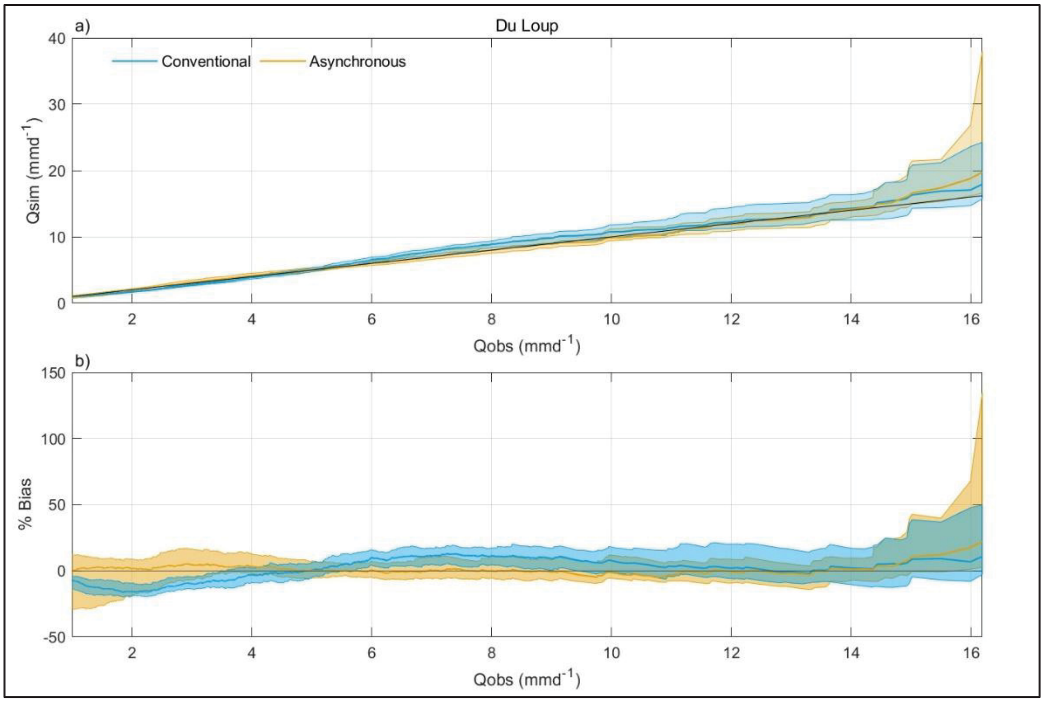

Figure AC.7 Same as Fig. AC.1 but for Du Loup catchment

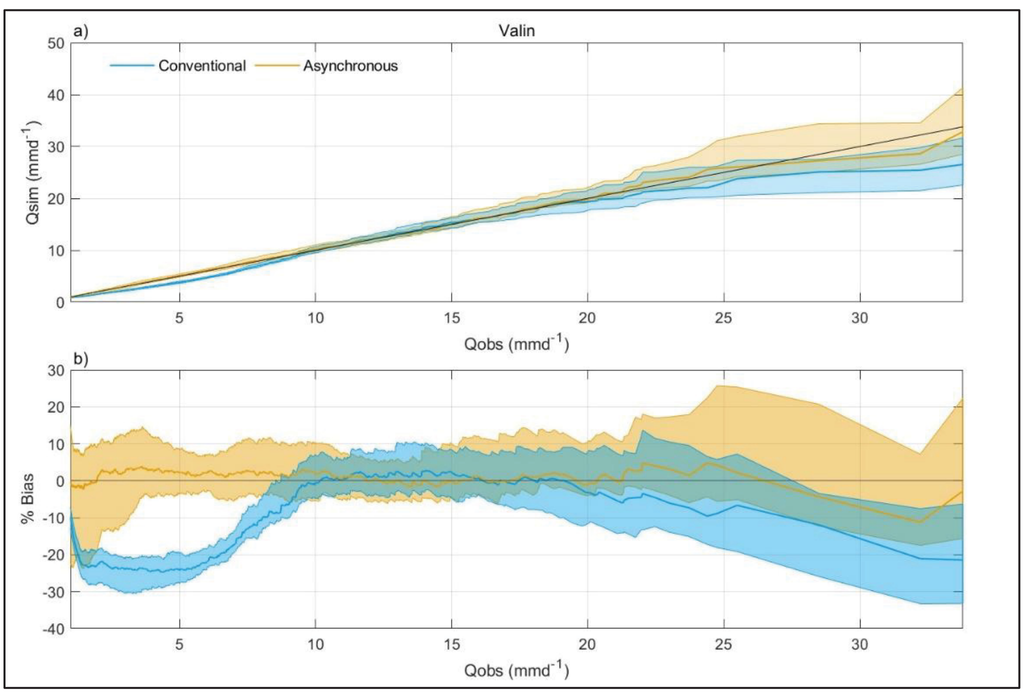

Figure AC.8 Same as Fig. AC.1, but for Valin catchment

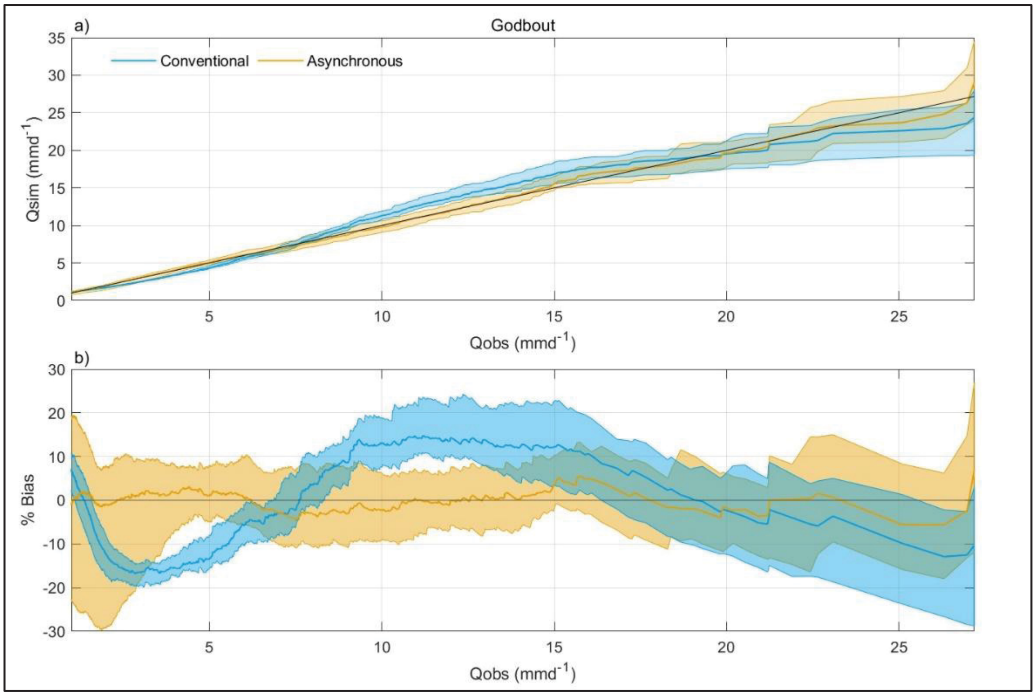

Figure AC.9 Same as Fig. AC.1, but for Godbout catchment

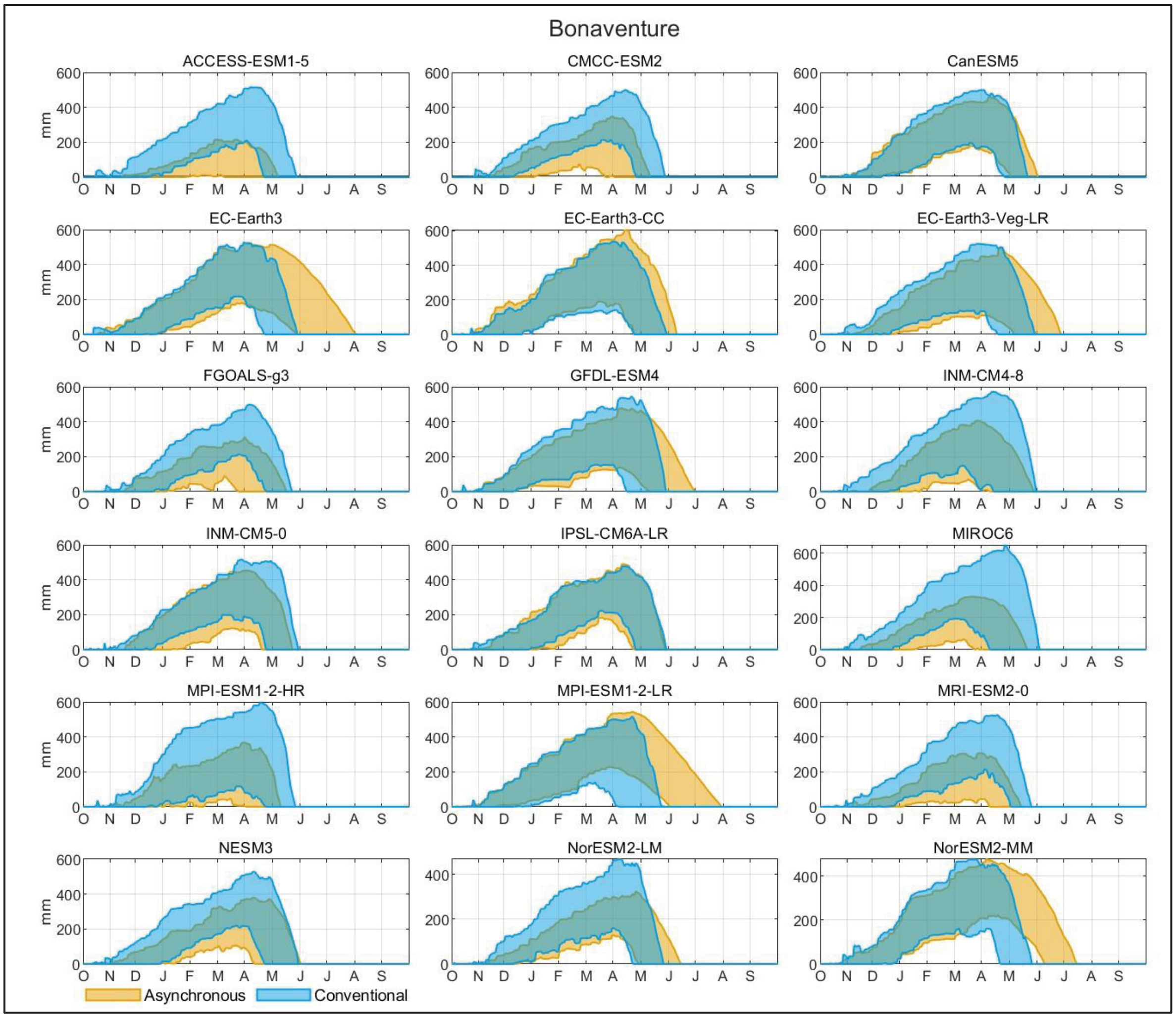

Figure AC.10 Snow water equivalent (SWE) comparison for the reference period (1981–2010) across various climate models for the Bonaventure Catchment

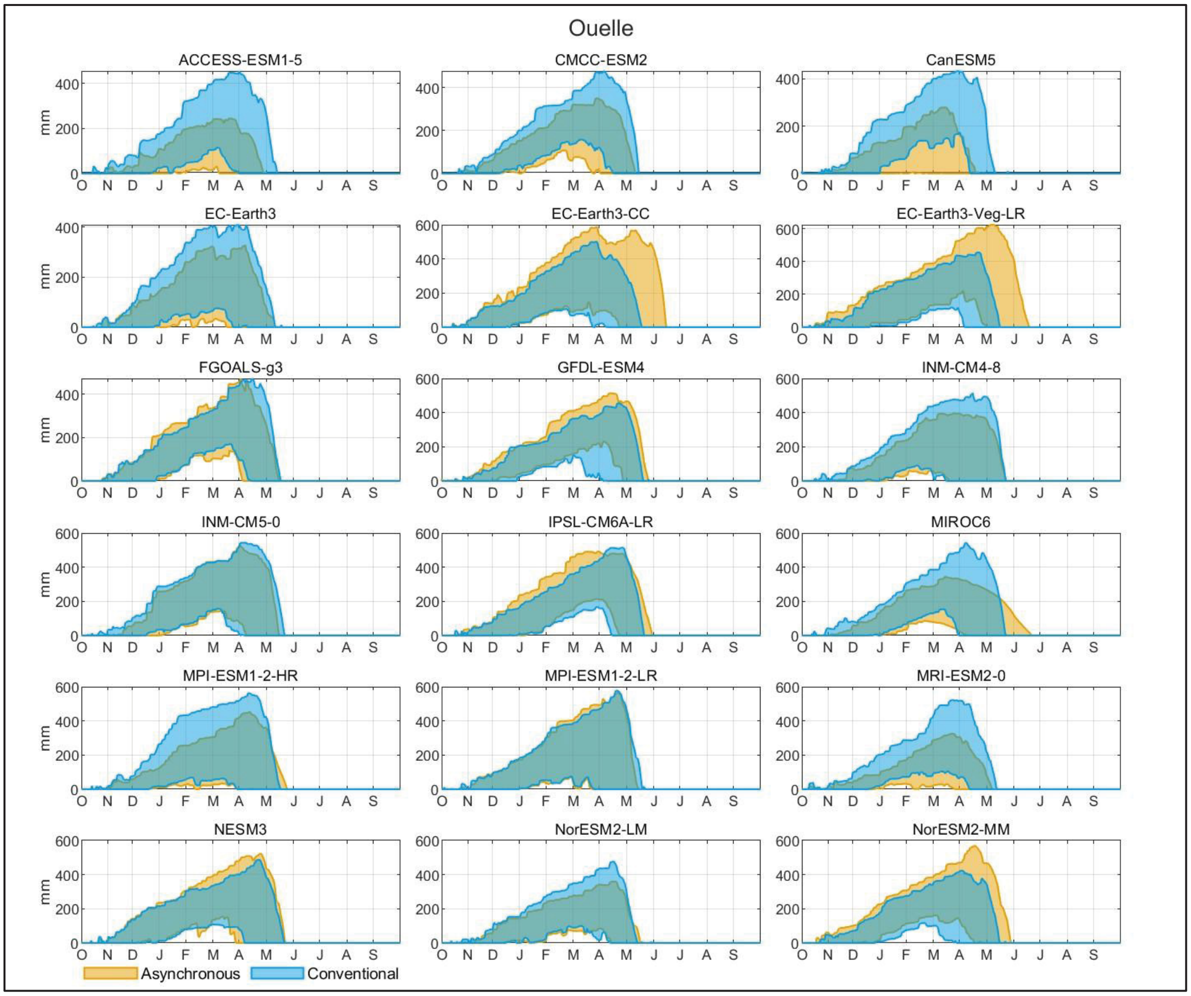

Figure AC.11 Same as Fig. AC.10, but for Ouelle catchment

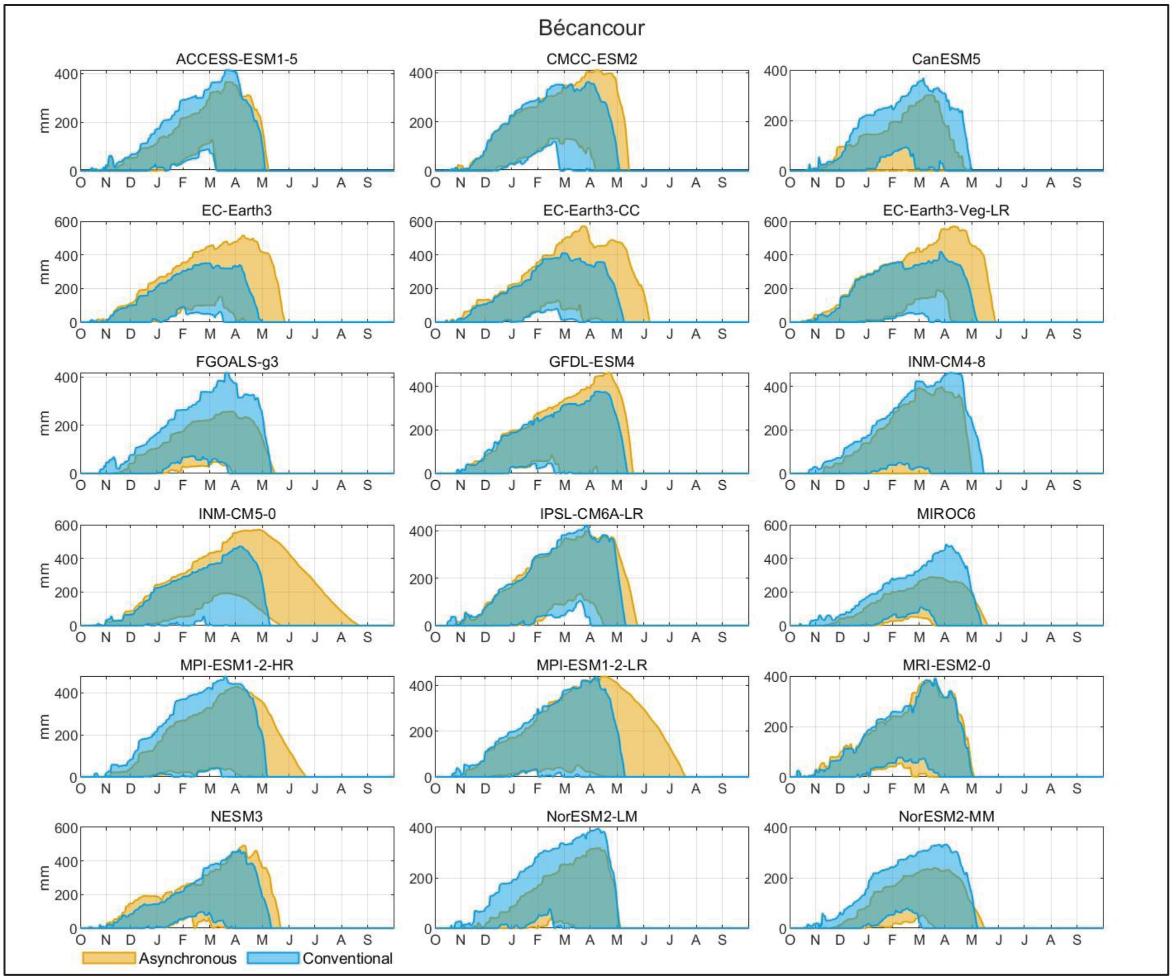

Figure AC.12 Same as Fig. AC.10, but for Bécancour catchment

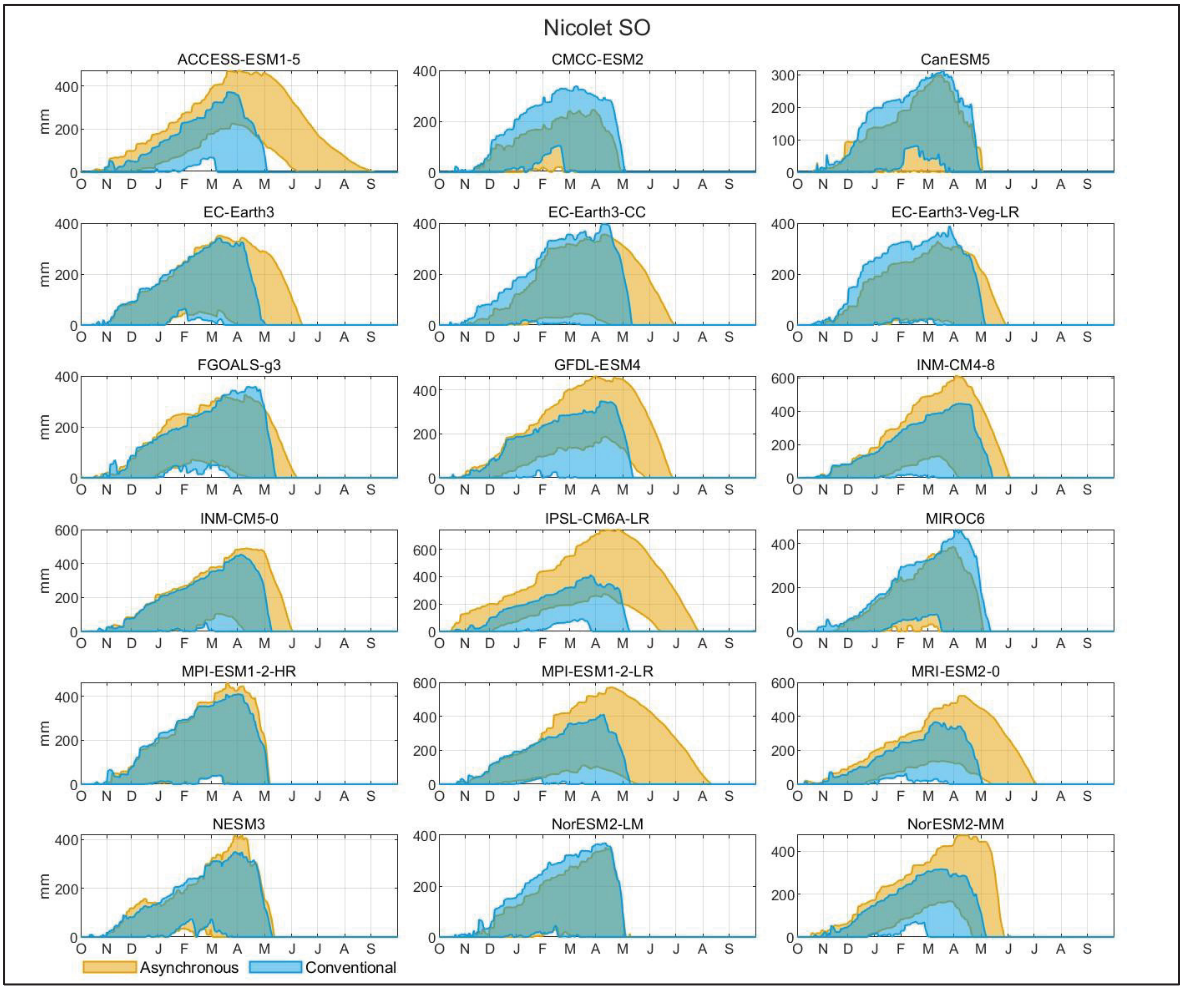

Figure AC.13 Same as Fig. AC.10, but for Nicolet Sud-Ouest catchment

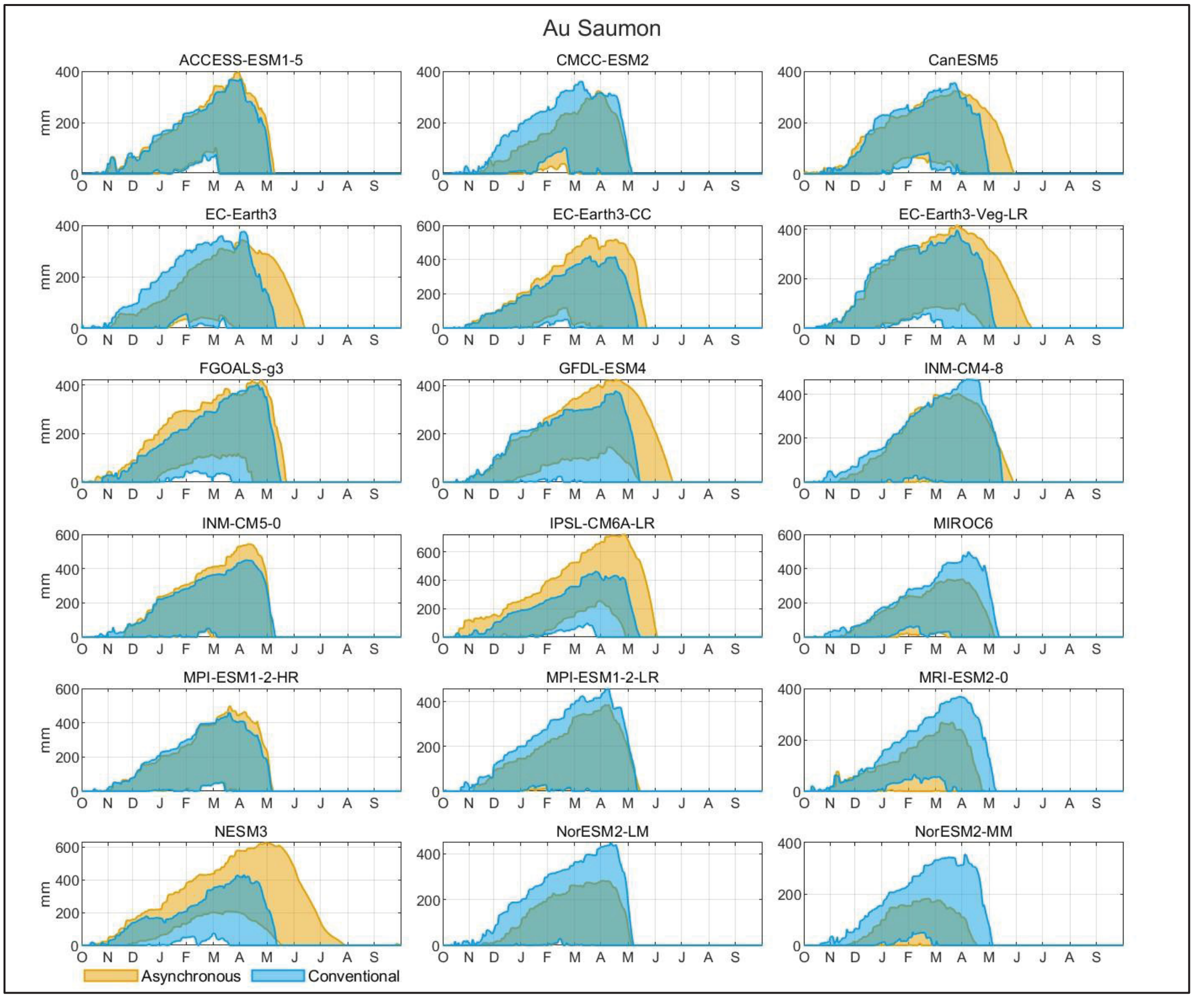

Figure AC.14 Same as Fig. AC.10, but for Au Saumon catchment

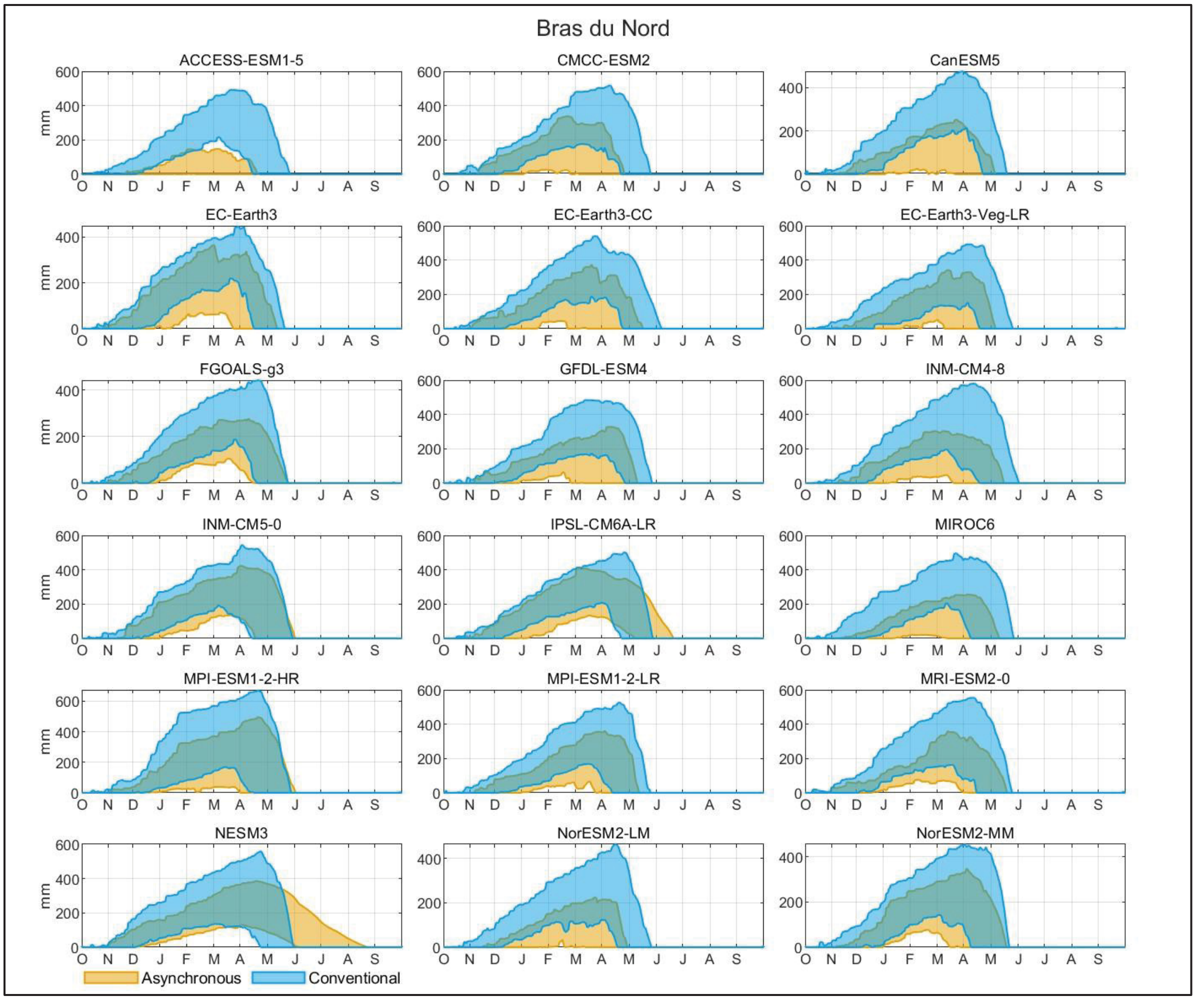

Figure AC.15 Same as Fig. AC.10, but for Bras du Nord catchment

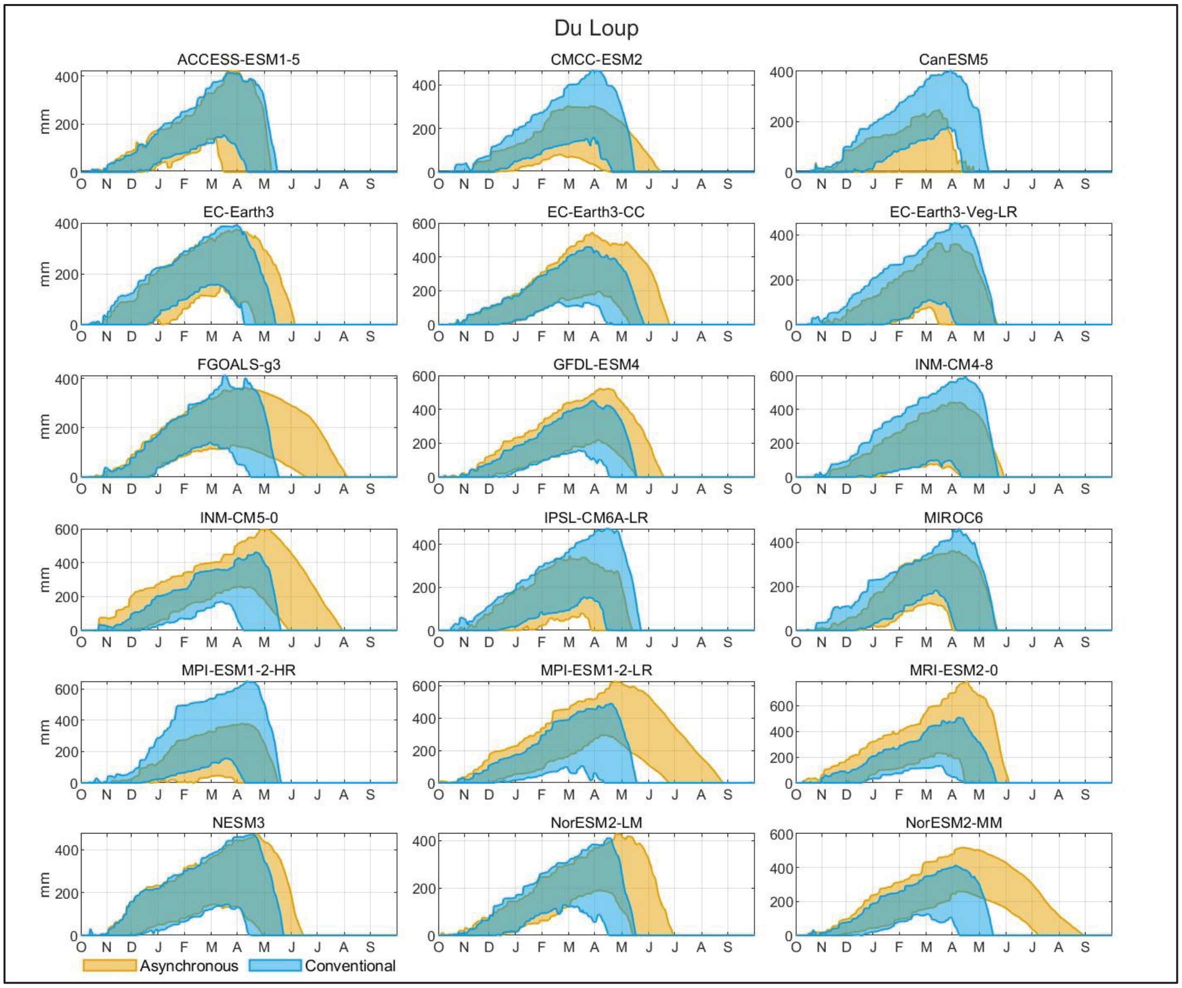

Figure AC.16 Same as Fig. AC.10, but for Du Loup catchment

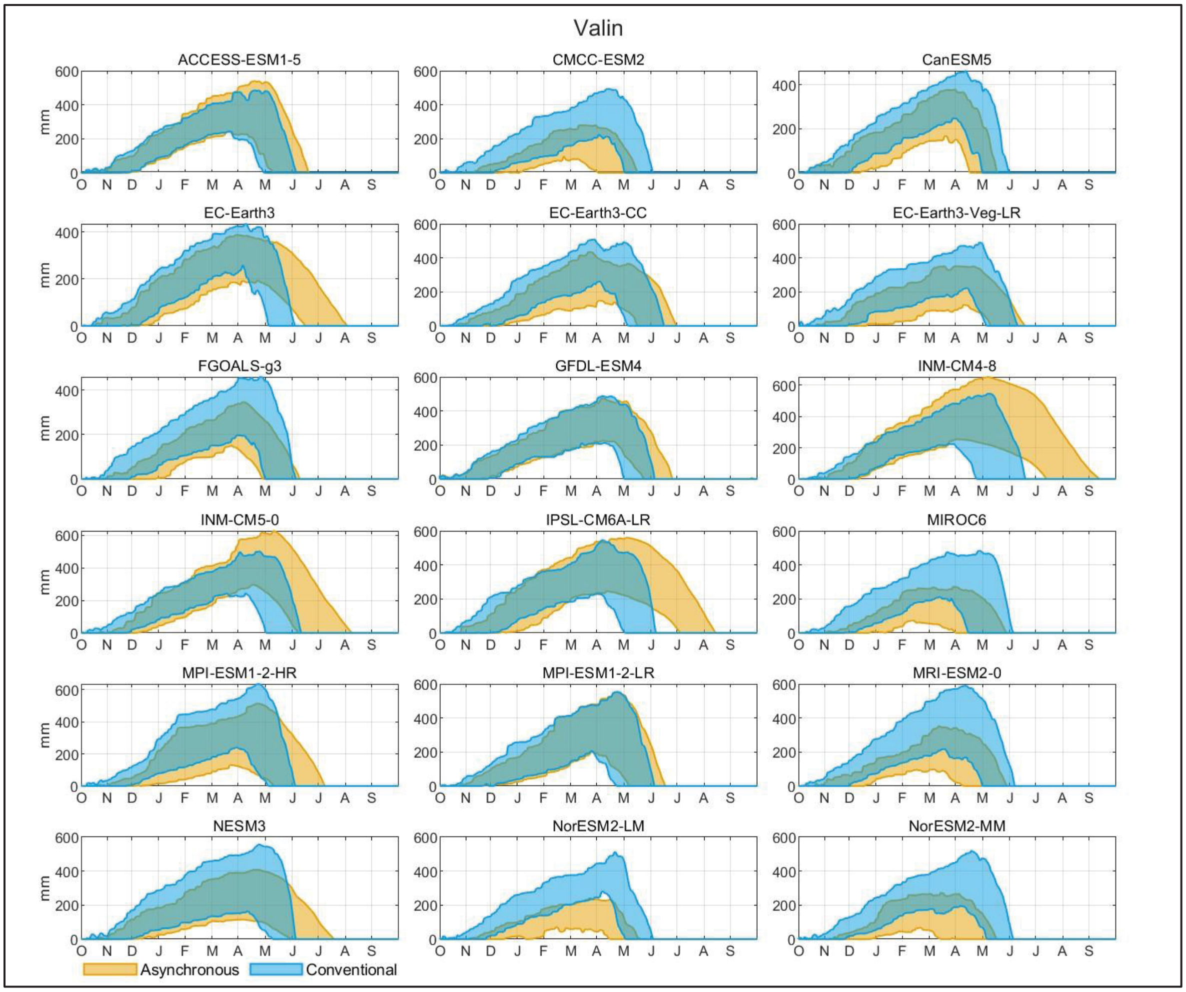

Figure AC.17 Same as Fig. AC.10, but for Valin catchment

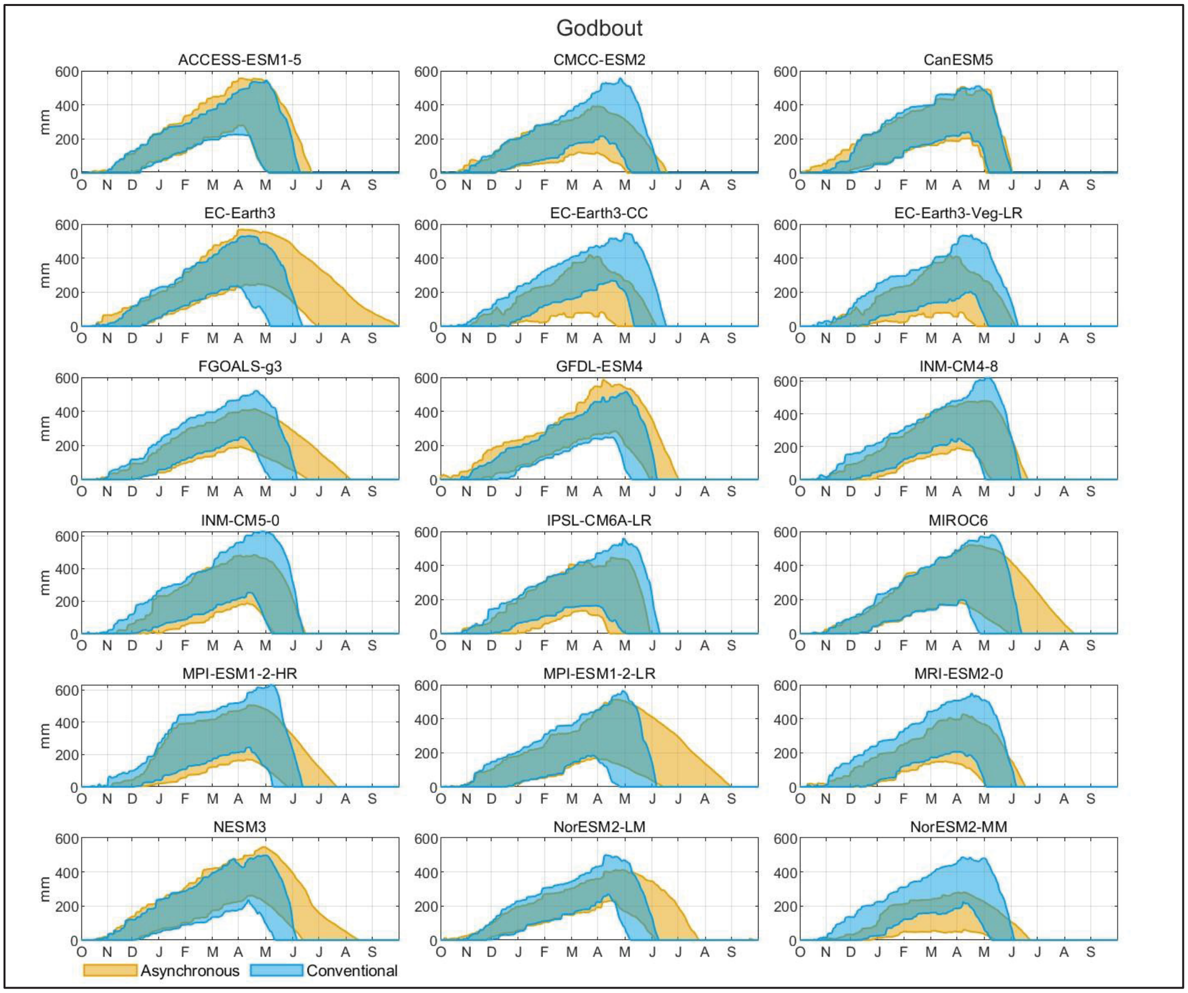

Figure AC.18 Same as Fig. AC.10, but for Godbout catchment

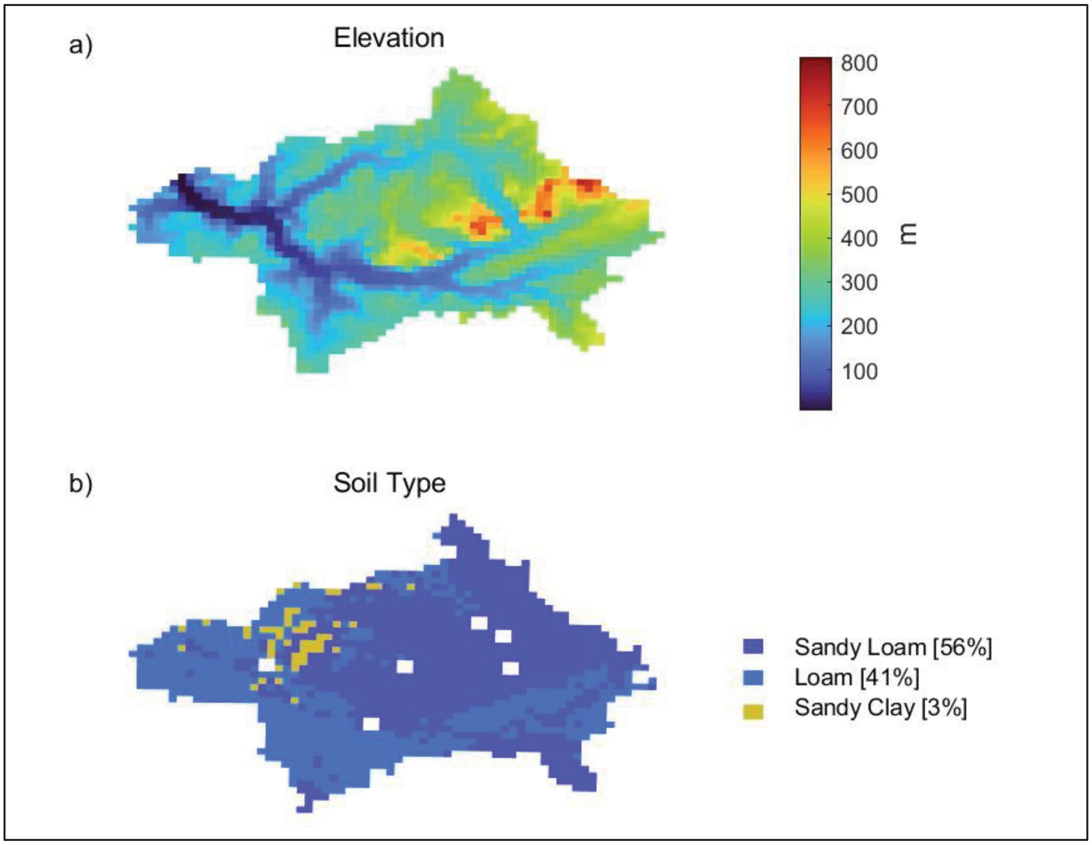

Figure AC.19 Topographic and soil type characteristics of the Matane catchment. Panel (a) shows the elevation map, with elevations ranging from 100 to 800 meters above sea level

APPENDICE D

CHAPITRE 5 - MATÉRIELS SUPPLÉMENTAIRES DE L'ARTICLE 3

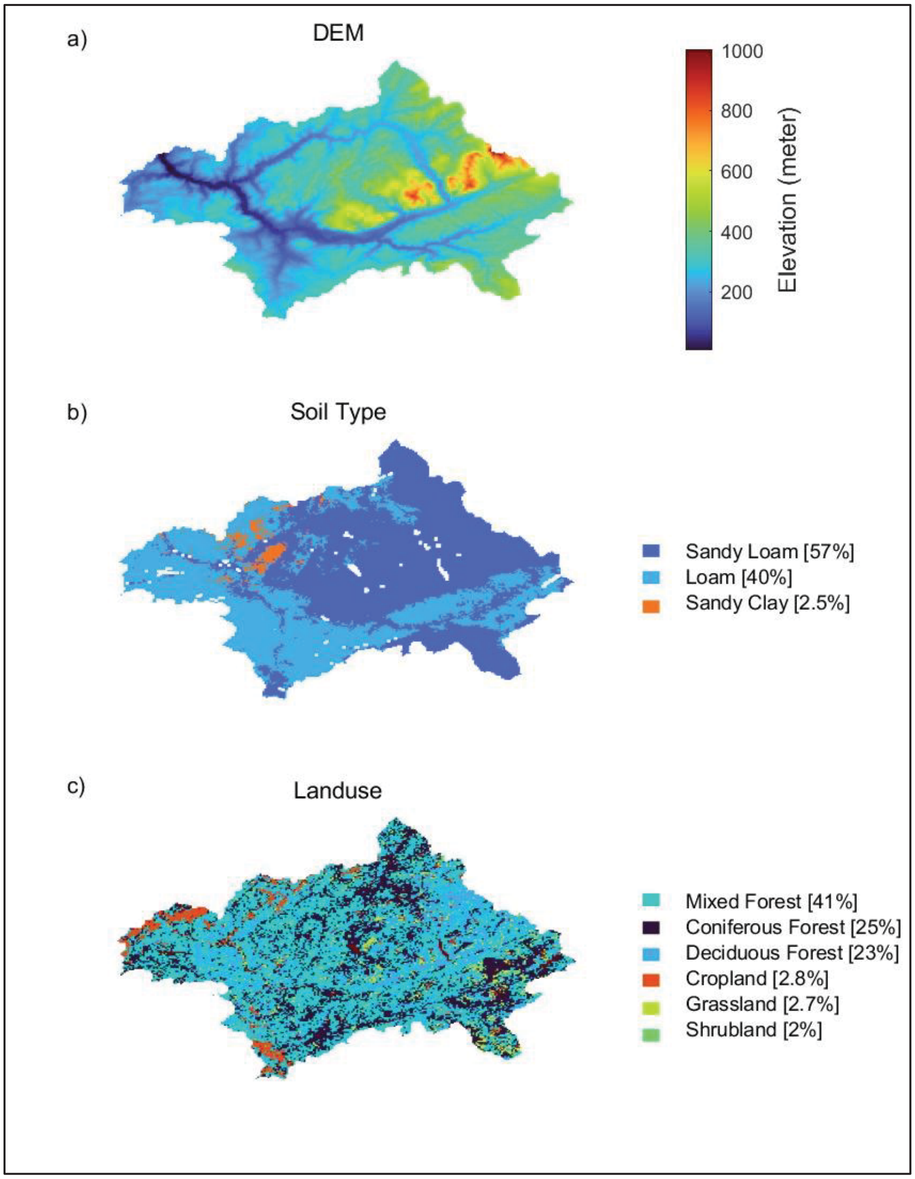

Figure AD.1 Matane catchment DEM (a), soil type (b) and land use (c)

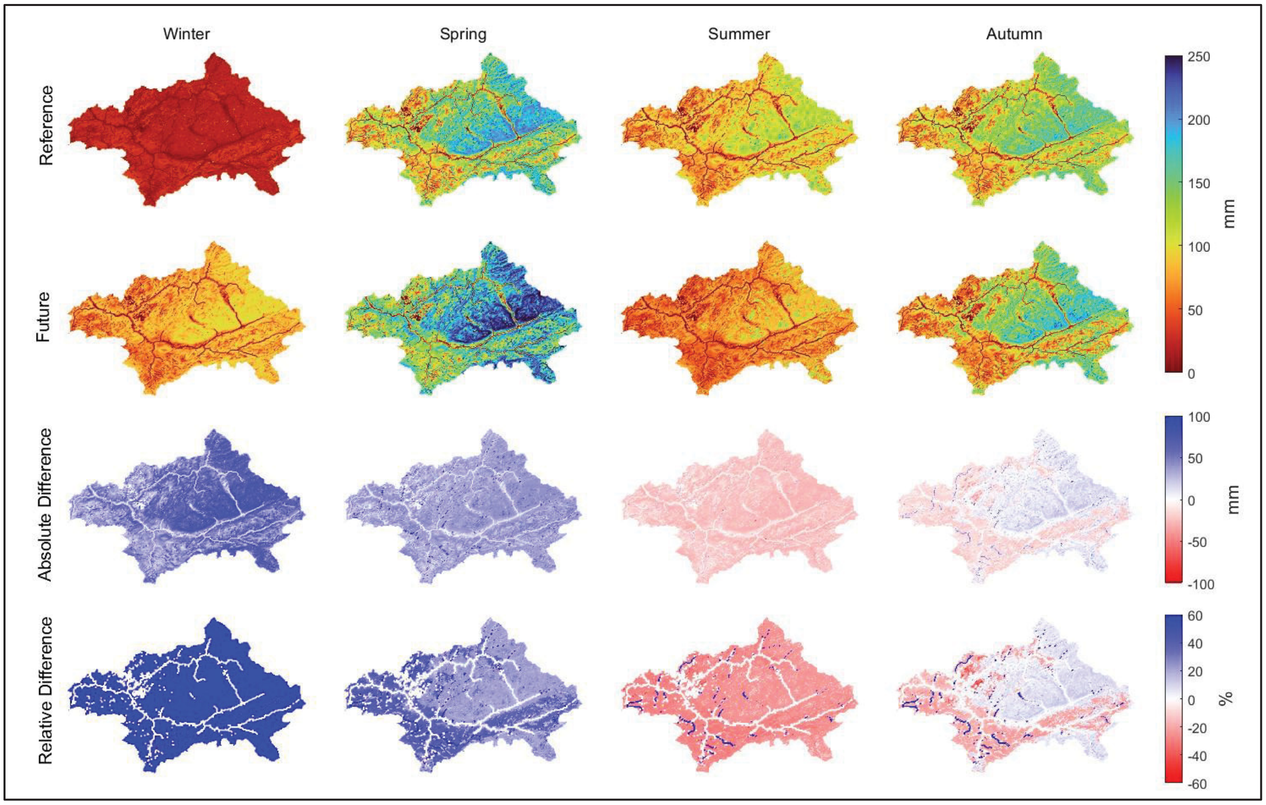

Figure AD.2 Seasonal interflow rates in the Matane catchment for reference and future periods, with absolute and relative differences

Table AD.1 Comparison of simulated hydroclimatic variables between the reference and future periods across the Matane catchment

Hydroclimatic Variables	**Unit**	**Reference (1981-2010)**			**Future (2070-2099)**		
		ERA5	CMIP6	Relative Bias	CMIP6	Relative change	
						μ	σ
Precipitation	mm yr^{-1}	821	798	-2.84%	1135	42%	15%
Snowfall	mm yr^{-1}	444	440	-0.98%	298	-32%	15%
Streamflow	mm yr^{-1}	718	699	-2.65%	714	2.2%	10%
Surface Runoff	mm yr^{-1}	247	254	3.02%	169	-34%	18%
Interflow	mm yr^{-1}	364	341	-6.41%	429	26%	16%
ETa	mm yr^{-1}	476	472	-0.68%	645	36%	8%
Baseflow	mm yr^{-1}	104	101	-3.02%	112	11%	18%
Groundwater Recharge	mm yr^{-1}	130	124	-4.30%	133	7%	15%
SWE	mm	338	336	-0.57%	178	-47%	17%
Soil Moisture	-	0.199	0.197	-0.81%	0.197	-0.20%	2%

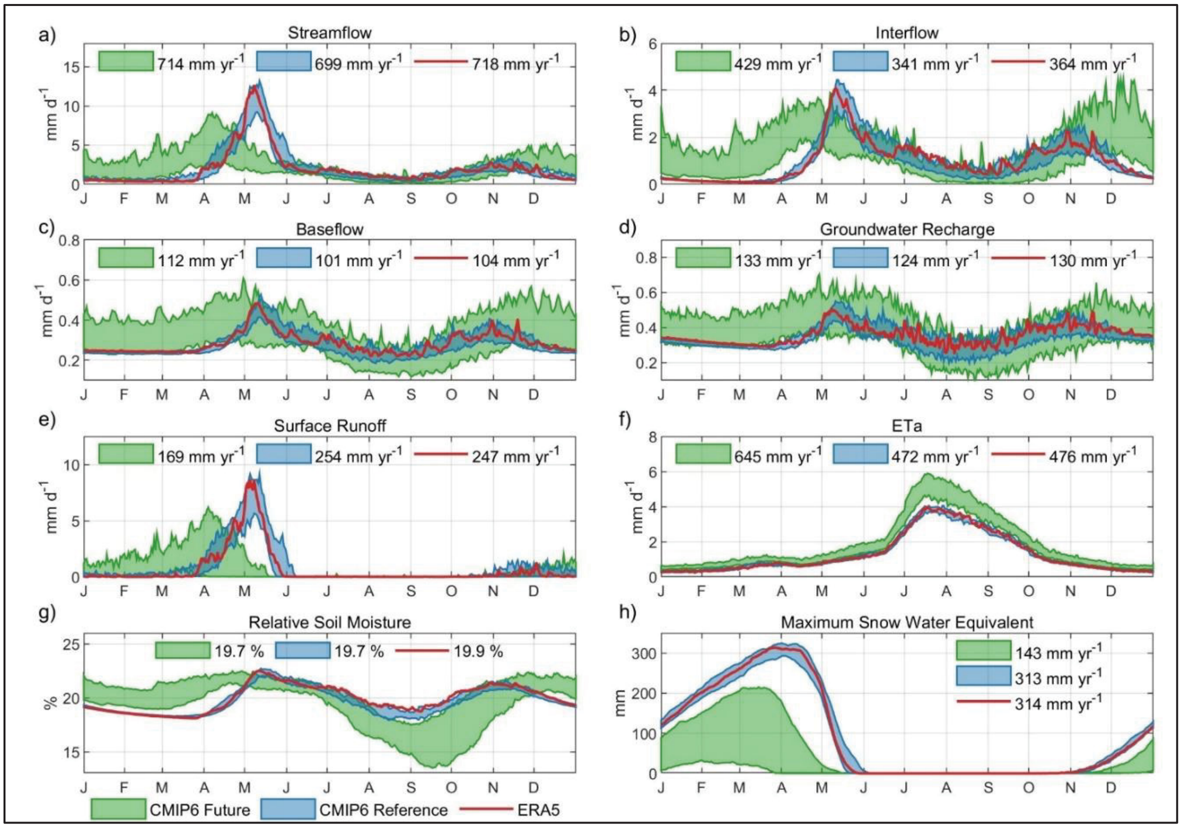

Figure AD.3 Comparative analysis of annual dynamics of daily hydroclimatic variables for the Matane catchment

LISTE DE RÉFÉRENCES BIBLIOGRAPHIQUES

Acero Triana, J. S., Chu, M. L., Guzman, J. A., Moriasi, D. N., & Steiner, J. L. (2019). Beyond model metrics : The perils of calibrating hydrologic models. *Journal of Hydrology*, *578*, 124032. https://doi.org/10.1016/j.jhydrol.2019.124032

Adeyeri, O. E., Laux, P., Lawin, A. E., & Oyekan, K. S. A. (2020). Multiple bias-correction of dynamically downscaled CMIP5 climate models temperature projection : A case study of the transboundary Komadugu-Yobe river basin, Lake Chad region, West Africa. *SN Applied Sciences*, *2*(7), 1221. https://doi.org/10.1007/s42452-020-3009-4

Alfieri, L., Feyen, L., Dottori, F., & Bianchi, A. (2015). Ensemble flood risk assessment in Europe under high end climate scenarios. *Global Environmental Change*, *35*, 199-212. https://doi.org/10.1016/j.gloenvcha.2015.09.004

Antwi, E. K., Burkhardt, H., Boakye-Danquah, J., Doucet, T., & Abolina, E. (2024). Review of climate change adaptation and mitigation implementation in Canada's forest ecosystems part I : Reporting, science, and institutional/governance supporting practices in Canada. *Environmental Reviews*, *32*(1), 16-41. https://doi.org/10.1139/er-2022-0130

Arsenault, R., Brissette, F., Chen, J., Guo, Q., & Dallaire, G. (2020). NAC2H : The North American Climate Change and Hydroclimatology Data Set. *Water Resources Research*, *56*(8), e2020WR027097. https://doi.org/10.1029/2020WR027097

Arsenault, R., Brissette, F., & Martel, J.-L. (2018). The hazards of split-sample validation in hydrological model calibration. *Journal of Hydrology*, *566*, 346-362. https://doi.org/10.1016/j.jhydrol.2018.09.027

Arsenault, R., Poulin, A., Côté, P., & Brissette, F. (2014). Comparison of Stochastic Optimization Algorithms in Hydrological Model Calibration. *Journal of Hydrologic Engineering*, *19*(7), 1374-1384. https://doi.org/10.1061/(ASCE)HE.1943-5584.0000938

Aygün, O., Kinnard, C., & Campeau, S. (2020). Impacts of climate change on the hydrology of northern midlatitude cold regions. *Progress in Physical Geography : Earth and Environment*, *44*(3), 338-375. https://doi.org/10.1177/0309133319878123

Banda, V. D., Dzwairo, R. B., Singh, S. K., & Kanyerere, T. (2022). Hydrological Modelling and Climate Adaptation under Changing Climate : A Review with a Focus in Sub-Saharan Africa. *Water*, *14*(24), 4031. https://doi.org/10.3390/w14244031

Bauer, A., & Steurer, R. (2014). Multi-level governance of climate change adaptation through regional partnerships in Canada and England. *Geoforum*, *51*, 121-129. https://doi.org/10.1016/j.geoforum.2013.10.006

Beck, H. E., Zimmermann, N. E., McVicar, T. R., Vergopolan, N., Berg, A., & Wood, E. F. (2018). Present and future Köppen-Geiger climate classification maps at 1-km resolution. *Scientific Data*, *5*(1), 180214. https://doi.org/10.1038/sdata.2018.214

Beven, K. (2006). A manifesto for the equifinality thesis. *Journal of Hydrology*, *320*(1), 18-36. https://doi.org/10.1016/j.jhydrol.2005.07.007

Beven, K., & Freer, J. (2001). Equifinality, data assimilation, and uncertainty estimation in mechanistic modelling of complex environmental systems using the GLUE methodology. *Journal of Hydrology*, *249*(1), 11-29. https://doi.org/10.1016/S0022-1694(01)00421-8

Beven, K. J. (2012). *Rainfall-Runoff Modelling : The Primer*. (S.l.): John Wiley & Sons. (Google-Books-ID: oB5G3ekgxpgC).

Bingeman, A. K., Kouwen, N., & Soulis, E. D. (2006). Validation of the Hydrological Processes in a Hydrological Model. *Journal of Hydrologic Engineering*, *11*(5), 451-463. https://doi.org/10.1061/(ASCE)1084-0699(2006)11:5(451)

Bormann, H., & Elfert, S. (2010). Application of WaSiM-ETH model to Northern German lowland catchments : Model performance in relation to catchment characteristics and sensitivity to land use change. Dans *Advances in Geosciences* (Vol. 27, pp. 1-10). Copernicus GmbH. https://doi.org/10.5194/adgeo-27-1-2010

Bouaziz, L. J. E., Fenicia, F., Thirel, G., de Boer-Euser, T., Buitink, J., Brauer, C. C., … Hrachowitz, M. (2021). Behind the scenes of streamflow model performance. *Hydrology and Earth System Sciences*, *25*(2), 1069-1095. https://doi.org/10.5194/hess-25-1069-2021

Brigode, P., Oudin, L., & Perrin, C. (2013). Hydrological model parameter instability : A source of additional uncertainty in estimating the hydrological impacts of climate change? *Journal of Hydrology*, *476*, 410-425. https://doi.org/10.1016/j.jhydrol.2012.11.012

Calvin, K., Dasgupta, D., Krinner, G., Mukherji, A., Thorne, P. W., Trisos, C., … Péan, C. (2023). *IPCC, 2023 : Climate Change 2023: Synthesis Report. Contribution of Working Groups I, II and III to the Sixth Assessment Report of the Intergovernmental Panel on Climate Change [Core Writing Team, H. Lee and J. Romero (eds.)]. IPCC, Geneva, Switzerland.* Intergovernmental Panel on Climate Change (IPCC). https://doi.org/10.59327/IPCC/AR6-9789291691647

Cannon, A. J. (2018). Multivariate quantile mapping bias correction : An N-dimensional probability density function transform for climate model simulations of multiple variables. *Climate Dynamics*, *50*(1), 31-49. https://doi.org/10.1007/s00382-017-3580-6

Castaneda-Gonzalez, M. (2018). *Effects of regional climate model spatial resolution on hydrological modelling of summer-fall floods in southern Quebec*. masters. École de technologie supérieure. Repéré à https://espace.etsmtl.ca/id/eprint/2048/

Chen, H., Sun, J., Lin, W., & Xu, H. (2020). Comparison of CMIP6 and CMIP5 models in simulating climate extremes. *Science Bulletin*, *65*. https://doi.org/10.1016/j.scib.2020.05.015

Chen, J., Arsenault, R., Brissette, F. P., & Zhang, S. (2021). Climate Change Impact Studies : Should We Bias Correct Climate Model Outputs or Post-Process Impact Model Outputs? *Water Resources Research*, *57*(5), e2020WR028638. https://doi.org/10.1029/2020WR028638

Chen, J., Brissette, F. P., & Chen, H. (2018). Using reanalysis-driven regional climate model outputs for hydrology modelling. *Hydrological Processes*, *32*(19), 3019-3031. https://doi.org/10.1002/hyp.13251

Chen, J., Brissette, F. P., & Leconte, R. (2011). Uncertainty of downscaling method in quantifying the impact of climate change on hydrology. *Journal of Hydrology*, *401*(3), 190-202. https://doi.org/10.1016/j.jhydrol.2011.02.020

Clark, M. P., Wilby, R. L., Gutmann, E. D., Vano, J. A., Gangopadhyay, S., Wood, A. W., … Brekke, L. D. (2016). Characterizing Uncertainty of the Hydrologic Impacts of Climate Change. *Current Climate Change Reports*, *2*(2), 55-64. https://doi.org/10.1007/s40641-016-0034-x

Cochand, F. (2014). Impact des changements climatiques et du développement urbain sur les ressources en eaux du bassin versant de la rivière Saint-Charles. Repéré à http://hdl.handle.net/20.500.11794/25465

Cochand, F., Therrien, R., & Lemieux, J.-M. (2019). Integrated Hydrological Modeling of Climate Change Impacts in a Snow-Influenced Catchment. *Groundwater*, *57*(1), 3-20. https://doi.org/10.1111/gwat.12848

Coron, L., Andréassian, V., Perrin, C., Bourqui, M., & Hendrickx, F. (2014). On the lack of robustness of hydrologic models regarding water balance simulation : A diagnostic approach applied to three models of increasing complexity on 20 mountainous catchments. *Hydrology and Earth System Sciences*, *18*(2), 727-746. https://doi.org/10.5194/hess-18-727-2014

Crawford, N. H., & Linsley, R. K. (1966). DIGITAL SIMULATION IN HYDROLOGY' STANFORD WATERSHED MODEL 4. Repéré à https://trid.trb.org/View/99040

Darcy, H. (1856). *Les fontaines publiques de la ville de Dijon*. Paris: Victor Dalmont.

de Lima Ferreira, P. M., & da Paz, A. R. (2024). Enhanced calibration of a distributed hydrological model in the Brazilian Semi-Arid : Integrating spatiotemporal evapotranspiration and streamflow data. *Environmental Earth Sciences*, *83*(11), 345. https://doi.org/10.1007/s12665-024-11663-6

Dembélé, M., Ceperley, N., Zwart, S. J., Salvadore, E., Mariethoz, G., & Schaefli, B. (2020). Potential of satellite and reanalysis evaporation datasets for hydrological modelling under various model calibration strategies. *Advances in Water Resources*, *143*, 103667. https://doi.org/10.1016/j.advwatres.2020.103667

Dembélé, M., Hrachowitz, M., Savenije, H. H. G., Mariéthoz, G., & Schaefli, B. (2020). Improving the Predictive Skill of a Distributed Hydrological Model by Calibration on Spatial Patterns With Multiple Satellite Data Sets. *Water Resources Research*, *56*(1), e2019WR026085. https://doi.org/10.1029/2019WR026085

Devia, G. K., Ganasri, B. P., & Dwarakish, G. S. (2015). A Review on Hydrological Models. *Aquatic Procedia*, *4*, 1001-1007. https://doi.org/10.1016/j.aqpro.2015.02.126

Dieng, D., Cannon, A. J., Laux, P., Hald, C., Adeyeri, O., Rahimi, J., … Kunstmann, H. (2022). Multivariate Bias-Correction of High-Resolution Regional Climate Change Simulations for West Africa : Performance and Climate Change Implications. *Journal* *of Geophysical Research : Atmospheres*, *127*(5), e2021JD034836. https://doi.org/10.1029/2021JD034836

Diskin, M. H., & Simon, E. (1977). A procedure for the selection of objective functions for hydrologic simulation models. *Journal of Hydrology*, *34*(1), 129-149. https://doi.org/10.1016/0022-1694(77)90066-X

Dubois, E., Larocque, M., Gagné, S., & Braun, M. (2022). Climate Change Impacts on Groundwater Recharge in Cold and Humid Climates : Controlling Processes and Thresholds. *Climate*, *10*(1), 6. https://doi.org/10.3390/cli10010006

Duethmann, D., Blöschl, G., & Parajka, J. (2020). Why does a conceptual hydrological model fail to correctly predict discharge changes in response to climate change? *Hydrology and Earth System Sciences*, *24*(7), 3493-3511. https://doi.org/10.5194/hess-24-3493-2020

Ebel, B. A., & Loague, K. (2006). Physics-based hydrologic-response simulation : Seeing through the fog of equifinality. *Hydrological Processes*, *20*(13), 2887-2900. https://doi.org/10.1002/hyp.6388

Edwards, P. N. (2011). History of climate modeling. *WIREs Climate Change*, *2*(1), 128-139. https://doi.org/10.1002/wcc.95

Estrada, F., Kim, D., & Perron, P. (2021). Spatial variations in the warming trend and the transition to more severe weather in midlatitudes. *Scientific Reports*, *11*(1), 145. https://doi.org/10.1038/s41598-020-80701-7

Eyring, V., Bony, S., Meehl, G. A., Senior, C. A., Stevens, B., Stouffer, R. J., & Taylor, K. E. (2016). Overview of the Coupled Model Intercomparison Project Phase 6 (CMIP6) experimental design and organization. *Geoscientific Model Development*, *9*(5), 1937-1958. https://doi.org/10.5194/gmd-9-1937-2016

Fan, H., Jiang, M., Xu, L., Zhu, H., Cheng, J., & Jiang, J. (2020). Comparison of Long Short Term Memory Networks and the Hydrological Model in Runoff Simulation. *Water*, *12*(1), 175. https://doi.org/10.3390/w12010175

Fankhauser, S. (2017). Adaptation to Climate Change. *Annual Review of Resource Economics*, *9*(Volume 9, 2017), 209-230. https://doi.org/10.1146/annurev-resource-100516-033554

Farjad, B., Gupta, A., & Marceau, D. J. (2016). Annual and Seasonal Variations of Hydrological Processes Under Climate Change Scenarios in Two Sub-Catchments of a Complex Watershed. *Water Resources Management*, *30*(8), 2851-2865. https://doi.org/10.1007/s11269-016-1329-3

Förster, K., Garvelmann, J., Meißl, G., & Strasser, U. (2018). Modelling forest snow processes with a new version of WaSiM. *Hydrological Sciences Journal*, *63*(10), 1540-1557. https://doi.org/10.1080/02626667.2018.1518626

Förster, K., Meißl, G., Marke, T., Pohl, S., Garvelmann, J., Schulla, J., & Strasser, U. (2017). A new snow-vegetation interaction extension for the Water Balance Simulation Model (WaSiM), 2620. Communication présentée au EGU General Assembly Conference Abstracts. Repéré à https://ui.adsabs.harvard.edu/abs/2017EGUGA..19.2620F

Gaudreau, J., Perez, L., & Drapeau, P. (2016). BorealFireSim : A GIS-based cellular automata model of wildfires for the boreal forest of Quebec in a climate change paradigm. *Ecological Informatics*, *32*, 12-27. https://doi.org/10.1016/j.ecoinf.2015.12.006

Gleick, P. H. (1989). Climate change, hydrology, and water resources. *Reviews of Geophysics*, *27*(3), 329-344. https://doi.org/10.1029/rg027i003p00329

Gombault, C., Sottile, M.-F., Ngwa, F. F., Madramootoo, C. A., Michaud, A. R., Beaudin, I., & Chikhaoui, M. (2015). Modelling climate change impacts on the hydrology of an agricultural watershed in southern Québec. *Canadian Water Resources Journal / Revue canadienne des ressources hydriques*, *40*(1), 71-86. https://doi.org/10.1080/07011784.2014.985509

Guo, K., Guan, M., & Yu, D. (2021). Urban surface water flood modelling – a comprehensive review of current models and future challenges. *Hydrology and Earth System Sciences*, *25*(5), 2843-2860. https://doi.org/10.5194/hess-25-2843-2021

Gupta, J. (2010). A history of international climate change policy. *WIREs Climate Change*, *1*(5), 636-653. https://doi.org/10.1002/wcc.67

Haguma, D., Leconte, R., Côté, P., Krau, S., & Brissette, F. (2014). Optimal Hydropower Generation Under Climate Change Conditions for a Northern Water Resources System. *Water Resources Management*, *28*(13), 4631-4644. https://doi.org/10.1007/s11269-014-0763-3

Han, F., Zheng, Y., Tian, Y., Li, X., Zheng, C., & Li, X. (2021). Accounting for field-scale heterogeneity in the ecohydrological modeling of large arid river basins : Strategies and relevance. *Journal of Hydrology*, *595*, 126045. https://doi.org/10.1016/j.jhydrol.2021.126045

Hankin, B. G., & Beven, K. J. (1998). Modelling dispersion in complex open channel flows : Equifinality of model structure (1). *Stochastic Hydrology and Hydraulics*, *12*(6), 377-396. https://doi.org/10.1007/s004770050026

Hausfather, Z., Marvel, K., Schmidt, G. A., Nielsen-Gammon, J. W., & Zelinka, M. (2022). Climate simulations : Recognize the « hot model » problem. *Nature*, *605*(7908), 26-29. https://doi.org/10.1038/d41586-022-01192-2

Houle, D., Bouffard, A., Duchesne, L., Logan, T., & Harvey, R. (2012). Projections of Future Soil Temperature and Water Content for Three Southern Quebec Forested Sites. https://doi.org/10.1175/JCLI-D-11-00440.1

Hydroclimatic Atlas of Southern Québec. (2022). Repéré à https://www.cehq.gouv.qc.ca/atlas-hydroclimatique/index-en.htm

Immerzeel, W. W., & Droogers, P. (2008). Calibration of a distributed hydrological model based on satellite evapotranspiration. *Journal of Hydrology*, *349*(3), 411-424. https://doi.org/10.1016/j.jhydrol.2007.11.017

Jasper, K., Calanca, P., & Fuhrer, J. (2006). Changes in summertime soil water patterns in complex terrain due to climatic change. *Journal of Hydrology*, *327*(3), 550-563. https://doi.org/10.1016/j.jhydrol.2005.11.061

Jehanzaib, M., Ajmal, M., Achite, M., & Kim, T.-W. (2022). Comprehensive Review : Advancements in Rainfall-Runoff Modelling for Flood Mitigation. *Climate*, *10*(10), 147. https://doi.org/10.3390/cli10100147

Jie, M.-X., Chen, H., Xu, C.-Y., Zeng, Q., & Tao, X. (2015). A comparative study of different objective functions to improve the flood forecasting accuracy. *Hydrology Research*, *47*(4), 718-735. https://doi.org/10.2166/nh.2015.078

Jones, R. N., Chiew, F. H. S., Boughton, W. C., & Zhang, L. (2006). Estimating the sensitivity of mean annual runoff to climate change using selected hydrological models. *Advances in Water Resources*, *29*(10), 1419-1429. https://doi.org/10.1016/j.advwatres.2005.11.001

K. Ajami, N., Gupta, H., Wagener, T., & Sorooshian, S. (2004). Calibration of a semi-distributed hydrologic model for streamflow estimation along a river system. *Journal of Hydrology*, *298*(1), 112-135. https://doi.org/10.1016/j.jhydrol.2004.03.033

Khakbaz, B., Imam, B., Hsu, K., & Sorooshian, S. (2012). From lumped to distributed via semi-distributed : Calibration strategies for semi-distributed hydrologic models. *Journal of Hydrology*, *418-419*, 61-77. https://doi.org/10.1016/j.jhydrol.2009.02.021

Kim, C., & Kim, C.-S. (2021). Comparison of the performance of a hydrologic model and a deep learning technique for rainfall- runoff analysis. *Tropical Cyclone Research and Review*, *10*(4), 215-222. https://doi.org/10.1016/j.tcrr.2021.12.001

Kling, H., Fuchs, M., & Paulin, M. (2012). Runoff conditions in the upper Danube basin under an ensemble of climate change scenarios. *Journal of Hydrology*, *424-425*, 264-277. https://doi.org/10.1016/j.jhydrol.2012.01.011

Kumar, J. R. R., Kalnawat, A., Pawar, A. M., Jadhav, V. D., Srilatha, P., & Khetani, V. (2024). Transparency in Algorithmic Decision-making : Interpretable Models for Ethical Accountability. *E3S Web of Conferences*, *491*, 02041. https://doi.org/10.1051/e3sconf/202449102041

Le Goff, H., Leduc, A., Bergeron, Y., & Flannigan, M. (2005). The adaptive capacity of forest management to changing fire regimes in the boreal forest of Quebec. *The Forestry Chronicle*, *81*(4), 582-592. https://doi.org/10.5558/tfc81582-4

Lee, M.-H., Lu, M., Im, E.-S., & Bae, D.-H. (2019). Added value of dynamical downscaling for hydrological projections in the Chungju Basin, Korea. *International Journal of Climatology*, *39*(1), 516-531. https://doi.org/10.1002/joc.5825

Lemieux, C. J., & Scott, D. J. (2011). Changing Climate, Challenging Choices : Identifying and Evaluating Climate Change Adaptation Options for Protected Areas Management in Ontario, Canada. *Environmental Management*, *48*(4), 675-690. https://doi.org/10.1007/s00267-011-9700-x

Ley, A., Bormann, H., & Casper, M. (2023). Intercomparing LSTM and RNN to a Conceptual Hydrological Model for a Low-Land River with a Focus on the Flow Duration Curve. *Water*, *15*(3), 505. https://doi.org/10.3390/w15030505

Manabe, S., & Bryan, K. (1969). Climate Calculations with a Combined Ocean-Atmosphere Model. Repéré à https://journals.ametsoc.org/view/journals/atsc/26/4/1520-0469_1969_026_0786_ccwaco_2_0_co_2.xml

Maraun, D. (2016). Bias Correcting Climate Change Simulations—A Critical Review. *Current Climate Change Reports*, *2*(4), 211-220. https://doi.org/10.1007/s40641-016-0050-x

Martel, J.-L., Brissette, F., Troin, M., Arsenault, R., Chen, J., Su, T., & Lucas-Picher, P. (2022). CMIP5 and CMIP6 Model Projection Comparison for Hydrological Impacts Over North America. *Geophysical Research Letters*, *49*(15), e2022GL098364. https://doi.org/10.1029/2022GL098364

McDonnell, J. J., Spence, C., Karran, D. J., van Meerveld, H. J. (Ilja), & Harman, C. J. (2021). Fill-and-Spill : A Process Description of Runoff Generation at the Scale of the Beholder. *Water Resources Research*, *57*(5), e2020WR027514. https://doi.org/10.1029/2020WR027514

Meehl, G. A., Boer, G. J., Covey, C., Latif, M., & Stouffer, R. J. (2000). The Coupled Model Intercomparison Project (CMIP). *Bulletin of the American Meteorological Society*, *81*(2), 313-318. Repéré à https://www.jstor.org/stable/26215108

Mei, Y., Mai, J., Do, H. X., Gronewold, A., Reeves, H., Eberts, S., … Hunt, R. J. (2023). Can Hydrological Models Benefit From Using Global Soil Moisture, Evapotranspiration, and Runoff Products as Calibration Targets? *Water Resources Research*, *59*(2), e2022WR032064. https://doi.org/10.1029/2022WR032064

Milly, P. C. D., Dunne, K. A., & Vecchia, A. V. (2005). Global pattern of trends in streamflow and water availability in a changing climate. *Nature*, *438*(7066), 347-350. https://doi.org/10.1038/nature04312

Minville, M., Brissette, F., Krau, S., & Leconte, R. (2009). Adaptation to Climate Change in the Management of a Canadian Water-Resources System Exploited for Hydropower. *Water Resources Management*, *23*(14), 2965-2986. https://doi.org/10.1007/s11269-009-9418-1

Minville, M., Brissette, F., & Leconte, R. (2008). Uncertainty of the impact of climate change on the hydrology of a nordic watershed. *Journal of Hydrology*, *358*(1), 70-83. https://doi.org/10.1016/j.jhydrol.2008.05.033

Miralha, L., Muenich, R. L., Scavia, D., Wells, K., Steiner, A. L., Kalcic, M., … Kirchhoff, C. J. (2021). Bias correction of climate model outputs influences watershed model nutrient load predictions. *Science of The Total Environment*, *759*, 143039. https://doi.org/10.1016/j.scitotenv.2020.143039

Mudryk, L. R., Derksen, C., Howell, S., Laliberté, F., Thackeray, C., Sospedra-Alfonso, R., … Brown, R. (2018). Canadian snow and sea ice : Historical trends and projections. *The Cryosphere*, *12*(4), 1157-1176. https://doi.org/10.5194/tc-12-1157-2018

Mulvany, T. (1850). On the use of self-registering rain and flood gauges. Dans *Proceedings of the Institure Civil Engineers* (Vol. 4, pp. 1-8). Dublin, Ireland.

Nand, V., & Qi, Z. (2023). Potential of implementing irrigation in rainfed agriculture in Quebec : A review of climate change-induced challenges and adaptation strategies. *Irrigation and Drainage*, *72*(4), 1165-1187. https://doi.org/10.1002/ird.2840

Natkhin, M., Steidl, J., Dietrich, O., Dannowski, R., & Lischeid, G. (2012). Differentiating between climate effects and forest growth dynamics effects on decreasing groundwater recharge in a lowland region in Northeast Germany. *Journal of Hydrology*, *448-449*, 245-254. https://doi.org/10.1016/j.jhydrol.2012.05.005

Nolin, A. F., Girardin, M. P., Adamowski, J. F., Barzegar, R., Boucher, M.-A., Tardif, J. C., & Bergeron, Y. (2023). Observed and projected trends in spring flood discharges for the Upper Harricana River, eastern boreal Canada. *Journal of Hydrology : Regional Studies*, *48*, 101462. https://doi.org/10.1016/j.ejrh.2023.101462

Novotná, B., van Bochove, E., & Thériault, G. (2013). Potential ecological impact of climate change on the water quality of an intensively managed agricultural watershed in Quebec, Canada. *Journal of Water and Climate Change*, *5*(1), 81-99. https://doi.org/10.2166/wcc.2013.121

Okiria, E., Okazawa, H., Noda, K., Kobayashi, Y., Suzuki, S., & Yamazaki, Y. (2022). A Comparative Evaluation of Lumped and Semi-Distributed Conceptual Hydrological Models : Does Model Complexity Enhance Hydrograph Prediction? *Hydrology*, *9*(5), 89. https://doi.org/10.3390/hydrology9050089

O'Neill, B. C., Tebaldi, C., van Vuuren, D. P., Eyring, V., Friedlingstein, P., Hurtt, G., … Sanderson, B. M. (2016). The Scenario Model Intercomparison Project (ScenarioMIP) for CMIP6. *Geoscientific Model Development*, *9*(9), 3461-3482. https://doi.org/10.5194/gmd-9-3461-2016

Perrin, C., Michel, C., & Andréassian, V. (2003). Improvement of a parsimonious model for streamflow simulation. *Journal of Hydrology*, *279*(1), 275-289. https://doi.org/10.1016/S0022-1694(03)00225-7

Piani, C., Haerter, J. O., & Coppola, E. (2010). Statistical bias correction for daily precipitation in regional climate models over Europe. *Theoretical and Applied Climatology*, *99*(1), 187-192. https://doi.org/10.1007/s00704-009-0134-9

Picketts, I. M., Andrey, J., Matthews, L., Déry, S. J., & Tighe, S. (2016). Climate change adaptation strategies for transportation infrastructure in Prince George, Canada. *Regional Environmental Change*, *16*(4), 1109-1120. https://doi.org/10.1007/s10113-015-0828-8

Pool, S., Fowler, K., & Peel, M. (2024). Benefit of Multivariate Model Calibration for Different Climatic Regions. *Water Resources Research*, *60*(4), e2023WR036364. https://doi.org/10.1029/2023WR036364

Poulin, A., Brissette, F., Leconte, R., Arsenault, R., & Malo, J.-S. (2011). Uncertainty of hydrological modelling in climate change impact studies in a Canadian, snow-dominated river basin. *Journal of Hydrology*, *409*(3), 626-636. https://doi.org/10.1016/j.jhydrol.2011.08.057

Pradhan, A., & Indu, J. (2019). Uncertainty in Calibration of Variable Infiltration Capacity Model, 89-108. https://doi.org/10.1007/978-3-030-02197-9_4

Rajib, A., Evenson, G. R., Golden, H. E., & Lane, C. R. (2018). Hydrologic model predictability improves with spatially explicit calib ration using remotely sensed evapotranspiration and biophysical parame ters. *Journal of Hydrology*, *567*, 668-683. https://doi.org/10.1016/j.jhydrol.2018.10.024

Riboust, P., & Brissette, F. (2015). Climate Change Impacts and Uncertainties on Spring Flooding of Lake Champlain and the Richelieu River. *JAWRA Journal of the American Water Resources Association*, *51*(3), 776-793. https://doi.org/10.1111/jawr.12271

Riboust, P., & Brissette, F. (2016). Analysis of Lake Champlain/Richelieu River's historical 2011 flood. *Canadian Water Resources Journal / Revue canadienne des ressources hydriques*, *41*(1-2), 174-185. https://doi.org/10.1080/07011784.2014.982190

Ricard, S., Lucas-Picher, P., & Anctil, F. (2021). Producing hydrologic scenarios from raw climate model outputs using an asynchronous modelling framework. *Hydrology and Earth System Sciences Discussions*, 1-24. https://doi.org/10.5194/hess-2021-451

Ricard, S., Lucas-Picher, P., Thiboult, A., & Anctil, F. (2023). Producing reliable hydrologic scenarios from raw climate model outputs without resorting to meteorological observations. *Hydrology and Earth System Sciences*, *27*(12), 2375-2395. https://doi.org/10.5194/hess-27-2375-2023

Ricard, S., Sylvain, J.-D., & Anctil, F. (2019). Exploring an Alternative Configuration of the Hydroclimatic Modeling Chain, Based on the Notion of Asynchronous Objective Functions. *Water*, *11*(10), 2012. https://doi.org/10.3390/w11102012

Ricard, S., Sylvain, J.-D., & Anctil, F. (2020). Asynchronous Hydroclimatic Modeling for the Construction of Physically Based Streamflow Projections in a Context of Observation Scarcity. *Frontiers in Earth Science*, *8*. Repéré à https://www.frontiersin.org/articles/10.3389/feart.2020.556781

Rössler, O., Diekkrüger, B., & Löffler, J. (2012). Potential drought stress in a Swiss mountain catchment—Ensemble forecasting of high mountain soil moisture reveals a drastic decrease, despite major uncertainties. *Water Resources Research*, *48*(4). https://doi.org/10.1029/2011WR011188

Rößler, O., & Löffler, J. (2010). Potentials and limitations of modelling spatio-temporal patterns of soil moisture in a high mountain catchment using WaSiM-ETH. *Hydrological Processes*, *24*(15), 2182-2196. https://doi.org/10.1002/hyp.7663

Sabzipour, B., Arsenault, R., Troin, M., Martel, J.-L., Brissette, F., Brunet, F., & Mai, J. (2023). Comparing a long short-term memory (LSTM) neural network with a physically-based hydrological model for streamflow forecasting over a Canadian catchment. *Journal of Hydrology*, *627*, 130380. https://doi.org/10.1016/j.jhydrol.2023.130380

Samek, W., & Müller, K.-R. (2019). Towards Explainable Artificial Intelligence. Dans W. Samek, G. Montavon, A. Vedaldi, L. K. Hansen, & K.-R. Müller (Éds), *Explainable AI: Interpreting, Explaining and Visualizing Deep Learning* (pp. 5-22). Cham: Springer International Publishing. https://doi.org/10.1007/978-3-030-28954-6_1

Schäfer, C., Fäth, J., Kneisel, C., Baumhauer, R., & Ullmann, T. (2023). Multidimensional hydrological modeling of a forested catchment in a German low mountain range using a modular runoff and water balance model. *Frontiers in Forests and Global Change*, *6*. https://doi.org/10.3389/ffgc.2023.1186304

Schulla, J. (2021). WaSiM-ETH Documentation. Repéré à http://www.wasim.ch/en/products/wasim_description.htm

Shen, H., Tolson, B. A., & Mai, J. (2022). Time to Update the Split-Sample Approach in Hydrological Model Calibration. *Water Resources Research*, *58*(3), e2021WR031523. https://doi.org/10.1029/2021WR031523

Singh, V. P. (2018). Hydrologic modeling : Progress and future directions. *Geoscience Letters*, *5*(1), 15. https://doi.org/10.1186/s40562-018-0113-z

Sivakumar, B. (2011). Global climate change and its impacts on water resources planning and management : Assessment and challenges. *Stochastic Environmental Research and Risk Assessment*, *25*(4), 583-600. https://doi.org/10.1007/s00477-010-0423-y

Sulis, M., Paniconi, C., Rivard, C., Harvey, R., & Chaumont, D. (2011). Assessment of climate change impacts at the catchment scale with a detailed hydrological model of surface-subsurface interactions and comparison with a land surface model. *Water Resources Research*, *47*(1), 2010WR009167. https://doi.org/10.1029/2010WR009167

Taylor, K. E., Stouffer, R. J., & Meehl, G. A. (2012). An Overview of CMIP5 and the Experiment Design. *Bulletin of the American Meteorological Society*, *93*(4), 485-498. https://doi.org/10.1175/BAMS-D-11-00094.1

Teufel, B., Sushama, L., Huziy, O., Diro, G. T., Jeong, D. I., Winger, K., … Nguyen, V.-T.-V. (2019). Investigation of the mechanisms leading to the 2017 Montreal flood. *Climate Dynamics*, *52*(7), 4193-4206. https://doi.org/10.1007/s00382-018-4375-0

Teutschbein, C., & Seibert, J. (2013). Is bias correction of regional climate model (RCM) simulations possible for non-stationary conditions? *Hydrology and Earth System Sciences*, *17*(12), 5061-5077. https://doi.org/10.5194/hess-17-5061-2013

Valencia Giraldo, M. del C., Ricard, S., & Anctil, F. (2023). Assessment of the Potential Hydrological Impacts of Climate Change in Quebec—Canada, a Refined Neutral Approach. *Water*, *15*(3), 584. https://doi.org/10.3390/w15030584

van Bellen, S., Garneau, M., & Bergeron, Y. (2010). Impact of Climate Change on Forest Fire Severity and Consequences for Carbon Stocks in Boreal Forest Stands of Quebec, Canada : A Synthesis. *Fire Ecology*, *6*(3), 16-44. https://doi.org/10.4996/fireecology.0603016

Yassin, F., Razavi, S., Wheater, H., Sapriza-Azuri, G., Davison, B., & Pietroniro, A. (2017). Enhanced identification of a hydrologic model using streamflow and sat ellite water storage data : A multicriteria sensitivity analysis and op timization approach. *Hydrological Processes*, *31*(19), 3320-3333. https://doi.org/10.1002/hyp.11267

Yue, X.-L., & Gao, Q.-X. (2018). Contributions of natural systems and human activity to greenhouse gas emissions. *Advances in Climate Change Research*, *9*(4), 243-252. https://doi.org/10.1016/j.accre.2018.12.003